Genetic control of melanin production in the polyextremotolerant fungus *Exophiala dermatitidis*

By

Kamaldeep S. Chhoker

A Thesis submitted to the Faculty of Graduate and Postdoctoral Studies of

The University of Manitoba

in partial fulfilment of the requirements of the degree of

Doctor of Philosophy

Department of Biological Sciences

University of Manitoba

Winnipeg, Manitoba, Canada

Abstract

Exophiala dermatitidis is a polymorphic black yeast found in various habitats such as soil, leaf litter and man-made environments including sinks, dishwashers and saunas. *E. dermatitidis* is also an opportunistic pathogen of humans where it can cause phaeohyphomycosis and skin infections. 1,8-DHN melanin found in *E. dermatitidis* has been shown to provide various functions that range from protection against cellular damage to conversion of visible UV energy into heat. Although the *E. dermatitidis* genome sequence has revealed the presence of genes responsible for production of melanin via three different pathways, relatively little is known about the relative contribution of these pathways to melanization. The aim of this study was to address this issue by using an unbiased genetic approach to determine which pathways are essential for melanin production. To this end, albino mutants lacking the ability to produce melanin were obtained using UV irradiation. Based on genome re-sequencing and SNVs analysis, all the albino mutants showed variants in the *PKS1* gene including mutations ranging from missense base substitutions to frameshifts and short deletions. When grown on different carbon sources, some albino mutants were able to recover melanin production. Ultimately, comparative transcriptomics was used as a tool to examine differentially expressed genes when the various albino mutants were grown on different carbon sources. Transcriptomics analysis allowed us to investigate the expression of alternative genes/pathways that can promote the recovery of melanin production in the conditional albino mutants.

Acknowledgements

I would like to thank Dr. Steven Harris for his commitment, guidance, and support that allowed me to learn more about different aspects of fungal biology. I would also like to thank Dr. Georg Hausner who was always there to provide feedback and guidance when I was stuck. I would like to thank my committee members Dr. Steven Whyard, Dr. Mark Belmonte and Dr. Aleeza Gerstein who provided me with valuable insight in my project and were always there to help.

I would also like to thank the Biological Sciences departmental staff (Jaime Stringer, Sylvia Lapointe, Doreen Davies) who were always there to provide support for any administrative and financial questions I had be it conference related, travel or ordering supplies for my project in a quick manner.

I would like to thank my grandpa, mom, dad, brother and my wife for their support all these years who were always there for me to keep my spirits up. I would like to thank my family and friends with whom I could share how my days went be it good or bad and who were always there to cheer me up.

A special thanks to my friends and colleagues Jennifer Doering, Alicia Fox and Emily Kaul with whom I could talk about my project and talk about the frustrations that came along some days including things not working properly.

I would like to dedicate this thesis to my grandma who passed away during my PhD and hopefully she can see it from the heaven and rejoice on her grandson's accomplishment.

Thesis, the publication status of chapters, and the role of each coauthor in each chapter

Chapter	**Author**	Contributions of each author	Article Status
1	Kamaldeep Chhoker	KC reviewed the literature, organized the chapter, and wrote the chapter. SH and GH edited the chapter	Part of Literature review (Sections 1.3.4 – 1.3.10) published in Frontiers in Fungal Biology
2	Kamaldeep Chhoker Steven Harris Georg Hausner	KC and SH generated the experiment and guided the process. KC obtained the mutants, conducted the experiments, collected the results and wrote the chapter. SH and GH edited the chapter	Published in G3 Genes| Genomes| Genetics
3	Kamaldeep Chhoker Steven Harris Georg Hausner	KC and SH generated the experiment and guided the process. KC performed the experiments, performed the analysis of the data and wrote the chapter. SH and GH edited the chapter	Submitted to Canadian Journal of Microbiology for publication
4	Kamaldeep Chhoker	Final discussion and conclusions were written by KC and edited by SH and GH	Not to be published

Table of Contents

List of Tables

List of Figures

CHAPTER 1: General introduction and literature review

Parts of Chapter 1 (Sections 1.3.4 – 1.3.10) have been published as a review paper in peer reviewed journal (Frontiers in Fungal Biology).

Chhoker K, Hausner G, Harris S. 2025. Regulation of melanin production in fungi. *Front. Fungal Biol.* 6: doi: 10.3389/ffunb.2025.1621764.

Abstract

Melanin is a dark macromolecule found in organisms ranging from animals to fungi and plants. In fungi, melanin is a secondary metabolite that is not essential *per se* for growth but does provide various benefits that facilitate adaptation to stressful conditions such as UV light, desiccation, oxygen radicals and extreme temperatures. The biosynthetic pathways of most types of melanin are known and documented but the regulation of those pathways is not well understood. In fungi, known pathways for melanin production include those directing the synthesis of 1,8-DHN melanin and L-DOPA melanin, as well as the tyrosine degradation pathway. Genetic studies have identified structural genes and enzymes that play a role in these different melanin biosynthesis pathways. Recent studies have focused on the roles of various transcription factors (TFs) and signaling circuits (e.g., cAMP/PKA and the HOG pathway) in regulating the expression of the biosynthetic pathways. The review will provide insight into what is known about these TFs and regulatory circuits in diverse fungi in an attempt to identify common themes.

1.1 Introduction and Rationale

Black yeasts are a group of fungi that have a unique black-brown appearance due to the production of the macromolecule melanin (Kejžar *et al*. 2013; Selbmann *et al*. 2015). Melanin is not essential for these organisms but does provide various benefits to help them adapt to stressful conditions and can provide competitive advantages to the fungus it is found in (Cordero and Casadevall 2017). Fungal melanin has been shown to help fungi adapt to stressful conditions such as providing protection against UV radiation (Wollenzien *et al*. 1995), it also helps protect the organism against lysis (Kohno 1983), provides protection from extreme temperatures and toxic metals (Jacobson *et al*. 1995; Rosas and Casadevall 1997) and aids in virulence of opportunistic pathogens and provides protection from hosts immune system (Wang *et al*. 1995; Nosanchuk and Casadevall 2003). Black yeasts have been found surviving in the Antarctic desert such as McMurdo Dry Valleys (Selbmann *et al*. 2005), where conditions are thought to be closely related to conditions on Mars. There is a growing interest in how black yeasts can adapt to such extreme conditions in fields such as exobiology (Onofri *et al*. 2004). Depending on the fungal species the melanin produced can vary and it can either be allomelanin, pyomelanin, eumelanin or pheomelanin (Funa *et al*. 2005; Simon and Peles 2010; Seo and Choi 2020; Cao *et al*. 2021). Some fungal species such as *Aspergillus fumigatus* can produce more than one type of melanin.

Many black yeasts can cause infections in humans and other vertebrates due to the presence of melanin. One such black yeast that can cause infection in humans is *Exophiala dermatitidis*. The first infection caused by *E. dermatitidis* was reported in 1934 (Hohl *et al*. 1983) and by 2011, at least 30 cases have been reported (Mukaino *et al*. 2006; Bulloch 2011; Chen *et al*. 2016). Due to the recent emergence of new cases, more focus needs to be placed on

understanding the mechanism involved in *E. dermatitidis* that allow it to survive during infections and on different conditions. The investigation of melanin production undertaken via this study will provide insight into the genes and functional pathways that might be beneficial for *E. dermatitidis* to survive in different conditions.

Until now most of the work on melanin production in *E. dermatitidis* has focused on targeted mutations of *PKS1* gene. Random mutagenesis represents an unbiased approach that promises to expand the number of identifiable genes with putative roles in melanin production. When combined with the analysis of mutant phenotypes and transcriptomics, this approach will provide new insights into the genes and pathways that contribute to melanin production in *E. dermatitidis*. This study could, identify key determinants of stress tolerance in the extremotolerant fungus *E. dermatitidis*. Since *E. dermatitidis* can thrive in stressful low nutrient conditions such as steam baths, saunas and dishwashers (Machouart *et al*. 2011) and also in airways of humans as a opportunistic pathogen (Kenney *et al*. 1992; Patel *et al*. 2013; Berger *et al*. 2017), this study will provide insight into genes and functional pathways that might be responsible for *E. dermatitidis* melanization that allows it to survive in such extreme niches.

1.2 Objectives

1. To obtain a repository of *E. dermatitidis* mutant strains with different pigmentation phenotypes (albino (*alb*) and hyperpigmented (*hyp*)) using an unbiased random mutagenesis approach. A combination of classical genetics, phenotyping, and genome re-sequencing will be used to identify candidate genes that might be involved in affecting the difference in phenotypes (Chapter 2).

2. Investigate the relative role of melanin of *E. dermatitidis* to various phenotypic stress and nutrient composition. Perform different phenotypic assays to determine if melanin plays a crucial

role in growth of *E. dermatitidis* and to determine if different nutrient composition can affect melanization (Chapter 2).

3. To determine the genes that might be implicated in the production of melanin in *E. dermatitidis*. Since *E. dermatitidis* can potentially produce three distinct types of melanin, RNA transcriptomics analysis was performed to examine the expression of genes implicated in melanin production. This approach leveraged a novel conditional albino phenotype to screen for yet unknown genes or pathways that may be involved in melanin production (Chapter 3).

1.3 Literature Review

1.3.1 Black Yeasts

Black Yeasts refers to a group of fungi that have black-brown appearance due to the presence of melanin in the cells and display meristematic development (Kejžar *et al*. 2013; Selbmann *et al*. 2013). Fungi whose vegetative cells contain melanin in the cell wall are often referred to as phaeoid or dematiaceous fungi. These dematiaceous fungi are among the most extreme-tolerant organisms found in different habitats (Coleine *et al*. 2022). Another interchangeable name that has been used for black yeasts is meristematic fungi, which are defined as any fungi that form aggregates of thick-walled, enlarged melanized cells (Sterflinger *et al*. 1999). Despite these two different definitions the species can be classified morphologically as either black yeast or meristematic fungi, but molecular approaches are needed to properly distinguish them (de Hoog and Hermanides-Nijhof 1977). In meristematic fungi each vegetative cell is highly resistant to desiccation, environmental stresses and capable of propagation (Sterflinger and Krumbein 1995). Black yeasts and meristematic fungi show slow growth rates in nature and for most species in lab conditions as well. Black yeasts are found in various habitats that are characterized by extreme conditions, such as rock surfaces, and in toxic niches that contain hydrocarbons and heavy metals (Coleine *et al*. 2022; Gostinčar *et al*. 2012; 2023). They

are sometimes also found in vertebrates as opportunistic pathogens (de Hoog 2014). Melanized fungal species have been found in the McMurdo Dry Valley of Antarctica, which is reportedly the coldest and driest habitat on the planet (Onofri *et al*. 2004). In these conditions the black yeasts are often found in microscopic niches found within rocks (Selbmann *et al*. 2005). The existence of black yeasts in these environments might be attributed to two main reasons: firstly, the presence of melanin that provides protection against UV and resists desiccation (Wollenzien *et al*. 1995) and secondly, meristematic growth that increases surface/volume ratio thereby facilitating water and nutrient transport in a manner that enables stress tolerance (Sterflinger *et al*. 1995; Wollenzien *et al*. 1997; Zalar *et al*. 1999; Gostinčar *et al*. 2012; 2023).

Several black yeasts species have been isolated from subglacial ice or polythermal glaciers (Gunde-Cimerman *et al*. 2003). An osmotolerant black yeast, *Aureobasidium pullulans* has been shown to thrive in polluted waters (Kogej *et al*. 2005), solar salterns (Gunde-Cimerman *et al*. 2000), and even arctic glaciers (Zalar *et al*. 2008). Species from the black yeast genus *Hortaea* are shown to survive in saturated salt solutions (Gunde-Cimerman *et al*. 2000), and under acidic conditions (Holker *et al*. 2004). A study conducted on *H. werneckii* showed that melanized cell walls helped retain high concentrations of glycerol when the samples were grown at low salinities (Kogej *et al*. 2007). Another study conducted in 2013 also showed that if melanin biosynthesis is inhibited, the growth of *H. werneckii* in hypersaline media also decreases (Kejžar *et al*. 2013). These studies provide evidence that in some part melanin might be responsible for the adaptability and survivability of black yeasts. Due to the adaptation of black yeasts to highly stressful conditions, they are generally not found in complex microbial populations but prefer nutrient poor environments where they can thrive without competition (de Hoog *et al*. 1999). Based on the preferred growing conditions, extremotolerant fungi are

subdivided into various categories: Psychrotolerant fungi can grow at or near 0°C, thermotolerant fungi grow above 45-50°C, halotolerant and fungi grow at various salinity ranges; acidotolerant fungi grow at acidic conditions ranging from pH 3-4 and xerotolerant fungi grow well in dry environments (Gostinčar *et al*. 2023).

1.3.2 Chaetothyriales

Black yeasts in the order *Chaetothyriales* (*Pezizomycotina*) are ascomycete fungi that are melanized and possess considerable morphological diversity. All species found in this order are consistently melanized (Quan *et al*. 2020). Members in this order comprise species with aquatic, rock-inhabiting, ant-associated, and mycoparasitic lifestyles, as well as species that can tolerate toxic compounds, indicating the different extremotolerance adaptations (Teixeira *et al*. 2017). The order Chaetothriales contains five different families: *Chaetothyriaceae, Cyphellophoraceae, Epibryaceae, Herpotrichiellaceae,* and *Trichomeriaceae* and out of these five there are two main families that are well studied (Teixeira *et al*. 2017). The first family *Chaetothyriaceae* generally includes epiphyte species that grow on plant leaves (Chommunti *et al*. 2012) and are mainly distributed in tropical regions (Hyde *et al*. 2011). Members of this family produce a sooty melanized mycelium which resembles a network of loosely joined hyphae (Teixeira *et al*. 2017). The second family known for its medicinal importance is *Herpotrichiellaceae* and exhibits highly diversified lifestyles and contains saprobic species that are found on plant debris as well as other clinically important species that can cause phaeohyphomycosis, chromoblastomycosis and primary cerebritis (Untereiner and Naveau 1998; Garnica *et al*. 2009; de Hoog 2014). Since mammalian tissue shares ecological similarities such as raised temperature, osmotic stress, and oxygenic action this makes it a favourable environment for these black yeasts since they are already preadapted to it in their natural habitats (Matos *et al*. 2002).

Of the two main families of Chaetothyriales, the family *Herpotrichiellaceae* has been the focus of recent research due to its diversified lifestyles and their potential as opportunistic pathogens of various vertebrate hosts (de Hoog 2014). Species found in the family *Herpotrichiellaceae* are categorized by their ecological preference and trends and fall into 5 different clades: bantiana-clade, carrionii-clade, jeanselmei-clade, dermatitidis-clade and salmonis-clade (de Hoog *et al*. 2014; Teixeira *et al*. 2017). Some members found in all five of these clades are opportunistic pathogens of cold and warm-blooded vertebrates that can cause disease despite the presence of an intact immune system (Crous *et al*. 2007; Seyedmousavi *et al*. 2013). Species of the family *Herpotrichiellaceae* can be found in extreme environments such as growing on exposed rock surfaces in toxic niches containing hydrocarbons or arid environments (Seyedmousavi *et al*. 2011; de Hoog 2014) or they can also be found in nutrient-poor habitats such as showers, sinks, dishwashers and steam baths (Hamada and Abe 2009; Liam and de Hoog 2010; Döğen *et al*. 2013; Zupančič *et al*. 2016) and ant-associated families are also found (Voglmayr *et al*. 2011). Species in this family generally reproduce asexually with conidia generated during the filamentous phase, an exception being *Exophiala* where yeast-like budding is prevalent (de Hoog *et al*. 2011).

1.3.3 *Exophiala dermatitidis*

Exophiala dermatitidis (Kano) also known as *Wangiella dermatitidis* (Kano) is an ascomycete black yeast (Figure 1.1). Another name used for *E. dermatitidis* was *Phialophora dermatitidis*, but this has not been used in the literature since 1960s. *E. dermatitidis* belongs to the dermatitidis-clade of the family *Herpotrichiellaceae* which contains thermophilic *Exophiala* species from hot, low-nutrient water systems that can cause disseminated infections in humans (de Hoog *et al*. 2011). *E. dermatitidis* is a polymorphic, dematiaceous fungus which mostly

exists as yeast but has also been known to produce structures such as pseudohyphae, hyphae and sclerotic bodies (Liu *et al*. 2004). The dematiaceous nature of *E*. *dermatitidis* is caused due to deposition of 1,8-dihydroxynaphthalene [1,8-DHN] melanin present in the cell wall (Geis *et al*. 1984; Taylor *et al*. 1987; Feng *et al*. 2001). *E*. *dermatitidis* has a world-wide distribution and can be found in natural habitats such as tropical rain forests, where it is most likely associated with fruits and fruit-eating animals (Sudhahham *et al*. 2008). There has also been emergence of *E*. *dermatitidis* in man-made environments such as bathrooms, kitchen sink drains, saunas, steam baths and railways ties (Matos *et al*. 2002; Hamada and Abe 2010). Other species in the genus *Exophiala* have shown destructive potential on older buildings and can even colonize hard materials such as marble, sandstone and glass (de Hoog 2014). Studies conducted on *E*. *dermatitidis* in the past have recorded the species has the ability of growing up to 42°C (Matos *et al*. 2002).

In *E*. *dermatitidis*, melanin is in the cell walls resulting in dark pigmentation, whereas albino mutants appear white (Gies *et al*. 1984; Wheeler and Bell 1988). A study conducted by Dixon *et al*. (1987) on *E*. *dermatitidis* showed that dark color of the cells is lost when the cell wall is removed, providing support that melanin is present in the cell wall. Compared to the albino mutant strains, invasive hyphal growth is only recorded in melanized *E*. *dermatitidis* samples (Dixon *et al*. 1987; 1989). A study conducted by Brush and Money (1999) found that penetration of agar by *E*. *dermatitidis* hyphae was dependent on melanin, providing evidence that melanin might be involved in hyphal penetration in tissue. In a study conducted by de Hoog *et al*. (1994), it was observed that *E*. *dermatitidis* can transform into a meristematic from at ultralow pH. This has also been observed in the human digestive tract, where *E*. *dermatitidis* forms meristematic aggregates to survive low pH conditions (Horre and de Hoog 1999). In

addition to the 1,8-DHN melanin pathways *E. dermatitidis* has also been shown to use the DOPA-melanin pathway to produce melanin (Chen *et al.* 2014; Poyntner *et al*. 2018; Carr *et al*. 2023). The third pathway to produce melanin using L-tyrosine degradation to produce pyomelanin as a side product is also present in *E. dermatitidis* (Chen *et al.* 2014; Solano 2014).

In *E. dermatitidis*, it has been observed that the 1,8-DHN melanin pathway genes were upregulated during pH stress, which might facilitate adaptation to its natural niches (Chen *et al*. 2014). In the PKS pathway melanin is produced via the polymerization of 1,8-dihydroxynaphthalene (DHN) as the last step (Taylor *et al*. 1987). This is different than *C. neoformans* where melanin is synthesized from 3,4-dihydroxyphenylalanine via tyrosine, which includes polymerization of dopachrome as the last step (Kwon-Chung *et al*. 1982). *E. dermatitidis* has also been shown to produce two carotenoids: torulene and torularhodin (Geis and Szaniszlo 1984). A study conducted by Geis and Szaniszlo (1984) showed that the carotenoids increase the post-UV irradiation survival rates in the *E. dermatitidis* mutant strain MEL-4 which lacks melanin. Previous studies have noted that carotenoid pigments help protect the organism from harmful effects of oxidants which are photochemically induced (Geis and Szaniszlo 1984; Schnitzler *et al*. 1999), so having carotenoids as a complement to melanin would act as an extra security measure in *E. dermatitidis*. Since *E. dermatitidis* produces both melanin and carotenoids it can be theorized that melanin helps shield the species from light to some extent, which can then be detected by photoreceptor proteins to trigger carotenoid synthesis (Chen *et al*. 2014). These carotenoids might be important at earlier stages of development and spore germination where melanin has not yet been produced in a larger quantity to help protect against oxidative damage caused by light (Chen *et al*. 2014).

One way *E. dermatitidis* copes with stressful conditions is by undergoing morphological change. *E. dermatitidis* has been shown to produce multiple morphologies such as budding yeast forms, moniliform hyphae, true hyphal forms and multicellular forms (Oujezdsky *et al*. 1973; Roberts and Szaniszlo 1978). Under acidic cultural conditions around pH 2.5, *E. dermatitidis* can transition from yeast to a meristematic multicellular form whereas at a neutral pH the yeast cells continue to bud (Szaniszlo *et al*. 1976). It was observed that under acidic conditions there is a cessation of bud formation which is followed by cell wall thickening, cellular enlargement, septum formation and an increase in melanin production (Roberts and Szaniszlo 1978). The reasoning for this phenomenon was shown in a study conducted by Chen *et al*. (2014), where they found that the genes that were induced under low pH included genes responsible for cell wall biosynthesis, melanin biosynthesis and chitin processing. This was also found in previous studies where under low pH stress cells experienced chitin enrichment and produced thicker cell walls by upregulating the cell wall biosynthesis genes (Szaniszlo *et al*. 1983). One advantage of thicker cells is that there is more space available for melanin storage which would allow them to survive and adapt better to stressful conditions (Chen *et al*. 2014).

There has also been evidence that *E. dermatitidis* can switch between yeast-like to multicellular morphology under different temperatures and nutrient composition. A study by Karuppayil and Szaniszlo (1997) demonstrated the ability of *E. dermatitidis* wildtype strain to transition from yeast to multicellular forms at both 25°C and 37°C by addition of calcium to the medium at pH 2.5. In a study conducted by Roberts and Szaniszlo 1978, it was observed that temperature sensitive mutants of *E. dermatitidis* switched between morphologies at different temperatures. Whereas the wildtype strain displayed yeast-like budding growth at both 25°C and 37°C, temperature sensitive mutants started showing multicellular forms at 37°C and went back

to yeast-like forms at 25°C (Roberts and Szaniszlo 1978). These studies provided evidence that *E. dermatitidis* is vegetatively polymorphic and changes its form depending on the stress it encounters. Before *E. dermatitidis* can convert into a hyphal form, the vegetative yeast form must become thick walled and spore-like (Oujezdsky *et al*. 1973). When *E. dermatitidis* is growing on a suitable substrate, bud formation allows rapid cellular growth and when the conditions become restrictive the hyphal and yeast buds transform into thick walled, resistant yeasts that show dormancy and considerable longevity (Oujezdsky *et al*. 1973).

E. dermatitidis possesses a variety of chitin synthases which are responsible for cell wall strengthening, cell wall remodeling, and protection from host immune systems (Abramczyk *et al*. 2009). Previous studies have also demonstrated that there is enhanced growth of *E. dermatitidis* under induced ionizing radiation (Dadachova *et al*. 2007; Robertson *et al*. 2012). In a study conducted by Chen *et al*. (2014), it was found that *E. dermatitidis* has multiple iron transport pathways and genes necessary to acquire iron from hosts during infection. This might also enable them to uptake iron from various niches hence providing an advantage against competitive species. In a study looking at the role of calcium concentration in regulating growth and polymorphism it was observed that acidic stress and low calcium concentration aids the transition of yeast cells to multicellular forms (Karuppayil and Szaniszlo 1997). In *E. dermatitidis* it was found that under acidic conditions cells regulate $Ca2^{+}$ providing evidence that calcium is critical for controlling cellular morphogenesis.

E. dermatitidis also possesses orthologues of the velvet family of regulatory proteins (Chen *et al*. 2014) which have been shown to play a key role in coordinating development and secondary metabolism in response to light (Bayram *et al*. 2008; Chen *et al*. 2014). There has been evidence that the carotenoid pigments produced by *E. dermatitidis* are involved in light

reception and provide protection against ionizing radiation (Robertson *et al*. 2012) and oxidative damage (Geis and Szaniszlo 1984). In a study conducted by Chen *et al*. (2014), it was found that wild type *E*. *dermatitidis* colonies that were grown in light had darker pigmentation than colonies grown in the dark. The same phenomenon was recorded in *WdPKS1* albino mutants where the colonies grown under light turned pink indicating carotenoid production compared to colonies grown in dark (Chen *et al*. 2014).

The genome of *E. dermatitidis* has been previously annotated. A study by Teixeira *et al*. (2017) looked at the genomic diversity of various members of the *Chaetothriales*. Genome size varied between 25.81 Mb (*Capronia coronate*) and 43.03 Mb (*Cladophialophora immunda*) with *E*. *dermatitidis* possessing a genome of 26.40 MB and the average genome size of the dermatitids-clade being 27.0 Mb. The number of scaffolds of *E*. *dermatitidis* was 11 and the total number of predicted genes was 9269. The number of cytochrome p450 genes (CYPs) which play a fundamental role in primary and secondary metabolism in various fungi was 62 in *E*. *dermatitidis* (van den Brink *et al*. 1998; Teixeira *et al*. 2017). Fungal genomes contain biosynthetic gene clusters coding for various secondary metabolites, and this was also observed in *E dermatitidis* where five terpene, one Type 3 PKS, two Type 1 PKS and five NRPS secondary metabolite gene clusters were observed (Teixeira *et al*. 2017).

(a) 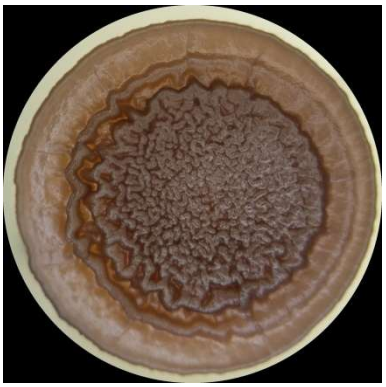 (b) 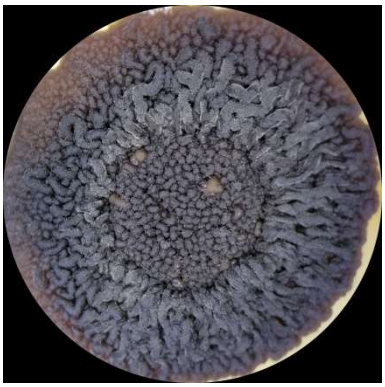

(c) 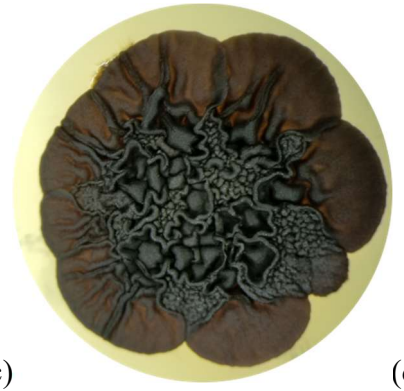 (d) 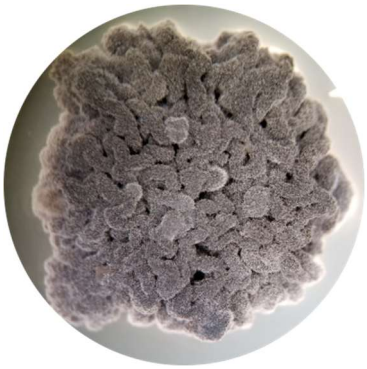

Figure 1.1: Images of *Exophiala dermatitidis* showing variety of coloration due to melanin and colony morphology (a) growing on YPD, (b) growing on YPG, (c) after one month of growth on YPD, (d) after one month of growth on YPG.

1.3.4 What is Melanin?

Melanin is a dark multifunctional pigment that is produced via the oxidative polymerization of phenolic and indolic compounds (Gomez and Nosanchuk 2003; Solano 2014; Suwannarach *et al*. 2019). The word melanin is derived from the Greek word "melanos", meaning "black" or "very dark" (Riley 1997; Gessler *et al*. 2014). The term melanin was first used by a Swedish chemist Berzalius to name a dark pigment extracted from eye membranes back in 1840 (Borovanský 2011). Melanin does not refer to a single substance but a group of substances that have similar properties (Bell and Wheeler 1986; Butler and Day 1998; Langfelder *et al*. 2003). Because they originate from different starting precursors, melanin particles can be found in a range of shapes and sizes that include rods, platelets, and planar arrays (Glass *et al*. 2012; Song *et al*. 2023). Based on the chemical precursor and the biosynthetic pathway, melanin pigments are classified into five different types: eumelanin, pheomelanin, neuromelanin, allomelanin and pyomelanin (Ambrico *et al*. 2016; Cao *et al*. 2021). These starting precursors condense and polymerize into nanometre to micron-size particles (Hong *et al*. 2012; 2018). Eumelanin, pheomelanin and neuromelanin are found associated with animal tissues whereas allomelanin and pyomelanin are found mostly in microorganisms, fungi and plants (Xie *et al*. 2019). Melanins are insoluble hydrophobic pigments which are negatively charged and have high molecular weight (Nosanchuk and Casadevall, 2003; Paolo *et al*. 2006; Solano 2014). Another key feature of melanin is the presence of a stable free radical population (Sealy *et al*. 1982).

Coloration of melanin can vary ranging from mainly dark brown to black, but in some instances, red or yellow coloration is also observed (Solano 2014). Features that distinguish melanin from other secondary compounds such as carotenoids and polyketides include (i) melanin is extremely heat-resistant and can withstand temperatures up to 600°C (Gallas *et al*.

2000), and (ii) it is highly insoluble and resistant to strong acids, detergents and reducing agents but is soluble in bases and phenols (Jacobson 2000). Because of these features, the structure is quite hard to identify since classical methods using aqueous or organic fluids end up disrupting its organization (Nosanchuk and Casadevall 2015). Like all naturally occurring pigments such as carotenoids, chlorophyll and flavonoids, melanin contains conjugate moieties such as aromatic rings that allow electronic resonance and mediate energy transfer reactions (Cordero and Casadevall 2017). Benefits and applied uses of melanin have been reviewed thoroughly (Cordero and Casadevall 2017; Tran-Ly *et al*. 2020; Mattoon *et al*. 2021; Suthar *et al*. 2023). Although the biosynthetic pathways that produce melanin are reasonably well understood (Eisenman and Casadevall 2012; Suthar *et al*. 2023; Qin and Xia 2024), much less is known about the regulation that ensures the proper timing and location of production such as in spores or deposition in the cell wall of the organism. Recent studies have implicated the PKA and HOG pathways as key signaling components of this regulation, while also identifying transcription factors that control expression of the biosynthetic pathways.

1.3.5 Fungal Melanin

In general, fungal melanin is typically found in the outer regions of the cell wall though it can also be found clustered on the cell wall surface (Bayry *et al*. 2014). In some fungi, melanin acts as a structural component of spores providing protection against various environmental stresses increasing the survivability of the fungi (Xu *et al*. 2022). In fungi, depending on the species melanin is either present all the time or is produced during specific development stages or in response to specific environmental cues (Bell and Wheeler, 1986). The term dematiaceous refers to species that produce melanin continuously, and species that produce melanin at specific stages (such as during conidia or filamentous growth) are referred to as “facultative melanotic”

fungi (Sterflinger *et al*. 1995; 1999). Melanin in many fungi is formed by a complex of differentially sized spherical particles that are approximately 200nm in diameter and are known as melanin granules (Franzen *et al*. 2006; Kogej *et al*. 2007). These granules are composed of fungal melanosomes which range from 30-120nm in diameter. Melanin granules allow macromolecules to pass through the melanin meaning that there are pores present in the melanin layers (Eisenman *et al*. 2005). Depending on the species, melanin tends to be stacked in layers with pores ranging between 1-4nm in diameter to facilitate the passage of macromolecules (Eisenman *et al*. 2005; Casadevall *et al*. 2012). Since the cell structures of different fungi vary in their organization and materials, so does the stacking distance of the melanin layers, examples include 4.15Å for *Exophiala dermatitidis* (also known as *Wangiella dermatitidis*), 4.45Å for *Aspergillus niger*, and 4.39Å for *Cryptococcus neoformans* (Nosanchuk *et al*. 2015). The indolic and/or phenolic monomers are ordered into planar arrangements of regularly interspaced stacked layers similar to graphite (Kim *et al*. 2016) and these layers can then cross-link into a more heterogeneous macromolecular configuration. This pattern of stacking is known as local-order-global-disorder and involves a combination of π-stacking, hydrogen and ionic bonded nanostructures with the melanin granules (Meredith and Sarna 2006; Nosanchuk *et al*. 2015; Kim *et al*. 2016).

For a pigment produced by fungi to be considered melanin and not a carotenoid, certain criteria need to be met: dark coloration, insolubility in cold, hot water and organic solvents, ability to solubilize and degrade in hot alkaline solutions and resistance to concentrated acid and bleaching by oxidizing agents (Meredith and Sarna 2006; Salgado-Castillo *et al*. 2023). Like other secondary metabolites produced by fungi, stress factors such as pH, temperature and nutrient starvation impact melanin synthesis (Salgado-Castillo *et al*. 2023). Light plays a

prominent role in production of melanin; strains grown under light tend to produce a higher quantity of melanin whereas strains grown in the dark tend to favour growth over melanin production (Pombeiro-Sponchiado *et al*. 2017). The concentration of copper also affects pigmentation and the production of melanin. Copper functions as a cofactor during oxidation and can be important for the biosynthesis of DHN and DOPA melanin (Eisenman and Casadevall 2012).

In fungi, laccases play a key role in polymerizing 1,8-DHN to melanin and oxidizing L-DOPA leading to series of spontaneous reactions that leads to the polymerization of DOPA melanin (Eiseman *et al*. 2007). Besides melanin production, laccases have also shown to be involved in the production of mycotoxins some of which share the PKS pathway that is responsible for the production of 1,8-DHN melanin (de Jonge *et al*. 2018; Gao *et al*. 2022). Laccases are diphenoloxidases that are associated with the cell wall of the fungi and catalyze the oxidation of diphenolic compounds to quinines (Williamson 1994; 1997; Zhu *et al*. 2001). In *C. neoformans* deletion of laccase genes led to the inhibition of melanin production and no pigmentation was observed even when media was supplemented by DOPA (Eisenman *et al*. 2007). Depending on the species of fungi, the number of laccases- encoding genes can vary. In *A. alternata* seven laccase-encoding genes have been identified (Gao *et al*. 2022). Deletion experiments of the seven laccase genes resulted in different observable phenotypes. Deletion of *lccB*-, *lccC-, lccD*- and *lccF*- did not have any significant effect on the melanization process when grown on mCDB media. But the deletion of *lccB* and *lccF* led to the reduction of melanin production for three days while growing on mCDB media with tomato puree. Double deletion mutants *lccC/D*- and *lccB/F*- showed highly reduced melanin production on both mCDB media and mCDB media with tomato puree. The study provided insight into the redundant nature of

laccase enzyme found in fungi (Gao *et al*. 2022). A study conducted by Dullah *et al*. (2021), found the laccase gene *lcc1* highly upregulated during fungal-fungal interaction where higher concentrations of melanin were also observed. These studies provide insight into the effect of various laccase enzymes on melanin production in fungi.

As the synthesis of melanin produces various highly reactive and toxic intermediates, fungal melanization occurs in specialized sphingolipid-enriched vesicles termed melanosomes which are generally similar to mammalian melanosomes (Walker *et al*. 2010). These vesicles contain laccase enzymes, leading to supramolecular buildup of melanin particles that are retained within the cell wall (Seiji *et al*. 1963; Camacho *et al*. 2019). The vesicles mediate transport of intercellularly synthesized macromolecules to targeted sites on the cell surface where they can be captured by the cell wall (Eisenman *et al*. 2009). Studies have revealed that the melanin polymer is covalently bonded to cell wall chitin and is also found associated with other cellular moieties including polysaccharides such as chitosan and plasma membrane derived lipids (Zhong *et al*. 2008; Chatterjee *et al*. 2015). Evidence of this has also been provided whereby mutations affecting chitin synthesis genes in different fungal species such as *E*. *dermatitidis*, *C*. *neoformans* and *Candida albicans* leads to a 'leaky melanin' phenotype such that strains are able to synthesize melanin but the cell wall is unable to retain the melanin granules which end up leaking into the extracellular space (Wang *et al*. 1999; Banks *et al*. 2005, Walton *et al*. 2005, Baker *et al*. 2007, Tsirilakis *et al*. 2012). Conversely, an increase in cell wall chitin or chitosan content reportedly increases melanin deposition (Banks *et al*. 2005; Baker *et al*. 2007; Tsirilakis *et al*. 2012). During the budding process of melanized yeasts, melanosomes in the cell wall are degraded or displaced allowing daughter cells to emerge (Nosanchuk and Casadevall, 2003; Eisenman *et al*. 2005). Much of the work in understanding melanin structure and morphology

has been performed on so-called melanin "ghosts", which are macromolecular structures obtained after hot acid digestion of melanized cells (Eisenman *et al*. 2009; Chatterjee *et al*. 2015). Melanin ghosts are composed of smaller melanin granules that are arranged in concentric layers embedded within the fungal cell wall (Eisenman *et al*. 2005). Melanin produced by fungi varies depending on the species that produces them. Most ascomycetes produce 1,8-DHN melanin via the polyketide synthase pathway (Nosanchuk *et al*. 2015), another type of melanin called L-DOPA melanin is produced mainly by basidiomycetes (Nosanchuk *et al*. 2015). Species such as *Aspergillus fumigatus* and *A*. *niger* can produce multiple different melanin types which can act as a failsafe during stressful conditions if certain nutrient requirements are not met (Pukkila-Worley *et al*. 2005). Some species such as *E*. *dermatitidis* have homologs of genes involved in 1,8-DHN melanin, L-DOPA melanin and L-tyrosine degradation melanin pathways but the exact mechanism or conditions that can trigger the production of L-DOPA or L-tyrosine melanin are not known (Paolo *et al*. 2006; Chen *et al*. 2014).

1.3.5 **Fungal Melanin biosynthesis**

The main type of melanin produced by fungi, especially by ascomycetes is 1,8-dihydroxynaphthalene [DHN] melanin via the polyketide synthase pathway (Nosanchuk et al. 2015). 1,8-DHN-melanin is named after one of the pathway intermediates, 1,8-dihydroxynaphthalene which was first identified in 1976 (Stipanovic and Bell 1976). Besides the polymerization of 1,8-DHN, different species can also utilize other pigment precursors such as: tyrosine, gama-glutaminyl-4-hydroxybenzene (GHB), catechol, homogentisic acid, and scytalone (Bell *et al*. 1976; Weijn *et al*. 2013; Belozerskaya *et al*. 2016). The second type of melanin, L-DOPA-melanin is named after one of the precursors, L-3,4-dihydroxyphenylalanine (Hamilton and Gomez 2002). The synthesis of eumelanin is catalyzed by phenoloxidases from DOPA

substrates by fungal species such as *C. neoformans* (Langfelder *et al*. 2003; Nosanchuk *et al*. 2015; Tran-Ly *et al*. 2020). L-DOPA melanin is mainly synthesized by basidiomycetes who occasionally also produce glutaminyl-3,4-dihydroxybenzene (GDHB) melanin (Henson *et al*. 1999; Selvakumar *et al*. 2008).

There are many fungal species that do not produce melanin under normal circumstances but when supplemented with L-DOPA tend to produce DOPA melanin (Butler *et al*. 1989; Butler and Day 1998). Despite the precursor, all fungal melanins tend to share similarities in the functional groups and physiochemical properties (Fogarty and Tobin 1996). During synthesis several enzymes such as tyrosinase, laccases, catechol oxidase carry out the rate-limiting initial oxidations of the starting phenolic precursors (Eisenman and Casadevall 2012; d'Ischia *et al*. 2013; Solano 2014) and activity of these enzymes depend on the copper ions present at the catalytic site (Mauch *et al*. 2013; Upadhyay *et al*. 2013).

In fungi three different categories of melanin include DHN melanin (Allomelanin and Pyomelanin), DOPA melanin (Eumelanin and Pheomelanin) and GHB melanin

1. **DHN-melanin (Allomelanin and Pyomelanin)**

   The word Allo refers to the Greek prefix meaning "heterogeneous" or "different" (Cao *et al*. 2021). The precursors of allomelanin can vary such that depending on the precursor allomelanins are referred to as DHN melanin, HPQ melanin or catechol melanin (Funa *et al*. 2005). The starting precursor for the synthesis of DHN-melanin, malonyl-CoA was first identified by Fujii *et al*. (2000) in *C. lagenarium*. Another precursor of DHN melanin is acetyl-CoA and both malonyl CoA and acetyl CoA are produced endogenously (Nosanchuk *et al*. 2015). It has been theorized that these starting precursors are obtained from glucose (Uran and Cano 2008). These starting precursors

are converted by polyketides synthase (PKS) to the first detectable intermediate 1,3,6,8-tetrahydroxynaphthalene (1,3,6,8-THN). 1,3,6,8-THN is reduced by hydroxynaphthalene reductase to produce scytalone (Alspaugh *et al*. 1997; Thompson *et al*. 2000). Scytalone is dehydrated enzymatically to 1,3,8-trihydoxynaphthalene (Alspaugh *et al*. 1998) which is then further reduced by a second reductase to vermelone (Basarab *et al*. 1999; Thompson *et al*. 2000). Vermelone is then further dehydrated by scytalone dehydratase to form the next intermediate 1,8-dihydroxynaphthalene (DHN). The pathway then involves a series of steps, including a dimerization of the 1,8-DHN molecules, followed by polymerization catalyzed by a laccase (Bloomfield and Alexander 1967). 1,8-DHN proceeds through C-C coupling reaction of the naphthalene rings, giving three DHN dimmers which are then further oxidized to form a mixture of longer oligomers, which self-assemble to form the melanin structure (Figure 1.2) (Cecchini *et al*. 2017; Manini *et al*. 2018). The structure of the DHN-melanin polymer is not well known but a study conducted by Beltran-Garcia *et al.* (2014) observed the presence of 50 DHN units in the polymer of melanin in the mycelium of *Mycosphaerella fijiensis*. The polyketide synthase responsible for the production of 1,8-DHN melanin generally possesses a similar structure across the fungi, including β-ketosynthase domain (β-KS), an acyl transferase domain (AT) and an acyl carrier domain (ACP). These are sometimes followed by a thiosterase domain (TE) which is responsible for detaching the polyketides from the enzyme (Watanabe *et al*. 2000; Fujii *et al*. 2001). DHN melanin production can be inhibited by tricyclazoles, pyroquilone, phthalide and clobenthiazone (Selvakumar *et al*. 2008).

Like allomelanins, pyomelanins are derived from the oxidative polymerization of nitrogen-free precursors such as homogentisic acid (HGA) (Funa *et al*. 2005; Seo and Choi 2020). Pyomelanin originates from the catabolism of either tyrosine or phenylalanine. The enzyme 4-hydroxyphenylpyruvic acid dioxygenase (HPPD) catalyzes the conversion of 4-hydroxyphenylpyruvate to HGA. Pyomelanin is generated through autooxidation to form benzoquinone acetic acid which are then self-polymerized to form HGA and the pyomelanin polymer (Turick *et al*. 2010; Keller *et al*. 2011). Pyomelanin polymers tend to be smaller compared to other melanin pigments (Figure 1.2).

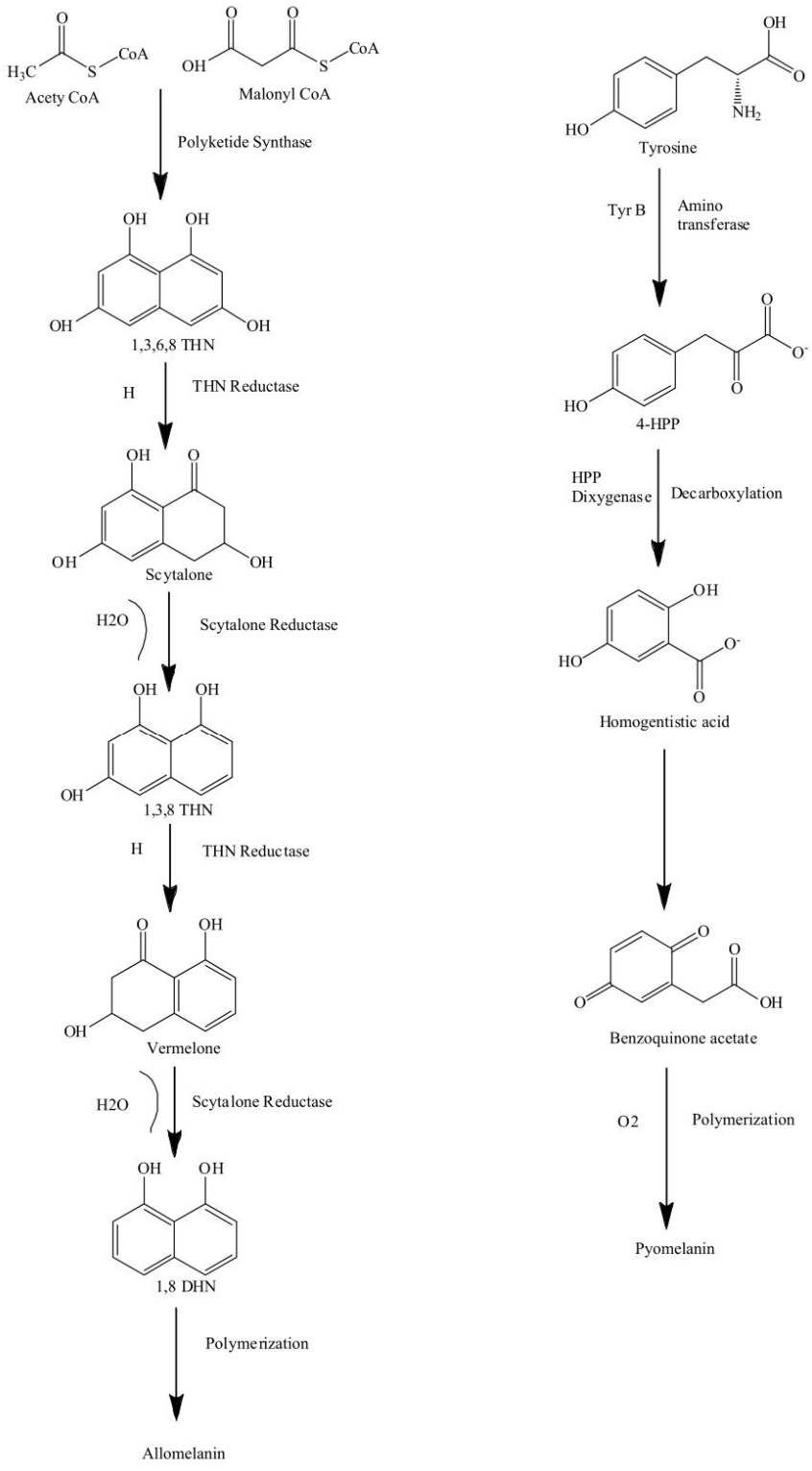

Figure 1.2: Biosynthesis pathway of allomelanin [1,8-DHN melanin] via the polyketide synthase (PKS) and pyomelanin derived from homogentistic acid. Pathways adapted from Suthar *et al*. (2023).

2. DOPA melanin (Eumelanin and Pheomelanin)

"Eu" is the Greek word for "good" or "well" and Pheo means "dark" in ancient Greek (Cao *et al*. 2021). The main difference between eumelanin and pheomelanin is attributed to the potential of eumelanin (Figure 1.3a) to act as a photoprotector and the phototoxic nature of pheomelanin (Figure 1.3b) (Cao *et al*. 2021). Pheomelanins are also believed to contain benzothiazine subunits that are synthesized from L-DOPA and cysteine (Simon and Peles 2010). Both eumelanin and pheomelanin are comprised of repeating units linked by carbon-carbon bonds (Costin *et al*. 2007). Phenoloxidases for DOPA melanin can either be laccases or tyrosinases, both of which have copper ligands and require copper ions for activity. Both play a different role where laccasses catalyze the one-step oxidation of dihydroxyphenols to quinones and tyrosinases catalyze the two-step oxidation of tyrosine (Langfelder *et al*. 2003). In brief the biosynthesis of eumelanin (Figure 1.4) begins with tyrosine, which is oxidized by oxygen followed by tyrosinase that forms levodopa (L-DOPA and then dopaquinone (Simon and Peles 2010; Cao *et al*. 2021). During the Dopa melanin pathway, hydroxylation of L-tyrosine to dopaquinone or the oxidation of L-DOPA to dopaquinone is catalyzed by tyrosinase or laccase respectively (Pomerantz and Warner 1967). If there are no thiol groups present dopaquinone forms leucodopachrome which is then oxidized to dopachrome. Hydroxylation and decarboxylation then yield dihydroxyindoles which is then further polymerized to form DOPA-melanin (Ozeki *et al*. 1997a, 1997b; Butler and Day 1998; Williamson 1994). Synthesis of DOPA-melanin has been shown to be inhibited by tropolone, kojic acid and diethyldithiocarbamete (Salgado-Castillo *et al*. 2023).

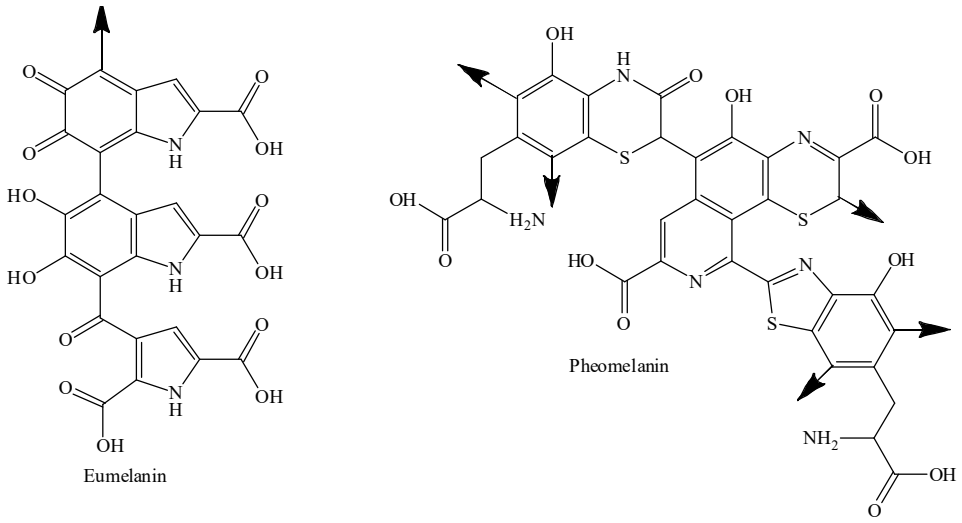

(a) (b)

Figure 1.3: Structures of eumelanin (a) and pheomelanin (b). Adapted from Sansinenea and Ortiz (2015).

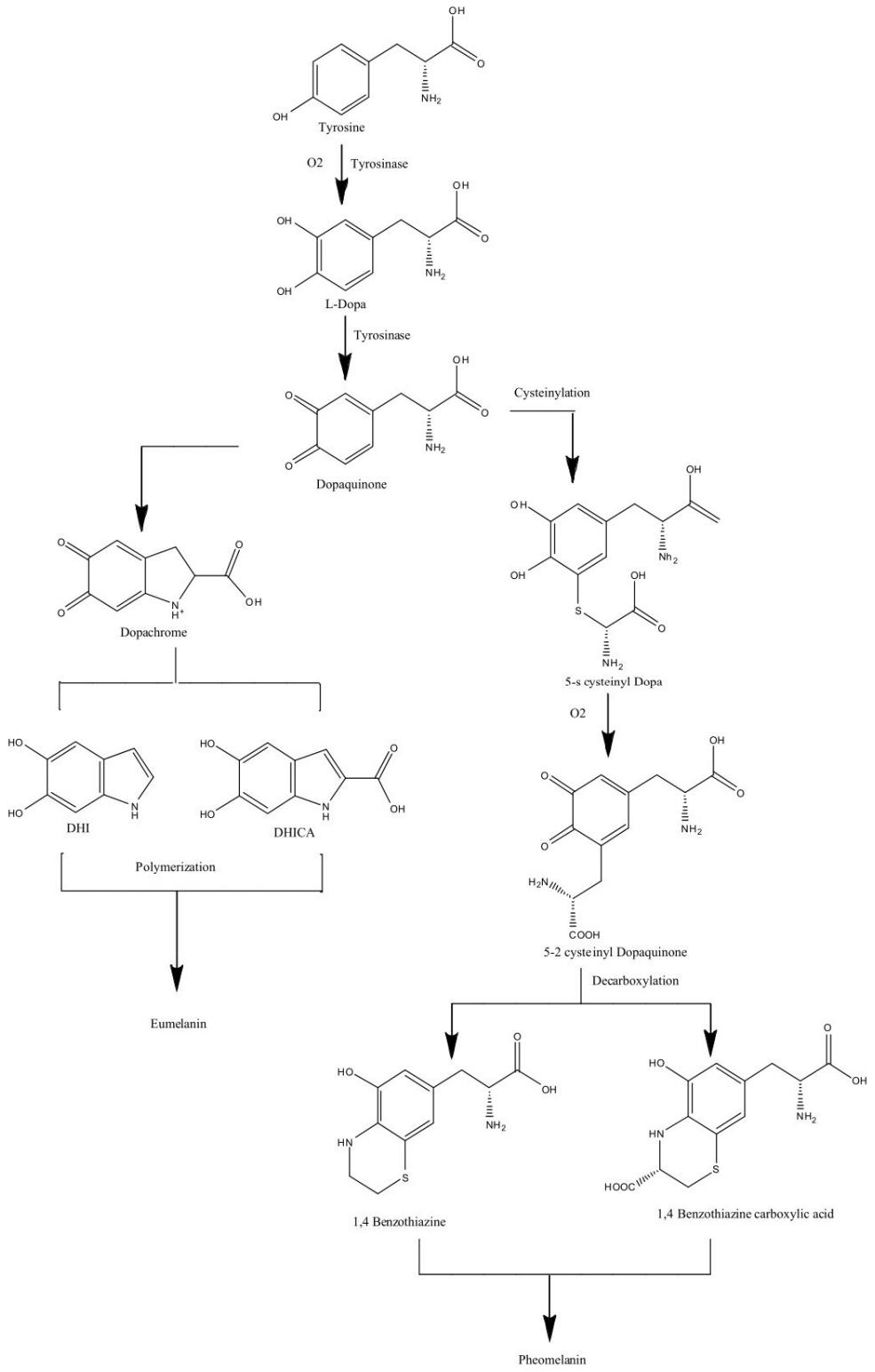

Figure 1.4: Biosynthesis pathway of eumelanin and pheomelanain (DOPA melanins) using tyrosinase enzymes. Pathways adapted from Suthar *et al*. (2023).

3. GHB melanin

In mushrooms such as *Agaricus bisporus* another type of melanin referred to as GHB is present. γ-L-glutaminyl4hydroxybenzene (GHB) is found in the mycelium and the fruiting body of *A*. *bisporus* whereas γ-L-glutaminyl-3,4_dydroxybenzene (GDHB) is found specifically in the reproductive hyphae (Stussi and Rast 1980). GHB melanin is also sometimes referred to as PAP-melanin as the initial substrate is *p*-aminophenol and the glutamyl are later removed before polymerization (Solano 2014). GHB melanin is formed from either phenolic precursors or GHB via the action of a tyrosinase (Figure 1.5) (Wejin *et al*. 2013). Chorismate which acts as the initial aromatic ring is converted to *p*-aminophenol and conjugated with a glutamyl residue to form GHB. GHB can then be further oxidized to form glutaminyl-3,4-dihydroxybenze (GDHB) or o-quinone, GBQ. The glutamyl residues are removed as from the final pigment (Bisko *et al*. 2007).

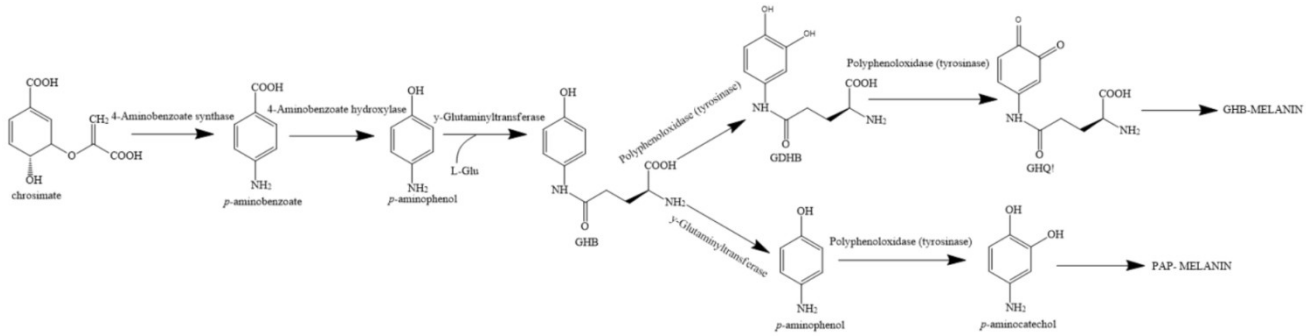

Figure 1.5: Biosynthesis pathway for GHB-melanin using chrosimate as a precursor. Pathway adapted from Wejin *et al*. (2013).

1.3.6 Genes involved in melanin synthesis pathways

Identification of the genes involved in the production of 1,8-DHN melanin and L-DOPA melanin has been achieved using gene knockout strategies (Schumacher 2016; Zhang *et al*. 2019; Nambu *et al*. 2021; Yang *et al*. 2022). The DHN melanin synthesis gene cluster is conserved in many fungi (Schumacher 2016; Ebert *et al*. 2018). The DHN-melanin pathway in *A*. *fumigatus* is comprised of a cluster of six genes: *abr1, abr2, ayg1, arp1, arp2* and *pksP* (Perez-Cuesta *et al*. 2020). Pheomelanin synthesis is related to the L-tyrosine degradation pathway that includes a cluster of six genes: *hppD, hmgX, hmgA, fahA, maiA* and *hmgR*. In *A*. *fumigatus* the DHN-melanin biosynthetic gene cluster spans roughly 10kb (Tsai *et al*. 1999). Genes encoded within this cluster are responsible for different steps of the DHN melanin biosynthetic pathway. The PKS gene *alb1* also referred to as *pksP* participates in the β-keotacyl condensation of malonyl-CoA and acetyl-CoA to generate 2,5,6,8-tetrahydroxy-2-methyl-2,3-dihydro-4H-naphtho(2,3-b) pyran-4-one (YWA1) (Gao *et al*. 2022). During the second step the *ayg1* gene hydrolyzes YWA1 to generate 1,3,6,8 tetrahydroxynaphthalene (1,3,6,8-THN). There are multiple reduction steps followed by aromatization/dehydration reactions that lead to oxidative polymerization (Perez-Cuesta *et al*. 2020). 1,3,6,8- THN is reduced to scytalone by the hydroxynaphthalene reductase gene *arp2* and the enzyme 1,3,6,8 reductase. The scytalone reductase gene *arp1*, is responsible for the dehydration of scytalone to 1,3,8-trihydroxynaphthalene which is followed by another reduction step by the enzyme hydroxynaphthalene reductase encoded by the gene *arp2* that reduces 1,3,8-trihydroxynaphthalene to vermelone. Vermelone is then dehydrated by a multicopper oxidase gene *abr1* which converts it to 1,8-dihydroxynaphthalene (1,8-DHN) which is polymerized into DHN-melanin by laccase enzymes encoded by the putative laccase *abr2*

gene (Perez-Cuesta *et al*. 2020). Genes with known functions involved in the 1,8-DHN pathway, L-DOPA pathway and tyrosine degradation pathway are summarized in Table 1.1.

Table 1.1: Genes involved in fungal melanin biosynthesis

Gene	Protein	Organism	Function	Reference
PKS/alb1 *PKS 12* and *PKS 13* *WdPKS1*	Polyketide Synthase	*A. fumigatus* *B. cinerea* *E. dermatitidis*	Production of 1,3,6,8-tetrahydroxynaphthalene (T4HN)	Gao *et al*. 2022 Schumacher *et al*. 2016 Paolo *et al*. 2006
Ayg1 *BRN1* and *BRN2*	Abhydrolase	*A. fumigatus* *M. laxa,* *M. fructicola,* *M. fructigena*	Reduction of 1,3,6,8 THN to scytalone	Gao *et al*. 2022 Verde-Yanez *et al*. 2023
arp1 *AISCD1* and *AISCD2* *SCD1*	Scytalone dehydratase	*A. fumigatus* *Ascochyta lentis* *M. laxa, M. laxa, M. fructicola, M. fructigena*	Reduction of scytalone to 1,3,8-THN	Gao *et al*. 2022 Debler and Henares 2020 Verde- Yáñez *et al*. 2023
arp2	Hydroxynaphthalene reductase	*A. fumigatus*	Reduction of 1,3,8-THN to vermelone	Gao *et al*. 2022
abr1	Vermelone dehydratase	*A. fumigatus*	Vermelone converted to 1,8-DHN	Gao *et al*. 2022 Upadhyay *et al*. 2013
abr2 *pbrB*	Oxydase	*A. fumigatus* *T. marneffei*	Polymerization of 1,8-DHN to DHN melanin	Gao *et al*. 2022 Upadhyay *et al*. 2013 Sapmak *et al*. 2015

Tat	Tyrosine aminotransferase	*A. fumigatus*	Converts tyrosine to 4-Hydroxyphenylpyruvate	Schmaler-Ripcke *et al*. 2009 Keller *et al*. 2011
hppD	4-hydroxyphenylpyruvate dioxygenase	*A. fumigatus* *A. niger*	Catalyzes precursor of pyomelanin, HGA	Schmaler-Ripcke *et al*. 2009 Koch *et al*. 2023
hmgA	Homogentisate dioxygenase	*A. fumigatus* *A. niger*	Degrades HGA to 4-Maleyl acetoacetate	Schmaler-Ripcke *et al*. 2009 Koch *et al*. 2023
fahA	Fumarylacetoacetate hydrolase	*A. fumigatus*	Degrades HGA to Fumarate	Heinekamp *et al*. 2013
maiA	Maleylacetoacetate isomerase	*A. fumigatus*	Degrades HGA to Acetoacetate	Heinekamp *et al*. 2013
melC2	Tyrosinase	*S. lincolnensis*	Oxidize L-DOPA to generate melanin	Endo *et al*. 2001

1.3.7 Benefits of melanin

Melanin provides various benefits to organisms that produce it. One key aspect that distinguishes melanin from other natural chromophores is its ability to absorb every wavelength of light (Riesz *et al*. 2006; Cordero *et al*. 2018). Melanin is not essential for the growth of fungi, but it does facilitate the ability to survive harmful conditions. The various benefits of melanin are reviewed in detail elsewhere (Cordero and Casadevall 2017; Suthar *et al*. 2023) and summarized in Table 1.2**.**

Table 1.2: Benefits of melanin in fungi

Benefits of Melanin in fungi	**Reference**
Protection from UV stress	Natarajan *et al*. 2014
Protection from various environmental stresses in fungi	Salgado-Castillo *et al*. 2023
Protection against microbes in fungi	Nosanchuk and Casadevall 2003
Protection against oxidative stress	Rosas and Casadevall 2006; Gorbushina *et al*. 2008; Kejžar *et al*. 2013; Cordero *et al*. 2018; Meredith and Sarna 2006
Protection against enzymatic lysis	Rosas and Casadevall 2001; Lin and Chen 2005
Protection against radiation	Gessler *et al*. 2014; Pacelli *et al*. 2017; El-Bialy 2019;
Provides structural support to the appressorium in plant pathogenic fungi	Belozerskaya *et al*. 2016; Chethana *et al*. 2021; Li *et al*. 2022

1.3.8 Applied uses of fungal melanin

For industrial use eumelanins are preferred over allomelanins, since allomelanins are attached to the inner side of the fungal cell wall making the extraction process more challenging (Mattoon *et al*. 2021). Over the years extraction protocols have been modified resulting in significant improvements in melanin yields. Examples include *Auricularia auricular*, where 10% of the biomass consisted of melanin following treatment with lytic enzymes, guanidinium thiocyanate, chloroform and HCL (Prados-Rosales *et al*. 2015), and *Armillaria cepistipes* in which a 99% yield increase (27.98 g/L) was obtained using simpler extraction procedures (Ribera *et al*. 2019). Besides extraction protocols, nutrient composition, temperature and pH have also been shown to play a part in melanin yield (Qin and Xia 2024). Recent studies have also examined the over expression of tyrosinase genes and its impact on melanin production (Tran-Ly *et al*. 2020; Mattoon *et al*. 2021).

Extracted melanin molecules possess a range of potentially useful applications (Table 1.3). For example, their ability to absorb and dissipate photons from ionizing radiation highlights the potential value of melanin as a sunscreen (Wolbarsht *et al*. 1981). It has been proposed that due to UV absorption and cytotoxic activities of melanin, they also have therapeutic potential in cancer patients during radiation and chemotherapy treatments (Table 1.3). With an increased consumer demand for natural ingredients in food, melanin has been considered as natural food coloring. Because the coloration of melanin can range from brown/black (i.e. eumelanin, allomelanin) to red/yellow (i.e. pheomelanin), these melanin molecules could be supplemented in food products as natural color agents instead of synthetic colors (Table 1.3) (Poorniammal *et al*. 2021; Yang *et al*. 2023). Various studies have also looked at the potential of melanin as industrial coatings for some packaging materials (Table 1.3).

Table 1.3: Potential uses of fungal melanin.

Species	**Applied use**	**Reference**
Agaricus bisporus	Protection from UV B	Olaizola *et al*. 2012
Agaricus bisporus	Packaging material	Łopusiewicz *et al*. 2018a
Agaricus bisporus	Antioxidant activity	Łopusiewicz *et al*. 2018b
Amorphotheca resinae	Absorption of both UV A And UV B	Oh *et al*. 2021
Aspergillus carbonarius	Potential yellow food coloring	Narendrababu and Shishupala 2017
Auricula auricila-judae	Protection from ionizing radiation	Revskaya *et al*. 2012
Auricularia auricular	Reduced oxidative stress in mouse liver	Hou *et al*. 2021
Blakeslea trispora	Potential source of β-carotene	Nabae *et al*. 2005
Cryptococcus antareticus	Survival and low mutation rate from space radiation	Onfori *et al*. 2020
Gliocephalotrichum simplex	Reduced oxidative stress in mouse liver	Kunwar *et al*. 2012
Monascus purpureus SM001	Red food coloring	Blanc *et al*. 1995
Penicillium aculeatum	Anticancer drug	Krishnamurthy *et al*. 2020
Penicillium europium	Pink food coloring	Khan *et al*. 2021
Talaromyces purpureogenus	Yellow food coloring	Pandit *et al*. 2020
Thermomyces sp	Food coloring and antioxidant	Poorniammal *et al*. 2021
Trichoderma viride	Brown color pigment	Chitale *et al*. 2012

1.3.9 Regulation of melanin synthesis

Although the biosynthetic pathways of melanin production are relatively well known in fungi, less is understood about the regulation of these pathways. However, increasing evidence suggests the PKA and HOG signaling pathways play a key role in the regulation of melanin production. The PKA-mediated cAMP signaling pathway is highly conserved among fungi and the regulation of factors involved in virulence via cAMP is quite common (Langfelder *et al*. 2003; Alspaugh 2015; Esher *et al*. 2018). A study by Alspaugh *et al*. (1997) identified the role of cAMP-dependent signaling pathway on melanin regulation in *C. neoformans*. A mutant strain with a defect in the GPA1 Gα-protein which showed reduced virulence and an inability to synthesize melanin could be partially complemented by addition of extracellular 3,5-cyclic adenosine monophosphate (cAMP) (Alspaugh *et al*. 1997;1998). This was followed by a study by D'Souza et al. (2001) where the deletion of *pkr1* and *pks1* (two genes encoding the regulatory and catalytic subunits of PKA, respectively) produced avirulent *C. neoformans* strains that lacked melanin production. Other studies highlight a relationship between cAMP signaling and melanin production in plant pathogenic fungi such as in *Ustilago hordei* where high levels of cAMP inhibited melanin formation (Lichter and Mills, 1998). Various studies have documented the relationship between the cAMP/PKA pathway and virulence in *C. neoformans* (reviewed by Caza and Kronstad (2019). In both *Magnaporthe oryzae* and *Colletotrichum lagenarium,* cAMP signaling is involved in appressoria formation which uses melanin to facilitate mechanical penetration of the host cell surface during infection (Adachi and Hamer 1998, Takano *et al*. 2001). Various studies have also confirmed the importance of cAMP/PKA signal transduction pathway and its involvement in the expression of genes involved in melanin biosynthesis (Brakhage and Liemann, 2005; Yu *et al*. 2017).

A link between glycolysis and melanin production mediated by cAMP/PKA activation in fungi has also been established by using mutant strains with defects in genes encoding phosphoglucose isomerase Pgil1 and trehalose synthesis (*TPS1* and *TPS2*) in both *C. neoformans* and *C. gattii* (Ngamskulrungroj *et al*. 2009; Zhang *et al*. 2015). These mutants had impaired cAMP/PKA activation with downstream effects on melanin production and the formation of the extracellular capsule (polysaccharide-based capsule). Further evidence of cAMP/pathway involvement was provided by Pukkila-Worley et al (2005), where *gpa1* mutants had a negative impact on melanin and capsule production in *C. neoformans* and *cac1* (adenylyl cyclase Cac1) mutants failed to produce melanin and capsules (Choi *et al*. 2015).

A study looking at transcription factors (TFs) in *C. neoformans* identified four melanin regulating TFs: *Bzp4*, *Usv101*, *Mbs1* and *Hob1* that are required for the induction of the laccase gene (*LAC1*) (Lee *et al*. 2019). The study found that the cAMP pathway is not involved in the regulation of these four TFs but the High Osmolarity Glycerol response (HOG) pathway has a negative impact on the induction of *BZP4* and *LAC1*. The study also focused on various protein kinases and identified Gsk3 and Kic1 deletion mutants as having a negative impact on LAC1 induction (Lee *et al*. 2019).

A recent study determined the effects of protein kinase A (PKA) on *Candida auris* melanization. By performing gene deletion experiments, it was observed that the catalytic subunits Tpk1 and Tpk2 of PKA are important for *C. auris* melanization whereas Ras1, Gpr1, Gpa2, and Cyr1 are not. Both *tpk1*Δ and *tpk2*Δ mutant strains formed melanin granules but these melanin granules failed to adhere to the cell wall (Kim and Bahn 2023). This study showed the importance of PKA catalytic subunits Tpk1 and Tpk2 in control of chitin synthesis related genes that are important for melanin granules to adhere to the cell wall. Since the melanin granules are

not strongly associated with the cell wall, *C. auris tpk1*Δ and *tpk2*Δ mutant strains were more susceptible to oxidative stress compared to the wildtype strain where both strains produced similar melanin (Kim and Bahn 2023).

In fungi mitogen-activated protein kinase (MAPK) signaling pathways play a critical role in many cellular processes including melanin biosynthesis by perceiving and responding to a variety of stresses or inputs (Gustin *et al*. 1998). Initial studies identified five MAPK pathways in *Saccharomyces cerevisiae* that were activated by different stimuli (Gustin *et al*. 1998; Saito 2010). Orthologs of these five MAPKs have also been determined to play critical roles in different fungi (Turrà *et al*. 2014). Membrane-spanning proteins such as Sho1, Msb2, Hkr1, Opy2, Sln1 and Ste2 are conserved in fungi and function as sensors that detect stimuli such as osmotic stress, oxidative stress, nutrients, cell wall defects, mating signals and developmental factors (Turrà *et al*. 2014; Kou and Naqvi 2016). In various fungi, the high osmolarity sensitive sensors (i.e. Sho1) activate the high osmolarity glycerol (HOG)-MAPK signalling pathway in response to osmotic stress. In *Verticillium dahliae* the mutant Δ*Sho1* strain showed a reduction in melanin accumulation and the expression of six genes involved in melanin synthesis was significantly affected in the Δ*Sho1* mutant strain (Li *et al*. 2019). Various studies have also confirmed the importance of cAMP/PKA signal transduction pathway and its involvement in the expression of genes involved in melanin biosynthesis (Brakhage and Liemann 2005; Yu *et al*. 2017).

Evidence of the HOG1 pathway negatively regulating synthesis of melanin was observed in a study conducted on *C. neoformans* by Bahn *et al*. (2005) that showed that the *hog1*ΔA mutant strain enhances capsule formation and had a significant increase in the production of melanin in the serotype A strain H99. To determine the impact of the HOG1 pathway and its

relationship with Pka1, it was observed that the deletion of *HOG1* gene resulted in restoring or in some instances enhancing the production of melanin in the serotype A *pka1*Δ mutants, suggesting that *HOG1* negatively modulates a downstream target of Pka1 in controlling melanin synthesis (Bahn *et al*. 2005). A follow up study by Bahn *et al*. (2007) demonstrated the effect of a single gene (*SSK2*) encoding an upstream MAPKKK element of Pbs2-Hog1 MAPK pathway. Ssk2 is known to activate the MAPKK pbs2 via phosphorylation. The *ssk2*Δ mutant strain had an enhanced production of capsules and melanin like the *hog1*Δ mutant indicating that Ssk2 functions as a key MAPKK controlling the Pbs2-Hog1 MAPK pathway in *C*. *neoformans* (Bahn *et al*. 2007).

1.3.10 Transcription factors (TFs) regulating fungal melanin production

Recent studies have focused on identifying the transcription factors (TFs) involved in the pathways that control melanin biosynthesis. These TFs can either work upstream or downstream of various fungal melanization pathways to influence expression of genes implicated in melanin production. Shelest (2017) identified 80 TF families in more than 200 fungal species using whole-genome annotation for TFs. Out of the 80 families of TFs, three (i.e. C6 Zn clusters, C2H2-like Zn fingers and Homeodomain-like TFs) were generally more prevalent. A previous study conducted by Tsuji *et al*. (2000) demonstrated the effect of the TFs Cmr1p and Pig1p in *C*. *lagenarium* and *M*. *oryzae* respectively. Both TFs contained C2H2 Zn finger and C6Zn cluster DNA binding motifs and deletion of the Zn cluster led to complete loss of melanin production whereas deletion of the C2H2 cluster led to reduced melanin production (Tsuji *et al*. 2000). The TFs involved in the melanization process tend to be conserved across fungi making them ideal targets to study the process of melanin production.

Cmr1 and its homologues are an example of a TF that is conserved in most melanin producing fungi. Specifically, it has been shown to regulate genes related to melanin biosynthesis by promoting the expression of the *PKS* gene clusters, thus impacting growth, development, stress response and virulence in various fungi such as *C*. *lagenarium*, *M*. *oryzae*, *Cochliobolus heterostrophus*, *Bipolaris oryzae* and *Alternaria alternata* (Tsuji *et al*. 2000; Eliahu *et al*. 2007; Kihara *et al*. 2008; Cho *et al*. 2012; Li *et al*. 2022). In some fungi the *PKS* gene and the *CMR1* gene show phylogenetic patterns suggesting they are subjected to co-evolution (Jia *et al*. 2021). Evidence of co-evolution (or functional dependency) of the *PKS* and *CMR1* genes has been provided by various knockout studies. In *Alternaria brassicicola* the Δ*amr1* (homologue of cmr1) mutants created melanin deficient colonies that were more sensitive to UV light (Cho *et al*. 2012). In *V*. *dahliae* both *VdCmr1* and *VdPKS1* were necessary for melanin production and the Δ*VdCmr1* strain, had a 50% reduction in survival when exposed to UV irradiation or high temperatures (40°C) (Wang *et al*. 2018). In *Botrytis cinerea*, Bcsmr1 is involved in the regulation of genes involved in melanogenesis and deletion of *bscmr1* led to defects in sclerotial melanogenesis and increase in expression of *bscmr1* led to accumulation of melanin (Zhou *et al*. 2017; Schumacher 2016). In *Setosphaeria turcica* deletion of the StMR1 a homologue of CMR1 led to production of lighter colonies and qPCR analyses confirmed that deletion mutants had significantly decreased expression of six key genes involved in the 1,8-DHN melanin synthesis pathway (Zhang *et al*. 2022). Another study identified two TFs, Pmr1 (homologue of Cmr1) and Pmr2 that regulate melanin biosynthesis, conidia development and secondary metabolism in *Pestalotiopsis microspora* by Zhou *et al*. (2022). Deletion mutant Δ*pmr1* showed defects in conidial pigmentation and the mutant Δ*pmr2* had decreased conidial pigmentation (Zhou *et al*. 2022). In *A*. *alternana* TF *AacmrA* homologue of cmr1 is required for

melanin biosynthesis and pathogenicity. Work on mutant strains Δ*AacmrA* showed severely decreased melanin production and the mutant strains were more sensitive to oxidative stress and cell wall inhibitors compared to the wildtype strain (Fetzner *et al*. 2014; Li *et al*. 2022). These studies provided evidence of potential co-evolution of TF Cmr1 and its homologues in various fungi and its involvement in fungal melanization and their effect on PKS.

Besides Cmr1 various other TFs have been identified that play a key role in melanin biosynthesis some of which are described below. Two genes encoding bHLH (*DevR*) and MADS-box (*Rlm*A) TFs, were identified in *A*. *fumigatus* located upstream of the melanin gene cluster acting as both a repressor and activators of the *pksP* promoter region to modulate the production of conidial melanin (Valiante *et al*. 2016). Another study identified two TFs genes, *PfmaH* and *PfmaF* that are part of the 1,8-DHN melanin biosynthetic gene cluster (*Pfma*) in *Pestalotiopsis fici* (Zhang *et al*. 2019). These studies showed that deleting the *PfmaF* did not affect melanin production but over expression of *PfmaF* lead to heavy pigment accumulation in *P*. *fici* hyphae (Zhang *et al*. 2019). In *V*. *dahliae* the TF VdMRTF1 is a bZip (Basic Leucine Zipper Domain) transcription factor that negatively regulates melanin biosynthesis (Lai *et al*. 2022). Transcriptomic analysis showed that VdMRTF1 regulates expression of genes associated with melanin biosynthesis, tyrosine metabolism, and oxidative activity in *V*. *dahliae* (Lai *et al*. 2022). Besides BcSMR1, two other TFs: BcZTF1 and BcZTF2 are involved in regulation of genes involved in melanogenesis in *B*. *cinerea* (Schumacher 2016). Over expression of *bcztf1* and *bcztf2* led to accumulation of pigmentation in young mycelia and the deletion mutants Δ*bcztf1* and Δ*bcztf2* led to colonies appearing white (Schumacher 2016).

In *C*. *neoformans* a GATA-type zinc finger TF (Cir1) which is involved in cAMP/PKA pathway regulation also showed involvement in melanin and capsule formation (Jung *et al*.

2006). In another study Cir1 was shown to regulate two genes involved in the HOG pathway which is involved in capsule regulation (Haynes *et al*. 2011). Laccases have been shown to play a key role in both 1,8-DHN and L-DOPA melanin (Upadhyay *et al*. 2013). Another study that demonstrated both the effects of TFs and MAPks was performed on *C*. *heterostrophus*. In this study it was found that two mitogen activated protein kinases (Chk1 and Mps1) were important for normal melanin production (Eliahu *et al*. 2007). Mutant strains Δ*chk* and Δ*mps1* both produced white colonies and showed an autolytic appearance. Besides Δ*chk* and Δ*mps1*, deletion of the CMR1 TFs also resulted in albino mutants and the acquisition of orange-pink coloration indicating the presence of other carotenoids or secondary metabolites besides melanin in *C*. *heterostrophus* (Eliahu *et al*. 2007). Table 1.4 summarizes various TFs in fungi and the impact on fungal melanization.

Table 1.4: Transcription factors (TFs) involved in melanin biosynthesis in various melanized fungi.

Transcription factor (TFs)	**Impact**	**Type of melanin**	**Species**	**Reference**
DevR RlmA	Production of conidial melanin	1,8-DHN	*A. fumigatus*	Valiante *et al*. 2016
Cmr1/PIG1/BMR1/Amr1 /CmMR1	Regulate melanin biosynthesis	1,8-DHN	*C. lagenarium*	Eliahu *et al*. 2007
		1,8-DHN	*M. oryzae*	Tsuji *et al*. 2000
		1,8-DHN	*B. oryzae*	Kihara *et al*. 2008
		1,8-DHN	*A. brassicicola*	Cho *et al*. 2012
		1,8-DHN	*C. minitans*	Luo *et al*. 2018
PfmaF	Overexpression leads to pigment accumulation	1,8-DHN	*P. fici*	Zhang *et al*. 2019
Pmr1 and Pmr2	Melanin biosynthesis/ conidia development	1,8-DHN	*P. microspora*	Zhou *et al*. 2022
AacmrA	Melanin production	1,8-DHN	*A. alternana*	Li *et al*. 2022
VdCmr1	Melanin biosynthesis/ pigment production	1,8-DHN	*V. dahliae*	Wang *et al*. 2018
VdMRTF1	Negative melanin regulation	1,8-DHN	*V. dahliae*	Lai *et al*. 2022
mtf1 and mtf2	Upregulation of PKSs genes	1,8-DHN	*U. maydis*	Reyes-Fernandez 2019

BcSMR1, BcZTF1 and BcZTF2	Regulation of gene involved in melanogenesis	1,8-DHN	*B. cinerea*	Schumacher 2016
Bzp4, Usv101, Mbs1 and Hob1	Induction of laccase gene (*LAC1*)	L-DOPA	*C. neoformans*	Lee *et al*. 2019
Cir1	Melanin deposition in the cell wall	L-DOPA	*C. neoformans*	Jung *et al*. 2006
VdZFP1 and VdZFP2	Involved in melanin deposition	1,8-DHN	*V. dahliae*	Li *et al*. 2023
Vta1/ VdpF	Involved in melanized microsclerotia development	1,8-DHN	*V. dahliae*	Harting *et al*. 2020

CHAPTER 2: Genetic analysis of pigment production in the fungus *Exophiala dermatitidis* mutant strains obtained via nontargeted UV mutagenesis

Published in G3. Genes| Genomes| Genetics (G3-2025-406059)

Chhoker K, Hausner G, Harris D. 2025. Genetic analysis of pigment production in the fungus *Exophiala dermatitidis* mutant strains obtained via nontargeted UV mutagenesis. *G3*(*Bethesda*). Sep 3: jkaf205. doi: 10.1093/g3journal/jkaf205.

Has also been submitted to bioRxiv

Chhoker K, Hausner G, Harris D. 2025. Genetic analysis of pigment production in the fungus *Exophiala dermatitidis* mutant strains obtained via nontargeted UV mutagenesis. *bioRxiv* 2025.03.19.644242. doi: https://doi.org/10.1101/2025.03.19.644242.

2.1 Abstract

Exophiala dermatitidis is a polyextremotolerant black yeast species. *E. dermatitidis* produces 1,8 dihydroxynaphthalene (DHN) melanin via the Polyketide Synthase 1 (*PKS1*) pathway enabling it to survive harmful conditions. This study focused on random nontargeted mutagenesis to obtain albino (*alb*) and hyper-pigmented (*hyp*) mutants. Notably, all 17 *alb* mutants possessed mutations in *PKS1* whereas the 113 hyper-pigmented (*hyp)* mutants harbored mutations impacting a range of functions. Cell morphology and phenotypic assays showed additional differences between the *alb* and *hyp* mutants. Strikingly, three of the albino mutants (*alb1*, *alb2*, and *alb3*) were conditional in that despite the presence of mutations in *PKS1* they were able to produce melanin upon exposure to different carbon sources. These mutants otherwise shared similar cell morphology and growth patterns with the obligate albinos. No additional shared mutations were found among the conditional albinos. Temperature and UV irradiation assays demonstrated reduced growth of albino mutants at higher temperatures (i.e., 42°C) and a greater sensitivity to higher doses of UV. Single nucleotide variant (SNVs) calling showed that some hyperpigmented mutants had a greater number of SNVs compared to albino strains. To date this is the first study to generate and characterize conditional albino mutants in *E. dermatitidis* with the ability to recover melanin production.

2.2 Introduction

Black yeasts, which are sometimes referred to as dematiaceous fungi, are a group of fungi that have black-brown appearance due to the association of melanin with their cell walls (Kejžar *et al.* 2013; Selbmann *et al.* 2015). Many species of black yeasts have been found growing in toxic niches, nutrient poor conditions and manmade environments (Onofri *et al.* 2008; Coleine *et al.* 2022; Gostinčar *et al.* 2012; 2023; Medina-Armijo *et al.* 2024). Another key aspect of black yeasts is morphological plasticity which refers to their ability to switch morphology thereby

enabling some of them to be opportunistic pathogens of both warm- and cold-blooded vertebrates (Slepecky and Starmer 2009; de Hoog 2014). Black yeasts can shift from single-celled yeasts to multicellular filamentous forms (Butin *et al.* 1996; Butler and Day 1998). This switch in their growth forms increases the surface/volume ratio of the fungi allowing them to absorb and transport more nutrients through the cell membrane when growing in nutrient poor habitats (Sterflinger *et al.* 1995; Zalar *et al.* 1999). *Exophiala dermatitidis* (also referred to as *Wangiella dermatitidis*; see Chen *et al*. 2014) is one such opportunistic black yeast found growing in soil, toxic and arid niches as well as in nutrient poor man-made environments ranging from steam baths, railway ties and dishwashers (Hamada and Abe 2009; Döğen *et al.* 2013; Zupančič *et al.* 2016). Emergence of *E. dermatitidis* as an opportunistic pathogen has been reported in immunocompromised patients where it is able to cause phaeohyphomycosis, chromoblastomycosis and fatal infections of central nervous system. Notably, the ability of *E. dermatitidis* to switch its morphology from yeast- like to a multicellular hyphal form at 37°C enables it to survive and adapt to the mammalian host (de Hoog 2014; Olsowski *et al.* 2018; Vasquez *et al.* 2018; Wang *et al.* 2019; Beniwal *et al.* 2023).

In general, melanization of the cell wall and the ability of some black yeasts to switch their growth form are two key adaptations that allow them to cope with stressful environmental conditions (Gorbushina 2007). Melanin is typically found in the outer regions of the cell wall in most species but in some cases can be found aggregated to the cell wall surface (Bayry *et al.* 2014). Fungal melanin provides various benefits to black yeasts such as protection against oxidative stress (Cordero *et al.* 2017), radiation (Dadachova *et al.* 2007), UV and hyperosmotic stress (Wollenzien *et el*. 1995; Kogez *et el*. 2007).

E. dermatitidis produces 1,8-Dihydroxynaphthalene (DHN) melanin, which has been shown to provide protection from oxidative stress, enzymatic lysis and phagocytosis during infection (Pihet 2009; Kurbessoian *et al.* 2023). The starting precursors for the synthesis of 1,8-DHN melanin can either be acetyl-CoA or malonyl-CoA which are produced endogenously (Nosanchuk *et al*. 2015). Besides 1,8-DHN melanin, genome annotation has revealed that *E. dermatitidis* also possesses the capacity to produce L-dihydroxyphenylalanine (L-DOPA) melanin and pyomelanin via the L-tyrosine degradation pathway (Chen *et al.* 2014; Poyntner *et al*. 2018; Carr *et al*. 2023). In brief the biosynthesis of DOPA melanin begins with tyrosine, which is oxidized by oxygen followed by tyrosinase that forms levodopa and then dopaquinone (Simon and Peles 2010; Cao *et al*. 2021). In the DOPA melanin pathway, hydroxylation of L-tyrosine to dopaquinone or the oxidation of L-DOPA to dopaquinone is catalyzed by tyrosinase or laccase respectively (Pomerantz and Warner 1967). Pyomelanins are derived from the oxidative polymerization of nitrogen-free precursors such as homogentisic acid (HGA) (Funa *et al*. 2005; Seo and Choi 2020). Pyomelanin originates from the catabolism of either tyrosine or phenylalanine. Nevertheless, the specific roles of these alternate types of melanin relative to that of 1,8-DHN melanin remain unknown. Notably, targeted mutagenesis of the *E. dermatitidis PKS1* gene is sufficient to generate albino mutants (Feng *et al.* 2001; Poyntner *et al.* 2018; Malo *et al.* 2021). This implies that the other melanin pathways might not provide any contribution to melanin production. Alternatively, the targeted nature of the prior mutagenic approaches might simply have precluded the identification of mutations affecting the alternate pathways. Accordingly, the objective of this study was to combine conventional random mutagenesis with whole genome sequencing to determine the spectrum of mutations that underlie both albino (*alb*) and hyperpigmented (*hyp*) phenotypes. Besides identifying genes that in addition to *PKS1* can

trigger an albino phenotype when mutated, the screen was also expected to provide insight into the regulatory mechanism that control melanin production in *E. dermatitidis*.

2.3 Materials and methods

2.3.1 Media and strains

Media used in this study include Yeast extract peptone dextrose (YPD): (10g yeast extract, 20g peptone, 20g dextrose and 20g agar per 1L), Yeast extract peptone galactose (YPG): (10g yeast extract, 20g peptone, 20g galactose and 20g agar per 1L), Malt extract agar (MEA): (20g malt extract, 2g peptone, 10g dextrose and 20g agar per 1L) and Minimal media (MN): (10g dextrose, 50ml 20x nitrate salts* and 1ml Hutner's TE** per 1L) * 20x Nitrate salts (1L: 120g NaNo3, 104g KCL, 10.4g MGSO4-7H2O, 30.4g KH2PO4. **Hutner's TE (100ml: 2.2g ZNSO4-7H20, 1.1g H2BO3, 0.5g MnCl2-4H20, 0.5g FeSO4-7H2O, 0.17g CoCl2-6H2O, 0.16g CuSO4-5H2O, 0.15g Na2MoO4-2H2O, 5g EDTA (Disodium salt).

The *E. dermatitidis* reference strain UT8656 (=ATCC 34100, =*Exophiala dermatitidis* CBS 525.76) was treated as the wildtype strain as described in (Chen *et al.* 2014). This strain was used for mutagenesis to obtain pigmentation mutant strains. For long term storage, the wildtype strain and the mutant strains (*alb* and *hyp*) obtained via UV mutagenesis were kept in 30% glycerol at -80°C.

2.3.2 UV mutagenesis

An unbiased forward genetic approach was employed to screen for *E. dermatitidis* mutants with altered pigmentation phenotypes ranging from complete loss of pigment to hyperpigmentation. Briefly, wildtype strain UT8656 was initially plated on YPD (Supplemental Figure S1). Four to five discrete colonies were isolated from the plates and combined into 1ml microcentrifuge tubes (Fisher Scientific, Nepean, ON, Canada) containing autoclaved sterile

distilled water. Diluted 250µl mixtures were plated onto YPD and subjected to UV mutagenesis (UVB) using a Stratagene Stratalinker UV1800 crosslinker (Marshall Scientific, Hampton, NH, United States) at setting Energy 1000 x 100µW/cm^2. The plates were removed, immediately wrapped in tinfoil to limit photoreactivation, and placed in an incubator at 28°C. After two days the plates were unwrapped and returned to the incubator. Growth was monitored and mutant colonies started to appear after about seven days at 28°C. After seven to ten days colonies were examined for color and morphology. The *E. dermatitidis* wildtype strain appears brown on YPD so any colonies that appeared white (*alb*) or black (*hyp*) were selected. One hundred YPD plates were subjected to random mutagenesis to obtain *E. dermatitidis* mutant strains. Mutant colonies that appeared fuzzy or crusty were also picked. The main difference between fuzzy and crusty was attributed to the presence of aerial hyphae in the fuzzy mutants whereas crusty mutants lacked aerial hyphae. Fuzzy mutants were easier to scrape off from the medium whereas crusty mutants tend to be invasive and embedded in the medium. Mutant isolates were sub-cultured on YPD plates to verify the selected phenotype and to generate material for subsequent phenotypic testing.

2.3.3 Study of cell morphology

To observe morphological phenotypes, wildtype and mutant isolates stocks were cultured onto YPD plates. Once the strains had grown, single colonies were picked and mounted in sterile water on glass slides for observation using an EVOS M5000 (Fischer Scientific) desktop microscope. Cell imaging software (FL Auto 2 Cell Imaging software) was used according to the manufacturer's guidelines to count the following cell types: unbudded yeast cells, budded yeast cells, chains, pseudohyphae, and hyphae (Figure 2.1). Manual counting was performed because small cell sizes resulted in discrepancies in the automated cell counts. For each strain three

replicates were examined, and photographs of the slides were taken using the built-in camera of EVOS M5000 (Supplemental Figure S5). Two hundred cells were counted from each photograph and the final cell count was based on the average number of different cells observed in the three replicates.

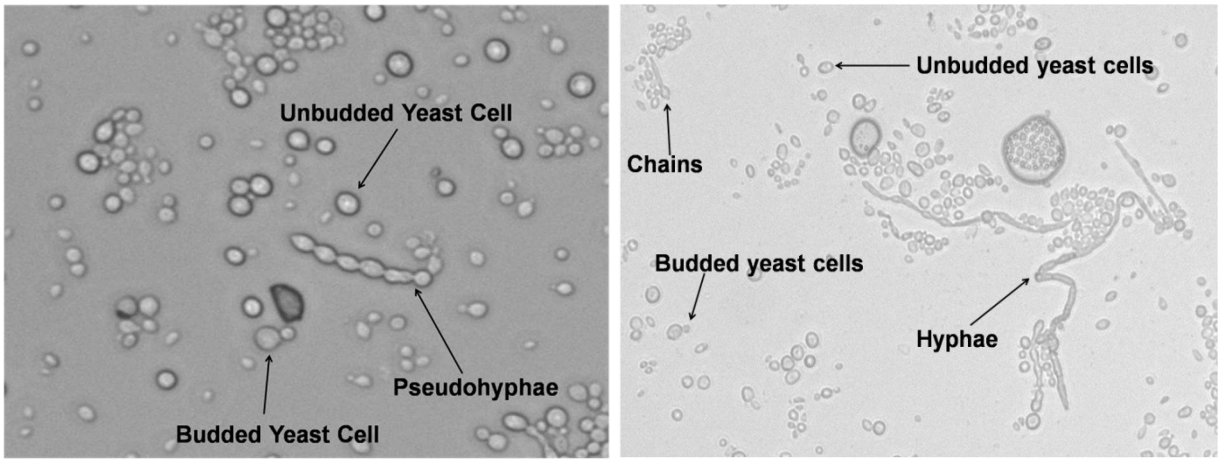

Figure 2.1: Different cell types observed in *E. dermatitidis* mutant strains (unbudded yeast cells, budded yeast cells, chains, pseudohyphae, and hyphae). Figure S2.5 represents additional examples of images obtained using an EVOS M5000 desktop microscope.

2.3.4 UV resistance and temperature assays:

Mutants were subjected to different phenotypic assays including UV tolerance as well as responses to different growth temperatures and media types. Briefly, *E. dermatitidis* mutants were plated onto YPD and left to grow at 28°C. Isolated colonies were suspended in sterile distilled water and diluted ten-fold. A semi-quantitative spot dilution method was used to observe the growth of the mutants in each assay (Supplemental Figure S2). For the temperature assay, four different temperatures were initially selected: 4°C, 10°C, 28°C and 42°C. No visible growth was observed at 4°C even after 3 months so only the other three temperature assays were recorded. For UV resistance, spot plates were subjected to six different treatments: no UV (control), 500, 750, 1000, 1250 and 1500 Energy 1000 x 100µW/cm^2. Growth was recorded after two weeks of incubation and again after an additional three weeks. Growth was scored on a scale of 1-7 where 1 indicated complete inhibition/no growth and 7 indicated no inhibition (Supplemental Figure S3).

2.3.5 Carbon source utilization

ID 32 C-strips (Mediray) were used to test the effect of different carbon sources on the growth and pigmentation of each mutant. For this analysis, wildtype and all 17 albino mutants were plated onto YPD and inoculated on the ID 32 C-strips following the manufacturer's protocol. Briefly, for each sample, several discrete colonies were picked and added to the provided ampule of API® Suspension Medium (2 ml). 250 µl of the suspension from the ampule AP1 was then added to the ampule of API C medium provided. Ampule API C was then homogenized and 135µl was added to each of the 32 wells of the ID32 C-strip. Once all the wells had been filled, the lid was placed on each strip, and they were incubated in a closed container. During the duration of the experiment paper towels dampened with autoclaved distilled water

were used to prevent desiccation of the strips. The containers were left at room temperature and photographed two weeks and four weeks after the start of the experiment. Two replicates were performed for the wildtype and for each of the 17 *alb* mutants.

2.3.6 DNA extraction

Whole cell DNA from *E. dermatitidis* wildtype and mutant strains was extracted using the DNeasy® PowerSoil® Pro Kit (Qiagen) following the manufacturer's protocol. Strains were initially plated on YPD. In total 51 mutant strains were picked which included the wildtype control, all 17 *alb* mutants, and 33 *hyp* mutants. The *hyp* mutants were picked based on cell morphology data such that the collection of mutants exhibited the greatest diversity of cell type morphologies. Other criteria taken into consideration were the results of the UV and temperature assays. The *hyp* mutants picked represented different growth and inhibition profiles for these phenotypic assays. DNA concentrations were determined using a NanoDrop 2000/2000c Spectrophotometer (Fisher Scientific). The samples were stored at -80°C for further downstream analysis.

2.3.7 Genome sequencing

Extracted whole cell DNAs from *E. dermatitidis* strains were shipped for sequencing to the Microbial Genome Sequencing Center (Pittsburgh, USA) or SeqCoast, LLC (Portsmouth, USA) with both vendors using the Illumina platform. The variant caller breseq (current version 0.35.4) was employed by each vendor to align and compare the sequencing data to the *E. dermatitidis* UT8656 reference genome (NCBI RefSeq Assembly GCF_000230625.1). *breseq* is a computational pipeline that employs NGS sequence reads in FASTQ format and aligns them to the reference genome sequence files in GenBank, GFF3 or Fasta format (Barrick *et al.* 2014, Deathrage and Barrick *et al.* 2014). The resulting dataset provided single nucleotide variants

(SNVs) that facilitated identification of the mutations potentially responsible for loss of melanin production and determining the degree of similarity between the mutations observed in the *alb* and *hyp* classes of mutants.

For each sample a summary statistic file is provided on the number of reads and their alignment rate to the reference genome (Supplemental Figure S4a). Percentages above >90% are favorable and anything below indicates low quality sequencing data due to poorly constructed DNA fragment libraries. *breseq* utilized three types of information to predict mutations: read alignment (RA), missing coverage (MC) and new junction (JC) evidence. For this dataset, RA evidence provided evidence to support mutations resulting in single nucleotide substitutions and deletions that are shorter than the read length. The index.html file obtained from the analysis displayed the "Mutation predictions" page that contained tables listing differences (SNVs) found in the samples and the reference genome. The SNVs were identified based on the RA evidence and the annotation found in the index.html file. The file also provided information regarding the gene and the description based on the reference genome (Supplemental Figure S4b). For each sample all the SNVs with RA evidence and annotations were pulled out and compiled in a single file (Supplemental File 1). The SNVs were prioritized based on the type of mutations. Small deletions or substitutions (coding) that shifted the reading frame and nonsense mutations were classified as high priority; non-synonymous missense mutations were classified as medium priority and synonymous missense mutations and mutations that resulted in no amino acid change were classified as low priority. The gene description was then taken into account to identify mutations that occurred in genes known to be involved in melanin production in black yeasts. Other genes known to be involved in cell morphology were also given priority. To confirm the geneID description obtained in the index.html files, all genes with mutations were

blasted in NCBI BLAST database to confirm their description and to identify if any new annotations for the hypothetical proteins have been added to the NCBI database for *E. dermatitidis*. The last part of the genome sequencing analysis involved searching for any shared mutations that occurred in all mutants (both *alb* and *hyp*), *alb* mutants only and *hyp* mutants only to see if any significant patterns can be observed between the mutant strains.

2.3.8 Pks1 structure and representation of mutated *PKS1* sites

To determine if there was a trend that appeared between the conditional *alb* and obligate *alb* mutants, *PKS1* SNVs were obtained from the genome sequences for all 17 *alb* mutants representing the two types (conditional and obligate) mutant strains. Domains and location of Pks1 in *E. dermatitidis* were determined using antiSMASH fungal version 7 (Blin *et al.* 2023) software and the *PKS1* sequences from each *alb* strains and the wildtype control. Based on the position, the *PKS1* sequence from the different *alb* strains aligned to different domains of the reference Pks1.

2.4 Results

2.4.1 Mutant Identification

Previous attempts to understand the genetic basis of pigment production in polyextremotolerant fungi have relied upon targeted mutagenesis of specific genes with predicted roles in the production of melanin or carotenoids. A limitation of this approach is its underlying bias towards known genes. We propose that a systematic unbiased screen offers the potential to identify any mutable gene with a role in pigment production. Although *E. dermatitidis* is not considered as routinely genetically tractable, the use of genome re-sequencing and variant calling makes it possible to provide some insight into the genetic basis of the recovered mutant phenotypes. Accordingly, UV mutagenesis was employed to recover 130

mutants with pigmentation defects that were selected for further analysis. Out of the 130 mutants that were isolated, 17 were classified as albino (*alb*) mutants and 113 as hyperpigmented (*hyp*) mutants (Figure 2.2a). *hyp* mutants were further subdivided into three subcategories; (i), those that exist primarily in the yeast form, which made up the vast majority of the *hyp* mutants (97), (ii), hyperpigmented (Fuzzy) mutants (12), and (iii), hyperpigmented (Crusty) mutants (4) (Figure 2.2b).

(a)

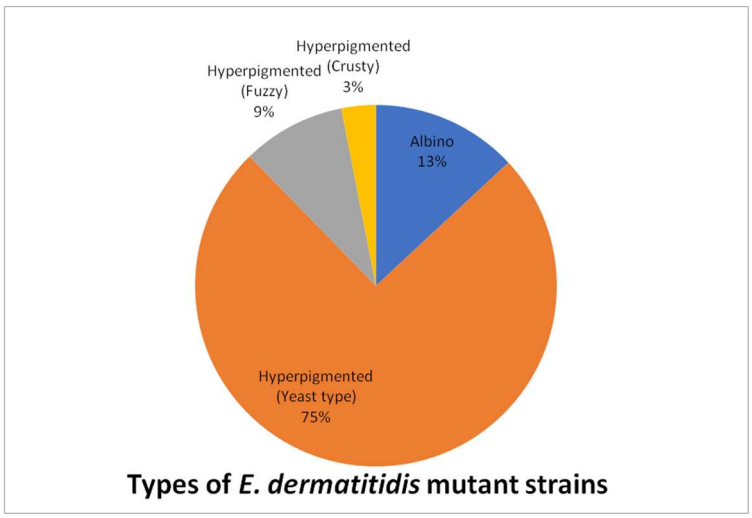

(b)

Wildtype *alb* *hyp*

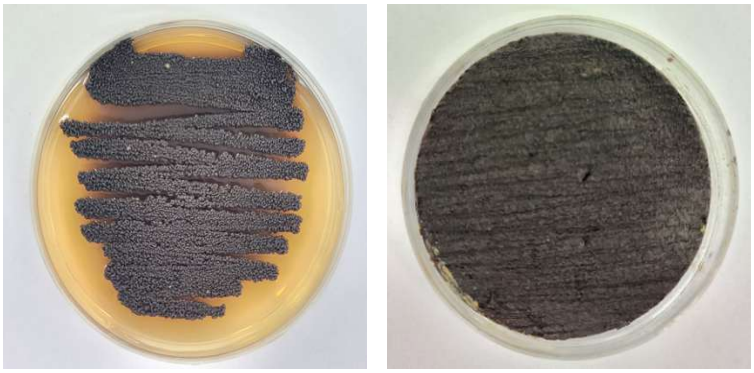

hyperpigmented (Fuzzy) hyperpigmented (Crusty)

Figure 2.2: (a) Breakdown of the 130 mutants based on phenotypes obtained using random UV mutagenesis on wildtype *E. dermatitidis* reference strain UT8656. (b) Images representing the wildtype and mutant *E. dermatitidis* mutant strains obtained in this study: *alb*, *hyp*, hyperpigmented (Fuzzy) and hyperpigmented (Crusty).

2.4.2 Cell and colony morphology

All the *alb* mutants had a yeast-like appearance that included the presence of both budded and unbudded cells (Figure 2.3a). The morphology of the *hyp* mutants varied, 50 possessed either unbudded or budded yeast cells, 13 exhibited three different cell types (unbudded yeast cells, budded yeast cells and chains), 24 showed four different cell types (unbudded yeast cells, budded yeast cells, chains and pseudohyphae) and 21 showed all five cell types (unbudded yeast cells, budded yeast cells, chains, pseudohyphae and hyphae) (Figure 2.3b) (Supplemental Figure S5). There were three hyperpigmented mutants with three cell types that did not contain chains but pseudohyphae instead (unbudded yeast cells, budded yeast cells, and pseudohyphae) (Figure 2.3b). Figure 2.3b only shows cell counts for a subset of *hyp* mutants (strains which were part of the SNV analysis), Supplemental Figure S6 shows the cell count morphology for the remaining *hyp* mutants.

a)

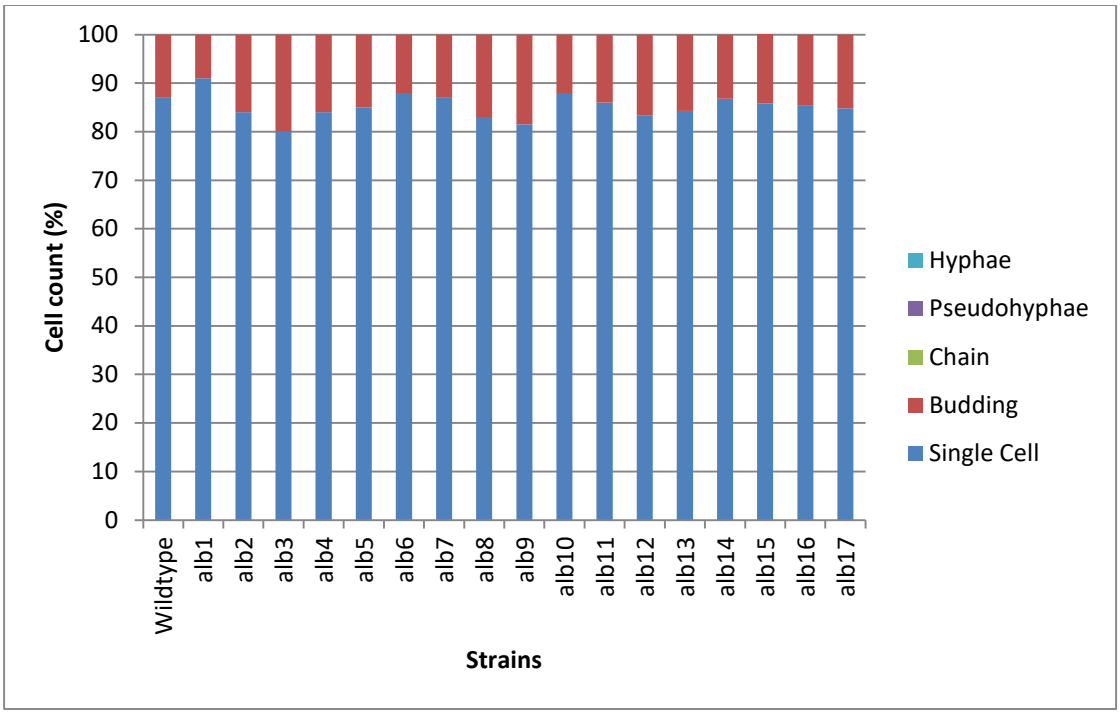

b)

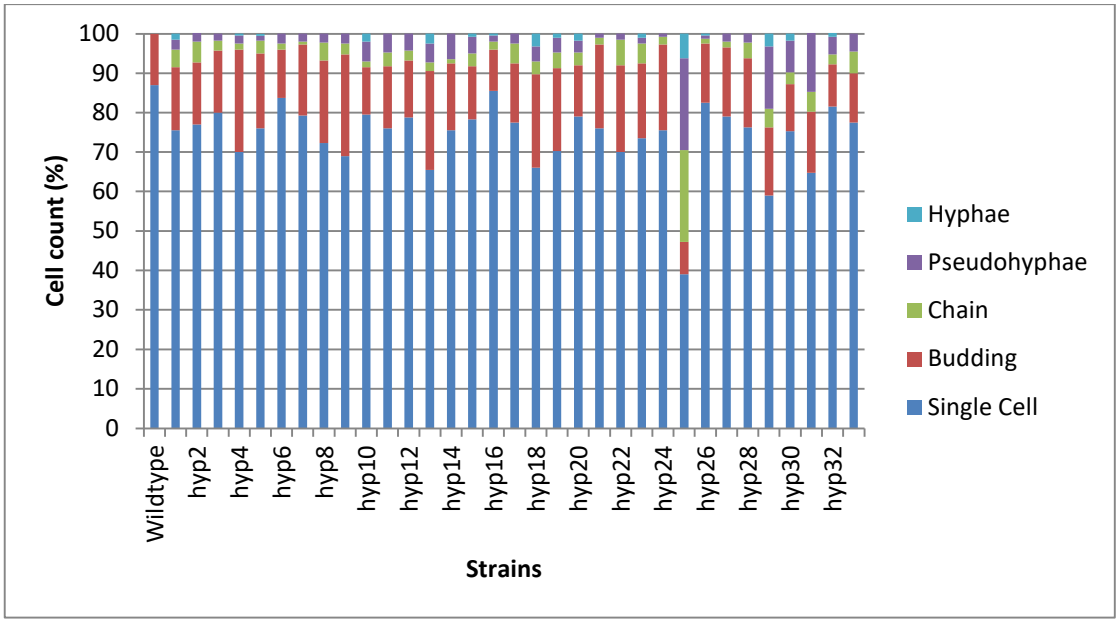

Figure 2.3: (a) Counts of different cell morphologies of *E. dermatitidis alb* mutant strains. (b) Counts of different cell morphologies of a subset of *hyp* mutant strains that were selected for genome sequencing (SNV analysis). Colors that define the type of observed cell morphologies as shown on the right. Cell count (%) on y-axis and strains on x-axis. Cell count of the remaining *hyp* mutants that were not selected for SNV analysis are shown in Supplemental data: Figure S2.6.

2.4.3 UV resistance and temperature sensitivity

Compared to wildtype, the *alb* mutants generally displayed moderate growth reduction at higher UV intensities (Supplemental Figure S3) when grown on YPD (Figure 2.4a) or MN (Figure 2.4b) plates. The only exceptions were, *alb1*, which showed similar growth to the wildtype on YPD and *alb2* which showed similar growth to the wildtype on MN. The *hyp* mutants exhibited a range of responses to UV irradiation when incubated on YPD and MN (Supplemental Figure S7a and S7b). Whereas some showed dose-dependent sensitivity similar to that of the *alb* mutants, others were indistinguishable from the wildtype. In relation to the media type, the overall trend showed better growth for all mutants on YPD compared to MN during the UV assays.

Profiling of growth at different temperatures revealed that the *alb* and *hyp* mutants displayed levels of growth comparable to wildtype controls when grown at 10°C or 28°C (Supplemental File 2). At 42°C, some reduction in growth of the *alb* mutants was observed at all dilutions with complete inhibition at the 1:1000 dilutions. Conversely, most of the *hyp* mutants were able to grow with little inhibition at 1:1, 1:10 and 1:100 dilutions with some reduction observed only at 1:1000 dilutions (Figure 2.5).


Strain
Control
500
750
1000
1250
1500
Wildtype
alb1
alb2
alb3
alb4
alb5
alb6
alb7
alb8
alb9
alb10
alb11
alb12
alb13
alb14
alb15
alb16
alb17
hyp1
hyp2
hyp3
hyp4
hyp5
7 6 5 4 3 2 1 0

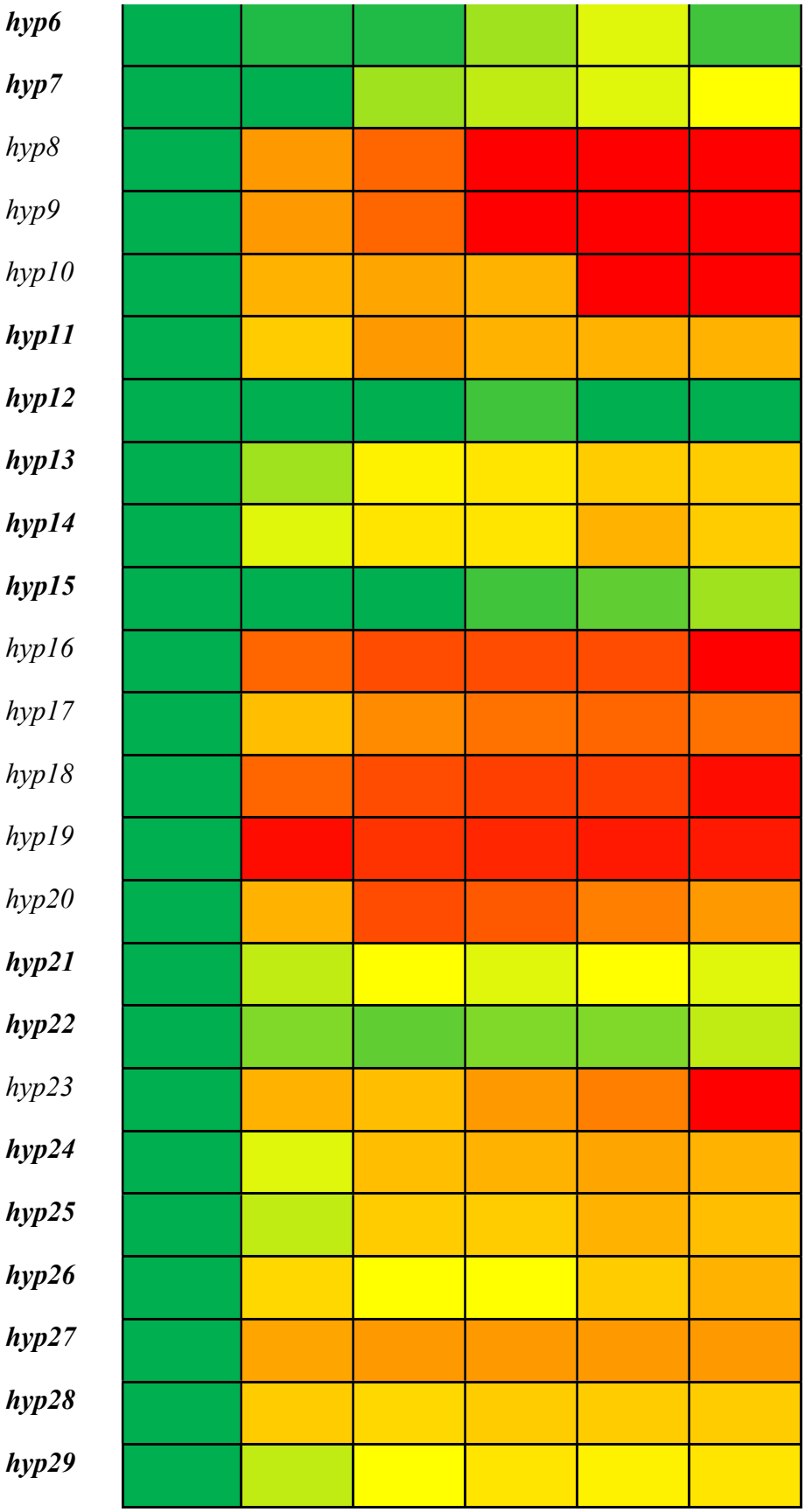
hyp6
hyp7
hyp8
hyp9
hyp10
hyp11
hyp12
hyp13
hyp14
hyp15
hyp16
hyp17
hyp18
hyp19
hyp20
hyp21
hyp22
hyp23
hyp24
hyp25
hyp26
hyp27
hyp28
hyp29

Figure 2.4a: Growth observed for *E. dermatitidis* wildtype, *alb* and subset of *hyp* strains (1:100 dilution) on YPD media at different UV intensities (control (no UV), 500, 750, 1000, 1250 and 1500 Energy 1000 x 100µW/cm^2). Colors of the heatmap represent the scores obtained by visualizing the type of growth observed for each spot and comparing them to growth patterns as indicated in Supplemental Figure S3. Mutant strains that had similar or lower UV intensity at each dose than the wildtype are in bold. Data for remaining *hyp* mutants for 1:100 dilution in Supplemental Figure S2.7a and data for 1:1, 1:10 and 1:1000 dilutions for all mutants in Supplemental File 2.


Strain
Control
500
750
1000
1250
1500
7 6 5 4 3 2 1 0
Wildtype
alb1
alb2
alb3
alb4
alb5
alb6
alb7
alb8
alb9
alb10
alb11
alb12
alb13
alb14
alb15
alb16
alb17
hyp1
hyp2
hyp3
hyp4
hyp5

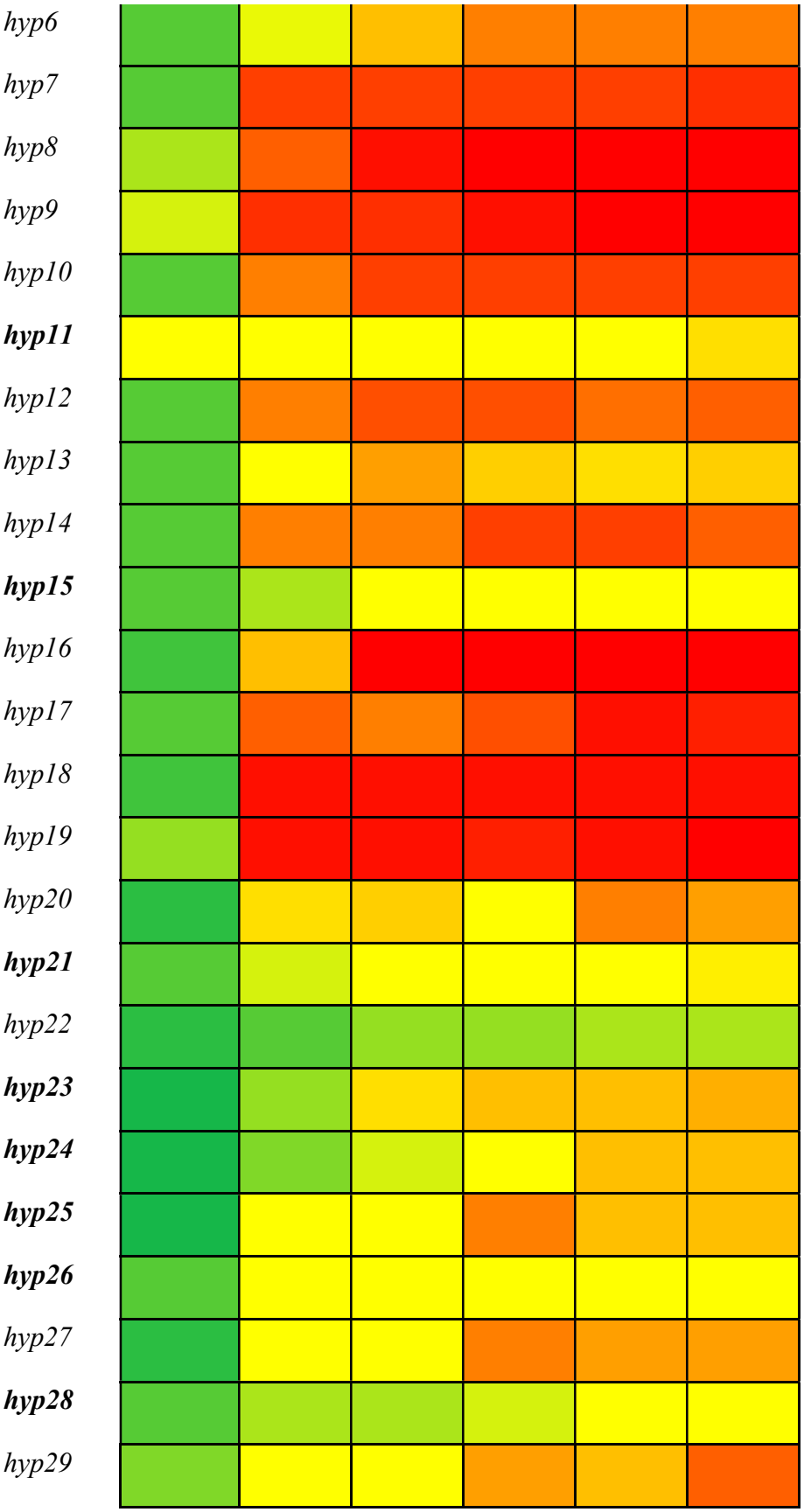
hyp6
hyp7
hyp8
hyp9
hyp10
hyp11
hyp12
hyp13
hyp14
hyp15
hyp16
hyp17
hyp18
hyp19
hyp20
hyp21
hyp22
hyp23
hyp24
hyp25
hyp26
hyp27
hyp28
hyp29

Figure 2.4b: Growth observed for *E. dermatitidis* wildtype, *alb* and subset of *hyp* strains (1:100 dilution) on MN media at different UV intensities (control (no UV), 500, 750, 1000, 1250 and 1500 Energy 1000 x 100µW/cm^2). Colors of the heatmap represent the scores obtained by visualizing the type of growth observed for each spot and comparing them to growth patterns as indicated in Supplemental Figure S3. Mutant strains that had similar or better UV resistance compared to the wildtype for each UV dose are in bold. Mutant strains that had similar or better UV resistance compared to the wildtype for each UV dose are in bold. Data for remaining *hyp* mutants for 1:100 dilution are shown in Supplemental Figure S2.7b and data for remaining dilutions for all mutants are shown in Supplemental File 2.

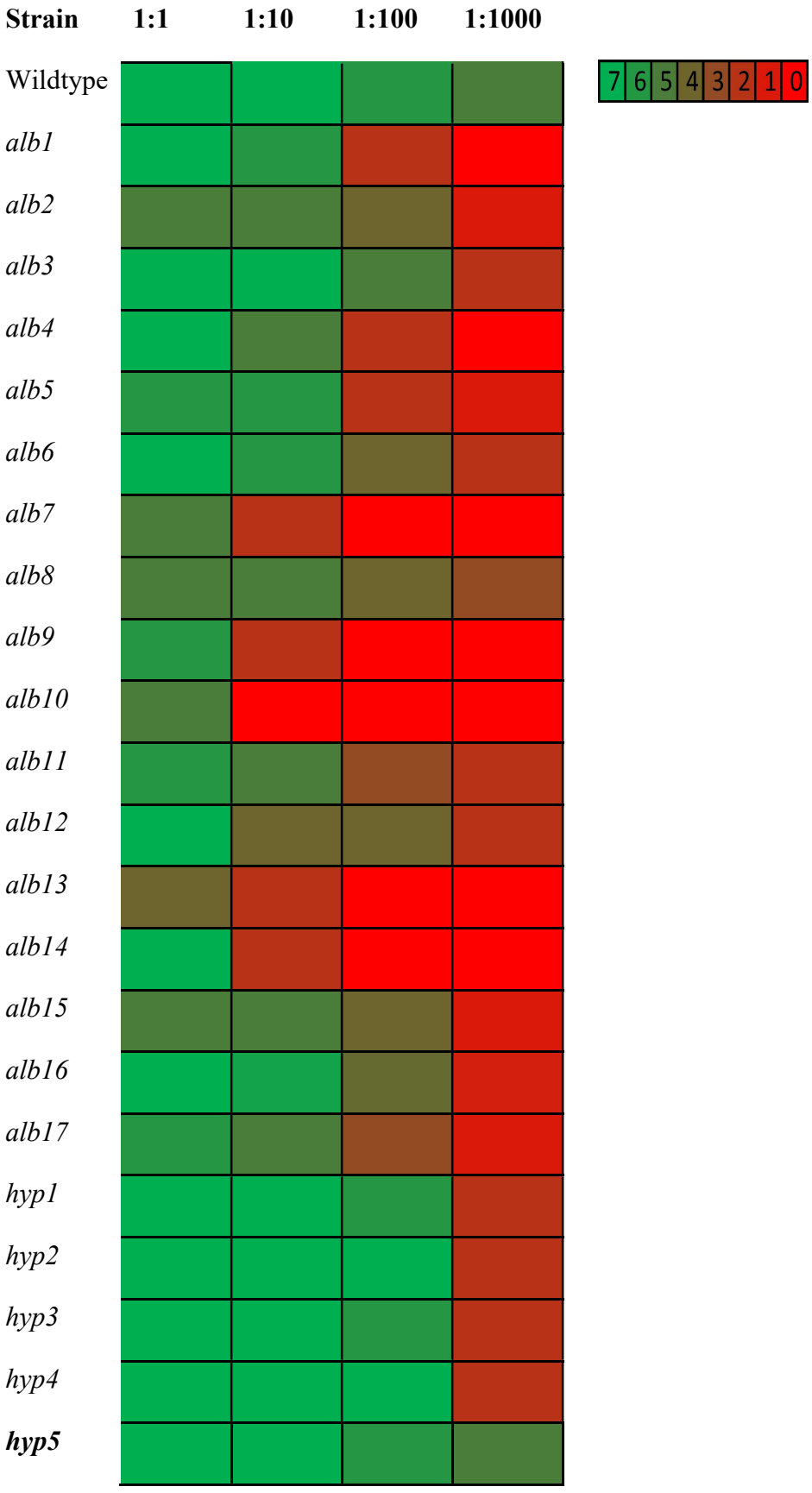
Strain
1:1
1:10
1:100
1:1000
7 6 5 4 3 2 1 0
Wildtype
alb1
alb2
alb3
alb4
alb5
alb6
alb7
alb8
alb9
alb10
alb11
alb12
alb13
alb14
alb15
alb16
alb17
hyp1
hyp2
hyp3
hyp4
hyp5

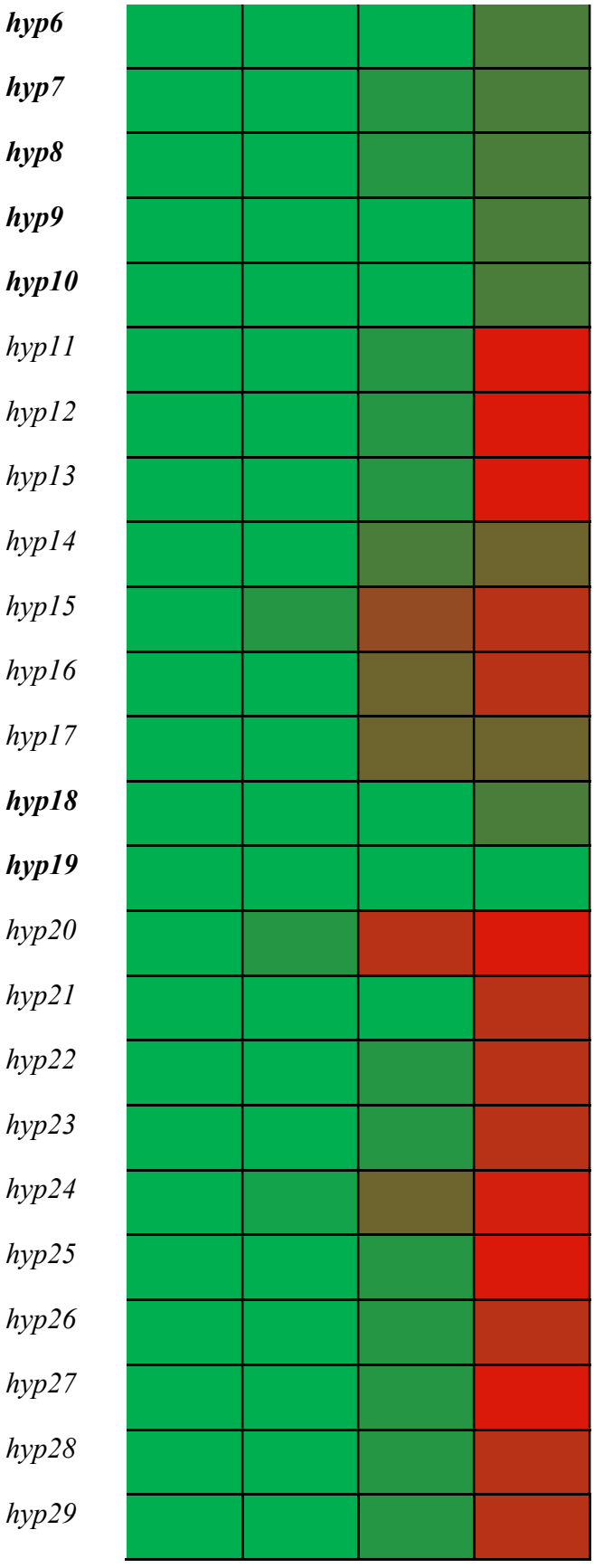
hyp6
hyp7
hyp8
hyp9
hyp10
hyp11
hyp12
hyp13
hyp14
hyp15
hyp16
hyp17
hyp18
hyp19
hyp20
hyp21
hyp22
hyp23
hyp24
hyp25
hyp26
hyp27
hyp28
hyp29

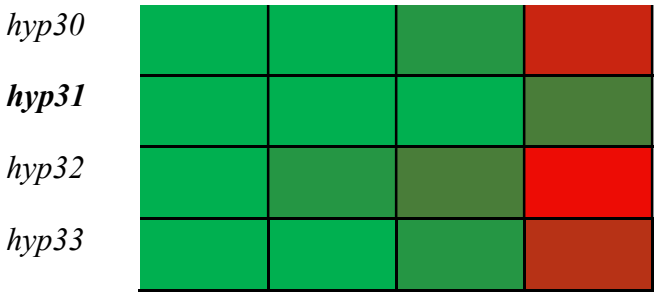

Figure 2.5: Heatmap representing the growth observed for different dilutions of *E. dermatitidis* wildtype, *alb* and subset of *hyp* mutant strains growing at 42°C. Samples were grown on YPD media. Colors of the heatmap represent the scores obtained by visualizing the type of growth observed for each spot and comparing them to growth patterns as indicated in Supplemental Figure S3. Mutant strains that had similar growth to wildtype at 42°C are in bold. Data for remaining *hyp* mutants at 42°C are shown in Supplemental Figure S2.8 and data for all mutants at 10°C and 28°C in Supplemental File 2.

2.4.4 Carbon source utilization

Preliminary testing of all 17 *alb* mutants for growth on YPD, YPG, MN and MEA media yielded the surprising observation that three albino mutants (*alb1*, *alb2* and *alb3*) were able to produce melanin on YPG. To determine in a more systematic manner how alternative carbon sources might impact the phenotypes displayed by the *alb* and *hyp* mutants, ID32-Cstrips were used (Supplemental Figure S9). The wildtype control was able to grow and produce melanin on all 32 carbon sources, whereas the same three *alb* mutants (*alb1*, *alb2*, and *alb3*) were unexpectedly able to produce melanin on multiple carbon sources (Figure 2.6). Pixel density obtained using colour intensity values less than 100 were used as a cutoff to determine if melanin production was observed. Based on the cutoff, *alb1* was able to reinitiate melanin production on 25 out of 32 carbon sources, *alb2* was able to reinitiate melanin production on 30 out of 32 carbon sources, and *alb3* was able to reinitiate melanin production on 14 out of 32 different carbon sources. All three conditional *alb* mutants (*alb1*, *alb2* and *alb3*) were able to produce melanin on the following 13 carbon sources: D-Galactose, cycloheximide (Actidione), acide Lactique, D-Raffinose, Methyl-αD-Glucopyranoside, D-LACtose (origine bovine), D-Sorbitol, D-Xylose, D-Ribose, Glycerol, Palatinose, Erythritol, D-Melibiose. Based on the cutoff the remaining 14 albino mutant strains were not able to recover melanin production (Figure 2.6).

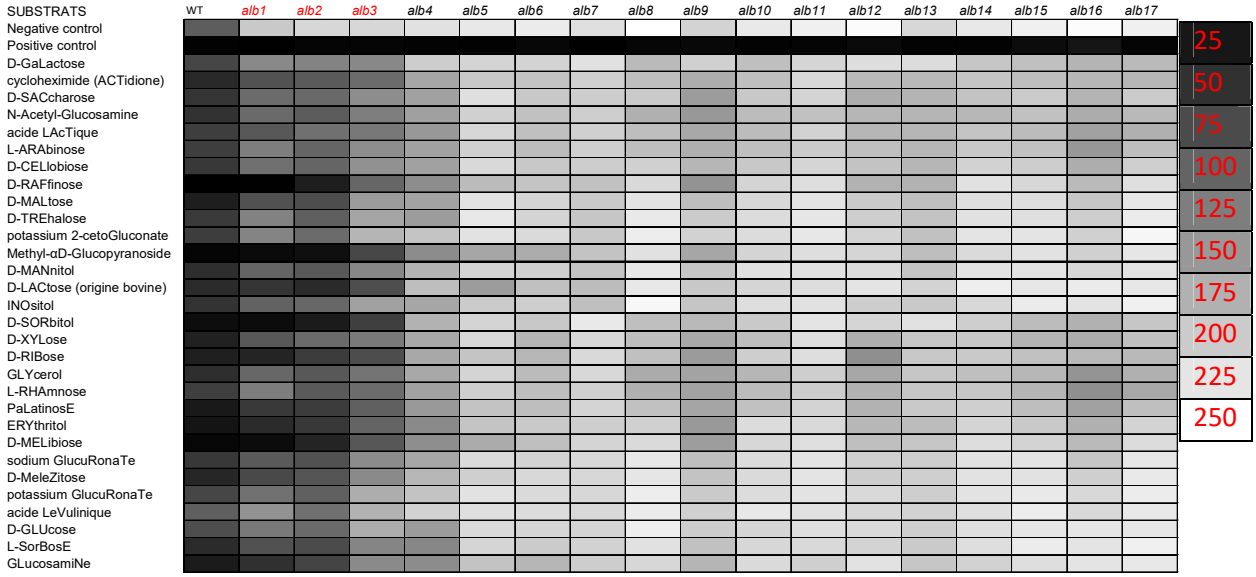

Figure 2.6: Heatmap representing the growth and melanin production of conditional albinos (in red) compared to the obligate albinos. Intensity values obtained using ImageJ and a cutoff of 100 was used to consider if melanin production was present. Negative control has no substrate and positive control= Esculinferric citrate.

2.4.5 Analysis of Single Nucleotide Variants (SNVs)

Genomic DNA from all 17 *alb* mutants and 33 selected *hyp* mutants (see the Materials and Methods for an explanation of the selection criteria) was prepared, submitted for sequencing, and sequences analyzed for variants as described in the Materials and Methods. The number of SNVs varied quite significantly between samples. The *E. dermatitidis* wildtype strain used for these studies (UT86568) possessed seven synonymous, four coding and 13 missense SNVs that were shared by all mutant strains and were not included in the number of unique SNVs found in each mutant strain. The lowest number of SNVs was zero for *hyp19* and *hyp24* and the highest number of SNVs observed was 106 for the *hyp28* mutant (Table 2.1). Among the albino mutants, the number of SNVs ranged from 48 (*alb15*) to one (*alb3*). Out of the 17 *alb* mutants, the top three mutants with the highest number SNVs predicted to have high impact were *alb12, alb15,* and *alb2* with 33, 32 and 31 respectively. Out of the 33 *hyp* mutants, the top three mutants with the highest number of high priority SNVs were *hyp28, hyp22,* and *hyp10* with 65, 45 and 43 high priority SNVs respectively. In all the mutant strains tested the largest numbers of mutations were missense mutations.

Table 2.1: Total number of SNVs found in the *alb* and *hyp* mutants. Variants classified as high impact include nonsense mutations, mutations affecting start codons, and frameshift mutations. Variants classified as medium impact include non-synonymous missense mutations. Variants classified as low impact include synonymous missense mutations and mutations that result in no amino acid change. Mutants denoted in red font display the conditional albino phenotype.

Strains	Total	High impact	Medium impact	Low Impact
alb1	13	3	5	5
alb2	44	5	26	13
alb3	16	1	12	3
alb4	23	2	20	1
alb5	44	2	28	14
alb6	35	2	25	8
alb7	6	0	5	1
alb8	14	0	10	4
alb9	12	3	5	4
alb10	25	5	17	3
alb11	37	4	21	12
alb12	43	8	25	11
alb13	2	0	2	0
alb14	10	2	4	4
alb15	48	3	29	16
alb16	24	2	15	7
alb17	45	8	22	15
hyp1	37	5	25	7
hyp2	1	1	0	0

hyp3	4	0	3	1
hyp4	43	9	21	13
hyp5	16	4	10	2
hyp6	17	3	8	6
hyp7	1	1	0	0
hyp8	26	10	11	5
hyp9	18	3	14	1
hyp10	64	8	35	21
hyp11	10	1	5	4
hyp12	9	1	4	4
hyp13	20	3	11	6
hyp14	9	2	1	6
hyp15	6	4	1	1
hyp16	49	9	23	17
hyp17	16	5	6	5
hyp18	2	0	2	0
hyp19	0	0	0	0
hyp20	22	3	13	6
hyp21	27	6	15	6
hyp22	63	12	33	18
hyp23	6	1	4	1
hyp24	0	0	0	0
hyp25	56	11	31	14
hyp26	8	2	4	2

hyp27	16	4	9	3
hyp28	106	12	56	38
hyp29	6	1	5	0
hyp30	7	2	5	0
hyp31	8	2	5	1
hyp32	21	4	13	4
hyp33	57	8	34	15

Strikingly, although the annotation of the *E. dermatitidis* genome sequence reveals the presence of genes associated with L-DOPA and pyomelanin melanin production, all 17 of the *alb* mutants possessed high or medium impact mutations in the *PKS1* gene (HMPREF1120_01373) (Table 2.2). No mutations were recovered in any other annotated melanin biosynthetic genes in these mutants. The a*lb15*, *alb16*, and *alb17* mutants possessed nonsense mutation whereas the rest of the albino strains had insertions, deletions and missense mutation in *PKS1*. None of the hyperpigmented mutants or the wildtype mutant had a mutation in *PKS1*. More generally, the vast majority of the recovered mutations were found in genes that are annotated as hypothetical proteins (Supplemental File 1).

Other than *PKS1*, there were only 54 examples of the same gene possessing SNVs in different mutants. Mutations in HMPREF1120_05524 (hypothetical protein) were shared between 16 mutant strains (three *alb* and 13 *hyp* mutants). Mutations in HMPREF1120_00737 (hypothetical protein) were shared between three *alb* and three *hyp* mutants. Mutations in HMPREF1120_02419 (hypothetical protein) were shared between three *alb* and three *hyp* mutants. Mutations in HMPREF1120_04157 (MFS transporter, SP family, sugar: H+ symporter) were shared between four *hyp* mutants. Mutation in HMPREF1120_06473 (mitogen-activated protein kinase spm1) was shared between four *hyp* mutants. Mutations in HMPREF1120_08863 (AP endonuclease 2) was shared between two *hyp* and 1 *alb* mutant. Mutations in HMPREF1120_08462 (hypothetical protein) was shared between two *hyp* and one *alb* mutant. Mutations in HMPREF1120_07859 (Ca2+-transporting ATPase) was shared between three *hyp* mutants and mutations in HMPREF1120_06469 (hypothetical protein) was shared between one *hyp* and two *alb* mutants (Table 2.3). Multiple other mutations were shared between two mutants (Supplemental File 1)

Table 2.2: Mutations observed in the Polyketide Synthase 1 (*pks1*) gene of the *E. dermatitidis* albino strains. Mutants in red are conditional albinos.

Strains	**Mutation**	**Impact on coding sequence**	***HMPREF1120_03173* (Polyketide Synthase)**
Wildtype	N/A	N/A	N/A
alb1	A→C Transversion	(AAC→CAC)	N578H
alb2	T→C Transition	(TTT→TCT)	F764S
alb3	T→C Transition	(TTC→CTC)	F439L
alb4	G→A Transition	(CAT→TAT)	H2065Y
alb5	A→G Transition	(TTT→TCT)	F429S
alb6	C→G Transversion	(TGG→TCG)	W1252S
alb7	A→G Transition	(CTC→CCC)	L577P
alb8	G→A Transition	(CAT→TAT)	H2152Y
alb9	A→T Transversion	(+52/+408)	1 bp Insertion
alb10	+G Insertion	coding (4727/6084 nt)	1 bp Insertion
alb11	Δ1 bp Deletion	coding (944/6202 nt)	1 bp DEL 944
alb12	2 bp→TC Substitution	coding (1068-1069/6084 nt)	2 bp substitution
alb13	Δ15 bp Deletion	coding (2319-2333/6202 nt)	15 bp DEL
alb14	G→A Transition	(CAG→TAG)	Q978*
alb15	C→T Transition	(TGG→TGA)	W198* Stop
alb16	G→A Transition	(CAG→TAG)	Q649* Stop
alb17	A→T Transversion	(TTG→TAG)	L251* Stop

Table 2.3: Shared mutations between different samples. Mutants in red are conditional albino and mutants in brown are obligate albinos.

Gene	Description	Strains found in
HMPREF1120_ 04157	MFS transporter, SP family, sugar:H+ symporter	*hyp9, hyp12*, *hyp17*, *hyp23*
HMPREF1120 _00737	hypothetical protein	*alb2*, *alb10*, *alb15*, *hyp3*, *hyp10*, *hyp23*
HMPREF1120 _02419	hypothetical protein	*alb2*, *alb5*, *alb12*, *hyp6*, *hyp8*, *hyp15*
HMPREF1120_06473	mitogen-activated protein kinase spm1	*hyp1*, *hyp4*, *hyp10*
HMPREF1120_05524	hypothetical protein	*alb9*, *alb12*, *alb17*, *hyp1*, *hyp2*, *hyp4*, *hyp5*, *hyp8*, *hyp14*, *hyp15*, *hyp16*, *hyp26*, *hyp28*, *hyp32*
HMPREF1120_08863	AP endonuclease 2	*alb6*, *hyp33*, *hyp10*, *hyp20*, *hyp25,*
HMPREF1120_08462	hypothetical protein	*alb11*, *hyp22*, *hyp20*,
HMPREF1120_07859	Ca2+-transporting ATPase	*hyp1*, *hyp4*, *hyp28*,
HMPREF1120_06469	hypothetical protein	*alb13*, *alb14, hyp28*

* Table showing shared mutations that are shared within at least three mutant strains or more. All shared mutations between two mutants are shown in Supplemental File 1.

2.4.6 Representation of PKS1 mutation sites

To assess the possibility that the conditional albino mutants *alb1*, *alb2*, and *alb3* might possess mutations that reside in a specific domain or region of Pks1, the locations of all *alb* mutations were mapped onto the protein domain map of Pks1 (Figure 2.7). Conditional albino strains *alb1* and *alb3* possess mutations in the ketoacyl Synthase (KS) domain and conditional albino *alb2* has a mutation in the Acyltransferase (AT) domain. Of the remaining 14 obligate albinos, two strains (*alb11* and *alb17*) had a mutation in the starter-unit acyltransferase (SAT) domain, four strains (*alb5, alb12, alb15* and *alb16*) harbored a mutation in the Ketoacyl Synthase (KS) domain, two strains (*alb13* and *alb14*) possess a mutation in the Acyltransferase (AT) domain, *alb6* has a mutation in the Phosphodiesterase (PT) domain, *alb10* possesses a mutation in the Acyl carrier protein (ACP) domain and four strains (*alb4, alb7, alb8* and *alb9*) exhibit mutations in the Thioesterase (TE) domain.

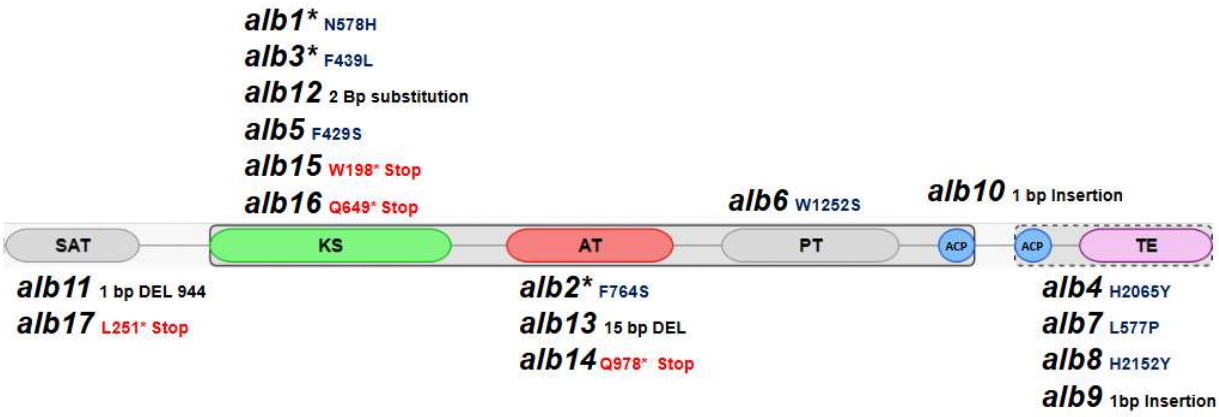

Figure 2.7: Mutations observed in the Polyketide Synthase 1 of the *E. dermatitidis* albino strains. The Pks1 domains a schematically represented (Starter unit: ACP transacylase (SAT), Ketosynthase (KS), Acyltransferase (AT), Product template (PT), Acyl-carrier protein (ACP) and Thioesterase (TE)) that are responsible for different aspects of the polyketide synthase pathway in *E. dermatitidis*. * Indicates to conditional albinos. Pks1 amino acid scale with regards to the position of the various domains: SAT: 4-241 AA, KS: 368-798AA, AT: 898-1194AA, PT: 1282-1598 AA, ACP: 1669-1733 and 1805-1870 AA, TE: 1921-2157 AA.

2.5 Discussion

This study represents the first systematic attempt to use unbiased random mutagenesis to investigate the genetic control of melanin production in the model polyextremotolerant fungus *E. dermatitidis*. Previous studies using targeted mutagenesis suggested that 1,8-DHN melanin synthesized via Pks1 is primarily responsible for melanin production. However, subsequent genome annotation showed the existence of additional melanin biosynthetic pathways whose relative contribution to melanin production is not known. Surprisingly, our genetic screen revealed that all recovered albino mutants possess mutations in the *PKS1* gene. However, an even more surprising observation is that pigmentation could be restored to a subset of these albino mutants by changing the carbon source. These results collectively emphasize the importance of 1,8-DHN melanin to growth and stress response in *E. dermatitidis*, while also hinting at surprisingly complex regulatory processes that appear to underlie melanin production.

2.5.1 *E. dermatitidis* and albino mutants due to mutations in *PKS1*

All *alb* mutants obtained via random mutagenesis shared a mutation in *PKS1* indicating a disruption in the production of 1,8-DHN melanin (Alspaugh *et al.* 1998; Fujii *et al.* 2000). The Pks1 enzyme possesses similar structures and domains across the fungi. The type 1 non-reducing Pks is a large complex protein found in fungi has three core domains: AcylTransferase (AT), Acyl carrier protein (ACP), and Ketosynthase (KS) domains (Sabatini *et al.* 2018; Jia *et al*. 2021). The ketosynthase (KS) domain is responsible for the elongation of the polyketide backbone by catalyzing repeated decarboxylative condensation, the AT domain is responsible for the selection of the extension unit, and the ACP domain contains a phosphopantetheinyl arm to act as a tether for the growing polyketide and the completed polyketides (Hopwood 1997; Bingle *et al.* 1999; Li *et al.* 2010). In addition to these three core domains, a Thioesterase (TE) domain

can also be present which is responsible for either the release of the bound enzyme intermediates or drives the final cyclization reaction hence releasing the final product (Du and Lou 2010). The final product can either be a heptaketide, hexaketide or pentaketide which is then released by the TE domain (Geyer *et al*. 2022).

Genome SNV analysis identified variation in the *PKS1* mutations observed in the *E. dermatitidis alb* strains. Mutations were observed in the KS, ACP, AT, and TE domains indicating that all domains are necessary to produce 1,8-DHN melanin and mutations in any of these domains can affect the intermediates necessary to produce 1,8-DHN melanin (Chen *et al.* 2021). Besides *PKS1* SNVs, the analysis did not identify mutations in any other gene clusters indicating that *PKS1* is the most important polyketide synthase for melanin production in *E. dermatitidis* under routine growing conditions.

In addition to 1,8-DHN melanin, genome annotation of *E*. *dermatitidis* reveals the presence of pathways that support the production of L-DOPA melanin and pyomelanin (Ito and Wakamatsu 2011; Chen *et al.* 2014; Solano 2014). In this study we obtained three *alb* mutants (*alb1*, *alb2* and *alb3*) referred to as conditional because of their ability to produce melanin in response to different carbon sources despite the presence of a mutation in *PKS1*. We speculate that these alternate pathways are responsible for the production of melanin when the 1,8-DHN pathway melanin is disrupted. Expression of genes involved in the L-DOPA pathway and L-Tyrosine degradation pathway has previously been observed in *E. dermatitidis* during skin infection. Under these conditions, expression levels of genes involved in the L-tyrosine degradation pathway were upregulated on skin compared to a negative control whereby *E. dermatitidis* was cultured on prewetted Nylon membrane (Poyntner *et al.* 2016; 2018).

2.5.2 Carbon utilization

Results from our study suggest that certain carbon sources might be better suited for promoting melanin production. Besides growth, carbon sources have also been shown to influence secondary metabolite production in different fungi (Fang and Zhong 2002; Shih *et al.* 2007). Genes involved in the sorbicillinoid biosynthesis production via Pks1 in *Ustilaginoidea virens* were shown to be affected by the 12 different carbon sources tested (Meng *et al.* 2016. Zhang *et al.* 2023). A recent study on *A. nidulans* found that DOPA-melanin production was increased when glucose was used as a carbon source (Campanhol *et al.* 2023). Carbon sources are likely to vary in their ability to produce intermediates involved in the production of different types of melanins in *E. dermatitidis*, which could then account for the differential ability of carbon sources to elicit melanin production in the conditional *alb* mutants. Future experiments will further investigate the expression of the L-DOPA melanin and pyomelanin biosynthetic pathways in these mutants to test this idea.

2.5.3 UV and temperature resistance

Melanin plays a key role in the adaptation of black yeasts to exposed surfaces. For example, in *A. niger* physiological stress caused by UV radiation was also able to enhance the synthesis of melanin as an adaptive response (Singaravelan *et al.* 2008). Unlike the *alb* mutants, the *hyp* mutants grew much better at higher UV doses indicating the benefit of melanization to counter and mitigate UV stress. Evidence of this comes from a study conducted on *Bipolaris oryzae,* where expression of 1,3,8-trihydroxy-napthalene reductase (*THR1*) gene involved in the production of DHN melanin pathway was also increased when subjected to UV radiation (Kihara *et al.* 2004).

Melanin can also provide protection from both heat and cold stress. Melanin can absorb heat energy and dissipate it to shield the cells against heat stress (Paolo *et al.* 2006). In our study the *alb* mutant and the *hyp* mutants were able to grow at 10°C and 28°C but at 42°C, the *hyp* mutants showed a higher growth rate compared to the *alb* mutants. This has been demonstrated in previous studies in *E. dermatitidis* where a *WdPKS1*Δ 1 mutation caused a lower survival rate compared to the WT strain that produced melanin (Paolo *et al.* 2006). In *C. neoformans* cells lacking melanin had a lower survival rate at extreme temperatures than melanized cells (Rosas and Casadevall 1997). The ability of fungi to respond to extreme conditions has led to different adaptations. In fungi the most important signaling pathway stimulated by low and high temperatures is the High-Osmolarity Glycerol (HOG) signal transduction pathway which is triggered by the sensors in the plasma membrane and leads to the mitogen-activated protein kinase (MAPK) Hog1 via signaling molecules (Winkler *et al.* 2002; Panadero *et al.* 2006; Hohmann *et al.* 2007; Wang *et al.* 2020). The mutant strains obtained in our study might be utilizing the genes involved in these pathways to mitigate environmental stressors.

2.5.4 *E. dermatitidis* and hyperpigmented mutant morphology

The genome SNV analysis of the 33 *hyp* mutants failed to reveal evidence for consistent association between a specific gene(s) and the observed phenotypes. The *hyp* mutants obtained in this study were subdivided into yeast-like, fuzzy or crusty morphologies which were attributed to the presence of multicellular pseudohyphae and hyphal filaments. Even within these subgroups there were no strong correlation between genes of known function that contained SNVs and the observed phenotypes. Indeed, the only obvious pattern in all *hyp* mutants was the lack of mutation in *PKS1*, indicating that all *hyp* mutants were able to produce 1,8-DHN melanin similar to the *E. dermatitidis* wildtype strain. Essentially, these results suggest that whereas there may

only be one (or at least a few) ways to generate albino mutants via random mutagenesis, there appears to be a multitude of ways to generate the hyperpigmented phenotype. The broader range of cellular morphologies observed among the *hyp* mutants substantiates this view. The apparent correlation between hyperpigmentation and the formation of hyphae and/or pseudohyphae supports the idea that these are related responses to conditions that reduce growth or cause stress. In that case, it would not be surprising that a greater number of mutations result in hyperpigmentation as this would be a secondary consequence of defects that impact growth or impose stress.

2.6 Conclusion

This study used an unbiased random mutagenesis approach to obtain *alb* and *hyp* mutant strains of the polyextremotolernant black yeast *E. dermatitidis*. The mutants were divided into *alb* and *hyp* mutants based on their phenotypes with regards to their ability to produce melanin. Based on phenotypic assays and melanin recoverability, the *alb* mutants were further subdivided into conditional *alb* that could recover melanin production on different carbon sources and obligate *alb* which had completely lost their ability to recover melanin. Phenotypic characterization based on UV and temperature tolerance revealed that the *hyp* mutants are more stress tolerant than the *alb* mutants. All *alb* mutants possess mutations in *PKS1*, which is involved in the production of 1,8-DHN melanin. Mutations in Pks1 appear to generate an albino phenotype that can be rescued in some mutant backgrounds by substituting dextrose with an alternative carbon source such as galactose as seen in the conditional *alb* mutants. Here galactose could activate signalling pathways that turn on alternative melanin producing pathways or there might be yet unknown functionally redundant components within the main melanin producing pathways that have not yet been deciphered. Future work will incorporate transcriptomics to

possibly identify candidate genes/pathways that might be involved in generating conditional albino mutants.

CHAPTER 3: Transcriptomic analysis of melanin production in *Exophiala dermatitidis* conditional albino mutants on two different carbon sources

This chapter has been submitted to Canadian Journal of Microbiology for publication.

Has also been submitted to bioRxiv

Chhoker K, Hausner G, Harris D. 2025. Transcriptomic analysis of melanin production in *Exophiala dermatitidis* conditional albino mutants on two different carbon sources. *bioRxiv* 2025.09.23.676125. doi: https://doi.org/10.1101/2025.09.23.676125.

3.1 Abstract

Exophiala dermatitidis is a polymorphic black yeast found in various habitats including soil and leaf litter and also in man-made environments such as sinks, dishwashers and saunas. Melanin plays a key role in *E. dermatitidis* virulence and environmental adaptation. The *E. dermatitidis* genome sequence has revealed the presence of genes responsible for production of melanin via three different pathways (1,8-DHN melanin, DOPA melanin, and pyomelanin) but besides DHN melanin not much is known about the activation of the other pathways. Our previous work identified three conditional albino mutants (*alb1*, *alb2* and *alb3*) that can recover melanin production despite mutation in *PKS1*. In this study RNA Transcriptomics was used as a tool to investigate gene expression differences between the three conditional albinos, two obligate albinos (*alb10* and *alb12*) and wildtype to account for variation in melanization using two treatments (dextrose and galactose) as carbon sources. Differential gene expression analysis revealed a higher number of significantly upregulated genes in the conditional albinos on galactose (YPG) compared to the obligate albinos. Overrepresentation analysis revealed a higher number of significantly enriched GO terms in the conditional albinos compared to the wildtype and the obligate albinos. Multiple genes involved in 1,8-DHN melanin and pyomelanin were also found to be upregulated on YPG in the conditional albinos. Besides genes involved in melanization, genes involved in various aspects of cell wall regulation were also upregulated on

YPG. To this date this is the first study that has demonstrated the activation of genes involved in multiple different melanin pathways in *E. dermatitidis* grown on different carbon sources.

3.2 Introduction

Fungal melanin plays a wide variety of roles that include protection from harmful environmental conditions (Salgado-Castillo *et al.* 2023) as well as the promotion of virulence in fungal pathogens of plants, animals and humans (Okuno *et al.* 1983; Howard and Valent 1996; Dean 1997; Adachi *et al.* 1998; Schnitzler *et al.* 1999). The main function attributed to fungal melanin is protection from UV irradiation (Patel *et al.* 1996; Khajo *et al.* 2011), which in some cases is associated with the quantity of melanin produced by cells (Dighton *et al.* 2008; Cordero and Casadevall 2017). Other studies have also demonstrated the ability of fungal melanin to confer protections by binding to toxic metals such as copper (Gadd and de Rome 1988), iron (Saiz-Jiminez and Shafizadeh 1984), zinc and tin (Rizzo *et al.* 1992).

Exophiala dermatitidis also known as *Wangiella dermatitidis* is an ascomycete black yeast with a world-wide distribution that can be found in natural habitats such as tropical rain forests, where it is most likely associated with fruits and wild fruit-eating animals (Sudhadham *et al.* 2008). There has also been emergence of *E. dermatitidis* recovered from man-made environments such as bathrooms, kitchen sink drains, saunas, steam baths and railways ties (Matos *et al.* 2002; Hamada and Abe 2010). The emergence of *E. dermatitidis* as an opportunistic pathogen has been noted in immunocompromised patients where it is able to cause phaeohyphomycosis, chromoblastomycosis and fatal infections of central nervous system (de Hoog 2014; Olsowski *et al.* 2018; Vasquez *et al.* 2018; Hagiya *et al.* 2019; Beniwal *et al.*2023). Several studies have identified DHN-melanin synthesized via the polyketide synthase Pks1 as a key attribute related to virulence in *E. dermatitidis*. Notably, mutant strains lacking Pks1 and

therefore unable to produce melanin show reduced virulence on skin and mouse model infections (Chen *et al.* 2014; Poyntner *et al.* 2016; 2018). Genome annotation of *E. dermatitidis* has revealed that besides 1,8-DHN melanin, *E. dermatitidis* also can produce L-DOPA melanin and pyomelanin via the L-tyrosine degradation pathway (Chen *et al.* 2014; Solano 2014).

As part of the ongoing study on the genetics of melanin production in *E. dermatitidis*, our previous work employed classical and unbiased random mutagenesis approach to generate albino mutant strains (Chhoker *et al*. 2025b). Unexpectedly, all recovered albino mutants possess mutations in the *PKS1* gene. The *alb* mutant strains could further be subdivided into conditional and obligate depending on the ability of different carbon sources to restore melanin production (Chhoker *et al*. 2025b). Specifically, the study identified 17 albino mutants all possessing a mutation in *PKS1*, but a subset of these, termed conditional albino (*alb1*, *alb2*, and *alb3*), were able to restore pigmentation on YPG. The ability of conditional albinos to restore pigmentation highlights the fact that fungal species that have genes involved in multiple different melanin biosynthetic pathways might be able to restore pigmentation if certain conditions are met. Previous studies on albino mutants of *E. dermatitidis* obtained via targeted mutations of *PKS1* using techniques such as Agrobacterium-mediated transformation (Feng *et al*. 2001) and CRISPR/Cas9 (Poyntner *et al*. 2018) have never observed pigment restoration, making this study the first of its kind where albino mutants of *E. dermatitidis* could restore pigmentation presumably via utilizing alternative melanin biosynthetic pathways. We propose that comparison of gene expression profiles in the conditional, obligate *alb* mutants and the wildtype presents an opportunity to identify genes and pathways involved in the activation of these alternative pathways, thereby providing novel insight into the regulation of melanin production in the polyextremotolerant fungus *E. dermatitidis*.

3.3 Materials and Methods

3.3.1 Media and strains

Two different media used in this study include Yeast extract peptone dextrose (YPD): (10g yeast extract, 20g peptone, 20g dextrose and 20g agar per 1L), and Yeast extract peptone galactose (YPG): (10g yeast extract, 20g peptone, 20g galactose and 20g agar per 1L)

Fungal strains

The *E. dermatitidis* reference strain UT8656 (=ATCC 34100, =*Exophiala dermatitidis* CBS 525.76) was treated as the wildtype strain as described in (Chen *et al.* 2014). Five *alb* mutants including three conditional albinos (*alb1*, *alb2*, and *alb3*) which produce melanin on YPG but not on YPD and two obligate albinos (*alb10* and *alb12*) to represent a subset of obligate albinos which have completely lost their ability to produce melanin on both YPD and YPG, were selected for this study (Chhoker *et al.* 2025b) (Figure 3.1). Obligate albinos were picked based on their ability to grow consistent and contamination free every time and that represented frameshifts mutations based on the SNV analysis (Chapter 2). Strains were obtained from -80°C stocks stored in 30% glycerol and grown at 28°C for a week until colonies started to appear on YPD plates. Single colonies were obtained, plated on YPD or YPG plates, and grown at 28°C for 7 days. Three replicates for each strain were used to obtain a total of 18 YPD plates and 18 YPG plates giving us 36 samples in total. After 7 days of growth, the fungal strains were subjected to RNA extraction.

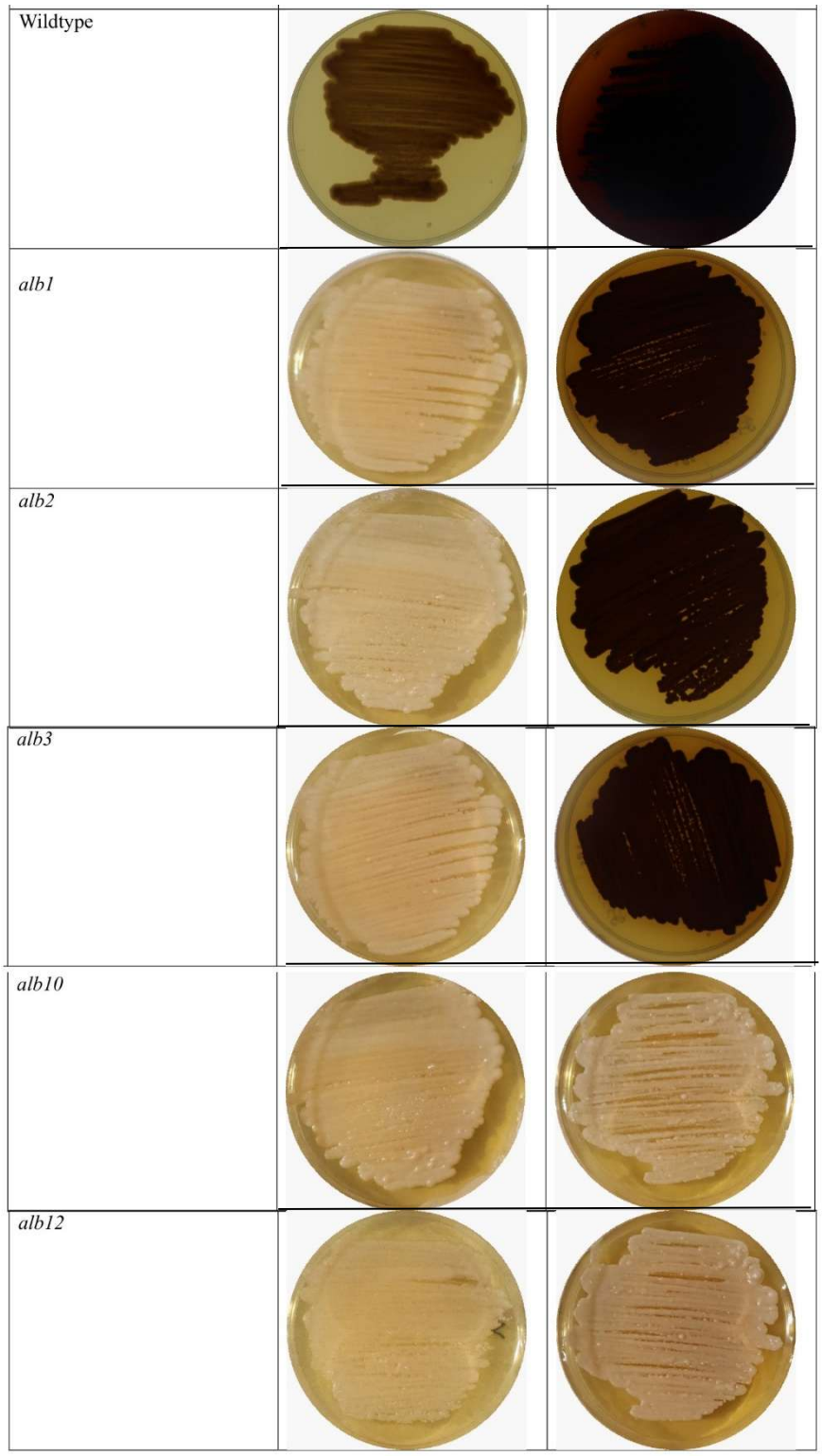

Figure 3.1: Images representing various strains of *E. dermatitidis* growth after 7 days at 28°C. Growth observed on YPD on the left and YPG on the right.

3.3.2 RNA extraction and Sequencing

Total RNA from all 36 samples was extracted using the RNeasy Mini Kit (Qiagen, Germantown, MD, United States) following manufacturers guidelines with slight modifications. Briefly, material from seven-day old YPD and YPG plates was scraped off using sterile flat toothpicks and added to 2ml screw cap collection tubes containing 500µl RLT buffer and 5µl β-ME (β-mercaptoethanol) on ice. Silica beads were added, and the tubes were run on a Bead Beater (Sigma-Aldrich, Missouri, United States) for 15 seconds to homogenize the samples. Samples were maintained on ice to minimize degradation, and all centrifugation was performed for 20 seconds at 8000G. DNA contamination was removed using the RNase-Free DNase Kit (Qiagen) following manufacturers' guidelines.

Initial readings to check the quality and quantity of extracted RNA were obtained using a NanoDrop 2000/2000c Spectrophotometer (Fisher Scientific). The Agilent TapeStation 4150 (AgilentTechnologies, Santa Clara, CA, United States) was used to obtain RIN values. Any sample that yielded RNA with a RIN value below 7 was re-extracted to obtain higher molecular weight RNA. The RNA (minimal concentration >30 (ng/µL) was shipped to the GenomeQuebec Innovation Centre (McGill University, Quebec, Canada). The RNA samples used for library preparations were enriched for PolyA mRNA, and sequencing of the RNA libraries (cDNA) was performed in both directions (paired-end reads of 100bp) on an Illumina NovaSeq 6000 platform (PE100 4 X 25 million reads/lane) aiming for 100 million reads per sample.

3.3.3 Transcriptomic analysis

RNA-seq analysis was performed on data obtained from all 36 samples utilizing tools available on the Galaxy platform (https://galaxyproject.org/usegalaxy/) (The Galaxy Community 2024). First, Fastq files containing the raw reads (as data obtained from GenomeQuebec) were subjected to quality checks using FastQC version 0.12.1 (Andrews 2010). Low Quality bases

with a phred score below 20 and adaptor sequences were trimmed using cutadapt version 5.9 (Martin 2011). The cleaned and trimmed sequences were mapped against the *E. dermatitidis* reference genome sequence (NCBI Refseq: GCF_000230625.1) using HISAT2 version 2.2.1 with paired end reads (Kim *et al.* 2015). The BAM files were visualized using the IGB browser to visualize read mapping on the reference genome (Freese *et* al. 2016). MultiQC version 1.27 (Ewels *et al.* 2016) was used after each step to summarize the analysis results from various tools to visualize all samples at once. FeatureCounts version 2.0.6 (Liao *et al.* 2013) was used to count the number of mapped reads to annotation elements present in the reference genome. The count matrix obtained using FeatureCounts for three replicates per treatment (YPD vs YPG) was used to identify differentially expressed genes (DEGs) using DESEQ2 version 2.11.40.8 (Love *et al.* 2014). Genes were considered differentially expressed between the two conditions (YPD vs YPG) if their adjusted p-value (referred to as FDR) was <0.05. Volcano plots were constructed to observe the number of significant up and down regulated genes based on FDR <0.05 and Log2(FC) > 2 or < -2. The obtained lists of differentially expressed genes for each of the *alb* mutants was compared with the lists of differentially expressed genes of the wildtype using BioVenn (https://www.biovenn.nl/index.php) (Hulsen *et al*. 2008) and were analysed for enriched Gene Ontology (GO terms) using FungiFun3 (https://fungifun3.hki-jena.de/) (Priebe *et al.* 2014; Lopez *et al.* 2024). The Fisher exact test was used to calculate the significance of the enriched GO terms and Benjamini-Hochberg Correction was used to obtain adjusted p-values.

3.4 Results

3.4.1 Overview of differentially expressed genes (DEGs)

The number of DEGs varied between the wildtype and the five mutant *alb* strains when observed using a significance cutoff of $p < 0.05$ and Log2(FC) > 2 or <-2 (Supplemental Figure S3.1). Several trends were observed. First, the numbers of upregulated and downregulated genes

were greater in the albino mutants compared to wildtype, except for the alb12 mutant that had fewer upregulated genes than wildtype (Figure 3.2). Second, all the conditional albinos (*alb1*, *alb2* and *alb3*) had a higher number of differentially upregulated genes (>400) and a higher number of downregulated genes (>1000) compared to the obligate albinos (*alb10*, and *alb12*) that had <400 upregulated genes and <1000 downregulated genes (Figure 3.2). Magnitude of down-regulation based on the number of downregulated genes was greater for all albino mutants and the wildtype. And, lastly, the number of shared upregulated and downregulated genes between the mutants and the wildtype were quite low (Figure 3.2).

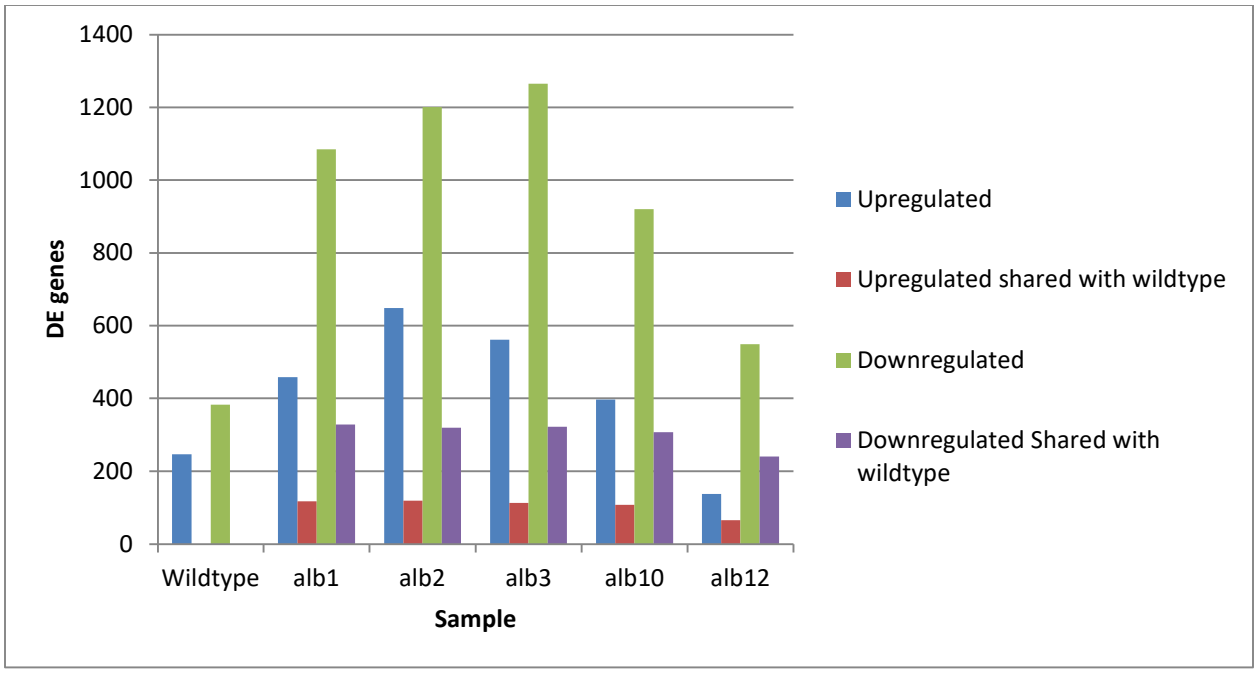

Figure 3.2: The number of genes differentially expressed, with a significant cutoff of p <0.05 and Log2(FC)> 2 or < -2 for each mutant strain, as well as shared with the wildtype. Graph represents the number of DEGs using the count matrix data obtained using FeatureCount with three replicates for each per treatment (YPD vs YPG).

3.4.2 Overrepresentation Analysis

To determine which GO terms were enriched among the various samples, Overrepresentation Analysis (ORA) (Chicco and Agapito 2022) was performed using the FungiFun3 platform. For each mutant strain, Venn diagrams represent significant DEGs sets (FDR < 0.05) based on unique and shared differentially expressed upregulated and downregulated genes between the wildtype and mutant *alb* strains (Supplemental Figure S3.2). Genes that correspond to specific GO terms for the wildtype and all five albino mutants are found in Supplemental File 3. Based on the ORA analysis performed on differentially expressed genes (DEGs) with $p < 0.05$ and Log2(FC) >2 or <-2, some trends appeared. With regards to shared upregulated genes between the wildtype and the *alb* mutants, none of the mutants showed any significantly enriched GO terms at FDR cutoff of 0.05 (Supplemental Figure S3.2 a-e). However, the wildtype strain showed significant enrichment in microtubule binding, microtubule motor activity and microtubule-based movement when considering upregulated genes not shared with the *alb* mutants (Supplemental Figure S3.2 a-e). The conditional *alb* mutants displayed a variable number (ranging from nine to twelve) of significantly enriched GO terms when subjected to one-by-one comparison with wildtype (Supplemental Figures S3.2 a-c). Both obligate albino mutants *alb10* and *alb12* had the lowest number with just one enriched GO terms (Supplemental Figure S3.2d, e). Strikingly, there were no shared upregulated GO terms amongst all the *alb* mutants but there were few GO terms that were shared between just the conditional *alb* mutants discussed in the section (Shared GO terms between albino mutants).

Overrepresentation analysis on significantly expressed unique downregulated genes revealed that the wildtype strain did not show any enriched GO terms for unique genes when compared with *alb1*, *alb2*, *alb3* and *alb10* mutants but had three enriched GO terms (obsolete oxidation-reduction process, transaminase activity and oxidoreductase activity while comparing

with *alb12* (Supplemental Figure S3.2 f -j). With regards to shared downregulated genes between the wildtype and the *alb* mutants, conditional albino mutants *alb1*, *alb2* and *alb3* had five, four and three enriched GO terms respectively, whereas obligate albino *alb10* had six enriched GO terms and *alb12* had the highest number with 14 enriched GO terms (Supplemental Figure S3.2 f- j). The conditional *alb* mutants displayed a variable number (ranging from one to three) of significantly enriched unique GO terms when subjected to one-by-one comparison with wildtype (Supplemental Figures S3.2 f-j). Obligate albino mutant *alb10* had no unique enriched GO terms and *alb12* had the highest number with 13 unique enriched GO terms when subjected to one-by-one comparison with the wildtype (Supplemental Figure S3.2 f- j). There were no shared downregulated GO terms amongst all the *alb* mutants.

Shared GO terms between albino mutants

Amongst up-regulated genes, there were four significantly enriched GO terms shared between all conditional *alb* mutants, transmembrane transport, transmembrane transporter activity, plasma membrane and zinc ion binding. Notably, none of these terms were found in the obligate albino mutants or the wildtype. One GO term (DNA-binding transcription factor activity, RNA polymerase II-specific) was only shared between the *alb1* and *alb2* conditional albinos. Two GO terms (acyl-CoA dehydrogenase activity and acylformamidase activity) were shared between the *alb2* and *alb3* conditional albinos (Figure 3.3) and not in either obligate albino mutants or the wildtype. The only significantly enriched GO term that was found in both conditional and obligate albino mutants was DNA-templated transcription which was enriched in all three conditional albinos (*alb1*, *alb2*, and *alb3*) and in one obligate albino (*alb10*) (Figure 3.3).

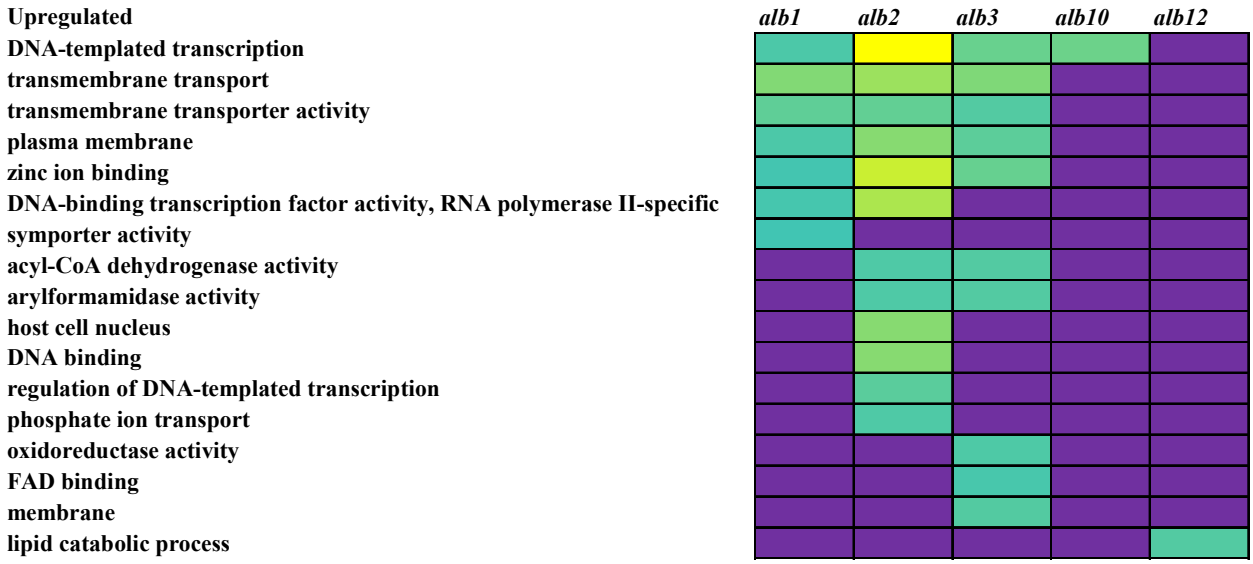

Figure 3.3: Heatmap representing the significantly enriched GO terms (FDR < 0.05) obtained from the FungiFun 3.0 platform that are shared between the five albino mutants and not the wildtype based on differentially expressed upregulated genes with $p < 0.05$ and Log2FC > 2. Yellow colour = more statistically enriched, purple colour= not statistically significant.

Most of the genes involved in the GO term transmembrane transport and transmembrane transporter activity were related to major facilitator superfamily transporters (MFS transporter). Other genes in these two GO terms corresponded with retrograde regulation protein and amino acid protein transporters. The GO term plasma membrane consisted of genes involved in MFS transporters, multiple genes involved in chitin synthesis and a Ras2 homologue. The GO term zinc-ion binding encompassed genes encoding various transcription factors (TFs) and transcriptional regulators such as GAL4 involved in galactose metabolism and multiple protein kinases such as stk16 protein kinase homologue (Supplemental File 3).

Based on downregulated DEGs with $p < 0.05$ and Log2(FC) <-2, there were no GO terms that were significantly enriched amongst all the albino mutants (Figure 3.4). However, the GO term carbon-sulfur lyase activity was shared between all conditional albino mutants (*alb1*, *alb2*, and *alb3*). This term encompasses genes encoding glutathione-dependent formaldehyde (GFA) activating enzymes (Supplemental File 3). An additional GO term transmembrane transport was significantly enriched among the conditional albino mutants *alb2* and *alb3* (Figure 3.4).

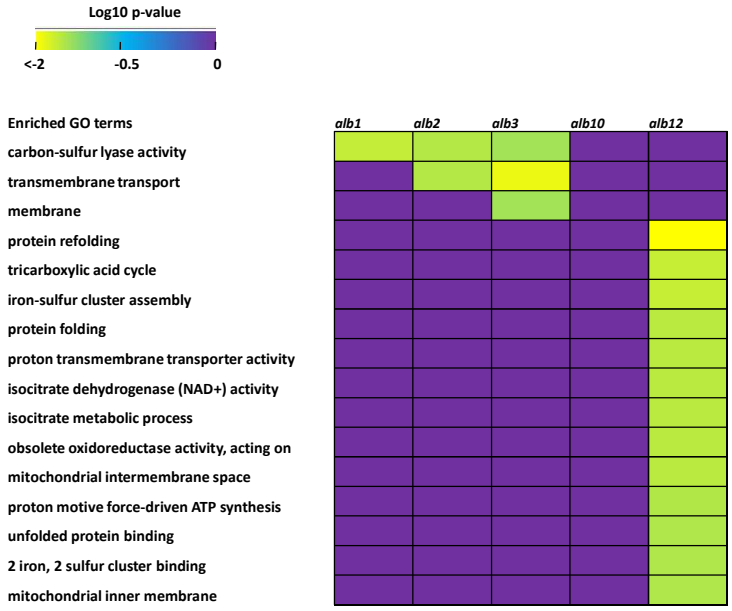

Figure 3.4: Heatmap representing the significantly enriched GO terms (FDR < 0.05) obtained from the FungiFun 3.0 platform that are shared between the five albino mutants based on differentially expressed downregulated genes with $p > 0.05$ and Log2FC < -2. Yellow colour = more statistically enriched, purple colour= not statistically significant.

3.4.3 Melanin biosynthetic pathways

Based on DEGs obtained via DESEQ2 between the two treatments (YPD vs YPG), there were several genes involved in the synthesis of 1,8-DHN melanin that were found to be upregulated (Figure 3.5). The Polyketide synthase (HMPREF1120_03173), 1,3,6,8-Tetrahydroxynaphthalene reductase (HMPREF1120_05939), Scytalone dehydratase (HMPREF1120_07724) and Fungal pigment MCO (HMPREF1120_02828) genes were each significantly upregulated in all three conditional albinos (*alb1*, *alb2*, and *alb3*) and the obligate albino *alb10*. L-ascorbate oxidase (HMPREF1120_03706) was only upregulated in two conditional albinos (*alb2* and *alb3*) and L-ascorbate oxidase (HMPREF1120_04536) was upregulated in the wildtype and conditional albino *alb1* (Figure 3.5).

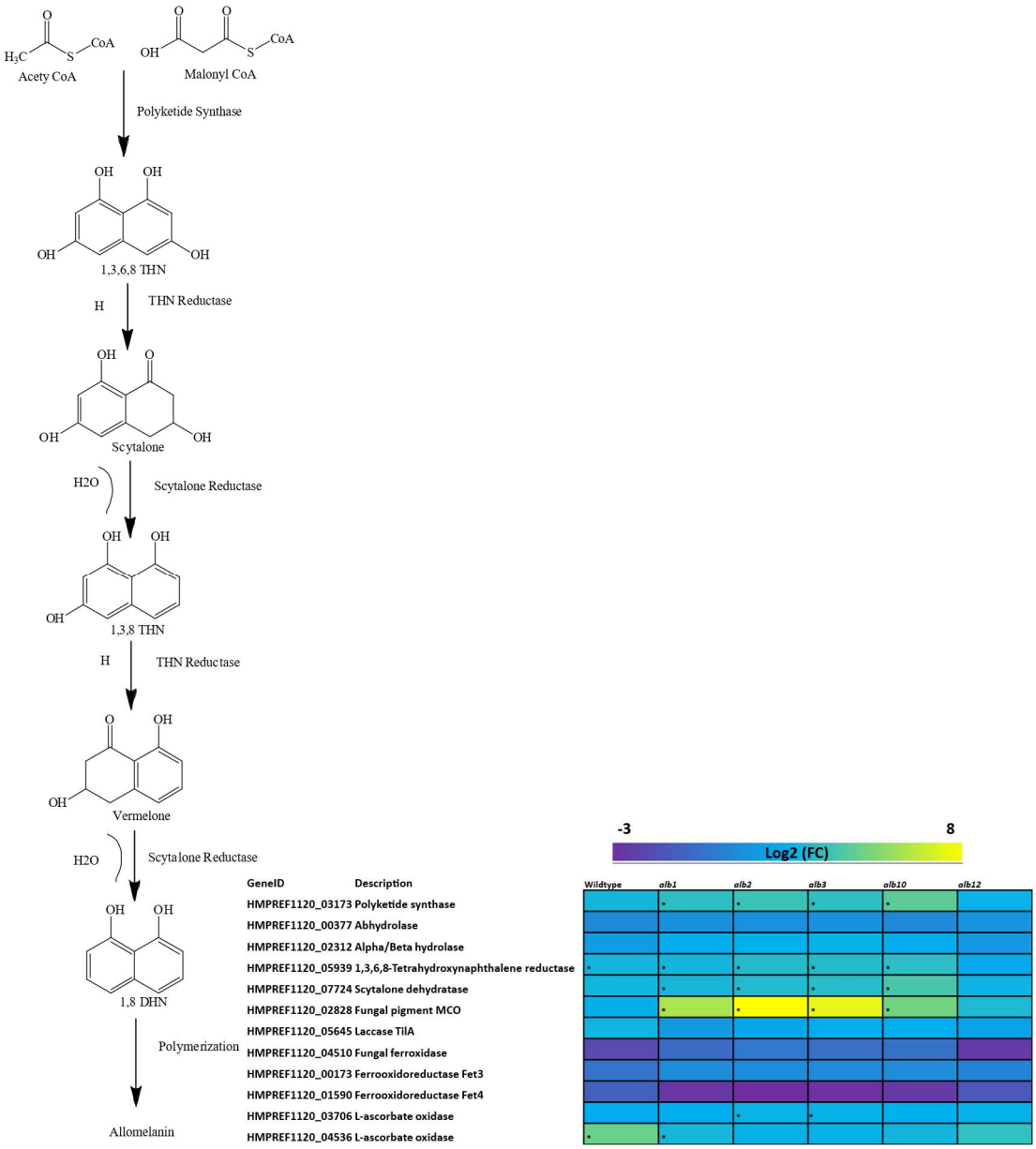

Figure 3.5: Heatmap representing the DEGs involved in the 1,8-DHN melanin biosynthetic pathway found to be upregulated or downregulated based on two treatments (YPD vs YPG) and three replicates each for the wildtype and three conditional albinos (*alb1*, *alb2* and *alb3*) and two obligate albinos (*alb10* and *alb12*). Yellow colour = upregulated DEGs, purple colour= downregulated DEGs. * Indicate significantly upregulated DEGs (Log2FC >1 and $p < 0.05$).

For the tyrosine degradation pathway, several genes were found to be upregulated on YPG. None of the genes involved in the tyrosine degradation pathway were upregulated in the wildtype and the obligate albino *alb12* (Figure 3.6). Tyrosine aminotransferase (HMPREF1120_02164) was significantly upregulated in all three conditional albino *alb1*, *alb2* and *alb3* and in the obligate albino mutant *alb10*. 4-Hydroxyphenylpyruvate dioxygenase (HMPREF1120_05584) was significantly upregulated in conditional albinos *alb2* and *alb3*, and obligate albino *alb10*. Fumarylacetoacetate hydrolase (HMPREF1120_03825) was significantly upregulated in only one conditional albino *alb2*. Maleylacetoacetate isomerase (HMPREF1120_03438) was significantly upregulated in all three conditional albinos (*alb1*, *alb2* and *alb3*), and obligate albino *alb10*. One gene, Homogentisate dioxygenase (HMPREF1120_03827) was significantly downregulated in the wildtype, conditional albinos *alb3* and the obligate albino alb10 (Figure 3.6).

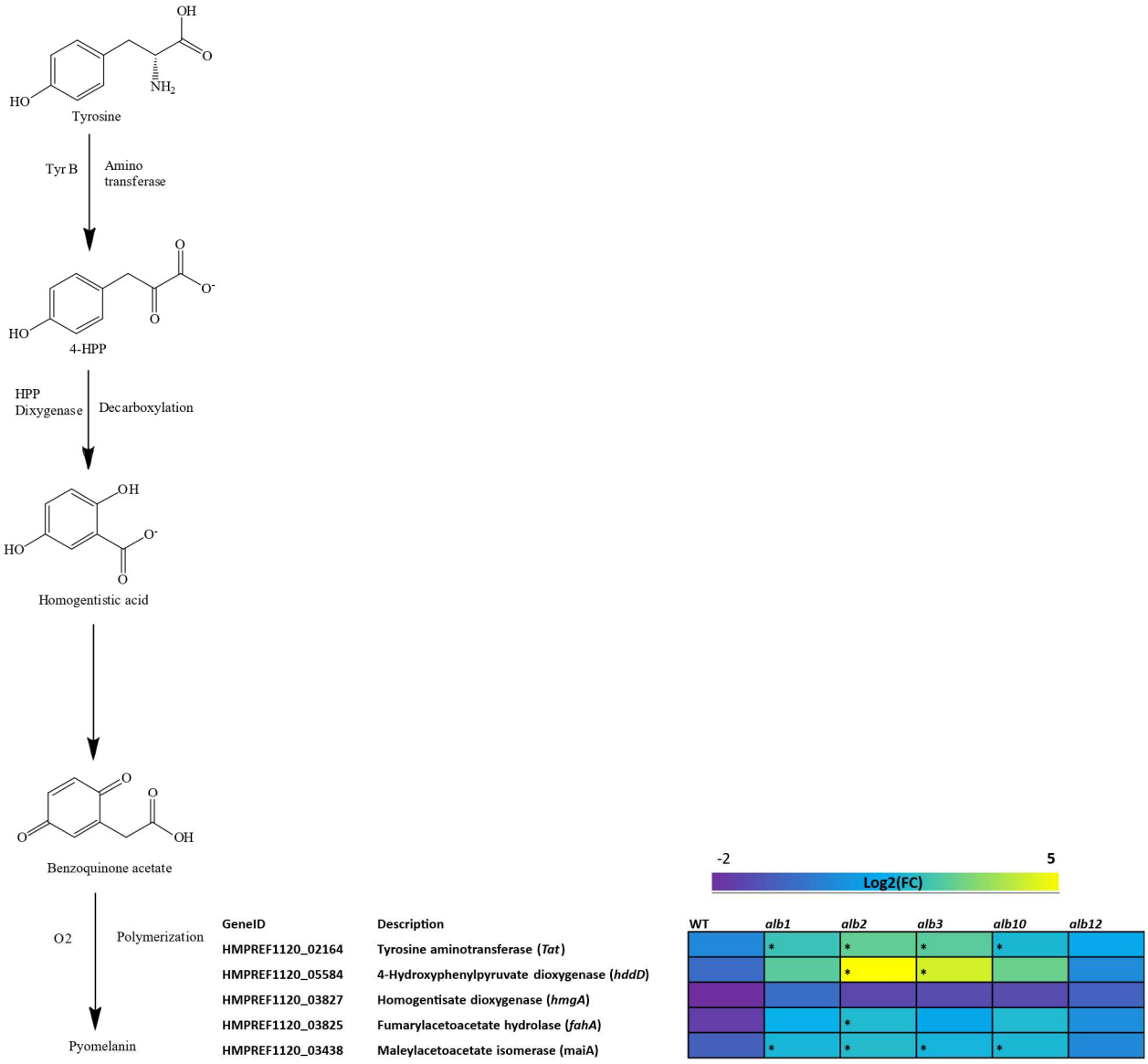

Figure 3.6: Heatmap representing the DEGs involved in the tyrosine degradation pathway found to be upregulated or downregulated based on two treatments (YPD vs YPG) and three replicates each for the wildtype and three conditional albinos (*alb1*, *alb2* and *alb3*) and two obligate albinos (*alb10* and *alb12*). Yellow colour = upregulated DEGs, purple colour= downregulated DEGs. * Indicate significantly upregulated DEGs (Log2FC >1 and $p < 0.05$).

Most of the genes involved in the DOPA melanin pathway did not show any differential upregulation in response to different treatments (YPD vs YPG) (Figure 3.7). Tyrosinase (HMPREF1120_07692) showed significant upregulation in the wildtype and obligate albino *alb12* in response to different treatments. Another gene, Multicopper oxidase (HMPREF1120_00199) was found to be upregulated in the wildtype and in all albino mutants (*alb1*, *alb2*, *alb3*, *alb10* and *alb12*) in response to different treatments (YPD vs YPG) (Figure 3.7).

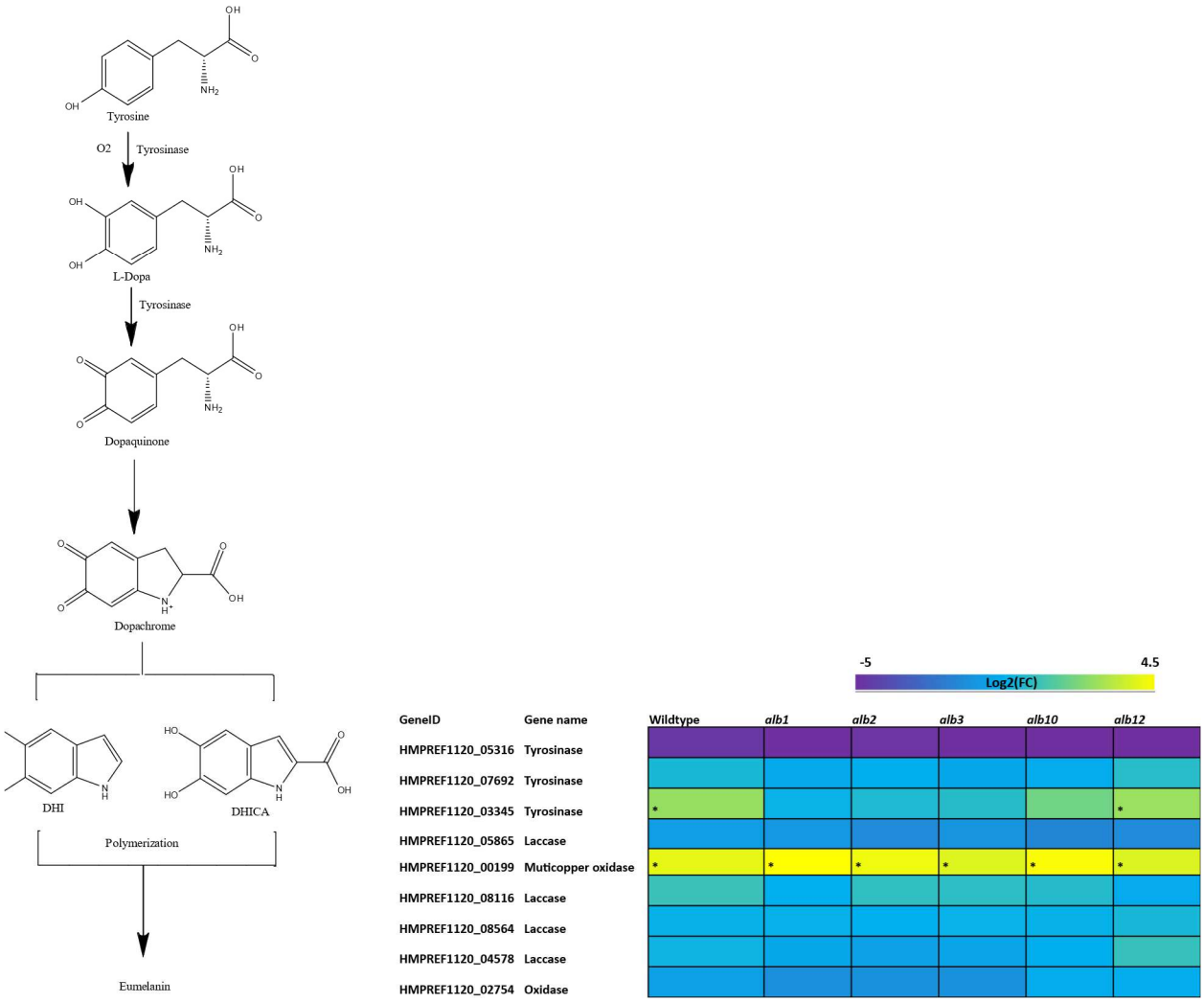

Figure 3.7: Heatmap representing the DEGs involved in the DOPA melanin pathway found to be upregulated or downregulated based on two treatments (YPD vs YPG) and three replicates each for the wildtype and three conditional albinos (*alb1*, *alb2* and *alb3*) and two obligate albinos (*alb10* and *alb12*). Yellow colour = upregulated DEGs, purple colour= downregulated DEGs. * Indicate significantly enriched upregulated DEGs (Log2FC >1 and $p < 0.05$).

3.4.4 Secondary metabolism and light sensing

Based on the DESEQ2 analysis between the two treatments (YPD vs YPG), a small number of genes involved in the production of secondary metabolites are significantly upregulated on YPG (Figure 3.8a). Superkiller protein 3 (HMPREF1120_06543) and 3-oxoacyl-[acyl-carrier-protein] synthase II (HMPREF1120_08091) were significantly upregulated in all three conditional albinos (*alb1*, *alb3* and *alb3*) but not in the obligate *alb* mutants or the wildtype (Figure 3.8a). Acetylaranotin, toxin (HMPREF1120_02993) was upregulated in all three conditional albinos (*alb1*, *alb2* and *alb3*) and the wildtype. Chromosome segregation ATPase family protein (HMPREF1120_01968) was upregulated in the wildtype and the conditional albino *alb3*. Transcription factor hoxa13 (HMPREF1120_08032) was significantly upregulated in the wildtype, conditional albino *alb1* and obligate albino *alb10*. Linear gramicidin synthetase subunit C (HMPREF1120_00598) was upregulated in the wildtype, and all five albino mutants. Calponin-homology (CH) domain-containing protein (HMPREF1120_09090) and Polyketide synthase (HMPREF1120_06568) was only significantly upregulated in the wildtype.

Two light sensing genes are upregulated on YPG. White collar 2 (HMPREF1120_04504) was upregulated in the conditional albinos *alb2* and *alb3* and Velvet domain-containing protein (HMPREF1120_02378) was only upregulated in the wildtype (Figure 3.8b). Most other light sensing genes did not show any upregulation but there were a few genes that were highly downregulated on YPG (Figure 3.8b).

(a)

GeneID	
HMPREF1120_00352	Clathrin, heavy polypeptide
HMPREF1120_01260	Cell morphogenesis protein
HMPREF1120_01968	Chromosome segregation ATPase family protein
HMPREF1120_02200	Dynein heavy chain, cytoplasmic
HMPREF1120_06543	Superkiller protein 3
HMPREF1120_07933	E3 ubiquitin-protein ligase TRIP12
HMPREF1120_08032	Transcription factor hoxa13
HMPREF1120_08132	Complex I intermediate-associated protein 84
HMPREF1120_09269	Hypothetical protein
HMPREF1120_08670	Minichromosome maintenance protein 3
HMPREF1120_09038	F-box protein 8
HMPREF1120_09090	Calponin-homology (CH) domain-containing protein
HMPREF1120_01440	Nonribosomal peptide synthase Pes1
HMPREF1120_02993	Acetylaranotin,toxin
HMPREF1120_04809	Nonribosomal peptide synthase
HMPREF1120_06043	L-aminoadipate-semialdehyde dehydrogenase
HMPREF1120_07636	Nonribosomal siderophore peptide synthase SidC
HMPREF1120_00598	Linear gramicidin synthetase subunit C
HMPREF1120_03318	Carrier domain-containing protein
HMPREF1120_07093	Carrier domain-containing protein
HMPREF1120_03173	Polyketide synthase
HMPREF1120_06568	Polyketide synthase
HMPREF1120_06570	*t1PKS*
HMPREF1120_07394	*t3PKS*
HMPREF1120_08091	3-oxoacyl-[acyl-carrier-protein] synthase II
HMPREF1120_02863	Phytoene synthase
HMPREF1120_03149	Terpene Cyclase
HMPREF1120_09198	Geranylgeranyl pyrophosphate synthetase AtmG

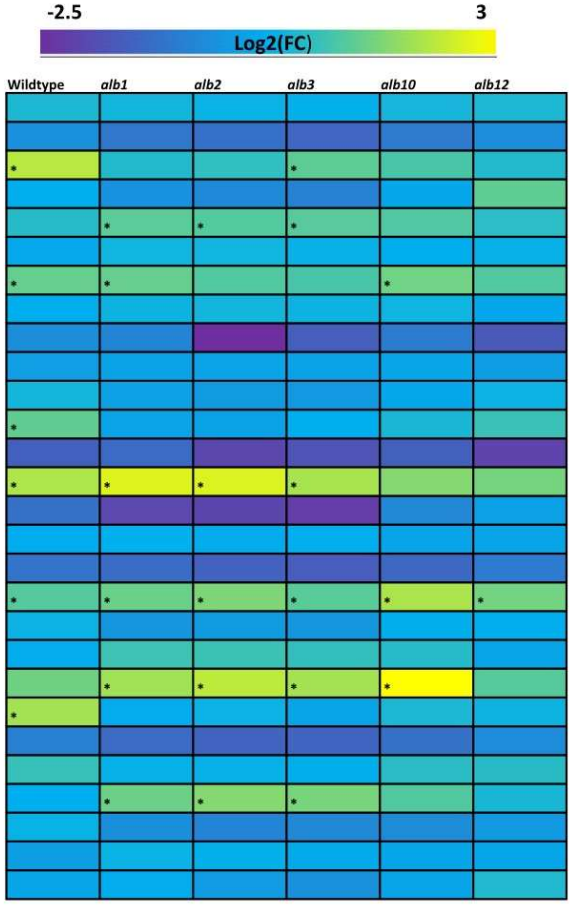

(b)

GeneID	Description
HMPREF1120_07867	Phytochrome, response to red light
HMPREF1120_06318	White-collar complex, response to blue light
HMPREF1120_04504	Cutinase
HMPREF1120_04357	Cryptochrome/photolyase, response to blue and UVA light
HMPREF1120_00264	Fungal opsin, green light−sensing
HMPREF1120_06677	Velvet complex (VelB/VeA/LaeA),
HMPREF1120_03349	Velvet domain-containing protein
HMPREF1120_00072	Velvet domain-containing protein
HMPREF1120_05878	Velvet family protein with homology to VeA
HMPREF1120_02378	Velvet domain-containing protein
HMPREF1120_06091	Velvet domain-containing protein
HMPREF1120_02861	Opsin-like protein
HMPREF1120_06324	Bacteriorhodopsin
HMPREF1120_02862	Phytoene dehydrogenase
HMPREF1120_02863	Carotene cyclase
HMPREF1120_02864	Carotenoid oxygenase

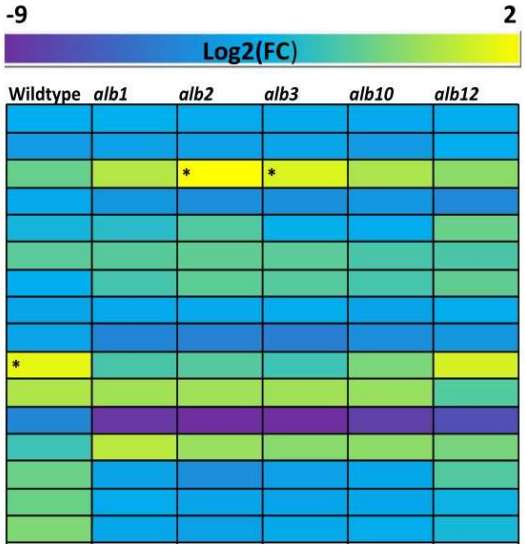

Figure 3.8: Heatmap representing the DEGs involved in (a) secondary metabolism, and (b) light sensing in *E. dermatitidis* found to be upregulated or downregulated based on two treatments (YPD vs YPG) (analysis based on three replicates for all strains examined). Significance based on DESeq2 analysis ($p < 0.05$ and Log2(FC) <1 or >-1). Yellow colour = upregulated DEGs, purple colour= downregulated DEGs. * Indicate significantly upregulated DEGs (Log2FC >1 and $p < 0.05$).

3.4.5 Cell wall regulation

Genes involved in the cell wall biosynthesis, were found to be upregulated on YPG (Figure 3.9). CHS2 Class I chitin synthase (HMPREF1120_06816), Class V chitinase (HMPREF1120_06669) and Chitinase (HMPREF1120_04557) were all found to be upregulated in the wildtype and all three conditional albinos (*alb1*, *alb2*, and *alb3*). Glucans Putative exo-1,3-b-glucanase family (HMPREF1120_05230) was only found to be upregulated in the obligate albino *alb12*. Bgl2-family of putative 1,3-b-transglucosylases (HMPREF1120_00547) was upregulated in the wildtype, all three conditional albinos (*al1*, *alb2*, and *alb3*) and obligate albino *alb10* (Figure 3.9).

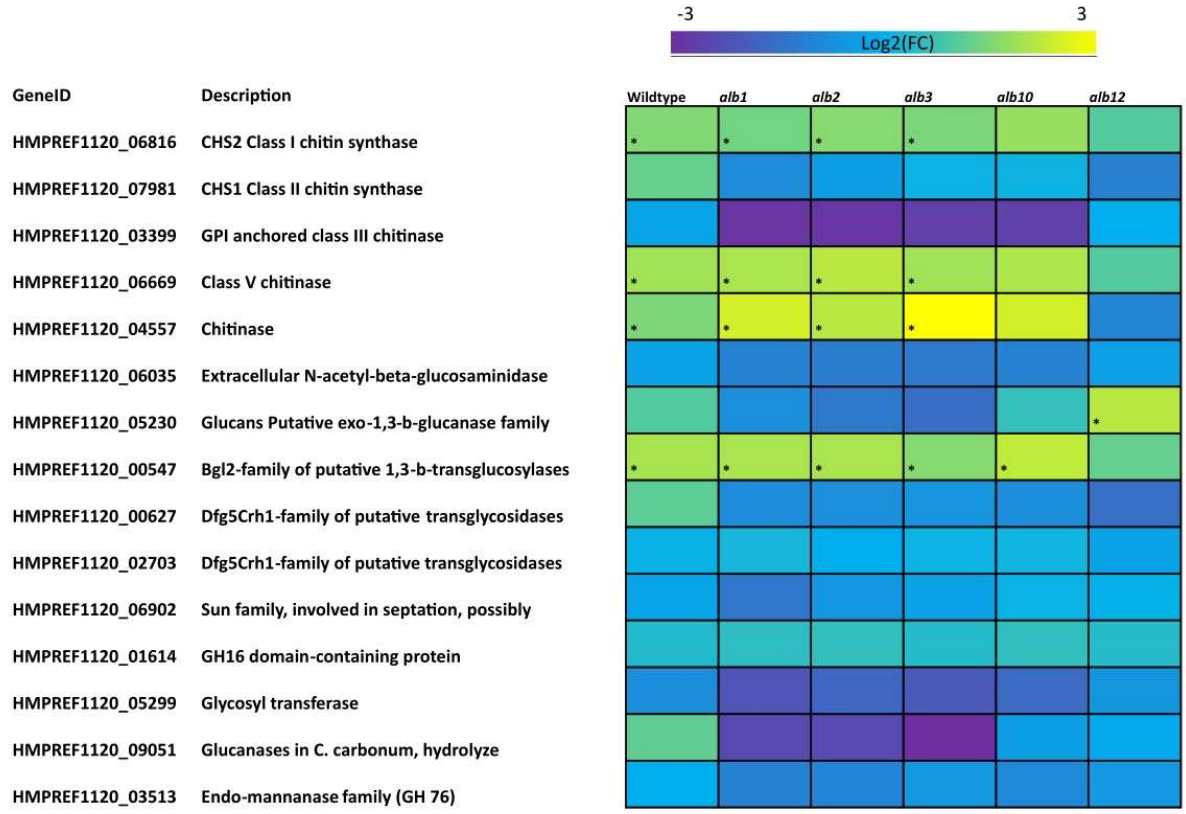

Figure 3.9: Heatmap representing the DEGs involved in cell wall regulation of *E. dermatitidis* found to be upregulated or downregulated based on two treatments (YPD vs YPG) (analysis based on three replicates for all strains examined). Significance based on DESeq2 analysis ($p <$ 0.05 and Log2(FC) <1 or >-1. Yellow colour = upregulated DEGs, purple colour= downregulated DEGs. * Indicate significantly upregulated DEGs (Log2FC >1 and $p < 0.05$).

3.4.6 Metal acquisition

In *E. dermatitidis*, the siderophore pathway is responsible for the uptake of iron via the reduction of Fe^{2+} to Fe^{3+} (Poyntner *et al*. 2016). Homologues of genes encoding the enzymes involved in the siderophore pathway, namely *sidA*, *sidC*, *sidD* and *sidF* and the transporter *sit1* were all significantly downregulated in the wildtype and all albino mutants on YPG (Figure 3.10). *Ftr1* and *Fet3*, genes involved in the reductive uptake pathway were also significantly downregulated in the wildtype and all albino mutants on YPG. There was no significant upregulation or downregulation of genes involved in the copper transport in either the wildtype or any of the albino mutants.

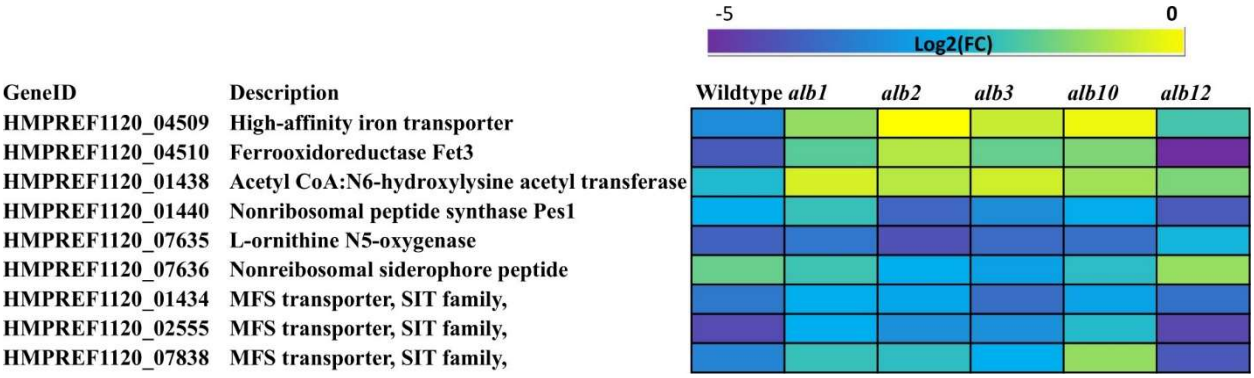

Figure 3.10: Heatmap representing the DEGs involved in metal uptake of *E. dermatitidis* found to be upregulated or downregulated based on two treatments (YPD vs YPG) (analysis based on three replicates for all strains examined). Significance based on DESeq2 analysis ($p < 0.05$ and Log2(FC) <1 or >-1. Yellow colour = slightly downregulated DEGs, purple colour= extremely downregulated DEGs.

3.4.7 Carbon uptake

Aconitate hydratase (HMPREF1120_03751), part of the glyoxylate cycle was significantly upregulated in all three conditional albinos (*alb1*, *alb2*, *alb3*) and the obligate albino mutant *alb10*. Malate dehydrogenase (HMPREF1120_06787) was significantly downregulated in all three conditional albinos (*alb1*, *alb2* and *alb3*) and both obligate albinos *alb10* and *alb12* (Figure 3.11).

In the gluconeogenesis pathway, Fructose-1,6-bisphosphatase (HMPREF1120_04809) was significantly downregulated in the wildtype and all three conditional albinos (*alb1*, *alb2* and *alb3*). Pyruvate carboxylase (HMPREF1120_06163) was significantly downregulated in all three conditional albinos. Fructose-bisphosphate aldolase class I (HMPREF1120_07847) was significantly downregulated in the wildtype and obligate albino mutant *alb10*. Fructose-biphosphate aldolase class II (HMPREF1120_08620) was significantly downregulated in all three conditional albinos and both obligate albinos (Figure 3.11).

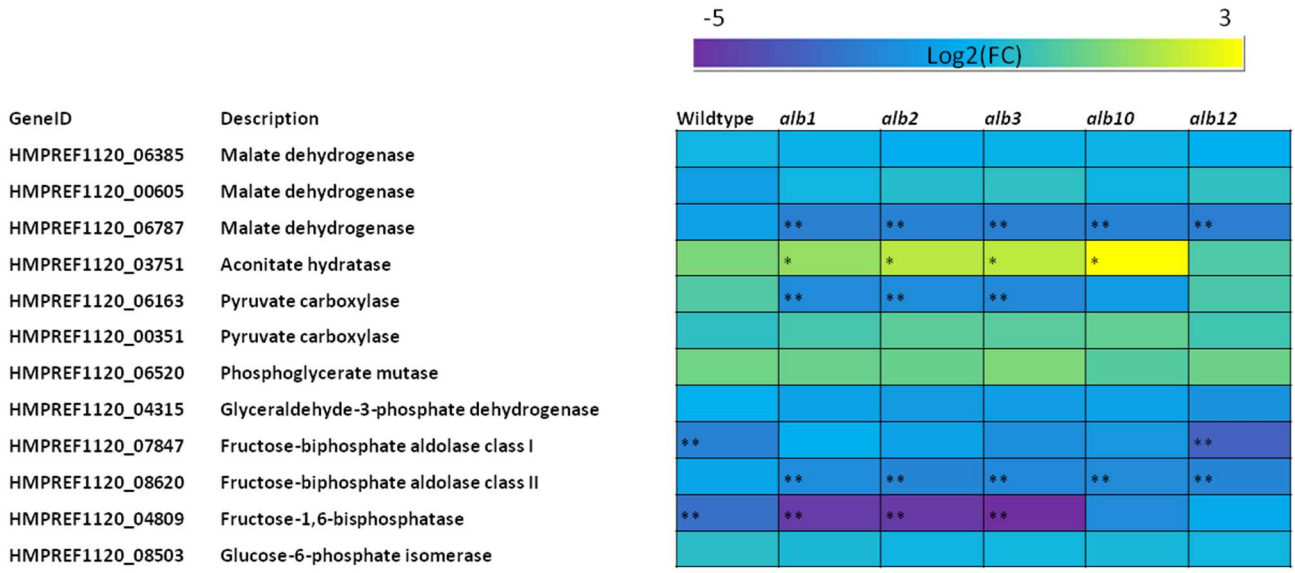

Figure 3.11: Heatmap representing the DEGs involved in the glyoxylate cycle and gluconeogenesis of *E. dermatitidis* found to be upregulated or downregulated based on two treatments (YPD vs YPG) (analysis based on three replicates for all strains examined). Significance based on DESeq2 analysis ($p < 0.05$ and Log2(FC) <1 or >-1. Yellow colour = upregulated DEGs, purple colour= downregulated DEGs. ** genes were significantly downregulated (Log2FC >1 and $p < 0.05$).

3.5 Discussion

For this study three conditional (*alb1*, *alb2* and *alb3*) and two obligate (*alb10* and *alb12*) mutants were picked representing both categories of *alb* mutants we obtained in our previous work (Chhoker *et al*. 2025b). Besides mutations in *PKS1*, our previous work (Chapter 2) did not find any other mutations that were shared between all three conditional *alb* mutants, indicating that the recovery of melanization caused by the carbon source shift might be governed by multiple different pathways and mechanisms that interact with each other. Based on the SNV analysis in Chapter 2, there weren't any mutants that shared multiple genes that had similar mutations indicating that the mutants were not isogenic and behaved differently from each other This study was performed to better understand the pathways whose expression might contribute to the conditional recovery of melanin synthesis in a subset of the albino mutants such as looking at genes involved in the production of melanin via different pathways. Certain trends were observed based on RNA transcriptomics. There were co-regulated genes in the wildtype and all albino mutants likely responding to the carbon shift. There were genes whose expression was shared between both the conditional and the obligate albino mutants but not the wildtype. These are likely a response to a combination of pigment loss and the carbon shift experienced by the mutants. Lastly, there were a small number of genes that were differentially expressed in the conditional albino mutants but not in the obligate mutants, thereby potentially identifying processes that could contribute to the recovery of melanization in the conditional *alb* mutants.

3.5.1 Enriched GO terms

There were no significantly enriched GO terms that were shared between all five albino mutants indicating that all five mutants behaved differently from each other. However, three GO terms (transmembrane transport, transmembrane transporter activity and plasma membrane)

were only enriched amongst the conditional albino mutants. These terms each relate to membrane function and solute transport across the membrane. Most of the genes in these GO terms corresponded with MFS transporters, which play key roles in multidrug resistance and growth during stress (Chen *et al*. 2017). In fungi, melanin production is typically a key component of stress response, which suggests that the conditional albino mutants might have experienced some type of stress during the carbon shift that uniquely triggered melanin production or the SNVs in these mutants allowed then to uniquely respond to stress in a different way compared to the obligate albino mutants or the wildtype. Since fungal melanization occurs in specialized vesicles that are moved and are deposited in the cell wall (Eisenman *et al*. 2009; Camacho *et al*. 2019) the shared nature of these GO terms which also included chitin synthase genes might indicate their roles in cell wall regulation which is important in melanization.

Another term that was shared between all conditional *alb* mutants was zinc ion binding. Most of the genes involved were TFs and transcriptional regulators. There is growing evidence of involvement of TFs that can act either upstream or downstream of various fungal melanization pathways to influence melanin production (Tsuji *et al*. 2000; Shelest 2017; Chhoker *et al*. 2025a). The upregulation of wide variety of TFs in the conditional albino mutants might be linked to the recovery of melanization observed in our study. Metal ions such as Zn^{2+} have been shown to result in the increase of free radical population of melanin (Buszman *et al*. 2006). In fungi, melanin can bind to a wide variety of metals which can also induce melanogenesis and the melanin allows for bioabsorption of essential metals from their environment (Cordero and Casadevall 2017). Since the conditional *alb* mutants were able to recover melanin production, the genes involved in bioabsorption and uptake of certain metals might be upregulated to increase the production of melanin and protect the organism from heavy metal toxicity. The best

way to test this phenomenon would be to grow these conditional *alb* mutants on media incorporating different concentrations of heavy metals and monitor the growth or inhibition of growth over time and compare it with the wildtype and the obligate *alb* mutants.

3.5.2 Melanization in *E. dermatitidis*

The dematiaceous nature of *E. dermatitidis* is attributed to the deposition of 1,8-dihydroxynaphthalene [1,8-DHN] melanin within the cell wall (Geis *et al.* 1984; Taylor *et al.* 1987; Feng *et al.* 2001). In *E. dermatitidis*, it has been observed that the DHN-melanin pathway genes were upregulated during pH stress, which might facilitate adaptation to its natural niches (Chen *et al.* 2014). In our study *PKS1* gene was upregulated in all three conditional albino mutants and one obligate albino mutant indicating that multiple genes in the PKS pathway are necessary for the production of DHN melanin. Since most of the biological processes including PKS1 require multiple steps, if the downstream genes such as laccases are nonfunctional the production of melanin can be affected. The conditional *alb* mutants in our study incorporated missense mutations (Chhoker *et al*. 2025b) whereas the obligate *alb* mutants had frameshift mutations (Chapter 2), so the *PKS1* gene might not have completely lost its function. In DHN pathway, Malonyl-CoA/acetyl-CoA acts as the precursor serving as initiator and extender units of PKS which catalyze the first step of the DHN melanin biosynthetic pathway to produce 1,3,6,8-tetrahydroxynaphthalene (T4HN) (Verde-Yáñez *et al.* 2023). The T4HN compound is then reduced to scytalone by THN reductase. Scytalone is dehydrated by scytalone dehydratase to form 1,3,8-trihydroxynaphthalene (T3HN). Another reduction reaction by the THN reductase forms vermelone from T3HN and the vermelone compound is then converted to DHN-melanin by scytalone dehydratase (Schumacher 2016; Verde-Yáñez *et al.* 2023). All three conditional albinos and one obligate albino showed an upregulation of THN reductase and Scytalone

dehydrates genes, showing that parts of the DHN-melanin could be functional and possibly producing intermediates. These intermediates might then be shunted off to other processes such as fatty acid synthesis which also uses similar precursors such as acetyl-CoA and malonyl-CoA (Zhang *et al*. 2022). In fungi, 3-oxoacyl-[acyl-carrier-protein] synthase II enzyme is involved with the fatty acid synthesis which can be responsible for producing carotenoids in fungi (Sandmann 2022).

In fungi, pyomelanin is produced by the tyrosine degradation pathway via the oxidative polymerization of homogentisate (HGA) (Schmaler-Ripcke *et al*. 2008; Lorquin *et al*. 2022). Two enzymes: 4-hydroxyphenylpyruvic acid dioxygenase and homogentisic acid oxidase are required to degrade L-tyrosine to acetoacetate and fumarate (Ruzafa *et al.* 1995; Kotob *et al.* 1995; Schmaler-Ripcke *et al.* 2008). Pyomelanin is then produced from the auto-oxidation followed by self-polymerization of HGA (Fernandes *et al.* 2021). Upregulation of multiple genes involved in the tyrosine degradation pathway indicates that certain aspects of the pathway are being triggered in all three conditional albinos but not the obligate *alb* mutants or the wildtype. This phenomenon has been previously observed in *E. dermatitidis* albino mutants where genes involved in the L-tyrosine pathway were upregulated during skin infection (Poyntner *et al.* 2016). During infection, *E. dermatitidis* experiences reprogramming of its carbon metabolism, and since our treatment focused on two different carbon sources, similar phenomenon might be at play here that is inducing the L-tyrosine pathway.

Some fungi can produce pyomelanin (DOPA melanin) through a pathway that involves cysteine and DOPA quinine reactions to form various intermediates that are polymerized to generate pheomelanin. Most of the genes involved in the production of DOPA melanin did not show any upregulation in our treatments. Previous studies on *E. dermatitidis* infection did not

show any upregulation of genes involved in DOPA melanin (Poyntner *et al.* 2016) but upregulation of specific laccasses and tyronises was observed at low pH (Chen *et al.* 2014) indicating that specific conditions are required for the activation of the DOPA melanin pathway. Since only the carbon source was changed between the two treatments (YPD and YPG), the cells might not have experienced the required conditions to trigger the activation of the pathway.

3.5.3 Secondary metabolism

In fungi, light is responsible for regulating critical aspects of life cycles including activation of biosynthetic pigments and regulation of melanin production (Tisch and Schmoll 2009; Estrada and Avalos 2008; Corrochano and Garre 2010; Dasgupta *et al.* 2015; Fuller *et al*. 2013; 2015; 2016). In *Neurospora crassa*, blue light has been shown to regulate carotenoid pigment production which is disrupted in mutants lacking the WC-1 or WC-2 photoreceptors (Froehlich *et al.* 2002; He *et al.* 2002). This has also been recorded in *Fusarium* species and *Botrytis cinerea*, where carotenoid pigment development and accumulation are regulated by light (Avalos and Estrada 2010; Canessa *et al*. 2013; Hevia *et al*. 2015). Besides melanin, *E. dermatitidis* is known to produce two carotenoids: torulene and torularhodin (Geis and Szaniszlo 1984). Since *E. dermatitidis* produces both melanin and carotenoids it can be theorized that melanin helps shield the species from light to some extent, which can then be detected by photoreceptor proteins to trigger carotenoid synthesis (Chen *et al.* 2014). Carotenoid production in fungi is triggered by light and most genes involved in secondary metabolism and light sensing did not show upregulation in either the conditional or obligate albinos. Since the cultures were grown in a benchtop incubator with no light:dark cycle inputs, we did not see any accumulation of carotenoids in the albino mutants, or the upregulation of genes involved in secondary

metabolism. This implies that in our mutants under the specific treatment tested, no other secondary metabolites are being produced that can compensate for the loss of melanin.

3.5.4 Cell wall regulation

E. dermatitidis hosts a variety of chitin syntheses which are responsible for cell wall strengthening, cell wall remodelling, and protection from host immune systems (Abramczyk *et al.* 2009). All three conditional albinos had upregulation of multiple chitin synthase genes on YPG compared to YPD. A study conducted on *C. neoformans* demonstrated that mutant *chs3*Δ and *csr2*Δ strains both produced melanin but lost their ability to retain it (Banks *et al*. 2005). In *E. dermatitidis* the deletion mutant *wdchs1*Δ exhibited hyperpigmentation whereas the mutation *wdchs2*Δ did not have much impact on pigmentation (Zheng *et al*. 2006). In our study we saw upregulation of *CHS2* in the wildtype and all three conditional albinos but no upregulation of *CHS1* in either the wildtype or mutant strains. The study conducted by Zheng *et al* (2006) also observed that addition of 1M sorbitol and temperature impacted the pigmentation in the *wdchs1*Δ and *wdchs2*Δ mutants but since our study was conducted at 28°C, the impact of these class 1 and class II synthase genes might not be that strong. In *E. dermatitidis* a class V chitin synthase (WdChs5p) is essential for sustained cell growth during infection and disruptions can lead to impaired melanin externalization affecting cell wall integrity (Liu *et al*. 2004). The upregulation of class V chitinase in the wildtype and the conditional albinos but not the obligate albinos indicates the carbon source is most likely affecting cell wall organization in a manner that also impacts melanization.

3.5.5 Metal acquisition

In fungi, iron plays an essential role in various processes and acts as a cofactor for many different enzymes (Do *et al*. 2020). In pathogenic fungi, iron is a key nutrient for survival in the

host environment where iron availability is limited. To overcome this, many pathogenic fungi have developed methods such as reductive iron transport and use of siderophore and heme uptake systems (Do *et al*. 2020; Voß *et al*. 2020). Siderophores are secondary metabolites that have a high affinity for ferric iron making them crucial for iron acquisition (Choi *et al*. 2024). In a study conducted by Chen *et al.* (2014), it was found that *E. dermatitidis* has multiple iron transport pathways and genes necessary to acquire iron from hosts during infection. This might also enable them to uptake iron from various niches hence providing an advantage against competitive species. In *E. dermatitidis* multiple enzymes responsible for the synthesis for siderophores were found upregulated during skin infection providing evidence of their importance during infection (Poyntner *et* al. 2016; 2018). In our study genes responsible for iron acquisition were found to be significantly downregulated in the wildtype and all our albino strains.

Besides iron, copper also plays an important role in the production of melanin by participating in both the DHN and L-DOPA pathways (Walton *et al*. 2005; Saitoh *et al*. 2010; Eisenman and Casadevall 2015). We did not see any significant upregulation or downregulation of the copper transporter or copper chaperone genes indicating that the nutrient composition of the two treatments did not have a major influence on copper homeostasis.

3.5.6 Carbon utilization

In fungi, D-galactose is catabolized via two different pathways: the Leloir pathway and oxido-reductive catabolic pathway (Fekete *et al*. 2004). Older studies looking at effects of galactose on the growth of fungi observed that galactose has an inhibitory effect on fungal growth (Horr 1936; Edgecombe 1938). In *E. dermatitidis,* upregulation of genes involved in the gluconeogensis pathway and the glyoxylate cycle have been observed during skin infection

(Poyntner *et al.* 2016). This includes the Snf1 kinase which is activated under gluconeogenic conditions leading to the activation of gluconeogensis (Poyntner *et al.* 2016). Since production of DHN-melanin is controlled by the PKS1 pathway in *E. dermatitis,* specific carbon sources might be better suited to produce the starting materials or the intermediates. Different carbon sources may cause shifts in various pathways that might be involved in the production of L-DOPA-melanin or pyomelanin or they might also be better suited to upregulate the expression of genes involved in those pathways.

3.6 Conclusion

The main purpose of this study was to identify genes involved in the melanin recovery of the conditional *alb* mutants during the carbon shift. This was obtained by performing RNA-seq analysis of the three conditional albino mutants (*alb1*, *alb2* and *alb3*) that had the ability to recover melanin production on different carbon sources even with mutations in *PKS1*. RNA-seq analysis demonstrated that the number of DEGs was much higher in the conditional *alb* mutants compared to the two obligate *alb* mutants indicating that fungal melanization might be controlled by multiple different regulatory pathways that work in conjunction with each other. ORA analysis showed GO terms associated with cell membrane and transport were shared between all conditional albino mutants which might play a role in the cell wall deposition of melanin. There was upregulation of genes involved in the 1,8-DHN melanin and pyomelanin and various chitin synthase in all three conditional *alb* mutants indicating that melanization and cell wall regulation in fungi tend to work together. Further experiments can utilize knockout strategies to delete certain genes in the DOPA and pyomelanin pathways such as *tat*, *hppd,* tyrosinase and laccase to observe the effects on melanization in the conditional *alb* mutants. Another approach can be to

utilize IR spectra studies to determine if the melanin produced by the conditional *alb* mutants is similar to the melanin produced by the wildtype.

CHAPTER 4: General discussion and conclusion

Melanin plays a key role in black yeasts helping them adapt to various niches and providing competitive advantages (Wollenzien *et al.* 1995; Rosas and Casadevall 1997; Cordero and Casadevall 2017). Studies have also underlined the effect melanin has on fungal pathogenicity and virulence where mutants lacking melanin showed reduced pathogenicity (Nosanchuk and Casadevall 2003; Fetzner *et al*. 2014; Li *et al*. 2022). Various studies have found that environmental stresses such as UV irradiation, pH, nutrient composition and temperature can have negative impact on black yeasts growth and fitness if there are mutations associated with melanin production leading to reduced melanin production or loss of melanization (Jacobson *et al*. 1995; Wang *et al*. 2018). Chapter 2 of this thesis discusses the loss of pigmentation in *E. dermatitidis* mutant strains and how this impacts their response to various types of stress. Chapter 3 focuses on the identification of genes that are potentially involved in the recovery of melanization in *alb* mutant strains where the pigmentation defect is conditional. This chapter concludes and addresses the overall findings of this thesis, the significance of the results in a broader context, and outlines future studies and directions that can explore the impact of the loss of pigmentation on *E. dermatitidis,* and the genes involved in regulating pigmentation.

4.1.1 Generation and characterization of *E. dermatitidis* mutant strains with different pigmentation phenotypes

E. dermatitidis is a black yeast that produces melanin and is an opportunistic pathogen of humans where it can cause phaeohyphomycosis and skin infections in immunocompromised patients (Garnica *et al.* 2009; de Hoog 2014). The latter has led to a greater interest in gaining a better understanding on the mechanism of melanization and the virulent aspects of *E. dermatitidis*. *E. dermatitidis* is known to produce 1,8-DHN melanin via the Polyketide Synthase (*PKS1*) pathway but the genome annotation has also revealed the presence of genes involved in

the production of L-DOPA melanin and pyomelanin via the L-tyrosine degradation pathway (Chen *et al.* 2014; Poyntner *et al*. 2018).

The goal of this study was to build a repository of *E. dermatitidis* mutants using an unbiased nontargeted UV mutagenesis approach to obtain mutants lacking melanin production or mutants with increased pigmentation. The goal was to use this unbiased genetic screen to determine which of the three pathways contribute to melanin production and to also identify potential pathway regulators or genes associated with melanin production. Previous work on *E. dermatitidis* focused on targeted mutation of the *PKS* gene responsible for the production of 1,8-DHN melanin. The aim of this study was to determine if any other mutations besides those previously noted in *PKS1* could lead to defects in melanin production in *E. dermatitidis*. The mutants obtained in this study could be categorized into albino (*alb*) and hyperpigmented (*hyp*) mutants. All the *alb* mutants shared a mutation in *PKS1*, indicating that *PKS1* is important for melanization in *E. dermatitidis* (Chapter 2). None of the *hyp* mutants had mutations in *PKS1*.

The ability of *E. dermatitidis* to switch from yeast-like to multicellular hyphal forms in response to pH stress (Szaniszlo *et al*. 1976), temperature sensitivity (Roberts and Szaniszlo 1978) and radiation (Dadachova *et al*. 2007; Robertson *et al*. 2012) has been demonstrated previously. All the *alb* mutants showed yeast-like colony appearance and only had two different cell morphologies ranging from yeast-like to budding cells (Chapter 2). The *hyp* mutants showed three different colony appearances (yeast-like, fuzzy and crusty) and five different cell morphologies (yeast-like, budding, chains, pseudohyphae and hyphae) (Chapter 2). The difference in morphology observed in *E. dermatitidis* has been theorized to provide a competitive advantage. Depending on the growth conditions, the ability of *E. dermatitidis* to switch from single cell to a multicellular form might be advantageous. If the substrate is suitable to grow on,

bud formation in *E. dermatitidis* allows cellular growth and when the conditions become restrictive such as during infection or under stress, the hyphal form and yeast buds can transform into thick walled meristematic cells that are, resistant to desiccation and show dormancy and considerable longevity (Oujezdsky *et al*. 1973). In many fungi, chitin acts as a scaffold for cellular membranes and melanin is found inside the cell walls. The colony morphology and different cell types observed in *hyp* mutants could be crucial for the accumulation of melanin in these mutants.

Based on the different phenotypic assays, the overall trend showed that most *hyp* mutants were able to grow similar to or better than the wildtype in most instances whereas most *alb* mutants struggled under similar conditions compared to the wildtype (Chapter 2). This is then in line with various studies that have shown the ability of melanin to provide competitive advantages when dealing with UV and temperature stress. Among the *alb* mutants obtained in this study, three were termed "conditional" due to their ability to restore melanin production when grown on different carbon sources (Chapter 2). As stated previously along with genes for 1,8-DHN melanin production, *E. dermatitidis* also has homologues of genes involved in the production of L-DOPA melanin and pyomelanin (Chen *et al*. 2014). Therefore, the three conditional *alb* mutants were picked for further analysis using RNA transcriptomics to determine if the different carbon sources could have potentially triggered the expression of other melanin biosynthetic pathways (Chapter 3). Since the wildtype produces melanin on all tested carbon sources it would not provide a snapshot of genes involved in other melanin biosynthetic pathways because the production of 1,8-DHN melanin would be constant. If one pathway is already active the need for the upregulation of other pathways might not be necessary.

4.1.2 Genes implicated in the production of melanin in *E. dermatitidis* based on transcriptomics.

Based on RNA-seq and differential gene expression analysis, the wildtype and all five *alb* mutants (three conditional (*alb1*, *alb2* and *alb3*) and two obligate (*alb10* and *alb12*)) behaved differently when grown on D-glucose vs galactose containing media. Overrepresentation analysis (ORA) revealed the presence of significantly enriched GO terms involved in transmembrane transport, transmembrane transporter activity, plasma membrane and zinc ion binding that was shared between all three conditional *alb* mutants but not the wildtype or the obligate *alb* mutants (Chapter 3). Even though the three conditional *alb* mutants all had a nonsynonymous mutation in the *PKS1* (Chapter 3) the type and location of the mutations in the Pks enzyme were not shared. There were some GO terms that were only enriched in one mutant. Other GO terms (DNA-binding transcription factor activity, RNA polymerase II-specific) were only shared between the *alb1* and *alb2* conditional albinos and two GO terms (acyl-CoA dehydrogenase activity and acylformamidase activity) were only shared between the *alb2* and *alb3* conditional albinos (Chapter 3). This demonstrated that even though a shared *PKS1* mutation was observed in all three conditional *alb* mutants and all three had the ability to recover melanin on galactose, they all behaved differentially from each other based on the RNA-seq data. This could potentially be attributed to the differences in the total number of overall SNVs found in the mutant genomes especially if they are high impact, the type of SNVs either being high impact, medium impact, or low impact and the overall impact these SNVs have on various functions observed in these mutants (Chapter 2). This was also observed during the ID32-C strips assays where melanin recovery among the mutant strains varied as to which carbon sources were able to re-store melanin production (Chapter 2). The difference in the number of upregulated and downregulated

genes between all three conditional *alb* mutants and their ability to restore melanin production on different carbon sources indicate that multiple different genes and TFs work in conjunction with each other during fungal melanization.

Based on differential gene expression all three conditional *alb* mutants and one obligate *alb* mutant showed an upregulation of the *PKS1* gene. Since all five mutants had either nonsynonymous or frameshift mutation in *PKS1* there is a possibility that the 1,8-DHN melanin pathway may not have been completely stopped, and the carbon shift might have triggered parts of the pathway, but the overall function of the pathway might be compromised. It can be theorized that the pathway is on at all times, but some mutations can either slow down the pathway or completely stop it. The carbon shift experienced by the mutants might compensate this and allow the pathway to keep going at a slower rate. As mentioned earlier, melanization in fungi can be impacted by nutrient composition and pH, the carbon shift experienced by these mutants might act as some sort of stress signal to the organism which might lead to the upregulation of *PKS1* to increase melanin production. Another key difference between the conditional and the obligate albinos was that many different genes involved in cellular transporters were found to be upregulated in the conditional *alb* mutants (Chapter 3). In fungi, melanin is produced in specialized vesicles that are deposited in the cell wall (Eisenman *et al*. 2009; Camacho *et al*. 2019) where they accumulate. The upregulation of multiple transporters observed in conditional *alb* mutants potentially suggests an increase in melanin deposition via various transporters and vesicle formation.

All three conditional *alb* mutants also shared the GO term for "Zinc Ion binding" which included multiple TFs and transcriptional regulators (Chapter 3). Recent studies have identified the roles of TFs, PKA and Hog1 (Bahn *et al.* 2005; 2007; Lee *et al*. 2019) signalling pathways

and their effects on fungal melanization. The upregulation of multiple TFs genes implicate that these genes might be involved in the recovery of melanin production by triggering the L-DOPA and the tyrosinase degradation pathways. This can be backed up by various genes involved in the tyrosine degradation pathway that were found to be upregulated in all three conditional *alb* mutants but not in the wildtype or the obligate *alb* mutants (Chapter 3).

Production of 1,8-DHN melanin involves several steps and different intermediates are produced along these steps. Based on differential gene expression, genes involved at the various stages of the 1,8-DHN melanin biosynthetic pathway were found to be upregulated in all three conditional *alb* and in one obligate *alb*, this also suggests that all components of the pathway are probably necessary for melanin production. The three conditional *alb* mutants showed nonsynonymous mutation in either the KS or the AT domain which are responsible for elongation of the polyketide backbone or the selection of the extension unit (Li *et al*. 2010), whereas obligate albino *alb10* had a frameshift mutation in the ACP domain which acts as a tether for the growing Polyketide (Chapter 2). The location of where the mutations occurred in *PKS1* may impact the functionality of the expressed protein and this could explain why all three conditional albino mutants and one obligate albino mutant had an upregulation of the *PKS1* gene, yet the obligate *alb* was not able to recover melanin production. As mentioned previously melanization in black yeasts is mediated by specialized vesicles and the genes involved in the various transporters might be crucial for melanin recovery in the conditional *alb* whereas the obligate *alb* lacked that transport mechanism as shown by the RNA-seq data (Chapter 3).

In fungi, chitin plays a key role during fungal melanization and mutant strains with defects in chitin synthesis tend to lose their ability to accumulate melanin leading to a ‘leaky melanin’ phenotype (Zheng *et al*. 2006; Baker *et al*. 2007; Tsirilakis *et al*. 2012). Thus, the

upregulation of multiple chitin synthase genes only in the conditional *alb* mutants might be involved in their ability to recover melanin production. This can be tested by knocking out specific genes such as *chs1* or *chs2* which can lead to negative impact on melanin deposition in *E. dermatitidis* and creates 'leaky' melanin phenotype.

4.1.3 Conclusions

This study is the first to identify conditional *alb* mutants for the polyextremotolerant black yeast *E. dermatitidis*. Colony and cell morphology varied significantly between the *alb* and *hyp* mutants and as observed in other studies conducted on black yeasts, melanin provided competitive advantages to *hyp* mutants under UV and temperature assays. Until now most studies on *E. dermatitidis* have only focused on targeted *PKS1* mutations that led to albino mutant strains, this study is the first to build a repository of *alb* and *hyp* mutants, with the latter exhibiting marked variation in morphology. Based on ORA and differential gene expression analysis, it was observed that even though all three conditional *alb* mutants possessed mutations in *PKS1* and the ability to restore melanin production on multiple different carbon sources, these mutants behaved differently from each other. This was backed up by the phenotypic UV, temperature and ID32-C strips assays where all three mutants yielded different results. Besides *PKS1*, the conditional *alb* did not share any other mutations indicating that the mutants were not isogenic. This was also observed during the RNA transcriptomics analysis where some genes were upregulated in all three conditional *alb* mutants and some genes were only upregulated in one or two conditional *alb* mutant.

This study provided some insight into the recovery of melanization in *E. dermatitidis* during the carbon shift. Melanization is a crucial step in *E. dermatitidis* which helps it to adapt to extreme environments as well as during infections. One thing that was notable regarding the

morphology of *E. dermatitidis* was the fact that only the hyperpigmented mutants possess multicellular hyphal forms and showed a variety of colony morphologies such as fuzzy and crusty whereas all *alb* mutants (both conditional and obligate) displayed yeast-like colony morphology and single yeasts cells. The switch in morphology is thought to be a key adaptation of *E. dermatitidis* during stressful conditions especially during infection. So, it can be theorized that both melanization and colony morphology might have similar triggers that activate those systems. The second key finding was that even with a mutation in *PKS1,* not all *alb* mutants had completely lost their ability to produce melanin. Even though the mutations were nonsynonymous the pathway might not have been completely shut down in some mutants and certain stresses might be able to trigger the activation of the 1,8-DHN melanin biosynthetic pathway again. Are there suppressor mutations or cryptic genes that can be reactivated and compensate for defective Pks1? These are questions for future studies.

Based on the phenotypic, genome sequencing and RNA-seq data, it was observed that all three conditional *alb* behaved differently from each other. The third finding was that there were a wide number of genes involved in various processes that were upregulated in all three conditional *alb* mutants. Some of the genes encode predicted membrane transporters which might play a key role in melanin deposition. Genes involved in the tyrosine degradation pathway were also upregulated indicating that certain stresses might also act as an activator for certain melanin biosynthetic pathways. Overall, the many DEGs (representing many different GO terms) provide evidence that melanin is important for *E. dermatitidis,* and many genes are involved in its production such as genes involved in regulation, signalling pathways, and alternative pathways for melanin production. These results point to functional redundancy where multiple genes can substitute for each other in case of mutations that could be detrimental for the fungus.

There were many genes that were significantly downregulated, but these genes did not correspond to any GO term that was shared between the *alb* mutants meaning that all mutants had different response during the carbon shift.

In summary, the conditional *alb* mutants while growing on galactose presumably somehow compensate for a defective Pks1 enzyme via an apparent range of mechanisms or expressing alternate genes that allow for melanin production and deposition into the cell wall of *E. dermatitidis*.

4.1.4 Future directions

Melanin as a biomolecule has been known for over 150 years. Most studies on melanin have focused on its roles in virulence, in pathogens infecting humans, animals and plants. Other research has highlighted the benefits of melanin to fungi such as protection from environmental stress that enable them to grow in harsh environments. Melanin pigments are complex polymers whose diversity has made it challenging to investigate their structural properties. However, better extraction protocols coupled with the identification of genes and factors involved in the regulation of melanin biosynthesis have enabled researchers to gain a better understanding of fungal melanization. The biosynthetic pathways for the main types of melanin 1,8 DHN-melanin and L-DOPA melanin are well known but recently focus has shifted towards identifying the various TFs and signalling pathways that regulate melanin production. TFs can act as either an activator or a repressor depending on where the TFs bind to their target DNA. Recent work has also provided insight into the regulation of melanin by the cAMP/PKA and the MAPK Hog1 pathways, including links between these pathways and downstream TFs (Lee et al., 2019; Cordero et al., 2020). The level of complexity underlying these links so far has only been explored extensively in *C. neoformans* (Jung et al., 2015; Lee et al., 2019; Cordero et al., 2020),

this suggests that comparable systems-level studies are needed in other fungi such as *E. dermatitidis* to determine the extent, if any, to which regulatory features are conserved across the fungi.

Different stresses can stimulate conditions necessary to produce melanin and the ability of some fungi to produce different types of melanin via the DHN or L-DOPA melanin pathway that can act as a failsafe mechanism if specific conditions for a particular type of melanin production pathway are not met. Understanding the mechanisms that control different melanin biosynthetic pathways in one fungal species can then be extrapolated to other related fungi. In our study the results demonstrated that some of those failsafe mechanisms can be triggered if certain conditions are met.

One of the major limitations of this study include the lack of robust annotation of the *E. dermatitidis* genome. Even though the genome of *E. dermatitidis* has been annotated there are only about 43% of genes that have been annotated excluding hypothetical or putative proteins and less than 5% of genes are annotated with Enzyme Commission (EC) numbers (Schroeder et al., 2020). Most of the SNVs obtained in this study correspond to hypothetical proteins making it hard to predict their function in the organism. The other limitation in this study was the lack of research on *E. dermatitidis* in general. Until now most studies on *E. dermatitidis* have focused on virulence mechanisms investigating the role of melanization on virulence. The lack of phenotypic studies such as effects of media, temperature and nutrient composition on mutants with more than one targeted mutation performed in this fungus have left a gap in the research that our study tries to fill by establishing how different mutations can affect overall growth and melanization of *E. dermatitidis*.

Future studies need to focus on the discovery and characterization of additional genes and TFs in fungal species that have homologues for different melanin biosynthetic pathways. Advancements and cost effectiveness of RNA transcriptomics can make it easier to identify novel genes and transcripts that are expressed under different conditions. Since melanin production is largely affected by different stresses, RNA-seq can help identify certain genes that are expressed under different conditions. Since only a subset of obligate mutants were picked for RNA-seq analysis, future work can focus on the remaining obligate *alb* mutants which can provide a better understanding on why one obligate *alb* mutant (*alb10*) behaved differently than the other obligate *alb* mutant (*alb12*). This will also allow us to focus on if there is any significant difference between the obligate *alb* mutant response to carbon shift if the *PKS1* mutation is nonsynonymous or nonsense in addition to frameshift mutation which was already tested. In addition to RNA-seq, CRISPR/cas9 reverse genetic strategies can be used to target and knock out specific genes which are potentially involved in regulating different melanin biosynthetic pathways. Genes known to play a key role in melanization in other fungi besides *PKS1,* such as PKA, Hog1 and multiple TFs including Cmr1 can be a starting point for such studies. Identification of the type of melanin produced by the conditional *alb* would also back up the data obtained using RNA transcriptomics and determine what genes determine the type of melanin that is being produced under different conditions and if the other melanin biosynthetic pathways are capable of producing melanin if 1,8-DHN melanin pathway is disrupted in *E. dermatitidis*. Spectroscopic techniques such as Ultraviolet-visible (UV-VIS) and Electron Paramagnetic Resonance (EPR) can be used to identify types of melanin present in the fungus. In a similar fashion some chemical assays such as different acids that inhibit growth of either DHN or L-DOPA melanin can also be used to identify the type of melanin the organism is producing.

Since in medical mycology the type of melanin that a fungus plays a key role in the type of antifungals that are administrated, by knowing if *E. dermatitidis* is producing 1,8-DHN, DOPA or pyomelanin during infection, proper antifungal drugs to fight off the infection can be administrated.

A more robust mechanistic understanding of the signaling pathways and TFs involved in fungal melanization will help in harnessing the potential benefits of melanin as bio-based components of sunscreens, natural food coloring agents and packaging materials. These applications have generated more interest in understanding regulatory pathways that can be manipulated to increase the concentration of melanin. In addition, melanin biosynthetic pathways produce many intermediates that have different properties. By genetically modifying strains to hamper or enhance the production of certain intermediates in these biosynthetic pathways, extraction and yield of the beneficial intermediates can be increased. Another way to increase melanin yield can be to genetically modify strains that leads to the expression of tyrosinases or laccases that play a key role in melanin production. Since melanin production is affected by environmental conditions, experimenting with nutrient composition and growth conditions such as pH, temperature and aeration may impact the yield of melanin as well.

At this time, it is fair to assume that additional pathways that regulate melanin production beyond those already known remain to be discovered. Systems-level studies that leverage new genetic and genomic-based resources in emerging polyextremotolerant fungi represent a promising approach towards addressing this challenge. Insights generated by such studies would provide a much more comprehensive understanding of how fungi coordinate melanin production with specific environmental inputs. For example, in those fungi capable of producing multiple types of melanin, do specific inputs direct the synthesis of a particular type of melanin? Obvious benefits

derived from such findings include enhanced capacities to engineer melanin production for specific applied purposes. Moreover, they would also create opportunities to delve into broader evolutionary questions regarding the role(s) that the regulation of melanin synthesis might have played in facilitating the adaptation of polyextremotolerant fungi to harsh environmental niches and in some instances their ability to be pathogenic on plant and animals.

Data availability

All data necessary for confirming the conclusions presented in this manuscript are present within the document, figures, and tables. Strains are available upon request. All DNA sequences (read files for SNV analysis) have been deposited under the NCBI BioProject accession: PRJNA1233822 (Chapter 2). All RNA raw sequence reads (RNA-seq analysis) have been deposited under the BioProject accession: PRJNA1196592 (Chapter 3).

Supplemental File breakdown

Supplemental File 1= Pages 196-199

Supplemental File 2= Pages 200-202

Supplemental File 3= Pages 203-239

References:

Abramczyk D, Park C, Szaniszlo PJ. 2009. Cytolocalization of the class V chitin synthase in the yeast, hyphal and sclerotic morphotypes of *Wangiella* (*Exophiala*) *dermatitidis*. *Fungal Genet. Biol*. 46(1): 28-41. doi: 10.1016/j.fgb.2008.10.004.

Adachi K, Hamer JE. 1998. Divergent cAMP signaling pathways regulate growth and pathogenesis in the rice blast fungus *Magnaporthe grisea*. *Plant Cell*. 10(8): 1361–1373. https://doi.org/10.2307/3870646.

Alspaugh JA, Perfect JR, Heitmann J. 1997. *Cryptococcus neoformans* mating and virulence are regulated by the G-protein a-subunit GPA1 and cAMP. *Genes Dev*. 11(23): 3206–3217. doi: 10.1101/gad.11.23.3206.

Alspaugh JA, Perfect JR, Heitmann J. 1998. Signal transduction pathways regulating differentiation and pathogenicity of *Cryptococcus neoformans*. *Fungal Genet Biol*. 25(1): 1–14. doi: https://doi.org/10.1006/fgbi.1998.1079.

Alspaugh JA. 2015. Virulence mechanisms and *Cryptococcus neoformans* pathogenesis. *Fungal Genet. Biol*. 78: 55–58. https://doi.org/10.1016/j.fgb.2014.09.004.

Ambrico M. 2016. Special Issue: Melanin, a long-lasting history bridging natural pigments and organic bioelectronics. *Polym. Int*. 65(11): 1249–1250. doi:10.1002/pi.5239.

Andrews S. 2010. *FastQC* A quality control tool for high throughput sequence data. http://www.bioinformatics.babraham.ac.uk/projects/fastqc/

Avalos J, Estrada AF. 2010. Regulation by light in *Fusarium*. *Fungal Genet. Biol*. 47(11): 930-938. doi: 10.1016/j.fgb.2010.05.001.

Bahn Y, Kojima K, Cox GM, Heitman J. 2005. Specialization of the HOG pathway and its impact on differentiation and virulence of *Cryptococcus neoformans*. *Mol. Biol. Cell*. 16(5): 2285-2300. https://doi.org/10.1091/mbc.e04-11-0987.

Bahn Y, Geunes-Boyer S, Heitman J. 2007. Ssk2 mitogen-activated protein kinase kinase kinase governs divergent patterns of the stress activated Hog1 signalling pathway in *Cryptococcus neoformans*. *Eukaryot. Cell*. 6(12): 2278-2289. https://doi.org/10.1128/ec.00349-07.

Baker LG, Specht CA, Donlin MJ, Lodge JK. 2007. Chitosan, the deacetylated form of chitin, is necessary for cell wall integrity in *Cryptococcus neoformans*. *Eukaryot. Cell*. 6(5): 855-867. https://doi.org/10.1128/ec.00399-06.

Banks IR, Specht CA, Donlin MJ, Gerik KJ, Levitz SM, Lodge JK. 2005. A chitin synthase and its regulator protein are critical for chitosan production and growth of the fungal pathogen *Cryptococcus neoformans*. *Eukaryot. Cell.* 4(11): 1902-12. doi: 10.1128/EC.4.11.1902-1912.2005.

Barrick JE, Colburn G, Deatherage DE, Traverse CC, Strand MD, Borges JJ, et al. 2014. Identifying structural variation in haploid microbial genomes from short-read resequencing data using breseq. *BMC Genomics*. 15(1): 1039. doi: 10.1186/1471-2164-15-1039 .

Basarab GS, Jordan DB, Gehret TC, Schwartz RS, Wawrzak Z. 1999. Design of scytalone dehydratase inhibitors as rice blast fungicides: derivatives of norephedrine. *Bioorg. Med. Chem. Lett*. 9(11): 1613–1618. doi: 10.1016/s0960-894x(99)00247-4.

Bayram O, Krappmann S, Ni M, Bok JW, Helmstaedt K, Valerius O, et al. 2008. VelB/VeA/LaeA complex coordinates light signal with fungal developmental and secondary metabolism. *Science*. 320(5882): 1504-1506. doi: 10.1126/science.1155888.

Bayry J, Beaussart A, Dufrene YF, Sharma M, Bansal K, Kniemeyer O, et al. 2014. Surface structure characterization of *Aspergillus fumigates* conidia mutated in the melanin synthesis pathway and their human cellular immune response. *Infect Immun.* 82(8): 3141-3153. doi: 10.1128/IAI.01726-14.

Bell AA, Puhalla JE, Tolmsoff WJ, Stipanovic RD. 1976. Use of mutants to establish (+)-scytalone as an intermediate in melanin biosynthesis by *Verticillium dahliae*. *Can. J. Microbiol*. 22(6): 787–799. https://doi.org/10.1139/m76-115.

Bell AA, Wheeler MH. 1986. Biosynthesis and functions of fungal melanins. *Ann. Rev. Phytopathol*. 24. 411-451. doi: 10.1146/annurev.py.24.090186.002211.

Beniwal AM, das AK, Nishant h, Rathod P, Tandon R. 2023. A rare case of *Exophiala dermatitidis* graft infection. *Indian J Ophthalmology.* 3(3): 671-672. doi: 10.4103/IJO.IJO_2907_22 .

Belozerskaya TA, Gessler NN, Aver'yanov AA. 2016. Melanin Pigments of Fungi, in: Merillon J-M, Ramawat KG (Eds), *Fungal Metabolites*. Springer International Publishing, Cham, pp. 1–29.

Beltran-Garcia MJ, Prado FM, Oliveira MS, Ortiz-Mendoz D, Scalfo AC, Pesso Jr A, et al. 2014. Singlet molecular oxygen generation by light activated DHN melanin of the fungal pathogen *Mycophaerella fijiensis* in Black Sigatoka Disease of Bananas. *PLoS One*. 19(3): e91616. https://doi.org/10.1371/journal.pone.0091616.

Berger JS, Cusumano LR, Derose JJ, Sarwar UN, Talhari S. 2017. *Exophiala* (*Wangiella*) *dermatitidis* prosthetic aortic valve endocarditis and prosthetic graft infection in an immune competent patient. *Case. Rep. Infect. Dis*. 2017: p.4839314-4. doi: 10.1155/2017/4839314.

Bienert S, Waterhouse A, de Beer TAP, Tauriello G, Studer G, Bordolo L, et al. 2017. The SWISS-MODEL Repository- new features and functionality. *Nucleic Acids Res*. 45(D1): D313-D319. doi: 10.1093/nar/gkw1132 .

Bisko NA, Shcherba VV, Mitropolskaya NY. 2007. Study of melanin complex from medicinal mushroom *Phellinus robustus*. *Int. J. Med. Mushrooms*. 9(2): 177-184. doi:10.1615/IntJMedMushr.v9.i2.80.

Bingle LE, Simpson TJ, Lazarus CM. 1999. Ketosynthase domain probes identify two subclasses of fungal polyketide synthase genes. *Fungal Genet Biol*. 26(3): 209–223. doi: 10.1006/fgbi.1999.1115 .

Blanc PJ, Loret MO, Goma G. 1995. Production of citrinin by various species of *Monascus. Biotechnol. Lett*.17: 291–294. https://doi.org/10.1007/BF01190639.

Blin K, Shaw S, Augustijn HE, Reitz ZL, Biermann F, Alanjary M, et al. 2023. antiSMASH 7.0: new and improved predictions for detection, regulation, chemical structures and visualisation. *Nucleic Acids Res*. 51(W1): W46-W50. doi: https://doi.org/10.1093/nar/gkad344.

Bloomfield BJ, Alexander M. 1967. Melanins and resistance of fungi to lysis. *J. Bacteriol*. 93(4): 1276– 1280. doi: 10.1128/jb.93.4.1276-1280.1967.

Borovanský J. 2011. History of Melanosome Research. In melanins and melanosomes; *John Wiley & Sons: Hoboken*, NJ, USA. pp. 1–19.

Brakhage AA, Liebmann B. 2005. *Aspergillus fumigatus* conidial pigment and cAMP signal transduction: significance for virulence. *Med. Mycol*. 43: S75-S82. https://doi.org/10.1080/13693780400028967.

Brush L, Money NP. 1999. Invasive hyphal growth in *Wangiella dermatitidis* is induced by stab inoculation and shows dependence upon melanin biosynthesis. *Fungal Genet. Biol*. 28(3): 190-200. doi: 10.1006/fgbi.1999.1176.

Bulloch MN. 2011. The treatment of pulmonary *Wangiella dermatitidis* infection with oral voriconazole. *J. Clin. Pharm. Ther*. 36(3): 433-436. doi: 10.1111/j.1365-2710.2010.01214.x

Buszman E, Pilawa B, Zdybel M, Wilczynski S, Gondzik A, Witoszynska T, et al. 2006. EPR examination of Zn2+ and Cu2+ binding by pigmented soil fungi *Cladosporium cladosporioides*. *Sci. Total Environ*. 363(1-3): 195–205. doi: 10.1016/j.scitotenv.2005.05.028.

Butin H, Pehl L, de Hoog GS, Wollenzien U. 1996. Trimmatostroma abietis sp. nov. (Hyphomycetes) and related species. *Antonie van Leeuwenhoek.* 69(3): 203–209. doi: 10.1007/BF00399607 .

Butler MJ, Lazarovits G, Higgins VJ, Lachance MA. 1989. Identification of a black yeast isolated from oak bark as belonging to genus *Phaecoccomyces* sp. Analysis of melanin produced by the yeast. *Can. J. Microbiol*. 35(7): 728-734. doi:10.1139/m89-118.

Butler MJ. Day AW. 1998. Fungal melanins: a review. *Can. J. Microbiol*. 44(12):1115-1136. doi: https://doi.org/10.1139/w98-119.

Camacho E, Vij R, Chrissian C, Prados-Rosales R, Gil D, O'Meally RN, et al. 2019. The structural unit of melanin in the cell wall of the fungal pathogen *Cryptococcus neoformans*. *J. Biol. Chem*. 294(27): 10471-10498. doi: 10.1074/jbc.RA119.008684.

Campanhol BS, Ribeiro BD, Casellato F, Medina KJD, Sponchiado SRP. 2023. Improvement of DOPA-melanin production by *Aspergillus nidulans* using eco-friendly and inexpensive substrates. *J Fungi*. 29(9): 714. doi: 10.3390/jof9070714 .

Canessa P, Schumacher J, Hevia MA, Tudzynski P, Larrondo LF. 2013. Assessing the effects of light on differentiation and virulence of the plant pathogen *Botrytis cinerea*: characterization of the White Collar Complex. *PloS ONE*. 8: p.e84223. https://doi.org/10.1371/journal.pone.0084223.

Cao W, Zhou X, McCallum NC, Hu Z, Ni QZ, Kapoor U, et al. 2021. Unraveling the structure and function of melanin through synthesis. *J. Am. Chem. Soc*. 143(7):2622–2637. doi: 10.1021/jacs.0c12322.

Carr EC, Barton Q, Grambo S, Sullivan M, Renfro CM, Kuo A, et al. 2023. Characterization of a novel polyextremotolerant fungus, *Exophiala viscosa*, with insights into its melanin regulation and ecological niche. *G3*, 13(8): jkad110. doi: 10.1093/g3journal/jkad110 .

Carr E, Bredeweg EL, Hamilton GE, Kurbessoian T, Williams AM. 2025. Pathogenic potential of polyextremotolerant fungi in a warming world. *PLoS Pathogens*. 21(4): e1013102. https://doi.org/10.1371/journal.ppat.1013102.

Casadevall A, Nakouzi A, Crippa PR, Eisner M. 2012. Fungal melanins differ in planar stacking distances. *PLoS One.* 7(2): e30299. https://doi.org/10.1371/journal.pone.0030299.

Caza M, Kronstad JW. 2019. The cAMP/Protein Kinase A pathway regulates virulence and adaptation to host conditions in *Cryptococcus neoformans*. *Front. Cell. Infect. Microbiol*. 9: 212. doi: 10.3389/fcimb.2019.00212 .

Chatterjee S, Prados-Rosales R, Itin B, Casadevall A, Stark RE. 2015. Solid-state NMR reveals the carbon-based molecular architecture of *Cryptococcus neoformans* fungal eumelanins in the cell wall. *J. Biol. Chem*. 290(22): 13779-13790. doi: 10.1074/jbc.M114.618389.

Chen Z, Martinez DA, Gujja S, Sykes SM Zeng Q, Szaniszlo PJ, et al. 2014. Comparative genomic and transcriptomic analysis of *Wangiella dermatitidis*, a major cause of phaeohyphomycosis and a model black yeast human pathogen. *G3*. 4(4): 561-578. doi: 10.1534/g3.113.009241.

Chen M, Zhang J, Dong Z, Wang E. 2016. Cutaneous phaeohyphomycosis caused by *Exophiala dermatitidis*: A case report and literature review. *Indian J. Dermatol. Venereol Leprol.*82(2): 173-177. doi: 10.4103/0378-6323.171013.

Chen X, Zhy C, Na Y, Ren D, Zhang C, He Y, et al. 2021. Compartmentalization of melanin biosynthetic enzymes contributes to self-defense against intermediate compound scytalone in *Botrytis cinerea*. *mBIO*. 12(2): e00007-21. doi: 10.1128/mBio.00007-21 .

Chen L, Tsai H, Yu P, Chung K. 2017. A major facilitator superfamily transporter-mediated resistance to oxidative stress and fungicides requires Yap1, Skn7, and MAP kinases in the citrus fungal pathogen *Alternaria alternata*. *PLoS One*. 12(1): e0169103. doi: 10.1371/journal.pone.0169103.

Chethana KWT, Jayawardena RS, Chen Y, Konta S, Tibpromma S, Abeywickrama PD, et al. 2021. Diversity and function of appresoria. *Pathogens* 10(6): 746. doi: 10.3390/pathogens10060746.

Chicco D, Agapito G. 2022. Nine quick tips for pathway enrichment anaylsis. *PLoS Comput. Biol.* 18(8): e1010348. https://doi.org/10.1371/journal.pcbi.1010348.

Chitale A, Jadhav DV, Waghmare SR, Sahoo AK, Ranveer RC. 2012. Production and characterization of brown coloured pigment from *Trichoderma viride*. *Electron. J. Environ. Agric. Food Chem.* 11(5): 529–537.

Chhoker K, Hausner G, Harris D. 2025a. Regulation of melanin production in fungi. *Front. Fungal Biol.* 6: doi: 10.3389/ffunb.2025.1621764.

Chhoker K, Hausner G, Harris D. 2025b. Genetic analysis of pigment production in the fungus *Exophiala dermatitidis*. *bioRxiv* 2025.03.19.644242. doi: https://doi.org/10.1101/2025.03.19.644242

Cho Y, Srivastava A, Ohm RA, Lawrence CB, Wang K, Grigoriev IV, et al. 2012. Transcription factor Amr1 induces melanin biosynthesis and suppresses virulence in *Alternaria brassicicola*. *PLoS Pathogens* 8(10): e1002974. https://doi.org/10.1371/journal.ppat.1002974.

Choi J, Jung WH, Kronstad JW. 2015. The CAMP/Protein kinase A signaling pathway in pathogenic basidiomycete fungi: Connections with iron homeostasis. *J. Microbiol*. 53(9): 579–587. doi: 10.1007/s12275-015-5247-5.

Choi S, Kronstad JW, Jung WH. 2024. Siderophore biosynthesis and transport systems in model and pathogenic fungi. *J. Microbiol. Biotechnol*. 34(8): 1151-1562. https://doi.org/10.4014/jmb.2405.05020.

Chomnunti P, Bhat DJ, Jones EBG, Chukeatirote E, Bahkali AH, Hyde KD. 2012. *Trichomeriaceae*, a new sooty mold family of *Chaetothyriales*. *Fungal Diversity*. 56(1): 63-76. doi: 10.1007/s13225-012-0197-2

Coleine C, Stajich J.E, Selbmann L. 2022. Fungi are key players in extreme ecosystems. *TREE*. 37(6): 517-528. doi: 10.1016/j.tree.2022.02.002 .

Cecchini MM, Reale S, Manini P, d'Ischia M, De Angelis F. 2017. Modeling fungal melanin buildup: Biomimetic polymerization of 1,8-Dihydroxynaphthalene mapped by mass spectrometry. *Chemistry*. 23(33): 8092−8098. doi: 10.1002/chem.201701951.

Colarusso A, Williams A, Gladfelter AS, Wirshing ACE, Lew DJ. 2025. Optimized vectors for genetic engineering of *Aureobasidium pullulans*. *bioRxiv*. Jan 27:2025.01.25.634885. doi: 10.1101/2025.01.25.634885.

Cordero RJB, Casadevall A. 2017. Functions of fungal melanin beyond virulence. *Fungal Biol. Rev*. 31(2): 99-112. doi: 10.1016/j.fbr.2016.12.003 .

Cordero RJB, Robert V, Cardinali G, Arinze ES, Thon SM, Casadevall A. 2018. Impact of yeast pigmentation on heat capture and latitudinal distribution. *Current Biol*. 28(16): 2657-2664. doi:10.1016/j.cub.2018.06.034.

Cordero RJB, Camacho E, Casadevall A. 2020. Melanization in *Cryptococcus neoformans* requires complex regulation. *mBIO*. 11(1): e03313-19. doi: 10.1128/mBio.03313-19.

Corrochano LM, Garre V. 2010. Photobiology in the Zygomycota: multiple photoreceptor genes for complex responses to light. *Fungal. Genet. Biol*. 47(11):893–899. https://doi.org/10.1016/j.fgb.2010.04.007.

Corrochano LM, Kuo A, Marcet-Houben M, Polaino S, Salanov A. et al. 2016. Expansion of signal transduction pathways in fungi by extensive genome duplication. *Current Biology*. 26(12): 1577-1584. doi: 10.1016/j.cub.2016.04.038.

Costin GE, Hearing VJ. 2007. Human skin pigmentation: melanocytes modulate skin color in response to stress. *FASEB J*. 21(4): 976–994. doi: 10.1096/fj.06-6649rev.

Crous PW, Schubert K, Braun U, de Hoog GS, Hocking AD, Shin HD, et al. 2007. Opportunistic, human-pathogenic species in the *Herpotrichiellaceae* are phenotypically similar to saprobic or phytopathogenic species in the *Venturiaceae*. *Stud. Mycol*. 58(1): 185-217. doi: 10.3114/sim.2007.58.07.

Dadachova E, Bryan RA, Huang X, Moadel T, Schweitzer AD, Aisen P, et al. 2007. Ionizing radiation changes the electronic properties of melanin and enhances the growth of melanized fungi. *PLoS one*. 2(5): p.e457. doi: https://doi.org/10.1371/journal.pone.0000457.

Dasgupta A, Chen C, Lee C, Gladfelter AS, Dunlap JC, Loros JJ. 2015. Biological significance of photoreceptor photocycle length: VIVID photocycle governs the dynamic VIVID-white collar complex pool mediating photo-adaption and response to changes in light intensity. *PLoS Genetics*. 11(5): p.e1005215. https://doi.org/10.1371/journal.pgen.1005215.

Dean RA. 1997. Signal pathways and appressorium morphogenesis. *Annu. Rev. Phytopathol*. 35(1): 211-234. doi: 10.1146/annurev.phyto.35.1.211 .

Deatherage DE, Barrick JE, Sun L, Shou W. 2014. Identification of mutations in laboratory evolved microbes from next-generation sequencing data using breseq. *Methods Mol. Biol*. 1151: 165-188. doi: 10.1007/978-1-4939-0554-6_12.

Debler JW, Henares BM. 2020. Targeted disruption of scytalone dehydratase gene using *Agrobacterium tumefaciens*-mediated transformation leads to altered melanin production in *Ascochyta lentis*. *J. Fungi (Basel)* 6(4): 314. doi: 10.3390/jof6040314.

de Hoog GS, Hermanides-Nijhof EJ. 1977. The black yeasts and allied Hyphomycetes. *Studies in Mycology*. 15:1-222.

de Hoog GS, Takeo K, Yoshida S, Gottlich E, Nishimura K, Miyaji M. 1994. Pleoanamorphic life cycle of *Exophiala* (*Wangiella*) *dermatitidis*. *Antonie van Leeuwenhoek*. 65(2): 143-153. doi: 10.1007/BF00871755.

de Hoog GS. 1999. Ecology and evolution of black yeasts and their relatives. *Stud. Mycol*. 43: 1-208.

de Hoog GS, Vicente VA, Najafzadeh MH, Harrak MJ, Badali H, Seyedmousavi S. 2011. Waterborne *Exophiala* species causing disease in cold-blooded animals. *Persoonia*. 27: 46-72. doi: 10.3767/003158511X614258.

de Hoog GS. 2014. Ecology and phylogeny of black yeast-like fungi: diversity in unexplored habitats. *Fungal Divers*. 65(1): 1-2. doi: 10.1007/s13225-014-0284-7.

de Jonge R, Ebert MK, Huitt-Roehl CR, Pal P, Suttle JC, Spanner RE, et al. 2018. Gene cluster conservation provides insight into cercosporin biosynthesis and extends production to the genus *Colletotrichum*. *Proc. Natl. Acad. Sci. USA.* 115:E5459–E5466. https://doi.org/10.1073/pnas.1712798115.

Diaz MH, Pedemonte CC. 2013. Emerging melanin protective pigment in the brain of *Xenopus laevis* to protect from the effects of UV radiation. *Int. J. Morph*. 31(3): 1120-1123. doi: 10.4067/S0717-95022013000300055 .

D'Ischia M. Wakamatsu K, Napolitano A, Briganti S, Garcia-Borron J, Kovacs D, et al. 2013. Melanins and melanogenesis: methods, standards, protocols. *Pigment Cell Melanoma Res* 26(5): 616-633. DOI: 10.1111/pcmr.12121.

Dighton J, Tugay T, Zhdanova N. 2008. Fungi and ionizing radiation from radionuclides. *FEMS Microbiol. Lett.* 281(2): 109-120. https://doi.org/10.1111/j.1574-6968.2008.01076.x.

Dixon DM, Polak A, Szaniszlo PJ. 1987. Pathogenicity and virulence of wild-type and melanin-deficient *Wangiells dermatitidis*. *J. Med. Vet. Mycol*. 25(2): 97-106. doi: 10.1080/02681218780000141.

Dixon DM, Polak A, Conner GW. 1989. Mel-negative mutants of *Wangiella dermatitidis* in mice: evaluation of multiple mouse and fungal strains. *J. Med. Vet. Mycol*. 27(5): 335-342.

Do E, Cho Y, Kim D, Kronstad JW, Jung WH. 2020. A transcriptional regulatory map of iron homeostasis reveals a new control circuit for capsule formation in *Cryptococcus neoformans*. *Genetics*. 215(4): 1171-1189. doi: 10.1534/genetics.120.303270.

Döğen A, Iikit M, de Hoog GS. 2013. Black yeast habitat choices and species spectrum on high altitude creosote-treated railways ties. *Fungal biol*. 117(10): 692-696. doi: 10.1016/j.funbio.2013.07.006

D'Souza CA, Alspaugh JA, Yue C, Harashima T, Cox GM, Perfect JR, et al. 2001. Cyclic AMP-dependent protein kinase controls virulence of the fungal pathogen *Cryptococcus neoformans*. *Mol. Cell Biol*. 21(9): 3179–3191. doi: 10.1128/MCB.21.9.3179-3191.2001 .

Du L. Lou L. 2010. PKS and NRPS release mechanisms. *Nat. Prod. Rep.* 27(2):255-278. doi: 10.1039/b912037h .

Dullah S, Hazarika DJ, Goswami G, Borgohain T, Ghosh A, Barooah M, et al. 2021. Melanin production and laccase mediated oxidative stress alleviation during fungal-fungal interaction among basidiomycete fungi. *IMA Fungus*. 12(1): 33. doi: 10.1186/s43008-021-00082-y.

Ebert MK, Spanner RE, Jonge E, Smith DJ, Holthusen J, Secor GA, et al. 2018. Gene cluster conservation identifies melanin and perylenequinone biosynthesis pathways in multiple plant pathogenic fungi. *Environ. Microbiol.* 21(3): 913-927. doi: 10.1111/1462-2920.14475 .

Edgecombe AE. 1938. The effect of Galactose on the growth of certain fungi. *Mycologia*. 30(6): 601-624. https://www.jstor.org/stable/3754358.

Eisenman HC, Nosanchuk JD, Webber JBW, Emerson RJ, Camesano TA, Casadevall A. 2005. Microstructure of cell wall-associated melanin in the human pathogenic fungus *Cryptococcus neoformans. Biochem*. 44(10): 3683-3693. https://doi.org/10.1021/bi047731m.

Eisenman HC, Mues M, Weber SE, Frases S, Chaskes S, Gerfen G, et al. 2007. *Cryptococcus neoformans laccase* catalyses melanin synthesis from D- and L-DOPA. *Microbiology*. 152(Pt12): 3954-3962. doi: 10.1099/mic.0.2007/011049-0.

Eisenman HC, Frases S, Nicola AM, Rodrigues ML, Casadevall A. 2009. Vesicle-associated melanization in *Cryptococcus neoformans*. *Microbiol.* 155: 3860–3867. doi: 10.1099/mic.0.032854-0.

Eisenman HC, Casadevall A. 2012. Synthesis and assembly of fungal melanin. *Appl. Microbiol. Biotechnol.* 93(3): 931-940. doi: 10.1007/s00253-011-3777-2.

El-Bialy HA, El-Gamal MS, Elsayed MA, Saudi HA, Khalifa MA. 2019. Microbial melanin physiology under stress conditions and gamma radiation protection studies. *Radiat. Phys. Chem.* 162:178−186. https://doi.org/10.1016/j.radphyschem.2019.05.002.

Eliahu N, Igbaria A, Rose MS, Horwitz BA, Lev S. 2007. Melanin biosynthesis in the maize pathogen *Cochliobolus heterostrophus* depends on two mitogen-activated protein kinases, Chk1 and Mps1, and the transcription factor Cmr1. *Eukaryot. Cell*. 6(3): 421-429. https://doi.org/10.1128/ec.00264-06.

Endo K, Kamo K, Hosono K, Bepu T, Ueda K. 2001. Characterization of mutants defective in melanogenesis and a gene for tyrosinase of *Streptomyces griseus*. *J. Antibiot*. (Tokyo). 54(10): 789-796. doi: 10.7164/antibiotics.54.789 .

Erdmann EA, Nitsche S, Gorbushina AA, Schumacher J. 2022. Genetic engineering of the rock inhabitant *Knufia petricola* provides insight into the biology of extremotolerant black fungi. *Frontiers*. *Fungal*. *Biol*. 3: 862429. doi: 10.3389/ffunb.2022.862429.

Esher SK, Zaragoza O, Alspaugh JA. 2018. *Cryptococcal* pathogenic mechanisms: a dangerous trip from the environment to the brain. *Mem. Inst. Oswaldo Cruz*. 113, e180057. doi: 10.1590/0074-02760180057 .

Estrada A, Avalos J. 2008. The White-Collar protein WcoA of *Fusarium fujikaroi* is not essential for photocarotenogenesis, but is involved in the regulation of secondary metabolism and conidiation. *Fungal Genet. Biol*. 45(5): 705-715. doi: 10.1016/j.fgb.2007.12.003.

Ewels P, Magnusson M, Lundin S, Käller M. 2016. MultiQC: summarize analysis results for multiple tools and samples in a single report. *Bioinformatics*. 32(19), 3047–3048. https://doi.org/10.1093/bioinformatics/btw354.

Fang QH, Zhong JJ. 2002. Submerged fermentation of higher fungus *Ganoderma lucidum* for production of valuable bioactive metabolites-ganoderic acid and polysaccharide. *Biochem. Eng. J.* 10(1): 61-66. doi: https://doi.org/10.1016/S1369-703X(01)00158-9.

Fekete E, Karaffa L, Sándor E, Banyai I, Seiboth B, Gyemant G, et al. 2004. The alternative d-galactose degrading pathway of *Aspergillus nidulans* proceeds via l-sorbose. *Arch. Microbiol.* 181(1) 35–44. https://doi.org/10.1007/s00203-003-0622-8.

Feng B, Wang X, Hauser M, Kaufmann S, Jentsch S, Haase G. 2001. Molecular cloning and characterization of *WdPKS1*, a gene involved in dihydroxynaphthalene melanin biosynthesis and virulence in *Wangiella* (*Exophiala*) *dermatitidis*. *Infect. Immun*. 69(3): 1781-1794. doi: 10.1128/IAI.69.3.1781-1794.2001.

Fernandes C, Mota M, Barros L, Dias MI, Ferreira ICF, Piedade AP, et al. 2021. Pyomelanin synthesis in *Alternaria alternata* inhibits DHN-melanin synthesis and decreases cell wall chitin content and thickness. *Front. Microbiol.* 27(12): 691433. doi: 10.3389/fmicb.2021.691433.

Fetzner R, Seither K, Wenderoth M, Herr A, Fishcer R. 2014. *Alternaria alternata* transcription factor CmrA controls melanization and spore development. *Microbiol*. 160(9): 1845-1854. doi: 10.1099/mic.0.079046-0 .

Fogarty RV, Tobin JM. 1996. Fungal melanins and their interactions with metals. *Enzyme Microb. Technol*. 19(4): 311–317. doi: 10.1016/0141-0229(96)00002-6.

Freese NH, Norris DC, Loraine AE. 2016. Integrated genome browser: Visual analytics platform for genomics. *Bioinformatics*. 32(14): 2089-2095. doi: 10.1093/bioinformatics/btw069.

Froehlich AC, Liu Y, Loros JJ, Dunlap JC. 2002. White Collar-1, a circadian blue light photoreceptor, binding to the frequency promoter. *Science*. 297(5582): 815-819. doi: 10.1126/science.1073681.

Fujii I, Mori Y, Watanabe A, Kubo Y, Tsuji G, Ebizuka Y. 2000. Enzymatic synthesis of 1,3,5,8-tetrahydroxynaphthalene solely from malonyl coenzyme A by a fungal iterative type I polyketide synthase PKS1. *Biochemistry*. 39(30): 8853–8858. doi: 10.1021/bi000644j .

Fujii I, Watanabe A, Sankawa U, Ebizuka Y. 2001. Identification of claisen cyclase domain in fungal polyketide synthase WA, a naphthopyrone synthase of *Aspergillus nidulans*. *Chem. Biol*. 8(2): 189–197. https://doi.org/10.1016/S1074-5521(00)90068-1.

Fuller KK, Ringelberg CS, Loros JJ, Dunlap JC, Heitman J. 2013. The fungal pathogen *Aspergillus fumigates* regulates growth, metabolism, and stress resistance in response to light. *mBio*. 4(2): 00142-13. doi: 10.1128/mBio.00142-13

Fuller KK, Loros JJ, Dunlap JC. 2015. Fungal photobiology: visible light as a signal for stress, space and time. *Current Genet*. 61(3): 275-288. doi: 10.1007/s00294-014-0451-0.

Fuller KK, Dunap JC, Loros JJ. 2016. Fungal light sensing at the bench and beyond. *Adv. Genet.* 96: 1-51. doi: 10.1016/bs.adgen.2016.08.002.

Franzen AJ, Cunha MM, Batista EJ, Seabra SH, de Souza W, Rozental S. 2006. Effects of tricyclazole (5-methyl-1,2,4-triazol[3,4] benzothiazole), a specific DHN-melanin inhibitor, on the morphology of *Fonsecaea pedrosoi* conidia and sclerotic cells. *Microsc. Res. Tech*. 69(9): 729–737. doi:10.1002/jemt.20344.

Funa N, Funabashi M, Ohnishi Y, Horinouchi S. 2005. Biosynthesis of hexahydroxyperylenequinone melanin via oxidative aryl coupling by cytochrome P-450 in *Streptomyces griseus*. *J. Bacteriol*, 187(23): 8149−55. doi: 10.1128/JB.187.23.8149-8155.2005.

Gadd GM, de Rome L. 1988. Biosorption of copper by fungal melanins. *Appl. Microbiol. Biotechnol*. 29(6): 610-617. https://doi.org/10.1007/BF00260993.

Geis PA, Szaniszlo PJ. 1984. Carotenoid pigments of the dematiaceous fungus *Wangiella dermatitidis*. *Mycologia*. 76(2): 268-273. https://doi.org/10.2307/3793103.

Gallas JM, Zajac GW, Sarna T, Stotter PL. 2000. Structural differences in unbleached and mildly bleached synthetic tyrosine-derived melanins identified by scanning probe microscopies. *Pigment Cell Res*.13(2): 99–108. doi: 10.1034/j.1600-0749.2000.130208.x.

Galvan A, Solano F. 2016. Bird integumentary melanins: Biosynthesis, forms function and evolution. *Int. J. Mol. Sci.* 17(4): 520. doi: 10.3390/ijms17040520 .

Gao J, Wenderoth M, Doppler M, Schumacher R, Marko D, Fischer R. 2022. Fungal melanin biosynthesis pathway as source for fungal toxins. *Food Microbiol.* 13(3): e00219-22. https://doi.org/10.1128/mbio.00219-22.

Garnica JE, Nucci M, Queiroz-Telles F. 2009. Difficult mycoses of the skin advances in the epidemiology and management of eumycetoma, phaeohyphomycosis and chromoblastomycosis. *Curr. Opi. Infect. Dis*. 22(6): 559-563. doi: 10.1097/QCO.0b013e328332bbc5.

Geis PA, Wheeler MH, Szaniszlo PJ. 1984. Pentaketide metabolites of melanin synthesis in the dematiaceous fungus *Wangiella dermatitidis*. *Archives Microbiol*. 137(4): 324-328. doi: 10.1007/BF00410729.

Gessler NN, Egorova AS. Belozerskaya TA. 2014. Melanin pigments of fungi under extreme environmental conditions. *Appl. Biochem. Microbiol*. 50: 105-113. https://doi.org/10.1134/S0003683814020094.

Geyer K, Hartmann S, Singh RR, Erb TJ. 2022. Multiple functions of the Type II thioesterase associated with the phoslactomycin polyketide synthase. *Biochemistry*, 61(23): 2662-2671. doi: 10.1021/acs.biochem.2c00234.

Glass K, Ito S, Wilby PR, Sota T, Nakamura A, Bowers CR, et al. 2012. Direct chemical evidence for eumelanin pigment from the Jurassic period. *Proc. Natl. Acad. Sci. USA.* 109: 10218-10223. doi: 10.1073/pnas.1118448109 .

Gomez BL, Nosanchuk JD. 2003. Melanin and fungi. *Curr. Opin. Infect. Dis*. 16(2): 91-96. doi: 10.1097/00001432-200304000-00005.

Gorbushina A. 2007. Life on the rocks. *Environ. Microbiol.* 9(7):1613-1631. doi: 10.1111/j.1462-2920.2007.01301.x .

Gorbushina AA, Kotlova ER, Sherstneva OA. 2008. Cellular responses of micro colonial rock fungi to long-term desiccation and subsequent rehydration. *Stud. Mycol*. 61: 91–97. doi:10.3114/sim.2008.61.09.

Gostinčar C. Muggia L. Grube. M. 2012. Polyextremotolerant black fungi: oligotrophism, adaptive potential, and a link to lichen symbiosis. *Front. Microbiol.* 3: 390-390. doi: 10.3389/fmicb.2012.00390.

Gostinčar C. Gunde-Cimerman N. 2023. Understanding fungi in glacial and hypersaline environments. *Annual Review Microbiol.* 77: 89-109. doi: 10.1146/annurev-micro-032521-020922 .

Gunde-Cimerman N, Zalar P, de Hoog S, Plemenitas A. 2000. Hypersaline waters in salterns-natural ecological niches for halophilic black yeasts. *FEMS Microbiol. Ecol*. 32(3): 235-240. https://doi.org/10.1111/j.1574-6941.2000.tb00716.x.

Gunde-Cimerman N, Sonjak S, Zalar P, Frisvad JC, Diderichsen B, Plemenitas A. 2003. Extremophilic fungi in Artic ice: a relationship between adaptation to low temperature and water activity. *Phys. Chem. Earth*. 28: 1273-1278.

Gustin MC, Albertyn J, Alexander M, Davenport K. 1998. MAP kinase pathways in the yeast *Saccharomyces cerevisiae*. *Microbiol. Mol. Biol. Rev.* 62(4): 1264–1300. doi: 10.1128/MMBR.62.4.1264-1300.1998 .

Hamada N, Abe N. 2009. Physiological characteristics of 13 common fungal species in bathrooms. *Mycoscience*. 50(6): 421-429. doi: https://doi.org/10.1007/S10267-009-0500-6

Hamada N, Abe N. 2010. Comparison of fungi found in bathrooms and sinks. *Biocontrol Sci*. 15(2): 51-56. doi: 10.4265/bio.15.51.

Hamilton AJ, Gomez BL. 2002. Melanins in fungal pathogens. *J. Med*. *Microbiol*. 51(3): 189–191. doi: 10.1099/0022-1317-51-3-189.

Hagiya H, Maeda T, Kusakabe S, Kawasaki K, Hori Y, Kimura K, et al. 2019. A fatal case of *Exophiala dermatitidis* disseminated infection in an allogenic hematopoietic stem cell transplant recipient during micafungin therapy. *J. Infect. Chemother.* 25(6): 463-466. doi: 10.1016/j.jiac.2018.12.009.

Harting R, Höfer A, Tran VT, Weinhold LM, Barghahn S, Schlüter R, et al. 2020. The Vta1 transcriptional regulator is required for microsclerotia melanization in *Verticillium dahliae*. *Fungal Biol*.124(5): 490–500. doi: 10.1016/j.funbio.2020.01.007 .

Haynes BC, Skowyra ML, Spencer SJ, Gish SR, Williams M, Held EP, et al. 2011. Toward an integrated model of capsule regulation in *Cryptococcus neoformans*. *PLoS Pathog*. 7(12): e1002411. https://doi.org/10.1371/journal.ppat.1002411.

He Q. 2002. White Collar-1, a DNA binding transcription factor and a light sensor. *Science.* 297(5582): 840-843. doi: 10.1126/science.1072795.

Heinekamp T, ThywiBen A, Macheleidt J, Keller S, Valiante V, Brakhage AA. 2013. *Aspergillus fumigatus* melanins: interference with the host endocytosis pathway and impact on virulence. *Front. Microbiol*. https://doi.org/10.3389/fmicb.2012.00440.

Henson JM, Butler MJ, Day AW. 1999. The dark side of the mycelium: melanins of phytopathogenic fungi. *Annu. Rev. Phytopathol*. 37: 447-471. doi: 10.1146/annurev.phyto.37.1.447.

Hevia MA, Canessa P, Muller-Esparza H, Larrondo LF. 2015. A circadian oscillator int he fungus *Botrytis cinerea* regulates virulence when infecting Arabidopsis thaliana. *Proc. Natl. Acad. Sci. USA*. 112(28): 8744-8749. doi: 10.1073/pnas.1508432112.

Hohl PE, Holley HP, Prevost E, Ajello L, Padhye AA. 1983. Infections due to *Wangiella dermatitidis* in humans: report of the first documented case from the United States and a report of the literature. *Rev. Infect. Dis*. 5(5): 854-864. doi:10.1093/clinids/5.5.854.

Hohmann S, Krantz M, Nordlander B. 2007. Yeast osmoregulation. In *osmosensing and osmosignaling*, ed. H Sies, D Haeussinger, pp. 29–45. *Methods Enzymol*. 428. San Diego, CA: Elsevier

Holker U, Bend J, Pracht R, Tetsch L, Muller T, Hofer M, et al. 2004. *Hortaea acidophila*, a new acid-tolerant black yeast from lignite. Antonie van Leeuwenhoek. 86(4): 287-294. Doi: 10.1007/s10482-005-0101-0.

Hong S, Na YS, Choi S, Song IT, Kim WY, Lee H. 2012. Non-covalent self-assembly and covalent polymerization co-contribute to polydopamine formation. *Adv. Funct. Mater*. 22(22): 4711-4717. doi:10.1002/adfm.201201156.

Hong S, Wang Y, Park SY, Lee H. 2018. Progressive fuzzy cation-π assembly of biological catecholamines. *Sci. Adv*. 4(9): eaat7457. doi: 10.1126/sciadv.aat7457 .

Hopwood DA.1997. Genetic contribution to understanding polyketide synthases. Chemical Reviews 97(7): 2456-2497. doi: https://doi.org/10.1021/cr960034i.

Horr WH. 1936. Utilization of galactose by *Aspergillus niger* and *Pencillium glaucum*. *Plant Physiol.* 11: 81-99.

Horre R, de Hoog GS. 1999. Primary cerebral infections by melanized fungi: a review. *Stud. Mycol*. 43: 176-193.

Hou R, Liu X, Wu X, Zheng M, Fu J. 2021. Therapeutic effect of natural melanin from edible fungus *Auricularia auricula* on alcohol-induced liver damage in vitro and in vivo. *Food Sci. Hum. Wellness.* 10(10): 514–522. https://doi.org/10.1016/j.fshw.2021.04.014.

Howard RJ, Valent B. 1996. Breaking and entering: host penetration by the fungal rice black pathogen *Magnoporthe grisea*. *Annu. Rev. Microbiol.* 50(1): 491-512. doi: 10.1146/annurev.micro.50.1.491 .

Hulsen T, de Vlieg J, Alkema W. 2008. BioVenn – a web application for the comparison and visualization of biological lists using area-proportional Venn diagrams. *BMC Genomics*. 9: 488. https://doi.org/10.1186/1471-2164-9-488.

Hyde KD, McKenzie EHC, Koko TW. 2011. Towards incorporating anamorphic fungi in a natural classification-checklist and notes for 2011. *Mycosphere*. 3(2): 157-228.

Idnurm A, Heitman J, Chory J. 2005. Light controls growth and development via a conserved pathway in the fungal kingdom. *PLoS Biol*. 3(4): p.e95-0626. https://doi.org/10.1371/journal.pbio.0030095.

Ito S, Wakamatsu K. 2011. Diversity of human hair pigmentation as studied by chemical analysis of eumelanin and phaeomelanin. *J EUR Acad Dermatol Venereol*. 25(12): 1369-1380. doi: 10.1111/j.1468-3083.2011.04278.x .

Jacobson ES, Hove E, Emery HS. 1995. Antioxidant function of melanin in black fungi. *Infect. Immun*. 63(12): 4944-5. doi: 10.1128/iai.63.12.4944-4945.1995.

Jacobson ES. 2000. Pathogenic roles for fungal melanins. *Clin. Microbiol. Rev*. 13(4): 708–717. doi: 10.1128/cmr.13.4.708-717.2000.

Jia S, Chi Z, Chen L, Liu G, Hu Z Chi Z. 2021. Molecular evolution and regulation of DHN melanin-related gene clusters are closely related to adaptation of different melanin-producing fungi. *Genomics*.113(4):1962-1975. doi: https://doi.org/10.1016/j.ygeno.2021.04.034.

Jung WH, Sham A, White R, Kronstad JW. 2006. Iron regulation of the major virulence factors in the AIDS-associated pathogen *Cryptococcus neoformans*. *PLoS Biol*. 4(12): e410. https://doi.org/10.1371/journal.pbio.1002410.

Jung KW, Yang DH, Maeng S, Lee KT, So YS, Hong J, et al. 2015. Systematic functional profiling of transcription factor networks in *Cryptococcus neoformans*. *Nat. Commun.*7: 6757. doi: 10.1038/ncomms7757.

Karuppayil SM, Szaniszlo PJ. 1997. Importance of calcium to the regulation of polymorphism in *Wangiella* (*Exophiala*) *dermatitidis*. *Med. Mycol*. 35: 379-388. https://doi.org/10.1080/02681219780001471.

Kejžar A, Gobec S, Plemenitas A, Lenassi M. 2013. Melanin is crucial for growth of the black yeast *Hortaea werneckii* in its natural hypersaline environment. *Fungal Biol.* 117(5): 368-379. doi: 10.1016/j.funbio.2013.03.006 .

Keller S, Macheleidt J, Scherlach K, Schmaler-Ripcke J, Jacobsen ID, Heinekamp T, et al. 2011. Pyomelanin formation in *Aspergillus fumigatus* requires HmgX and the transcriptional activator HmgR but is dispensable for virulence. *PLoS One*. 6(10): e26604. doi 10.1371/journal.pone.0026604.

Kenney RT, Kwon-Chung KJ, Waytes AT, Meinick DA, Pass H, Merino MJ. 1992. Successful treatment of systemic *Exophiala dermatitidis* infection in a patient with chronic granulomatous disease. *Clin. Infect. Dis*. 14(1): 235-242. doi: 10.1093/clinids/14.1.235.

Khajo A, Bryan RA, Friedman M, Burger RM, Levitsky Y, Casadevall A, et al. 2011. Protection of melanized *Cryptococcus neoformans* from lethal dose gamma irradiation involves changes in melanin's chemical structure and paramagnetism. *PLoS One*. 6(9): p.e25092. doi: 10.1371/journal.pone.0025092 .

Khan AA, Alshabi AM, Alqahtani YS, Alqahtani AM, Bennur RS, Shaikh IA, et al. 2021. Extraction and identification of fungal pigment from *Penicillium europium* using different spectral studies. *J. King Saud Univ. Sci.* 33,101437. https://doi.org/10.1016/j.jksus.2021.101437.

Kihara J, Moriwaki A, Ito M, Arase S, Honda Y. 2004. Expression of THR1, a 1, 3, 8-trihydroxynaphthalenereductase gene involved in melanin biosynthesis in the phytopathogenic fungus *Bipolaris oryzae*, is enhanced by near-ultraviolet radiation. *Pigment Cell Melanoma Res.* 17(1):15–23. doi: 10.1046/j.1600-0749.2003.00102.x.

Kihara J, Moriwaki A, Tanaka N, Tanaka C, Ueno M, Arase S. 2008. Characterization of the BMR1 gene encoding a transcription factor for melanin biosynthesis genes in the phytopathogenic fungus *Bipolaris oryzae*. *FEMS Microbiol. Lett*. 281(2): 221–227. doi: 10.1111/j.1574-6968.2008.01101.x .

Kim D, Langmead B, Salzberg SL. 2015. HISAT: a fast spliced aligner with low memory requirements. *Nature Methods*. 12(4), 357–360. https://doi.org/10.1038/nmeth.3317.

Kim YJ, Khetan A, Wu W, Chun S, Viswanathan V, Whitacre JF, et al. 2016. Evidence of porphyrin-like structure in natural melanin pigments using electrochemical fingerprinting. *Adv. Mater*. 28(16): 3173-3180. https://doi.org/10.1002/adma.201504650.

Kim KS, Bahn YS. 2023. Protein Kinase A controls the melanization of *Candida auris* through the alteration of cell wall components. *Antioxidents (Basel).* 12(9): 1702. doi: 10.3390/antiox12091702 .

Koch SM, Pohl CF, Siontas O, Cortesao M, Mota A, Runzheimer K, et al. 2023. *Aspergillus niger* as a cell factory for the production of pyomelanin, a molecule with UV-C radiation shielding activity. *Frontiers*. *Microbiol*. 14, https://doi.org/10.3389/fmicb.2023.1233740 .

Kogej T, Ramos J, Plemenitas A, Gunde-Cimerman N. 2005. The halophilic fungus *Hortaea werneckii* and the halotolerant fungus *Aureobasidium pullularis* maintain low intercellular cation concentrations in hypersaline environments. *Appl. Environ. Microbiol*. 71(11): 6600-6605. doi: 10.1128/AEM.71.11.6600-6605.2005.

Kogej S, Stein M, Volkmann M, Gorbushina AA, Galinski EA, Gunde-Cimerman N. 2007. Osmotic adaptation of the halophilic fungus *Hortaea werneckii*: role of osmolytes and melanisation. *Microbiology*. 153(12): 4261-4273. doi: 10.1099/mic.0.2007/010751-0 .

Kohno M, Ishizaki H, Lin P.H, Yamamori K, Kunoh H. 1983. Effect of polyoxin on fungi (IX): ultrastructural and cytochemical analysis of polyoxin treated hyphae of *Alternaria kikichiana* Tanaka. *Ann. Phytopath. Soc. Japan*. 49: 38-46.

Kotob SI, Coon SL, Quintero EJ, Weiner RM. 1995. Homogentisic acid is the primary precursor of melanin synthesis in *Vibrio cholerae*, a hyphomonas strain, and *Shewanella colwelliana*. *Appl. Environ. Microbiol*. 61(4): 1620-1622. https://doi.org/10.1128/aem.61.4.1620-1622.1995.

Kou Y, Naqvi NI. 2016. Surface sensing and signaling networks in plant pathogenic fungi. *Sem. Cell Dev. Biol*. 57: 84–92. doi: 10.1016/j.semcdb.2016.04.019 .

Krishnamurthy S, Narasimha MK, Thirumale S. 2020. Characterization of ankaflavin from *Penicillium aculeatum* and its cytotoxic properties. *Nat. Prod. Res*. 34(11): 1630-1635. doi: 10.1080/14786419.2018.1522633 .

Kunwar A, Adhikary B, Jayakumar S, Barik A, Chattopadhyay S, Raghukumar et al. 2012. Melanin, a promising radioprotector: Mechanisms of actions in a mice model. *Toxicol. Appl. Pharmacol*. 264(2): 202–211. doi: 10.1016/j.taap.2012.08.002 .

Kurbessoian T, Murante D, Crocker A, Hogan DA, Stajich JE. 2023. In host evolution of *Exophiala dermatitidis* in cystic fibrosis lung micro-environment.*G3 (Bethesda)*. 13(8): jkad126. doi: 10.1093/g3journal/jkad126 .

Kwon-Chung KJ, Polachek I, Popkin TJ. 1982. Melanin lacking mutants of *Cryptococcus neoformans* and their virulence for mice. *J. Bacteriol*. 150(3): 1414-1421. doi: 10.1128/jb.150.3.1414-1421.1982.

Lai M, Cheng Z, Xiao L, Klosterman SJ, Wang Y. 2022. The bZip transcription factor VdMRTF1 is a negative regulator of melanin biosynthesis and virulence in *Verticillium dahliae*. *Microbiol. Spectrum*. 10(2): e0258121. doi: 10.1128/spectrum.02581-21 .

Langfelder K, Stribel M, Jahn B, Haase G, Brakhage AA. 2003. Biosynthesis of fungal melanins and their importance for human pathogenic fungi. *Fungal Genet. Biol.* 38(2): 143-158. doi: 10.1016/s1087-1845(02)00526-1 .

Lee D, Jang E, Lee M, Kim S, Lee Y, Lee K-T, et al. 2019. Unraveling melanin biosynthesis and signalling networks in *Cryptococcus neoformans*. *mBIO*. 10(5): e02267. https://doi.org/10.1128/mbio.02267-19.

Li Y, Xu W, Tang Y. 2010. Classification, prediction, and verification of the regioselectivity of fungal polyketide synthase product template domains. *J Biol Chem.* 285(3):22764-22773. doi: 10.1074/jbc.M110.128504 .

Li J, Zhou L, Yin C, Zhang D, Klosterman SSJ, Wang B, et al. 2019. The *Verticillium dahliae* Sho1-MAPK pathway regulates melanin biosynthesis and is required for cotton infection. *Environ. Microbiol.* 21(12): 4852-4874. doi: 10.1111/1462-2920.14846.

Li R, Li Y, Xu W, Zhang M, Jiang Q, Liu Y, et al. 2022. Transcription factor AacmrA mediated melanin synthesis regulates the growth, appressorium formation, stress response and pathogenicity of pear fungal *Alternaria alternate*. *Fungal Biol*. 126(10): 687-695. doi: 10.1016/j.funbio.2022.08.008 .

Li H, Sheng R, Zhang C, Wang L. 2023. Two zinc finger proteins, VdZFP1 and VdZFP2, interact with VdCmr1 to promote melanized microsclerotia development and stress tolerance in *Verticillium dahlia*. *BMC Biol*. 21(1): 237. doi: 10.1186/s12915-023-01697-w.

Liam X, de Hoog GS. 2010. Indoor wet cells harbour melanized agents of cutaneous infection. *Med. Mycol*. 48: 622-628. doi: 10.3109/13693780903405774.

Liao Y, Smyth GK, Shi W. 2013. featureCounts: an efficient general purpose program for assigning sequence reads to genomic features. *Bioinformatics*. 30(7), 923–930. https://doi.org/10.1093/bioinformatics/btt656.

Lichter A, Mills D. 1998. Control of pigmentation of *Ustilago hordei*: the effect of pH, thiamine, and involvement of the cAMP cascade. *Fungal Genet Biol.*25(1): 63-74. doi: 10.1006/fgbi.1998.1087 .

Lin L, Chen W. 2005. The study of antioxidant effects in melanins extracted from various tissues of animals. Asian-Australas. *J. Anim. Sci*. 18(2): 277-281. https://doi.org/10.5713/ajas.2005.277

Liu H, Kauffman S, Becker JM, Szaniszlo PJ. 2004. *Wangiella* (*Exophiala*) *dermatitidis* WdChs5p, a class V chitin synthase, is essential for sustained cell growth at temperature of infection. 3(1): 40-51. doi: 10.1128/EC.3.1.40-51.2004.

Liu D, Wei L, Guo T, Tan W. 2014. Detection of DOPA-melanin in the dimorphic fungal pathogen *Penicillium marneffei* and its effect on macrophage phagocytosis in vitro. *PLoS One.* 9(3): p.e92610-e92610. https://doi.org/10.1371/journal.pone.0092610.

Lopez GA, Albrecht-Eckardt D, Panagiotou G, Schäuble S. 2024. FungiFun3: systemic gene set enrichment analysis for fungal species. *Bioinformatics*. 40(11): btae620. https://doi.org/10.1093/bioinformatics/btae620.

Łopusiewicz Ł, Jędra F, Bartkowiak A. 2018a. The application of melanin modified gelatin coatings for packaging and the oxidative stability of pork lard. *World Sci. News*. 101: 108–119.

Łopusiewicz Ł, Jędra F, Mizielińska M. 2018b. New poly (lactic acid) active packaging composite films incorporated with fungal melanin. *Polymers*. 10(4): 386. https://doi.org/10.3390/polym10040386.

Lorquin F, Piccerelle P, Orneto C, Robin M, Lorquin J. 2022. New insights and advances on pyomelanin production: from microbial synthesis to applications. *J. Ind. Microbiol. Biotechnol.* 49(4): kuac013. doi: 10.1093/jimb/kuac013.

Luo C, Zhao H, Yang X, Qiang C, Cheng J, Xie J, et al. 2018. Functional analysis of the melanin-associated gene *CmMR1* in *Coniothyrium minitans*. *Frontiers Microbiol.* 8: 2658. doi: 10.3389/fmicb.2018.02658.

Love MI, Huber W, Anders S. 2014. Moderated estimation of fold change and dispersion for RNA-seq data with DESeq2. *Genome Biology*. 15(12). https://doi.org/10.1186/s13059-014-0550-8.

Machouart M, Gueidan C, Khemisti A, Dulongcourty R, Sudhadham M, de Hoog GS. 2011. Use of ribosomal introns as new markers of genetic diversity in *Exophiala dermatitidis*. *Fungal Biol*. 115(10): 1038-1050. doi: 10.1016/j.funbio.2011.05.002.

Malo ME, Schultzhaus Z, Frank C, Romsdahl J, Wang Z, Dadachova E. 2021. Transcriptomic and genomic changes associated with radioadaptation in *Exophiala dermatitidis*. *Comput Struct Biotechnol J*. 19: 196-205. doi: https://doi.org/10.1016/j.csbj.2020.12.013.

Manini P, Bietti M, Galeotti M, Salamone M, Lanzalunga O, Cecchini MM, et al. 2018. Characterization and fate of hydrogen-bonded free-radical intermediates and their coupling products from the hydrogen atom transfer agent 1,8-Naphthalenediol. *ACS Omega.* 3(4): 3918−3927. doi: 10.1021/acsomega.8b00155.

Martin M. 2011. Cutadapt removes adapter sequences from high-throughput sequencing reads. *EMBnet. Journal*. 17(1), 10. https://doi.org/10.14806/ej.17.1.200.

Mattoon ER, Cordero RJB, Casadevall A. 2021. Fungal melanins and applications in healthcare, bioremediation and industry. *J. Fungi (Basel).* 7(6): 488. doi: 10.3390/jof7060488.

Matos T, de Hoog GS, de Boer AG, de Crom I, Hasse G. 2002. High prevalence of the neurotrope *Exophiala dermatitidis* and related oligotrophic black yeasts in sauna facilities. *Mycoses*. 45(9-10): 373-377. doi: 10.1046/j.1439-0507.2002.00779.x.

Mauch RM, Cunha Vde O, Dias AL. 2013. The copper interference with the melanogenesis of *Cryptococcus neoformans*. *Rev. Inst. Med. Trop. Sao. Paulo.* 55(2): 117–120. doi: 10.1590/s0036-46652013000200009.

Medina-Armijo C, Yousef I, Berná A, Puerta A, Esteve-Núñez A, Viñas M, Prenafeta-Boldu FX. 2024. Characterization of melanin from *Exophiala mesophila* with the prospect of potential biotechnological applications. *Front. Fungal Biol*. 5:1390724. doi: 10.3389/ffunb.2024.1390724

Meng J, Wang X, Xu D, Fu X, Zhang X, Lai D, Zhou L, Zhang G. 2016. Sorbicillinoids from Fungi and Their Bioactivities. *Molecules*. 21(6), 715. doi: 10.3390/molecules21060715.

Meredith P, Sarna T. 2006. The physical and chemical properties of eumelanin. *Pigment Cell Res*. 19(6): 572-594. https://doi.org/10.1111/j.1600-0749.2006.00345.x.

Mukaino T, Koga T, Oshita Y, Narita Y, Obata S, Aizawa H. 2006. *Exophiala dermatitidis* infection in non-cystic fibrosis bronchiectasis. Respiratory Medicine. 100(11): 2069-2071. doi: 10.1016/j.rmed.2006.03.003.

Nabae K, Ishiharam T, Hagiwaram A, Hirota T, Toda Y, Tamano S, et al. 2005. A 90-day oral toxicity study of beta-carotene derived from *Blakeslea trispora*, a natural food colorant, in F344 rats. *Food Chem. Toxicol*. 43(7): 1127-1133. doi: 10.1016/j.fct.2005.03.003 .

Nambu N, Tsai HF, Chang YC, Kwon-Chung KJ. 2021. Novel angular naphthopyrone formation by Arp1p dehydratase involved in *Aspergillus fumigatus* melanin biosynthesis. *Environ. Microbiol. Report.* 13(6): 822-829. doi: 10.1111/1758-2229.13013.

Narendrababu B, Shishupala S. 2017. Spectrophotometric detection of pigments from *Aspergillus* and *Penicillium* isolates. *J. App. Biol. Biotechnol*. doi:10.7324/JABB.2017.50109

Natarajan VT, Ganju P, Ramjumar A, Grover R, Gokhale RS. 2014. Multifaceted pathways protect human skin from UV radiation. *Nat. Chem. Biol*. 10(7): 542-551. doi: 10.1038/nchembio.1548 .

Ngamskulrungroj P, Himmelreich U, Breger JA, Wilson C, Chayakulkeeree M, Krockenberger MB, et al. 2009. The trehalose synthesis pathway is an integral part of the virulence composite for *Cryptococcus gattii*. *Infect. Immun*. 77(10): 4584–4596. doi: 10.1128/IAI.00565-09 .

Nosanchuk JD, Casadevall A 2003. Budding of melanized *Cryptococcus neoformans* in the presence or absence of L-dopa. *Microbiol*. 149(Pt 7): 1945–1951. doi: 10.1099/mic.0.26333-0 .

Nosanchuk JD, Stark RE, Casadevall A. 2015. Fungal melanin: what do we know about structure? *Front. Microbiol*. 6, 1463. https://doi.org/10.3389/fmicb.2015.01463 .

Oh J, Kim JY, Son SH, Jung W, Kim DH, Seo J, et al. 2021. Fungal melanin as a biocompatible broad-spectrum sunscreen with high antioxidant activity. *RSC advances*. 11(32): 19682-19869. doi: 10.1039/d1ra02583j.

Okuno T, Matsuura K, Furusawa I. 1983. Recovery of appressorial penetration by some melanin precursors in *Pyricularia oryzae* treated with tricyclazole and in a melanin deficient mutant. *J Pest. Sci*. 8(3): 357-360.

Olaizola C, Abramowski ZA, Ayala MJ. 2012. Photoprotective effect of fungal melanins against UVB in human skin cells. *Mycologia Aplicada International*. 25(1): 3-12.

Olsowski M, Hoffmann F, Hain A, Kirchhoff L, Theegarten D, Todt D, et al. 2018. *Exophiala dermatitidis* isolates from various sources: using alternative invertebrate host organisms (*Caenorhabditis elegans* and *Galleria mellonella*) to determine virulence. *Sci. Rep.* 8(1): 12747-13. DOI: 10.1038/s41598-018-30909-5 .

Onofri S, Selbmann L, Zucconi L. 2004. Antarctic microfungi as models for exobiology. *Plant Space Sci*. 52(1-3): 229-237. https://doi.org/10.1016/j.pss.2003.08.019.

Onofri S, Barreca D, Selbmann L, Isola D, Rabbow E, Horneck G, et al. 2008. Resistance of Antarctic black fungi and cryptoendolithic communities to simulated space and Martian conditions. *Stud Mycol*. 61: 99-109. doi: 10.3114/sim.2008.61.10 .

Onofri S, Pacelli C, Selbmann L, Zucconi L. 2020. The amazing journey of *Cryomyces antarcticus* from Antarctica to space. In: Seckbach J., Stan-Lotter H., editors. Extremophiles as Astrobiological Models. Wiley; New York, NY, USA: 2020. pp. 237–254. doi:10.1002/9781119593096.ch11.

Oujezdsky KB, Grove SN, Szaniszlo PJ. 1973. Morphological and structural changes during the yeast to mold conversion of *Phialophora dermatitidis*. *J. Bacteriol*. 113(1): 468-477. doi: 10.1128/jb.113.1.468-477.1973.

Ozeki H, Shosuke I, Wakamatsu K, Ishiguro I. 1997a. Chemical characterisation of pheomelanogenesis starting from dihydroxy phenylalanine or tyrosine and cysteine. Effects of tyrosine and cysteine concentrations and reaction time. *Biochem. Biophys. Acta*. 1336(3): 539–548. doi: 10.1016/s0304-4165(97)00068-8.

Ozeki H, Wakamatsu K, Ito S, Ishiguro I. 1997b. Chemical characterization of eumelanins with special emphasis on 5,6- dihydroxyindole-2-carboxylic acid content and molecular size. *Anal. Biochem*. 248(1): 149–157. doi: 10.1006/abio.1997.2079.

Pacelli C, Bryan RA, Onofri S, Selbmann L, Shuryak I, Dadachova E. 2017. Melanin is effective in protecting fast and slow growing fungi from various types of ionizing radiation. *Environ. Microbiol*. 19(4): 1612−1624. doi: 10.1111/1462-2920.13681 .

Panadero J, Pallotti C, Rodríguez-Vargas S, Randez-Gil F, Prieto JA. 2006. A downshift in temperature activates the high osmolarity glycerol (HOG) pathway, which determines freeze tolerance in *Saccharomyces cerevisiae*. *J. Biol. Chem.* 281(8): 4638–45. doi: 10.1074/jbc.M512736200 .

Pandit SG, Puttananjaiah MH, Peddha MS, Dhale MA. 2020. Safety efficacy and chemical profiling of water-soluble *Talaromyces purpureogenus* CFRM02 pigment. *Food Chem*. 310: 125869. doi: 10.1016/j.foodchem.2019.125869 .

Paolo WF, Dadachova E, Mandal P, Casadevall A, Szaniszlo PJ, Nosanchuk JD. 2006. Effects of disrupting the polyketide synthase gene *WdPKS1* in *Wangiella* [*Exophiala*] *dermatitidis* on melanin production and resistance to killing by antifungal compounds, enzymatic degradation, and extremes in temperature. *BMC Microbiol.* 19: 55. doi: 10.1186/1471-2180-6-55 .

Patel KR, Wyman JA, Patel KA, Burden BJ. 1996. A mutant of *Bacillus thuringiensis* producing a dark brown pigment with increased UV resistance and insecticidal activity. *J. Invertebr. Pathol*. 67(2): 120-124. doi: https://doi.org/10.1006/jipa.1996.0018.

Patel AK, Patel KK, Darji P, Sinqh R, Shivaprakash MR, Chakrabarti A. 2013. *Exophiala dermatitidis* endocarditis on native aortic valve in a postrenal transplant patient and review of literature on *E. dermatitidis* Infections. *Mycoses*. 56(3): 365-372. doi: 10.1111/myc.12009.

Perez-Cuesta U, Aparicio-fernandez L, Guruceaga X, Martin-Souto L, Abad-Diaz-de-Cerio A, Antoran A, et al. 2020. Melanin and pyomelanin in *aspergillus fumigatus* from its genetic to host interaction. *Int. Microbio.* 23(1): 55-63. doi:10.1007/s10123-019-00078-0.

Pihet M, Carrere J, Cimon B, Chabasse D, Delhaes L, Symoens F, et al. 2009. Occurrence and relevance of filamentous fungi in respiratory secretions of patients with cystic fibrosis- a review. *Med Mycol*. 47(4): 387-397. doi: 10.1080/13693780802609604 .

Polacheck I, Kwon-Chung KJ. 1988. Melanogenesis in *Cryptococcus neoformans*. *J. Gen Microbiol.* 134(4): 1037-1041. doi: 10.1099/00221287-134-4-1037.

Pomerantz SH, Warner MC. 1967. 3,4-Dihydroxy-L-phenylalanine as the tyrosine cofactor: occurrence in melanoma and binding constant. *JBC.* 242(22): 5308-5314. doi: https://doi.org/10.1016/S0021-9258(18)99429-9 .

Pombeiro-Sponchiado SR, Sousa GS, Reyes J, Lisboa HF. Production of melanin pigment by fungi and its biotechnological applications. *Melanin*. 4: 47-75.

Poorniammal R, Prabhu S, Dufosse L, Kannan J. 2021. Safety evaluation of fungal pigments for food applications. *J. Fungi (Basel).* 7(9): 692. doi: 10.3390/jof7090692.

Prados-Rosales R, Toriola S, Nakouzi A, Chatterjee S, Stark R, Gerfen G, et al. 2015. Structural characterization of melanin pigments from commercial preparations of the edible mushroom *Auricularia auricula*. *J. Agric. Food Chem*. 63(33): 7326–7332. https://doi.org/10.1021/acs.jafc.5b02713.

Pukkila-Worley R, Gerrald QD, Kraus PR, Boily MJ, Davis MJ, Giles SS, et al. 2005. Transcriptional network of multiple capsule and melanin genes governed by the *Cryptococcus neoformans* cyclic AMP cascade. *Eukaryot. Cell*. 4(1): 190–201. doi: 10.1128/EC.4.1.190-201.2005 .

Poyntner *C,* Blasi B, Arcalis E, Mirastschijski U, Sterflinger K, Tafer H. 2016. The transcriptome of *Exophiala dermatitidis* during ex-vivo skin model infection. *Frontiers in Cell and Infec Microbiol*. 6:136. doi: 10.3389/fcimb.2016.00136 .

Poyntner C. Mirastschijski U. Sterflinger K. Tafer H. 2018. Transcriptome study of an *Exophiala dermatitidis PKS1* mutant on an ex-vivo skin model: Is melanin important for infection? *Front. Microbiol.* 9: 1457. doi: 10.3389/fmicb.2018.01457 .

Priebe S, Kreisel C, Horn F, Guthke R, Linde J. 2014. FungiFun2: a comprehensive online resource for systematic analysis of gene lists from fungal species. *Bioinformatics*. 31(3): 445-446. doi: 10.1093/bioinformatics/btu627.

Qin Y, Xia Y. 2024. Melanin in fungi: advances in structure, biosynthesis, regulation, and metabolic engineering. *Microbial Cell Factories*. 23: 334. https://doi.org/10.1186/s12934-024-02614-8.

Quan Y, Muggia L, Moreno LF, Wang M, Al-Hatmi AMS, Menezes NS, et al. 2020. A re-evaluation of the *Chaetothyriales* using criteria of comparative biology. *Fungal Diversity*. 103: 47-85. https://doi.org/10.1007/s13225-020-00452-8

Revskaya E, Chu P, Howell RC, Schweitzer AD, Bryan RA, Harris M, et al. 2012. Compton scattering by internal shields based on melanin-containing mushrooms provides protection of gastrointestinal tract from ionizing radiation. *Cancer Biother. Radiopharm*. 27(9): 570–576. doi: 10.1089/cbr.2012.1318.

Reyes-Fernandez EZ, Shi Y, Grun P, Bode HB, Bolker M. 2019. An unconventional melanin biosynthetic pathway in *Ustilago maydis*. *Appl. Environ. Microbiol.* 87(3): e01510-20. doi: 10.1128/AEM.01510-20

Ribera J, Panzarasa G, Stobbe A, Osypova A, Rupper P, Klose D, et al. 2019. Scalable biosynthesis of melanin by the Basidiomycete *Armillaria cepistipes*. *J. Agric. Food Chem*. 67(1): 132–139. doi: 10.1021/acs.jafc.8b05071 .

Riesz J, Gilmore J, Meredith P. 2006. Quantitative scattering of melanin solutions. *Biophysical journal*. 90(11): 4137-4144. https://doi.org/10.1529/biophysj.105.075713.

Riley PA. 1997. Melanin. *Int. J. Biochem. Cell Biol*. 29(11): 1235– 1239. doi: 10.1016/s1357-2725(97)00013-7.

Rizzo DM, Blanchette RA, Palmer MA. 1992. Biosorption of metal compounds by *Armillaria rhizomorphs*. *Can. J. Bot*. 70(8): 1515-1520. doi: 10.1139/b92-190.

Roberts RL, Szaniszlo PJ. 1978. Temperature-sensitive multicellular mutants of *Wangiella dermatitidis*. *J. Bacteriol.* 135(2): 622-632. doi: 10.1128/jb.135.2.622-632.1978.

Robertson KI, Mostaghim A, Cuomo CA, Soto CM, Lebedev N. 2012. Adaptation of the black yeast *Wangiella dermatitidis* to ionizing radiation: molecular and cellular mechanisms. *PLoS One*. 7: p.e48674. https://doi.org/10.1371/journal.pone.0048674.

Rosas AL, Casadevall A. 1997. Melanization affects susceptibility of *Cryptococcus neoformans* to heat and cold. *FEMS Microbiol. Lett.* 153(2): 265–272. doi: 10.1111/j.1574-6968.1997.tb12584.x.

Rosas AL, Casadevall A. 2001. Melanization decreases the susceptibility of *Cryptococcus neoformans* to enzymatic degradation. *Mycopathologia* 151(2): 53–56. doi: 10.1023/a:1010977107089.

Rosas ÁL, Casadevall A. 2006. Melanization affects susceptibility of *Cryptococcus neoformans* to heat and cold1. *FEMS Microbiol. Lett*. 153(2): 265–272. doi: 10.1111/j.1574-6968.1997.tb12584.x .

Rosas AL, Casadevall A: Melanization affects susceptibility of *Cryptococcus neoformans* to heat and cold. *FEMS Microbiol Lett*. 1997. 153(2): 265-272. doi: 10.1111/j.1574-6968.1997.tb12584.x .

Ruzafa C, Sanchez-Amat A, Solano F. 1995. Characterization of the melanogenic system in *Vibrio cholera*, ATCC 14035. *Pigment Cell Research.* 8(3): 147-152. https://doi.org/10.1111/j.1600-0749.1995.tb00656.x,

Sabatini M, Comba S, Altabe S, Recio-Balsells A, Labadie GR, Takano E, et al. 2018. Biochemical characterization of the minimal domains of an iterative eukaryotic polyketide Synthase. *FEBS J.* 285(23):4494-4511. doi: 10.1111/febs.14675 .

Saito H. 2010. Regulation of cross-talk in yeast MAPK signaling pathways. *Curr. Opin. Microbiol*. 13(6): 677–683. https://doi.org/10.1016/j.mib.2010.09.001.

Saitoh Y, Izumitsu K, Morita A, Tanaka C. 2010. A copper-transporting ATPase BcCCC2 is necessary for pathogenicity of *Botrytis cinerea*. *Mol. Gen. Genomics*. 284(1):33–43. doi: 10.1007/s00438-010-0545-4.

Saiz-Jiminez C, Shafizadeh F. 1984. Iron and copper binding by fungal phenolic polymers: an electron spin resonance study. *Current Microbiol*. 10: 281-286. https://doi.org/10.1007/BF01577142.

Salgado-Castillo SN, Lopez-Peria HA, Diaz R, Pena-Solis K, Ponce-Alquicira E, Soriano-Santos J, et al. 2023. Fungal melanins and their potential applications: *A Review. BioResources*. 18(4): 8688-8706. doi:10.15376/biores.18.4.Castillo.

Sandmann G. 2022. Carotenoids and their biosynthesis in fungi. *Molecules*. 27(4): 1431. https://doi.org/10.3390/molecules27041431.

Sansinenea E, Ortiz A. 2015. Melanin: A photoprotection for photoprotection of *Bacillus thuringiensis* based biopesticides. *Biotechnol. Lett*. 37(3): 483-490. doi: 10.1007/s10529-014-1726-8.

Sapmak A, Boyce KJ, Andrianopoulos A, Vanittanakom N. 2015. The *pbrB* gene encodes a laccase required for DHN-melanin synthesis in conidia of *Talaromyces* (*Penicillium*) *marneffei*. *PLoS One*. 10(4): e0122728. https://doi.org/10.1371/journal.pone.0122728.

Schnitzler N, Peltroche-Llacsahuanga H, Bestier N, Zundorf J, Lutticken R, Haase G. 1999. Effect of melanin and carotenoids of *Exophiala* (*Wangiella*) *dermatitidis* on phagocytosis, oxidative burst, and killing by human neutrophils. *Infect. Immun*. 67(1): 94–101. doi: 10.1128/IAI.67.1.94-101.1999 .

Schmaler-Ripcke J, Sugareva V, Gebhardt P, Winkler R, Kniemeyer O, Heinekamp T, et al. 2008. Production of pyomelanin, a second type of melanin, via the tyrosine degradation pathway in *Aspergillus fumigates*. *Appl. Environ. Microbiol.* 75(2): 493-503. doi: 10.1128/AEM.02077-08.

Schroeder WL, Harris SD, Saha R. 2020. Computation-driven analysis of model polyextremo-tolerant fungus *Exophiala dermatitidis*: defensive pigment metabolic costs and human applications. *iScience*. 23(4): 100980. https://doi.org/10.1016/j.isci.2020.100980.

Schumacher J. 2016. DHN melanin biosynthesis in the plant pathogenic fungus *Botrytis cinerea* is based on two developmentally regulated key enzyme (PKS)-encoding genes. *Mol. Microbiol.* 99(4): 729-748. doi: 10.1111/mmi.13262.

Sealy RC, Hyde JS, Felix CC, Menon I, Prota G. 1982. Eumelanins and pheomelanins: characterization by electron spin resonance spectroscopy. *Science* 217(4559): 545–547. doi: 10.1126/science.6283638

Seiji M, Fitzpatrick TB, Simpson RT, Birbeck MS. 1963. Chemical composition and terminology of specialized organelles (melanosomes and melanin granules) in mammalian melanocytes. *Nature*. 197: 1082-1084. doi: 10.1038/1971082a0 .

Selbmann L, de Hoog S, Mazzaglia A, Friedmann EI. 2005. Fungi at the edge of life: Cryptoendolithic black fungi from Antarctic desert. *Stud. Mycol.* 51(51): 1-32.

Selbmann L, Egidi E, Isola D, Onofri S, Zucconi L. 2013. Biodiversity, evolution and adaptation of fungi in extreme environments. *Plant Biosystems*. 147(1): 237-246. Doi: 10.1080/11263504.2012.753134.

Selbmann L, Zucconi L, Isola D. 2015. Rock black fungi: excellence in the extremes, from the Antarctic to space. *Curr Genet.* 61(3): 335-345. doi: 10.1007/s00294-014-0457-7 .

Selvakumar P, Rajasekar S, Periasamy K, Raaman N. 2008. Isolation and characterization of melanin pigment from *Pleurotus cystidiosus*. *Microbiol. Biotechnol*. 24(10): 2125-2131. doi:10.1007/s11274-008-9718-2.

Seo D, Choi K, 2020. Heterologous production of pyomelanin biopolymer using 4-hydroxyphenylpyruvate dioxygenase isolated from *Ralstonia pickettii* in *Escherichia coli*. *J. Biochem. Engr*. 157, 107548. doi:10.1016/j.bej.2020.107548.

Seyedmousavi S, Badali H, Chlebicki A, Zhao J, Prenafeta-boldu FX, de Hoog GS. 2011. *Exophiala sideris*, a novel black yeast isolated from environments polluted with toxic alkyl benzenes and arsenic. *Fungal Biol*. 115(10): 1030-1037. doi: 10.1016/j.funbio.2011.06.004.

Seyedmousavi S, Guillot J, de Hoog GS. 2013. Phaeohyphomycoses, emerging opportunistic diseases in animals. *Clin*. *Microbiol. Rev.* 26(1): 19-35. doi: 10.1128/CMR.00065-12.

Shelest E. 2017. Transcription factors in fungi: TFome dynamics, three major families, and dual-specificity TFs. *Frontiers Genet*. 8:53. https://doi.org/10.3389/fgene.2017.00053 .

Shih IL, Tsai KL, Hsiech C. 2007. Effects of culture conditions on the mycelial growth and bioactive metabolite production in submerged culture of *Cordyceps militaris*. *Biochem Eng J*. 33(3): 193-201. doi:10.1016/j.bej.2006.10.019.

Simon JD, Peles DN. 2010. The red and the black. *Acc. chem. res.* 43(11): 1452-1460. https://doi.org/10.1021/ar100079y.

Singaravelan N, Grishkan I, Beharav A, Wakamatsu K, Ito S, Nevo E. 2008. Adaptive melanin response of the soil fungus *Aspergillus niger* to UV radiation stress at "Evolution Canyon", Mount Carmel, Israel. PLoS One. 3(8):e2993. doi: 10.1371/journal.pone.0002993 .

Slepecky RA, Starmer WT. 2009. Phenotypic plasticity in fungi: a review with observations on *Aureobasidium pullulans*. *Mycologia*. 101(6): 823-832. doi: 10.3852/08-197.

Solano F. 2014. Melanins: skin pigments and much more- types, structural models, biological functions, and formation routes. *New Journal of Science*. 2014(1): 1-28. doi: https://doi.org/10.1155/2014/498276.

Song W, Yang H, Liu S, Yu H, Dan Li, Li P, et al. 2023. Melanin: insights into structure, analysis, and biological activities for future development. *J. Mater. Chem. B*. 11: 7528-7543. doi:10.1039/D3TB01132A.

Sterflinger K, Krumbein WE. 1995. Multiple stress factors affecting growth of rock inhabiting fungi. *Botanica. Acta*. 108(6): 490-496. doi: https://doi.org/10.1111/j.1438-8677.1995.tb00526.x.

Sterflinger K, de Hoog GS, Haase G, 1999. Phylogeny and ecology of meristematic ascomycetes. *Stud. Mycol.* 43 5–22.

Stipanovic RD, Bell AA. 1976. Pentaketide metabolites of *Verticillium Dahliae* 0.3. Identification of (−)-3,4-dihydro-3,8- dihydroxy-1(2h)-naphthalenone [(−)-vermelone] as a precursor to melanin. *J. Org. Chem*. 41(14): 2468−2469. doi: 10.1021/jo00876a026.

Stüssi H, Rast DM. 1981. The biosynthesis and possible function of γ-glutaminyl-4-hydroxybenzene in *Agaricus bisporus*. *Phytochemistry*. 20(10): 2347-2352. https://doi.org/10.1016/S0031-9422(00)82663-1.

Sugumaram M, Barek H. 2016. Critical analysis of the melanogenic pathway in insects and higher animals. *Int. J. Mol. Sci*. 17(10): 1753. doi: 10.3390/ijms17101753 .

Sudhadham M, Prakitsin S, Sivichai S, Chaiwat R, Dorrestein GM, Menken SBJ, et al. 2008. The neurotropic black yeast *Exophiala dermatitidis* has a possible origin in the tropical rain forest. *Stud. Mycol.* 61: 145-155. doi: 10.3114/sim.2008.61.15.

Suwannarach N, Kumla J, Watanabe B, Matsui K, Lumyong S. 2019. Characterization of melanin and optimal conditions for pigment production by an endophytic fungus, *Spissiomyces endophytica* SDBR-CMU319. *PLoS One.* 14, e0222187. https://doi.org/10.1371/journal.pone.0222187.

Suthar M, Dufosse L, Singh SK. 2023. The enigmatic world of fungal melanin: A comprehensive Review. *J. Fungi (Basel)*. 9(9): 891. doi: 10.3390/jof9090891 .

Szaniszlo PJ, Hseih PH, Marlowe JD. 1976. Induction and ultrastructure of the multicellular (sclerotic) morphology in *Phialophora dermatitidis*. *Mycologia*. 68: 117-130. https://doi.org/10.1080/00275514.1976.12019889.

Szaniszlo PJ, Geis PA, Jacobs CW, Cooper CR, Harris JL. 1983. Cell wall changes associated with yeast to multicellular form conversion in *Wangiella dermatitidis*. *Microbiology*. 239-244. https://doi.org/10.1007/978-1-4684-4982-2_9

Szpoganicz B, Gidanian S, Kong P, Farmer P. 2002. Metal binding by melanins: studies of colloidal dihydroxyindole-melanin, and its complexation by Cu(II) and Zn(II) ions. *J. Inorg. Biochem*. 89(1-2): 45–53. doi: 10.1016/s0162-0134(01)00406-8.

Takano Y, Komeda K, Kojima K, Okuno T. 2001. Proper regulation of cyclic AMP-dependent protein kinase is required for growth, conidiation, and appressorium function in the anthracnose fungus *Colletotrichum lagenarium*. *MPMI*. 14(10): 1149–1157. doi: 10.1094/MPMI.2001.14.10.1149.

Taylor B, Wheeler MH, Szaniszlo PJ. 1987. Evidence for pentaketide melanin biosynthesis in dematiaceous human pathogenic fungi. *Mycologia*. 79: 320-322. doi: 10.1080/00275514.1987.12025711.

Tisch D, Schmoll M. 2009. Light regulation of metabolic pathways in fungi. *Appl. Microbiol. Biotechnol*. 85(5): 1259-1277. doi: 10.1007/s00253-009-2320-1.

The Galaxy Community. 2024. The Galaxy platform for accessible, reproducible, and collaborative data analyses: 2024 update, *Nucleic Acids Research*. *52(W1): W83-W94.* https://doi.org/10.1093/nar/gkae410.

Thompson JE, Fahnestock S, Farrall L, Liao DI, Valent B, Jordan DB. 2000. The second naphthol reductase of fungal melanin biosynthesis in *Magnaporthe grisea*: tetrahydroxynaphthalene reductase. *J. Biol. Chem*. 275(45): 34867–34872. doi: 10.1074/jbc.M006659200.

Tran-Ly AN, Reyes C, Schwarze FWMR, Ribera J. 2020. Microbial production of melanin and its various applications. *World J. Microbiol. Biotechnol.* 36(11): 170. https://doi.org/10.1007/s11274-020-02941-z.

Tsai HF, Wheeler MH, Chang YC, Kwon-Chung KJ. 1999. A developmentally regulated gene cluster involved in conidial pigment biosynthesis in *Aspergillus fumigatus*. *J. Bacteriol*. 181(20): 6469–6477. doi: 10.1128/JB.181.20.6469-6477.1999 .

Tsirilakis K, Kim C, Vicencio AG, Christopher A, Casadevall A, Goldman DL. 2012. Methylxanthine inhibit fungal chitinases and exhibit antifungal activity. *Mycopathologia*. 173: 83-91. doi: 10.1007/s11046-011-9483-x.

Tsuji G, Kenmochi Y, Takano Y, Sweigard J, Farrall L, Furusawa I, et al. 2000. Novel fungal transcriptional activators, Cmr1p of *Colletotrichum lagenarium* and pig1p of *Magnaporthe grisea*, contain Cys2His2 zinc finger and Zn(II)2Cys6 binuclear cluster DNA-binding motifs and regulate transcription of melanin biosynthesis genes in a developmentally specific manner. *Mol. Microbiol*. 38(5): 940–954. doi: 10.1046/j.1365-2958.2000.02181.x .

Teixeira MM, Moreno LF, Stielow BJ, Muszewska A, Hainaut M, Gonzaga L. 2017. Exploring the genomic diversity of black yeasts and relatives (*Chaetothyriales, Ascomycota*). *Stud. Mycol.* 86: 1-28. https://doi.org/10.1016/j.simyco.2017.01.001.

Turick CE, Knox AS, Becnel JM, Ekechukwu AA, Milliken CE. 2010. Properties and Function of Pyomelanin. *Biopolymers*. 449–472. doi:10.5772/10273.

Turrà D, Segorbe D, Di Pietro A. 2014. Protein kinases in plant-pathogenic fungi: conserved regulators of infection. *Annu. Rev. Phytopathol*. 52: 267–288. doi: 10.1146/annurev-phyto-102313-050143 .

Untereiner WA, Naveau FA. 1998. Molecular systematic of the *Herpotrichiellaceae* with an assessment of the phylogenetic positions of *Exophiala dermatitidis* and *Phialophora Americana*. *Mycologia*. 91(1): 67-83.

Upadhyay S, Guadalupe T, Xiaorong L. 2013. Laccases involved in 1,8-dihydroxynaphthalene melanin biosynthesis in *Aspergillus fumigatus* are regulated by developmental factors and copper homeostasis. *Eukaryot. Cell*. 12(12): 1641-1652. https://doi.org/10.1128/ec.00217-13.

Upadhyay S, Xu X, Lowry D, Jackson JC, Roberson RW, Lin X. 2016. Subcellular compartmentalization and trafficking of the biosynthetic machinery for fungal melanin. *Cell reports*. 14(11): 2511-2518. https://doi.org/10.1016/j.celrep.2016.02.059.

Uran ME, Cano LE. 2008. Melanin: implications in some disease pathogenesis and its capacity to evade the host immune system. *Infectio*. 12(2): 128-148.

Valiante V, Baldin C, Hortschansky P, Jain R. 2016. The *Aspergillus fumigatus* conidial melanin production is regulated by the bifunctional bHLH DevR and MADS-box RlmA transcription factors: MADS-box and bHLH transcription factors regulate conidial melanin of *Aspergillus fumigatus*. *Mol Microbiol*. 102(2): 321-335. doi: 10.1111/mmi.13462 .

van den Brink HM, van Gorcom RF, van den Hondel CA. 1998. Cytochrome P450 enzyme systems in fungi. *Fungal. Genet. Biol*. 23(1):1–17. doi: 10.1006/fgbi.1997.1021.

Vasquez A, Zavasky D, Chow NA, Gade L, Zlatanic E, Elkind S, et al. 2018. Management of an outbreak of *Exophiala dermatitidis* bloodstream infections at an outpatient oncology clinic. *Clin Infect Dis.* 66(6): 959-962. doi: 10.1093/cid/cix948 .

Verde-Yáñez L, Núria Vall-llaura N, Usall J, Teixidó N, Torreblanca-Bravo E, Torres R. 2023. Identification and biosynthesis of DHN-melanin related pigments in the pathogenic fungi *Monilinia laxa, M. fructicola*, and *M. fructigena*. *J Fungi (Basel)*. 9(2): 138. doi: 10.3390/jof9020138.

Verde-Yanez L, Usall J, Teixido N, Vall-llaura N, Torres R. 2023. Deciphering the effect of light wavelengths in *Monilinia* spp. DHN-melanin production and their interplay with ROS metabolism in *Monilinia fructicola*. *J. Fungi*. 9(6): 653. doi: 10.3390/jof9060653 .

Voß B, Kirschhöfer F, Brenner-Weiß G, Fischer R. 2020. *Alternaria alternata* uses two siderophore systems for iron acquisition. *Nature*. 3587(2020). https://doi.org/10.1038/s41598-020-60468-7.

Voglmayr H, Mayer V, Maschwitz U, Moog J, Djieto-Lordon C, Blatrix R. 2011. The diversity of ant-associated black yeasts: insights into a newly discovered world of symbiotic interactions. *Fungal Biol*. 115(10): 1077–1091. doi: https://doi.org/10.1016/j.funbio.2010.11.006.

Walker CA, Gomez BL, Mora-Montes HM, Mackenzie KS, Munro CA, Brown AJ, et al. 2010. Melanin externalization in *Candida albicans* depends on cell wall chitin structures. *Eukaryot Cell*. 9(9): 1329–1342. doi: 10.1128/EC.00051-10.

Walton FJ, Idnurm A, Heitman J. 2005. Novel gene functions required for melanization of the human pathogen *Cryptococcus neoformans*. *Mol. Microbiol*. 57(5): 1381–1396. https://doi.org/10.1111/j.1365-2958.2005.04779.x.

Wang Y, Aisen P, Casadevall A. 1995. *Cryptococcus neoformans* melanin and virulence: mechanism of action. *Infect Immun*. 63(8): 3131-3136. doi: 10.1128/iai.63.8.3131-3136.1995.

Wang Z, Zheng L, Hauser M, Becker JM, Szaniszlo PJ. 1999. WdChs4p, a homolog of chitin synthase 3 in *Saccharomyces cerevisiae*, alone cannot support growth of *Wangiella (Exophiala) dermatitidis* at the temperature of infection. *Infect. Immun*. 67(12): 6619–6630. doi: 10.1128/IAI.67.12.6619-6630.1999 .

Wang Y, Hu X, Fang Y, Anchieta A, Goldman PH, Hernandez G, et al. 2018. Transcription factor VdCmr1 is required for pigment production, protection from UV irradiation, and regulates expression of melanin biosynthetic genes in *Verticillium dahlia*. *Microbiol*. 164(4): 685-696. doi: 10.1099/mic.0.000633 .

Wang C, xing H, Jiang X, Zeng J, Liu Z, Chen J, Wu Y. 2019. Cerebral phaeohyphomycosis caused by *Exophiala dermatitidis* in a Chinese *CARD9-Deficient patient*: A case report and literature review. *Frontiers*: 10: 938. doi: 10.3389/fneur.2019.00938 .

Wang L, Chen R, Weng Q, Lin S, Wang H, Li L, et al. 2020. SPT20 regulates the Hog1-MAPK pathway and is involved in *Candida albicans* response to hyperosmotic stress. *Front. Microbiol.* 11: 213. doi:10.3389/fmicb.2020.00213 .

Watanabe A, Fujii I, Tsai HF, Chang YC, Kwon-Chung KJ, Ebizuka Y. 2000. *Aspergillus fumigatus* alb1 encodes naphthopyrone synthase when expressed in *Aspergillus oryzae*. *FEMS Lett*. 192(1): 39–44. doi: 10.1111/j.1574-6968.2000.tb09356.x.

Waterhouse A, Bertoni M, Bienert S, Studer G, Tauriello G, Gumienny Ret al. 2018. SWISS-MODEL: homology modeling of protein structures and complexes. *Nucleic Acids Res*. 46(Web Server issue): W296-W303. doi: 10.1093/nar/gky427.

Wejin A, Berg-Somhorst DBPM, Slootweg JC, Vincken JP, Gruppen H, Wichers HJ, et al. 2013. Main phenolic compounds of the melanin biosynthetic pathway in bruising tolerant and bruising sensitive button mushroom (*Agaricus bisporus*) strains. *J. Food Chem*. 61(34): 8224-8231. doi: 10.1021/jf4020558.

Williamson PR. 1994. Biochemical and molecular characterization of the diphenol oxidase of *Cryptococcus neoformans*: identification as a laccase. *J. Bacteriol*. 176(3): 656–664. doi: 10.1128/jb.176.3.656-664.1994.

Williamson PR. 1997. Laccase and melanin in the pathogenesis of *Cryptococcus neoformans*. *Front. Biosci.* 2: e99-107. doi: 10.2741/a231.

Wheeler MH, Bell AA. 1988. Melanins and their importance in pathogenic fungi. *Curr. Top. Med. Mycol*. 2: 338-387. doi: 10.1007/978-1-4612-3730-3_10.

Winkler A, Arkind C, Mattison CP, Burkholder A, Knoche K, Ota I. 2002. Heat stress activates the yeast high-osmolarity glycerol mitogen-activated protein kinase pathway, and protein tyrosine phosphatases are essential under heat stress. *Eukaryot. Cell.* 1(2): 163–173. doi: 10.1128/EC.1.2.163-173.2002.

Wolbarsht ML, Walsh AW, George G. 1981. Melanin, a unique biological absorber. *Appl. Opt*. 20(13): 2184-2186. https://doi.org/10.1364/AO.20.002184.

Wollenzien U, de Hoog GS, Krumbein WE, Urzi C. 1995. On the isolation of microcolonial fungi occurring on and in marble and other calcareous rocks. *Science of the total Environment*. 167(1-3): 287-294. doi: https://doi.org/10.1016/0048-9697(95)04589-S.

Wollenzien U, de Hoog GS, Krumbein WE, Uijthof JMJ. 1997. *Sarcinomyces petricola*, a new microcolonial fungus from marble in the Mediterranean basin. *Antonie van Leeuwenhock*. 71(3): 281-288. doi: 10.1023/a:1000157803954.

Xie W, Pakdel E, Liang Y, Kim YJ, Liu D, Sun L, et al. 2019. Natural eumelanin and its derivatives as multifunctional materials for bioinspired applications: A review. *Biomacromolecules* 20(12): 4312−4331. doi: 10.1021/acs.biomac.9b01413.

Xu X, Cao R, Li K, Wan Q, Xu G, Lin Y, et al. 2022. The protective role and mechanism of melanin for *Aspergillus niger* and *Aspergillus flavus* against chlorine-based disinfectants. *Water Res.* 223: 119039. https://doi.org/10.1016/j.watres.2022.119039.

Yang F, Cheng L, Du Y, Xia L, Long C. 2022. Functional identification of the DHN melanin synthesis gene cluster and its role in UV-C tolerance in citrus postharvest pathogenic fungus *Penicillium digitatum*. *Fungal Biol*. 126(9): 566-575. doi: 10.1016/j.funbio.2022.07.002 .

Yang X, Tang C, Zhao Q, Jia Y, Qin Y, Zhang J. 2023. Melanin: A promising source of functional food ingredient. *J. Functional Foods*. 105: 105574. https://doi.org/10.1016/j.jff.2023.105574.

Yu X, Liu H, Niu X, Akhberdi O, Wei D, Wang D, et al. 2017. The Gα1-cAMP signaling pathway controls conidiation, development and secondary metabolism in the taxol-producing fungus *Pestalotiopsis microspora*. *Microbiol. Research*. 203: 29-39. https://doi.org/10.1016/j.micres.2017.06.003.

Zalar P. de Hoog GS. Gunde-Cimerman N. 1999. *Trimatostroma salinum*, a new species from hypersaline water. *Stud. Mycol*. 43: 57-62.

Zalar P, Gostincar C, de Hoog GS, Ursic V, Sudhadham M, Gunde-Cimerman N. 2008. Redefinition of *Aureobasidium pullulans* and its varieties. *Stud. Mycol*. 61: 21-38. doi: 10.3114/sim.2008.61.02.

Zhang P, Wei D, Li Z, Sun Z, Pan J, Zhu X. 2015. *Cryptococcal* phosphoglucose isomerase is required for virulence factor production, cell wall integrity and stress resistance. *FEMS Yeast Res*. 15(7): fov072. doi: 10.1093/femsyr/fov072 .

Zhang P, Zhou S, Wang G, An Z, Liu X, Li K, et al. 2019. Two transcription factors cooperatively regulate DHN melanin biosynthesis and development in *Pestalotiopsis fici*. *Mol Microbiol.* 112(2): 649-666. doi: 10.1111/mmi.14281 .

Zhang Z, Jia H, Liu N, Li H, Meng Q, Wu N, et al. 2022. The zinc finger protein StMR1 affects the pathogenicity and melanin synthesis of *Setosphaeria turcica* and directly regulates the expression of DHN melanin synthesis pathway genes. *Mol. Microbiol*. 117(2): 261-273. doi: 10.1111/mmi.14786 .

Zhang X, Li B, Huang B, Wang F, Zhang Y, Zhao S, et al. 2022. Production, Biosynthesis, and Commercial Applications of Fatty Acids From Oleaginous Fungi. *Front. Nutr.* 9: 873657. doi: 10.3389/fnut.2022.873657.

Zhang X. Hou X. Xu D. Xue M. Zhang J. Wang J. Yang Y. Lai D. Zhou L. 2023. Effects of carbon, nitrogen, ambient pH and light on mycelial growth, sporulation, sorbicillinoid biosynthesis and related gene expression in *Ustilaginoidea virens*. *J. Fungi.* 9(4): 390. doi: 10.3390/jof9040390 .

Zheng L, Mendoza L, Wang Z, Liu H. 2006. WdChs1p, a class II chitin synthase, is more responsible than WdChs2p (Class I) for normal yeast reproductive growth in the polymorphic, pathogenic fungus *Wangiella* (*Exophiala*) *dermatitidis*. *Archives Microbiol.* 185(4): 316-329. doi:10.1007/s00203-006-0101-0.

Zhong J, Frases S, Wang H, Casadevall A, Stark RE. 2008. Following fungal melanin biosynthesis with solid-state NMR: biopolymer molecular structures and possible connections to cell-wall polysaccharides. *Biochem*. 47(16): 4701-4710. https://doi.org/10.1021/bi702093r.

Zhou Y, Yang L, Wu M, Chen W, Li G, Zhang J. 2017. A single-nucleotide deletion in the transcription factor gene bcsmr1 causes sclerotial-melanogenesis deficiency in *Botrytis cinerea*. *Front. Microbiol*. 8: 2492. https://doi.org/10.3389/fmicb.2017.02492 .

Zhou M, Li Z, Liu Y, Zhang P, Hao X, Zhu X. 2022. Transcription factors Pmr1 and Pmr2 cooperatively regulate melanin biosynthesis, conidia development and secondary metabolism in *Pestalotiopsis microspora*. *J. Fungi*. 8(1): 38. doi: 10.3390/jof8010038 .

Zhu X, Gibbons J, Garcia-Rivera J, Casadevall A, Williamson PR. 2001. Laccase of *Cryptococcus neoformans* is a cell wall-associated virulence factor. *Infect. Immun.* 69: 5589–5596. https://doi.org/10.1128/iai.69.9.5589-5596.2001.

Zupančič J, Babič MN, Zalar P, Gunde-Cimerman N. 2016. The black yeast *Exophiala dermatitidis* and other selected opportunistic human fungal pathogens spread from dishwashers to kitchens. *PLoS One.* 11(2): p.e0148166. doi: 10.1371/journal.pone.0148166 .

Appendix:

Supplemental Images

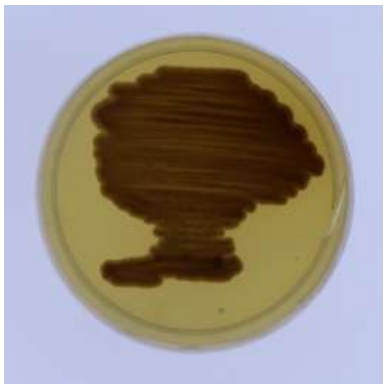

Figure S2.1: *Exophiala dermatitidis* wildtype strain UT8656 growing on YPD media.

Figure S2.2: Example images of spot test plates used to calculate growth and inhibition during UV and temperature assays. Solid spots indicate no inhibition in growth; transparent and scattered spots indicate growth inhibition.

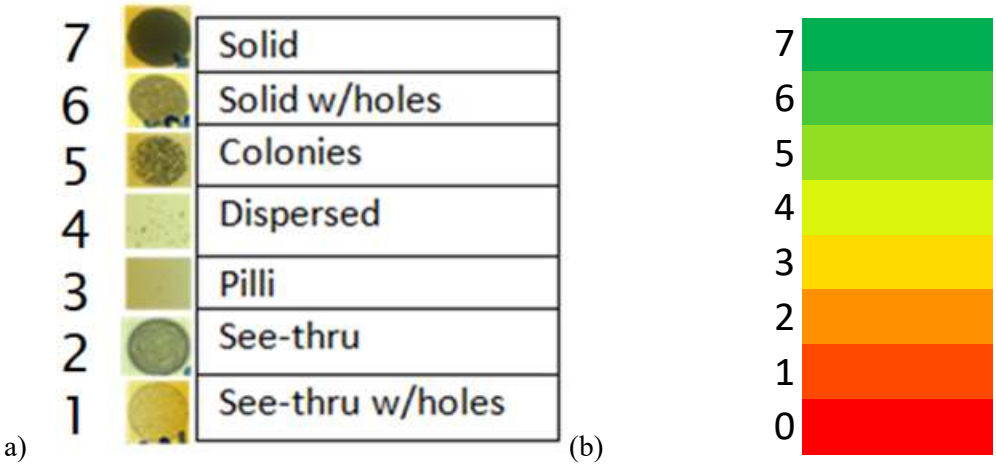

Figure S2.3: Scoring method used to categorize growth and inhibition of *E. dermatitidis* mutant strains during the UV and Temperature Assays. (a) A score of 7 indicates no inhibition and 1 indicates complete inhibition. (b) Image representing the colors associated with the scoring method for heatmaps.

breseq version 0.35.4
mutation predictions | marginal predictions | summary statistics | genome diff | command line log

Read File Information

	read file	reads	bases	passed filters	average	longest	mapped
errors	11020_S83_R1_001	5,651,745	674,156,273	100.0%	119.3 bases	149 bases	95.4%
errors	11020_S83_R2_001	5,647,400	673,567,540	99.9%	119.3 bases	149 bases	95.3%
	total	**11,299,145**	**1,347,723,813**	99.9%	119.3 bases	**149** bases	95.3%

Reference Sequence Information

		seq id	length	fit mean	fit dispersion	% mapped reads	description
coverage	distribution	NW_008751646	4,245,248	49.9	2.9	16.3%	Exophiala dermatitidis NIH/UT8656 unplaced genomic scaffold
coverage	distribution	NW_008751647	4,219,124	49.6	2.9	16.0%	Exophiala dermatitidis NIH/UT8656 unplaced genomic scaffold
coverage	distribution	NW_008751648	3,712,203	49.5	2.9	14.0%	Exophiala dermatitidis NIH/UT8656 unplaced genomic scaffold
coverage	distribution	NW_008751649	3,623,950	49.4	3.0	13.6%	Exophiala dermatitidis NIH/UT8656 unplaced genomic scaffold
coverage	distribution	NW_008751650	3,507,949	49.5	2.9	13.3%	Exophiala dermatitidis NIH/UT8656 unplaced genomic scaffold
coverage	distribution	NW_008751651	2,894,154	49.1	2.9	10.9%	Exophiala dermatitidis NIH/UT8656 unplaced genomic scaffold
coverage	distribution	NW_008751652	2,701,005	49.1	3.0	9.9%	Exophiala dermatitidis NIH/UT8656 unplaced genomic scaffold
coverage	distribution	NW_008751653	1,185,917	48.9	3.0	4.4%	Exophiala dermatitidis NIH/UT8656 unplaced genomic scaffold
coverage	distribution	NW_008751654	254,587	48.8	2.8	0.9%	Exophiala dermatitidis NIH/UT8656 unplaced genomic scaffold
coverage	distribution	NW_008751655	6,626	NA	NA	0.0%	Exophiala dermatitidis NIH/UT8656 unplaced genomic scaffold
coverage	distribution	NW_008751656	26,004	80.7	38.2	0.7%	Exophiala dermatitidis NIH/UT8656 mitochondrion, whole genome
		total	**26,376,767**			100.0%	

(a) **fit dispersion** is the ratio of the variance to the mean for the negative binomial fit. It is =1 for Poisson and >1 for over-dispersed data.

(b)

Predicted mutations						
evidence	seq id	position	mutation	annotation	gene	description
RA	NW_008751646	334,072	A→G	intergenic (+592/-2471)	*HMPREF1120_00122* → / → *HMPREF1120_00123*	hypothetical protein/hypothetical protein
RA	NW_008751646	334,795	A→G	intergenic (+1315/-1748)	*HMPREF1120_00122* → / → *HMPREF1120_00123*	hypothetical protein/hypothetical protein
RA	NW_008751646	335,148	C→T	intergenic (+1668/-1395)	*HMPREF1120_00122* → / → *HMPREF1120_00123*	hypothetical protein/hypothetical protein
RA	NW_008751646	335,164	C→T	intergenic (+1684/-1379)	*HMPREF1120_00122* → / → *HMPREF1120_00123*	hypothetical protein/hypothetical protein
RA	NW_008751646	343,384	C→T	intergenic (-265/-850)	*HMPREF1120_00126* ← / → *HMPREF1120_00128*	succinate dehydrogenase [ubiquinone] iron-sulfur subunit, mitochondrial/hypothetical protein
JC	NW_008751646	642,712	+28 bp	coding (3111/3141 nt)	*HMPREF1120_00237* ←	transcriptional activator SPT7
RA	NW_008751646	844,506	T→A	intergenic (+13762/-5833)	*HMPREF1120_00301* → / → *HMPREF1120_00303*	hypothetical protein/hypothetical protein
RA	NW_008751646	912,768	C→T	intergenic (-9757/+5193)	*HMPREF1120_00323* ← / ← *HMPREF1120_00324*	hypothetical protein, variant 2/hypothetical protein
RA	NW_008751646	1,384,766	A→G	intergenic (-1858/-15)	*HMPREF1120_00499* ← / → *HMPREF1120_00500*	topoisomerase (DNA) II binding protein 1/sterol O-acyltransferase
RA	NW_008751646	1,475,191	C→T	S61S (TCG→TCA)	*HMPREF1120_00537* ←	AAT family amino acid transporter
RA	NW_008751646	1,551,414	A→C	F936L (TTT→TTG)	*HMPREF1120_00561* ←	hypothetical protein
RA	NW_008751646	1,936,020	T→C	intergenic (-114/+2210)	*HMPREF1120_00699* ← / ← *HMPREF1120_00700*	hypothetical protein/transcriptional regulatory protein GAL4
RA	NW_008751646	2,408,143	T→C	A338A (GCT→GCC)	*HMPREF1120_00863* →	hypothetical protein
RA	NW_008751646	2,541,571	C→T	A82V (GCC→GTC)	*HMPREF1120_00918* →	DNA-directed RNA polymerase I subunit A12
RA	NW_008751646	2,583,552	A→G	L373P (CTG→CCG)	*HMPREF1120_00933* ←	hypothetical protein
RA	NW_008751646	2,587,971	C→T	intergenic (+997/-652)	*HMPREF1120_00934* → / → *HMPREF1120_00935*	importin subunit alpha-1/alcohol dehydrogenase

Figure S2.4: Example images for one of the samples showing (a) summary statistic file showing the alignment rate and (b) index.html file of the showing the predicted mutations obtained via the breseq computation pipeline showing the evidence, annotation, gene ID and description of the gene.

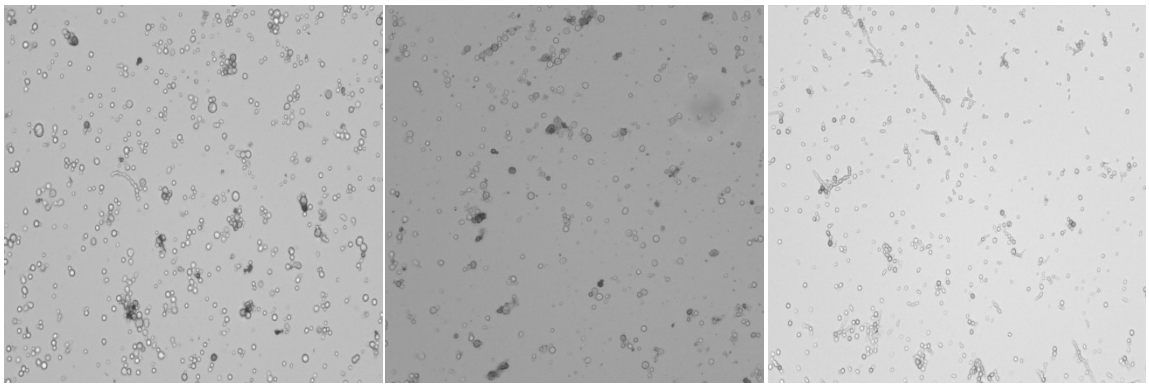

Figure S2.5: Images obtained using EVOS M5000 (FL Auto 2 Cell Imaging software) representing the different cell morphology observed in the wildtype and mutant *E. dermatitidis* strains.

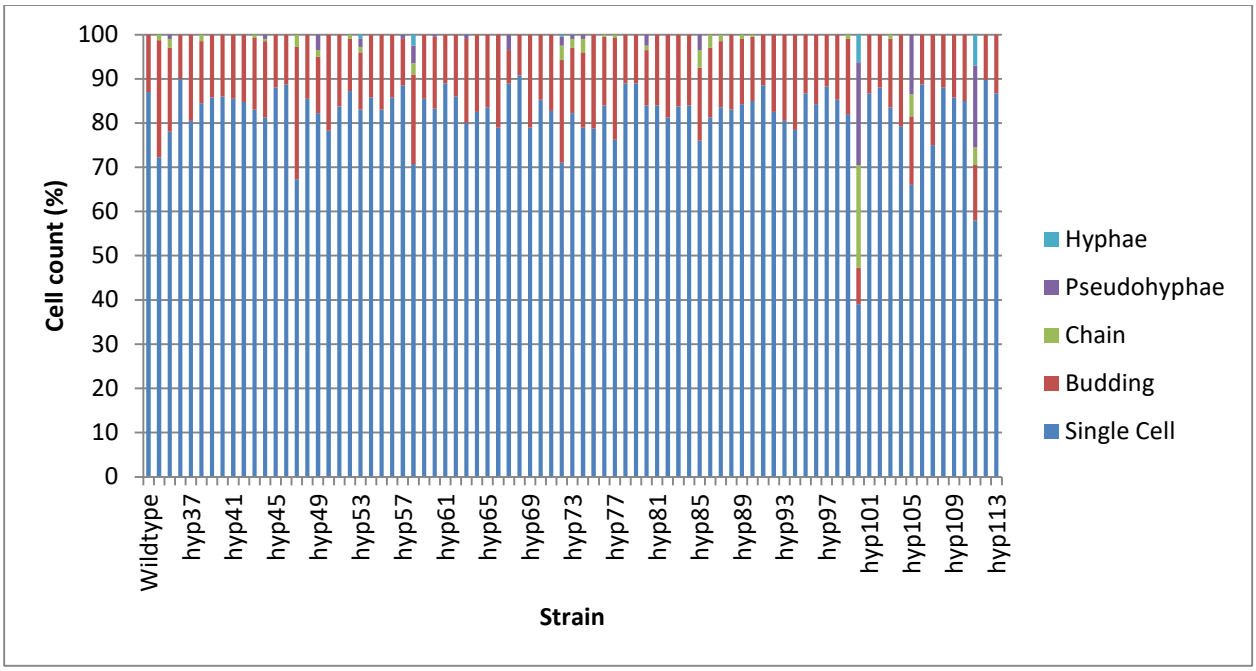

Figure S2.6: Counts of different cell morphologies of the remaining E. *dermatitidis hyp* mutant strains that were not selected for genome sequencing (SNV analysis). Legend indicating the type of cells observed. Cell count (%) on y-axis and strains on x-axis.

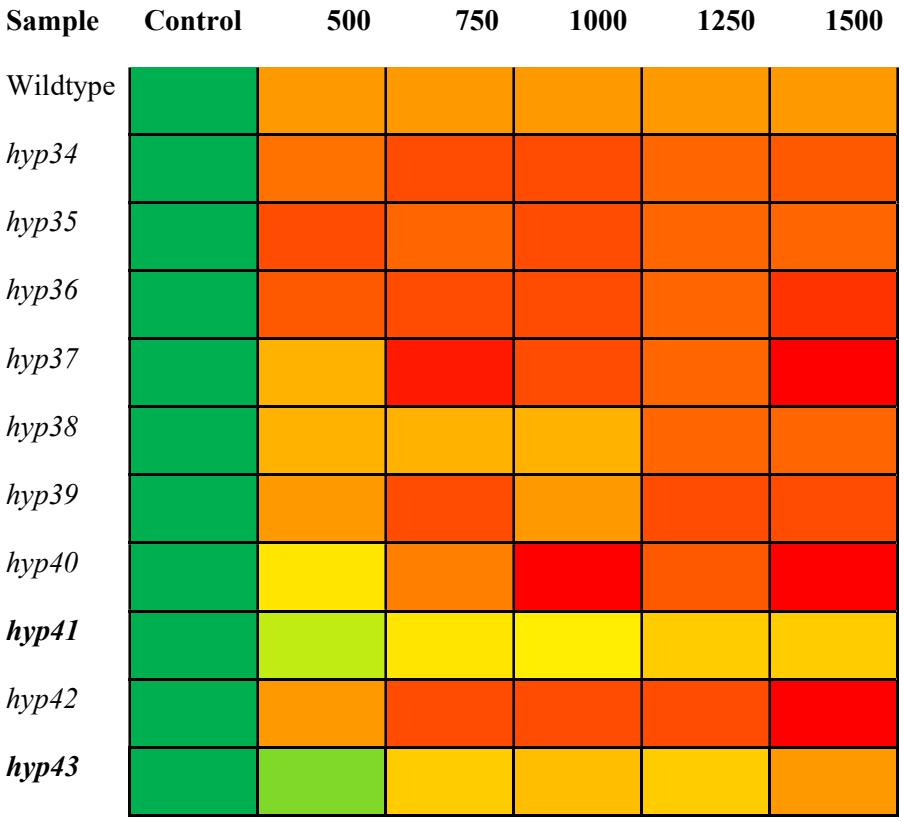

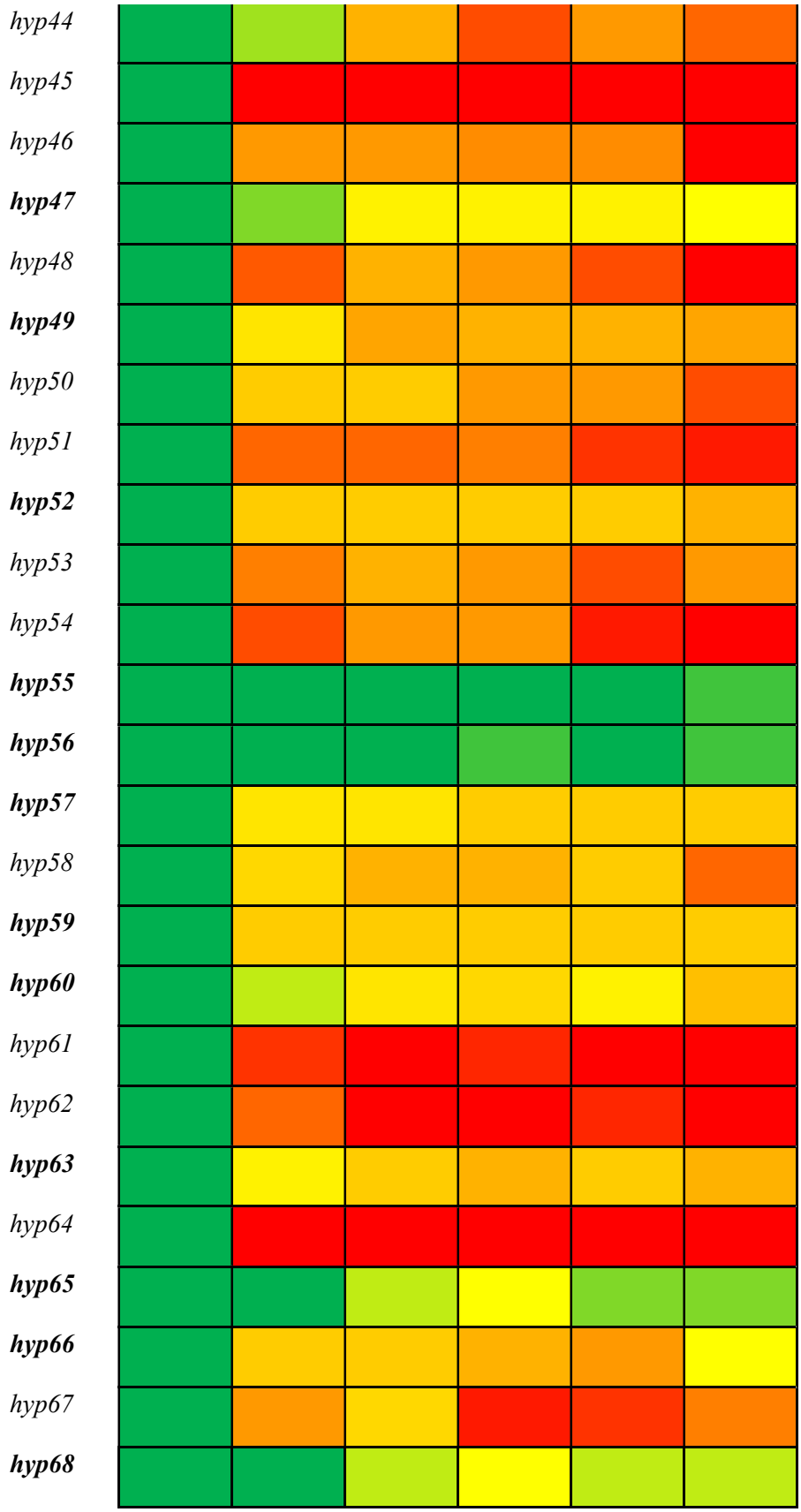
hyp44
hyp45
hyp46
hyp47
hyp48
hyp49
hyp50
hyp51
hyp52
hyp53
hyp54
hyp55
hyp56
hyp57
hyp58
hyp59
hyp60
hyp61
hyp62
hyp63
hyp64
hyp65
hyp66
hyp67
hyp68

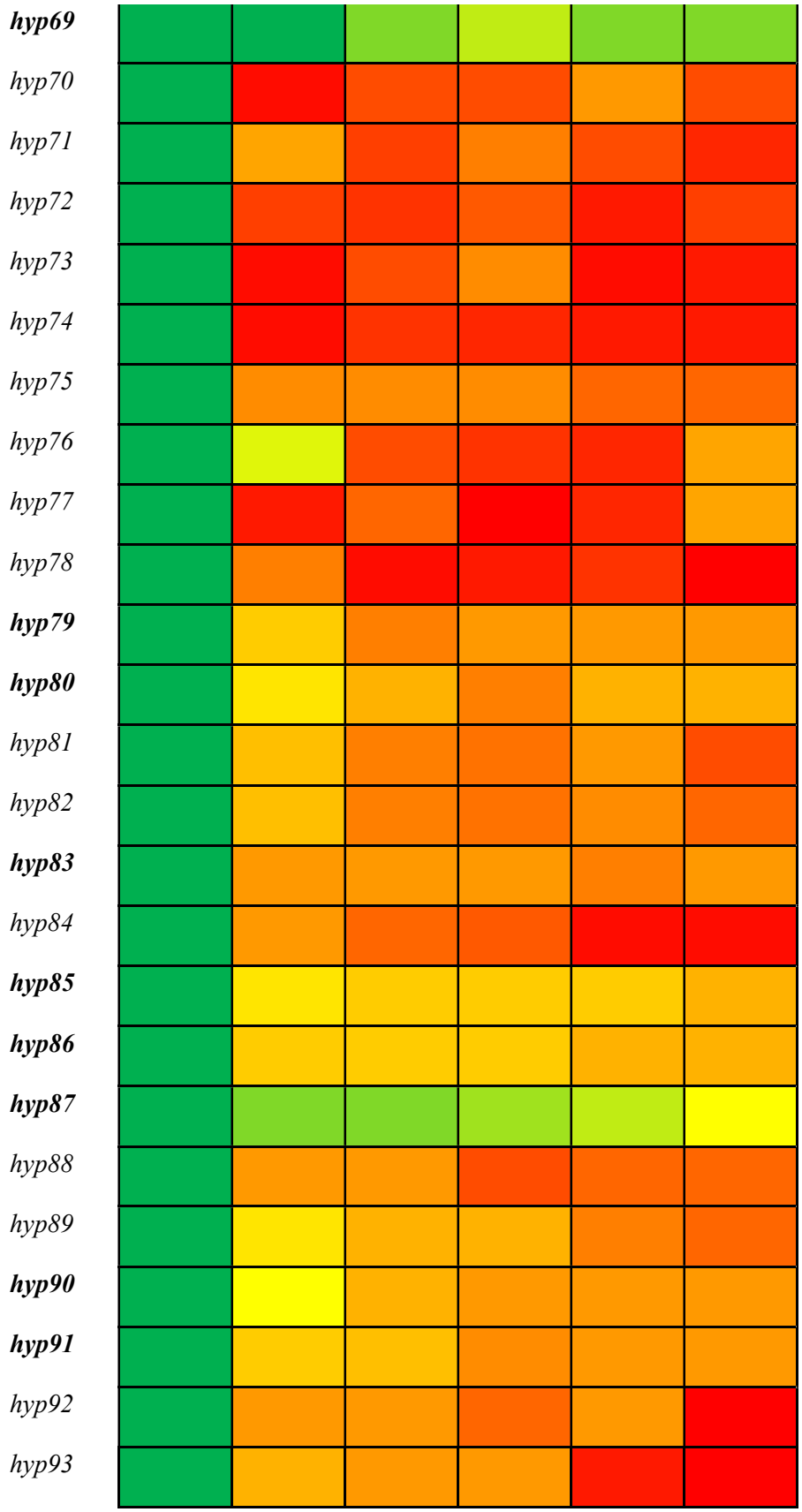
hyp69
hyp70
hyp71
hyp72
hyp73
hyp74
hyp75
hyp76
hyp77
hyp78
hyp79
hyp80
hyp81
hyp82
hyp83
hyp84
hyp85
hyp86
hyp87
hyp88
hyp89
hyp90
hyp91
hyp92
hyp93

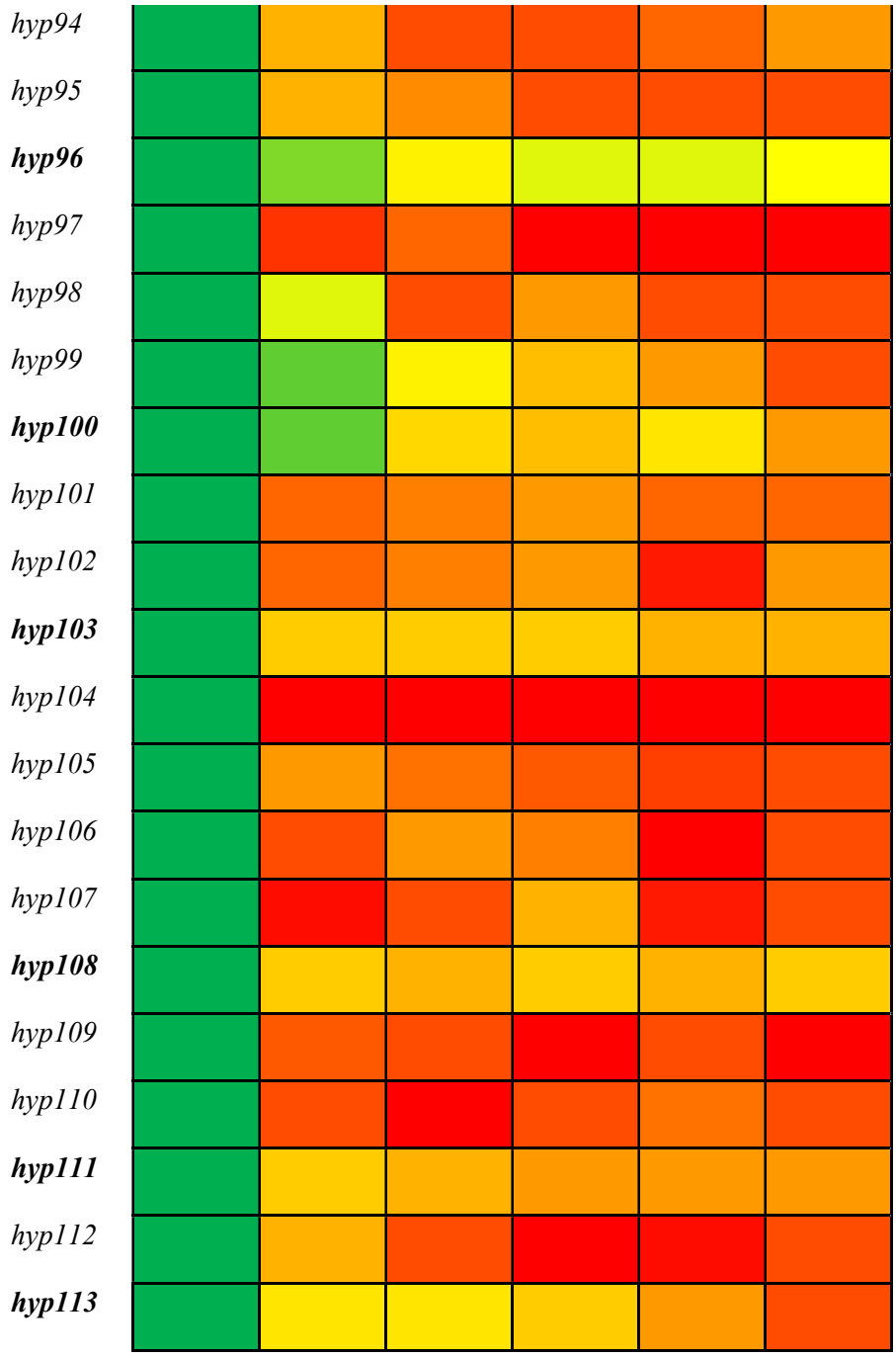

Figure S2.7a: Growth observed for the remaining *E. dermatitidis hyp* strains (1:100 dilution) on YPD media at different UV intensities (control (no UV), 500, 750, 1000, 1250 and 1500 Energy 1000 x 100µW/cm^2). Colors of the heatmap represent the scores obtained by visualizing the type of growth observed for each spot and comparing them to growth patterns as indicated in Supplemental Figure S3. Mutant strains that had similar or lower UV intensity than the wildtype are in bold. Data for 1:1, 1:10 and 1:1000 dilutions for all mutants in Supplemental File 2.

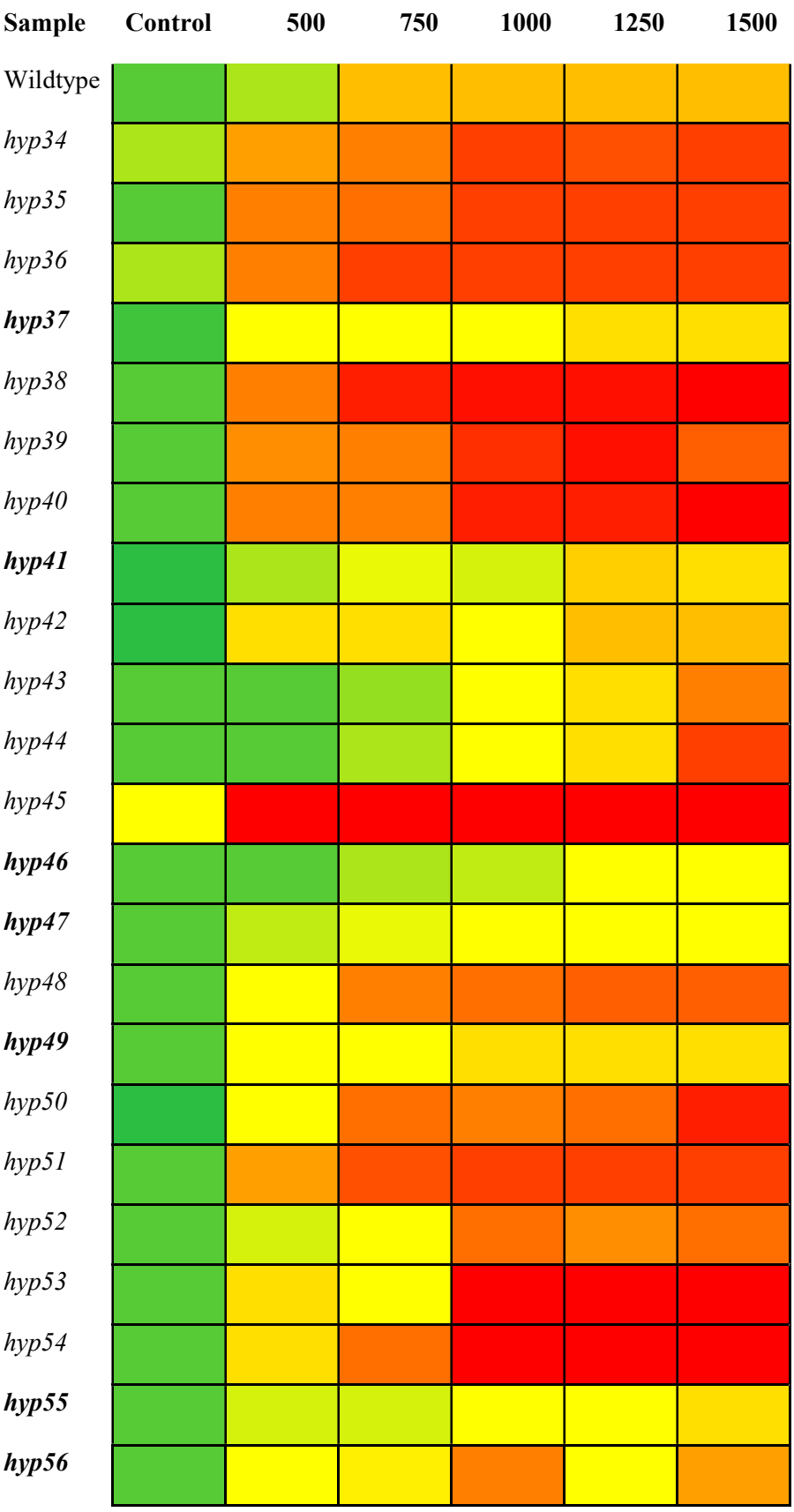
Sample
Control
500
750
1000
1250
1500
Wildtype
hyp34
hyp35
hyp36
hyp37
hyp38
hyp39
hyp40
hyp41
hyp42
hyp43
hyp44
hyp45
hyp46
hyp47
hyp48
hyp49
hyp50
hyp51
hyp52
hyp53
hyp54
hyp55
hyp56

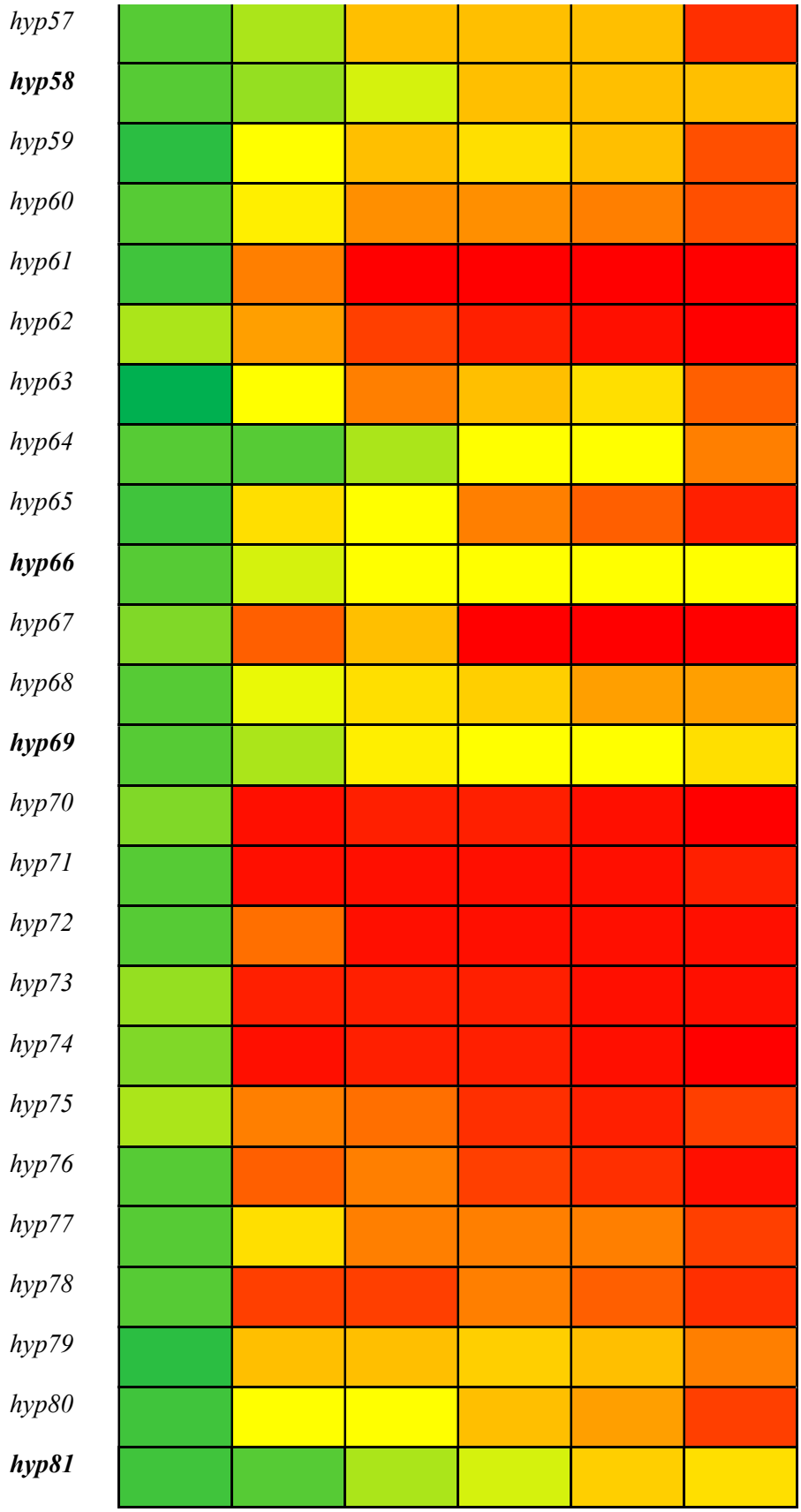
hyp57
hyp58
hyp59
hyp60
hyp61
hyp62
hyp63
hyp64
hyp65
hyp66
hyp67
hyp68
hyp69
hyp70
hyp71
hyp72
hyp73
hyp74
hyp75
hyp76
hyp77
hyp78
hyp79
hyp80
hyp81

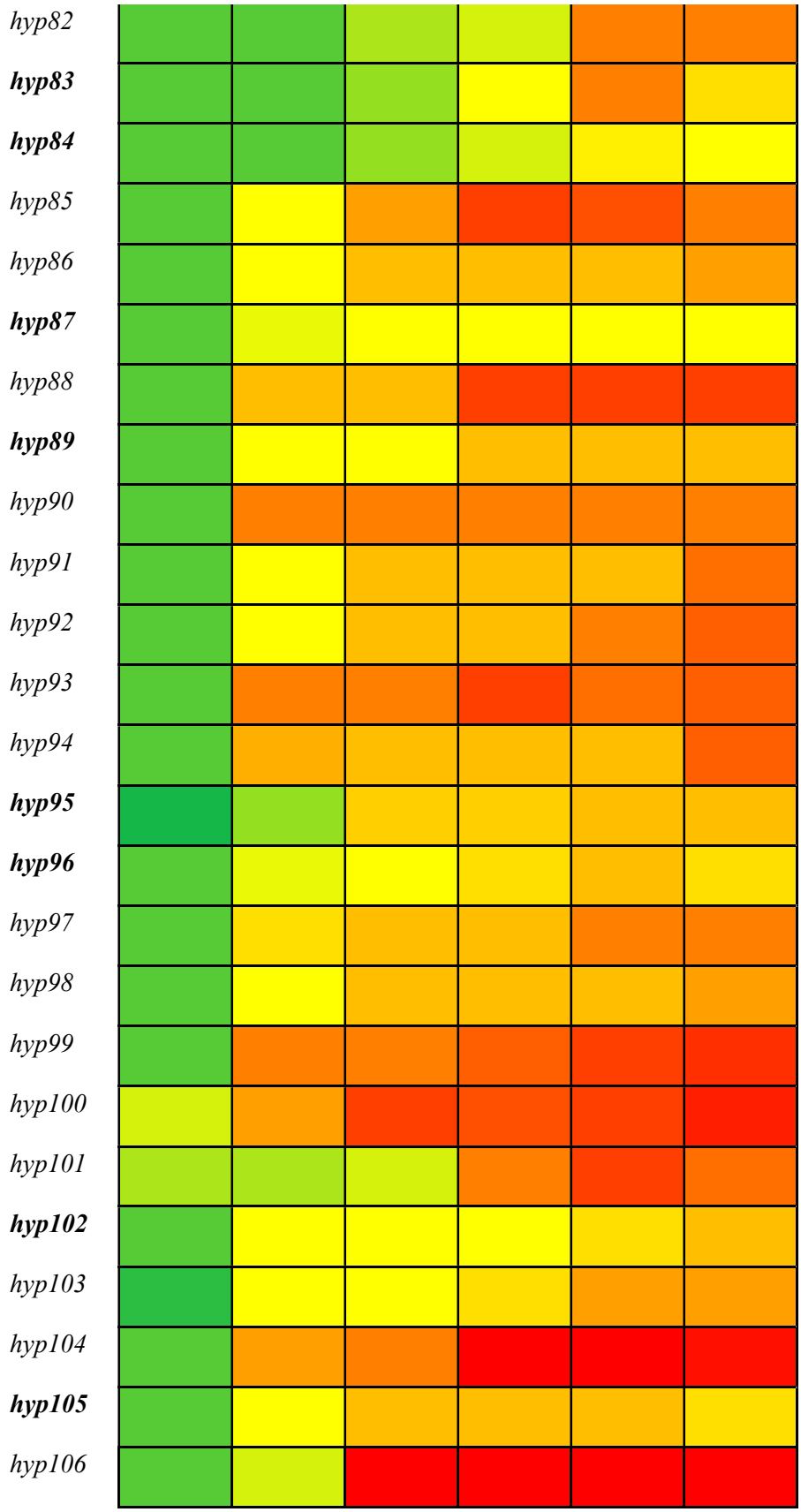
hyp82
hyp83
hyp84
hyp85
hyp86
hyp87
hyp88
hyp89
hyp90
hyp91
hyp92
hyp93
hyp94
hyp95
hyp96
hyp97
hyp98
hyp99
hyp100
hyp101
hyp102
hyp103
hyp104
hyp105
hyp106

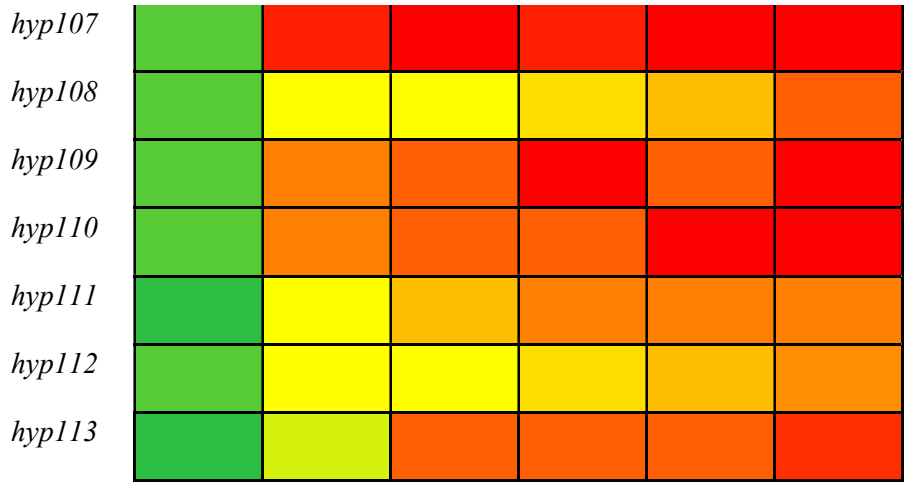

Figure S2.7b: Growth observed for the remaining *E. dermatitidis hyp* strains (1:100 dilution) on MN media at different UV intensities (control (no UV), 500, 750, 1000, 1250 and 1500 Energy 1000 x 100µW/cm^2). Colors of the heatmap represent the scores obtained by visualizing the type of growth observed for each spot and comparing them to growth patterns as indicated in Supplemental Figure S3. Mutant strains that had similar or lower UV intensity than the wildtype are in bold. Data for 1:1, 1:10 and 1:1000 dilutions for all mutants in Supplemental File 2.

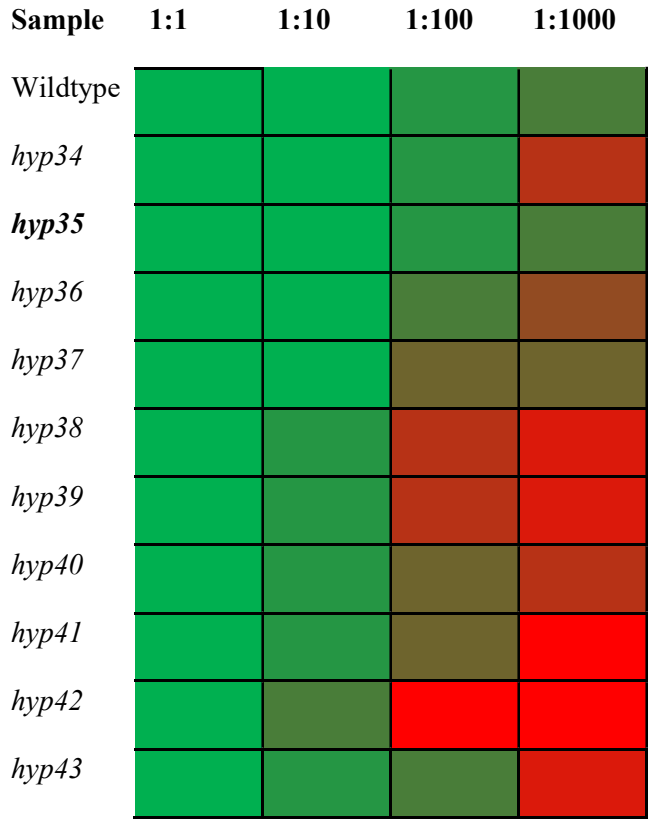

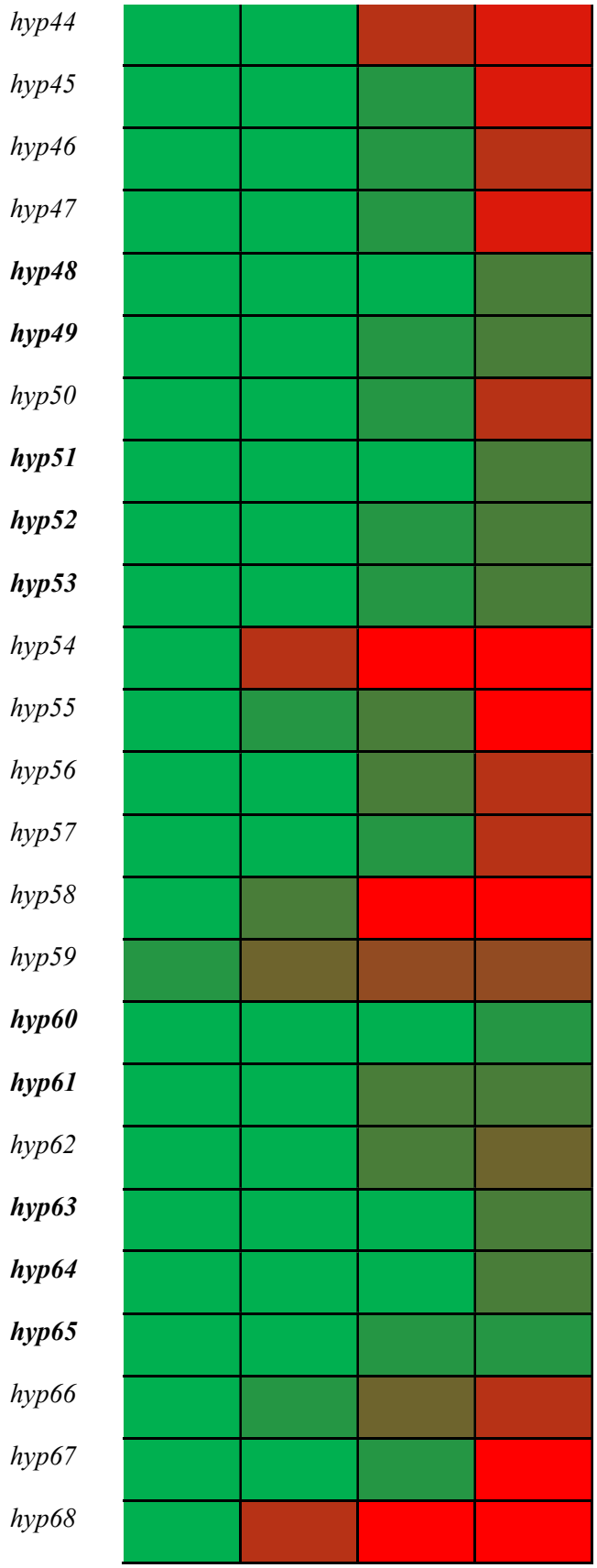
hyp44
hyp45
hyp46
hyp47
hyp48
hyp49
hyp50
hyp51
hyp52
hyp53
hyp54
hyp55
hyp56
hyp57
hyp58
hyp59
hyp60
hyp61
hyp62
hyp63
hyp64
hyp65
hyp66
hyp67
hyp68

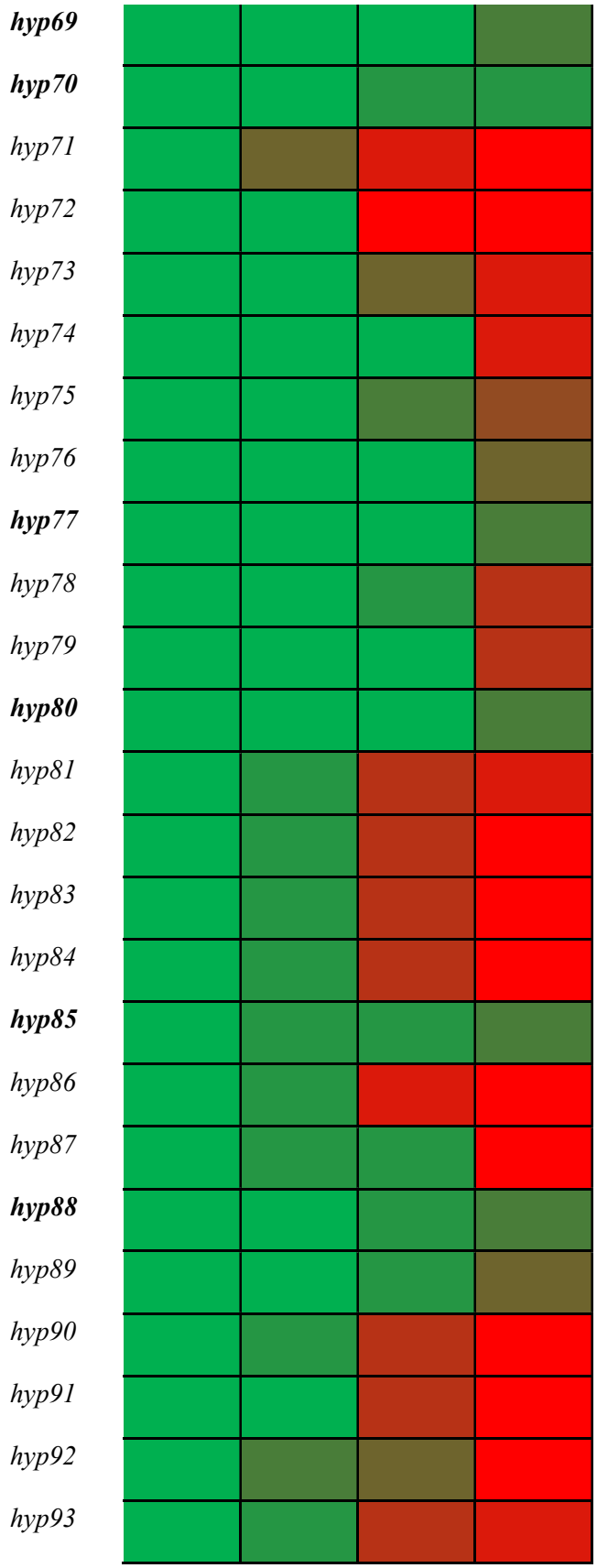
hyp69
hyp70
hyp71
hyp72
hyp73
hyp74
hyp75
hyp76
hyp77
hyp78
hyp79
hyp80
hyp81
hyp82
hyp83
hyp84
hyp85
hyp86
hyp87
hyp88
hyp89
hyp90
hyp91
hyp92
hyp93

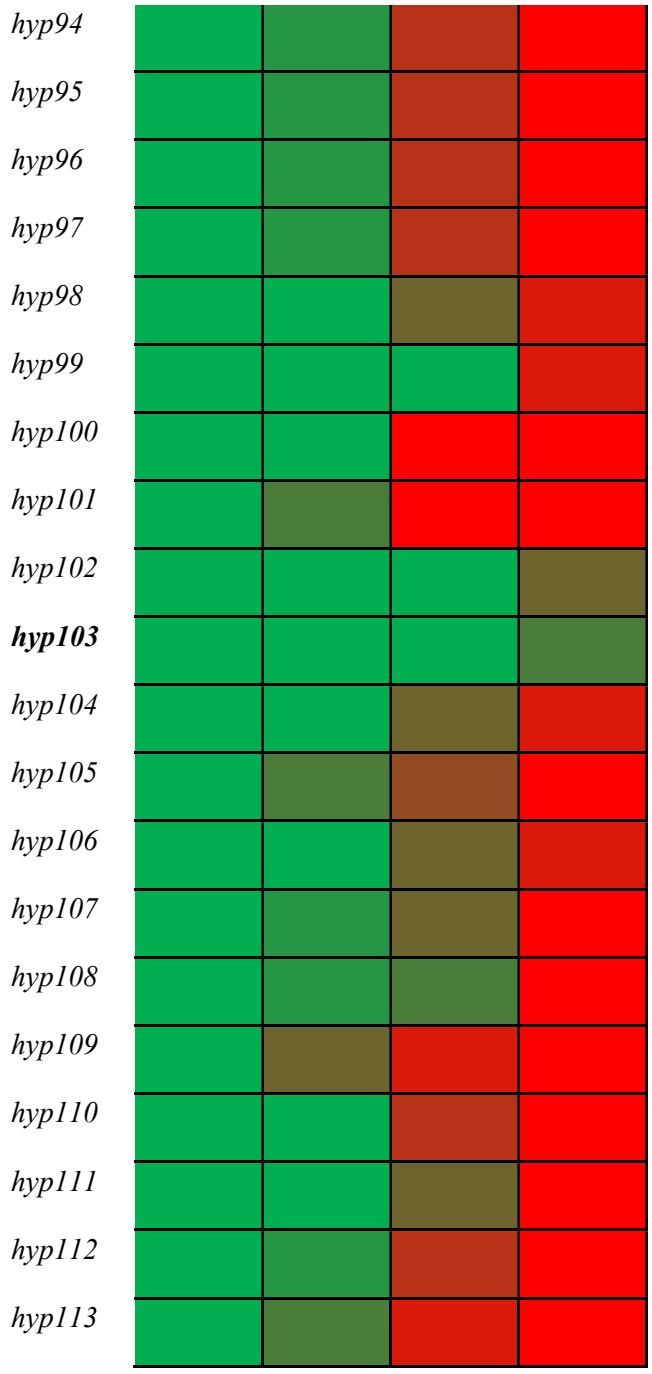

Figure S2.8: Heatmap representing the growth observed for different dilutions of remaining *hyp* mutant strains growing at 42°C. Samples were grown on YPD media. Colors of the heatmap represent the scores obtained by visualizing the type of growth observed for each spot and comparing them to growth patterns as indicated in Supplemental Figure S3. Mutant strains that had similar growth to wildtype at 42°C are in bold. Data for 10°C and 28°C for all mutants in Supplemental File 2.

(a)

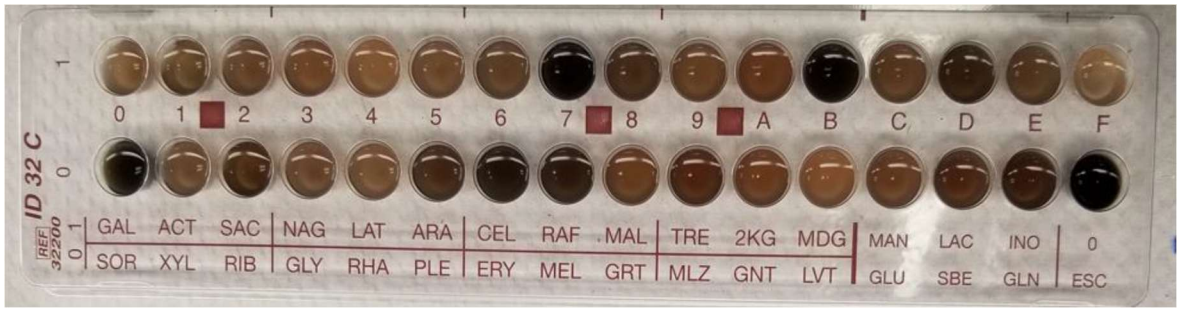
ID 32 C
REF 32200
0 1 2 3 4 5 6 7 8 9 A B C D E F
GAL ACT SAC NAG LAT ARA CEL RAF MAL TRE 2KG MDG MAN LAC INO 0
SOR XYL RIB GLY RHA PLE ERY MEL GRT MLZ GNT LVT GLU SBE GLN ESC

(b)

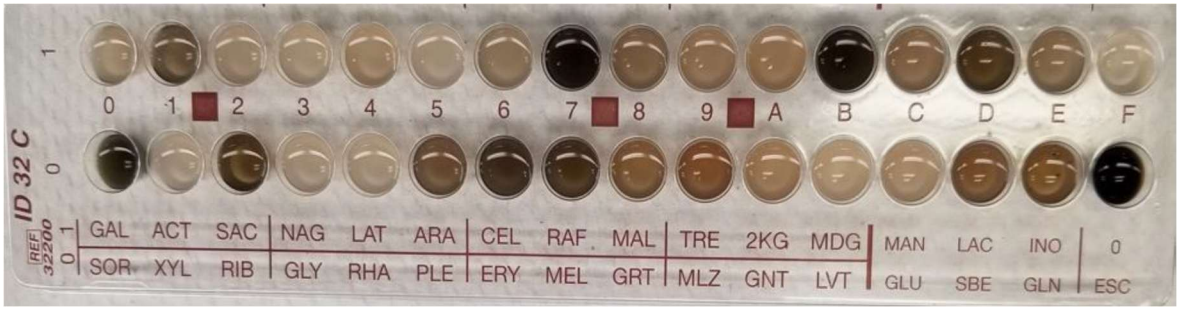
ID 32 C
REF 32200
0 1 2 3 4 5 6 7 8 9 A B C D E F
GAL ACT SAC NAG LAT ARA CEL RAF MAL TRE 2KG MDG MAN LAC INO 0
SOR XYL RIB GLY RHA PLE ERY MEL GRT MLZ GNT LVT GLU SBE GLN ESC

(c)

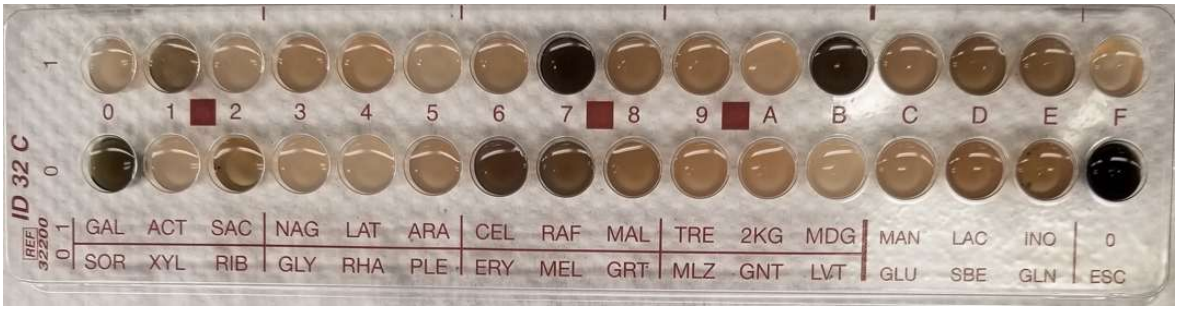
ID 32 C
REF 32200
0 1 2 3 4 5 6 7 8 9 A B C D E F
GAL ACT SAC NAG LAT ARA CEL RAF MAL TRE 2KG MDG MAN LAC INO 0
SOR XYL RIB GLY RHA PLE ERY MEL GRT MLZ GNT LVT GLU SBE GLN ESC

(d)

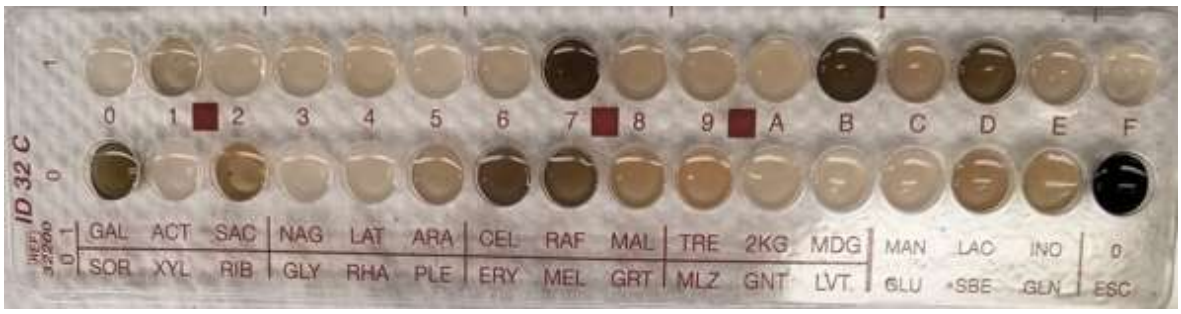
ID 32 C
REF 32200
0 1 2 3 4 5 6 7 8 9 A B C D E F
GAL ACT SAC NAG LAT ARA CEL RAF MAL TRE 2KG MDG MAN LAC INO 0
SOR XYL RIB GLY RHA PLE ERY MEL GRT MLZ GNT LVT GLU SBE GLN ESC

(e)

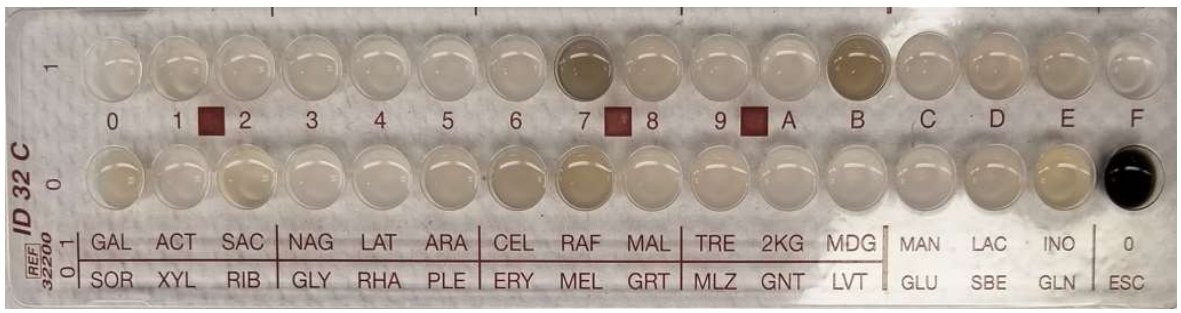
ID 32 C
REF 32200
0 1 2 3 4 5 6 7 8 9 A B C D E F
GAL ACT SAC NAG LAT ARA CEL RAF MAL TRE 2KG MDG MAN LAC INO 0
SOR XYL RIB GLY RHA PLE ERY MEL GRT MLZ GNT LVT GLU SBE GLN ESC

(f)


ID 32 C
0 1 2 3 4 5 6 7 8 9 A B C D E F
GAL ACT SAC NAG LAT ARA CEL RAF MAL TRE 2KG MDG MAN LAC INO 0
SOR XYL RIB GLY RHA PLE ERY MEL GRT MLZ GNT LVT GLU SBE GLN ESC

(g)


ID 32 C
0 1 2 3 4 5 6 7 8 9 A B C D E F
GAL ACT SAC NAG LAT ARA CEL RAF MAL TRE 2KG MDG MAN LAC INO 0
SOR XYL RIB GLY RHA PLE ERY MEL GRT MLZ GNT LVT GLU SBE GLN ESC

(h)


ID 32 C
0 1 2 3 4 5 6 7 8 9 A B C D E F
GAL ACT SAC NAG LAT ARA CEL RAF MAL TRE 2KG MDG MAN LAC INO 0
SOR XYL RIB GLY RHA PLE ERY MEL GRT MLZ GNT LVT GLU SBE GLN ESC

(i)

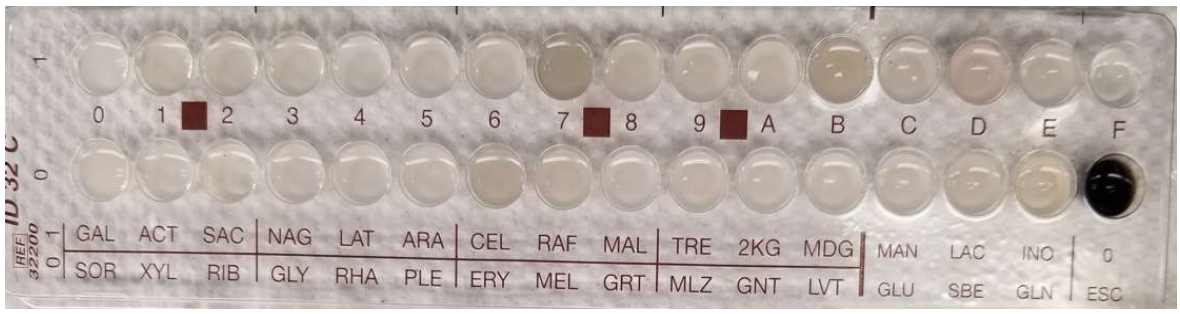
0 1 2 3 4 5 6 7 8 9 A B C D E F
GAL ACT SAC NAG LAT ARA CEL RAF MAL TRE 2KG MDG MAN LAC INO 0
SOR XYL RIB GLY RHA PLE ERY MEL GRT MLZ GNT LVT GLU SBE GLN ESC

(j)

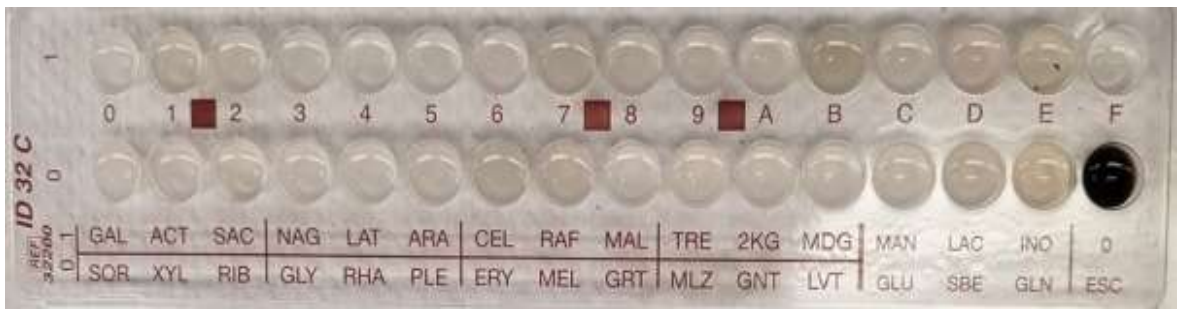
ID 32 C
0 1 2 3 4 5 6 7 8 9 A B C D E F
GAL ACT SAC NAG LAT ARA CEL RAF MAL TRE 2KG MDG MAN LAC INO 0
SOR XYL RIB GLY RHA PLE ERY MEL GRT MLZ GNT LVT GLU SBE GLN ESC

(k)


ID 32 C
REF 32200
0 1 2 3 4 5 6 7 8 9 A B C D E F
GAL ACT SAC NAG LAT ARA CEL RAF MAL TRE 2KG MDG MAN LAC INO 0
SOR XYL RIB GLY RHA PLE ERY MEL GRT MLZ GNT LVT GLU SBE GLN ESC

(l)


ID 32 C
REF 32200
0 1 2 3 4 5 6 7 8 9 A B C D E F
GAL ACT SAC NAG LAT ARA CEL RAF MAL TRE 2KG MDG MAN LAC INO 0
SOR XYL RIB GLY RHA PLE ERY MEL GRT MLZ GNT LVT GLU SBE GLN ESC

(m)

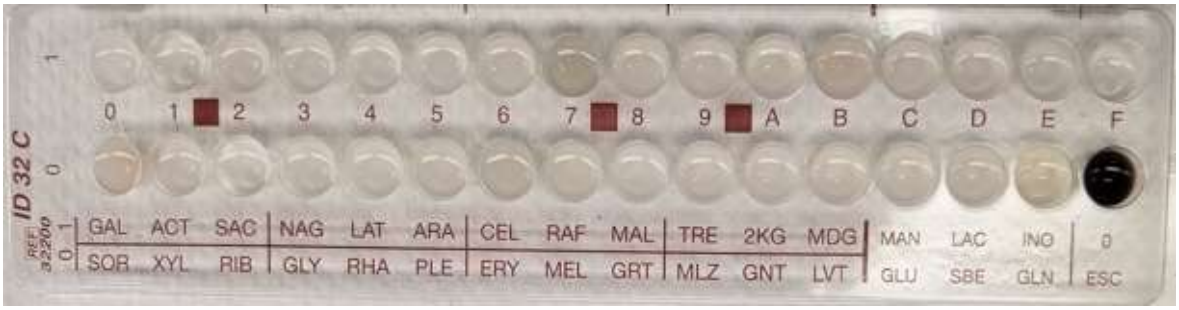
ID 32 C
REF 32200
0 1 2 3 4 5 6 7 8 9 A B C D E F
GAL ACT SAC NAG LAT ARA CEL RAF MAL TRE 2KG MDG MAN LAC INO 0
SOR XYL RIB GLY RHA PLE ERY MEL GRT MLZ GNT LVT GLU SBE GLN ESC

(n)

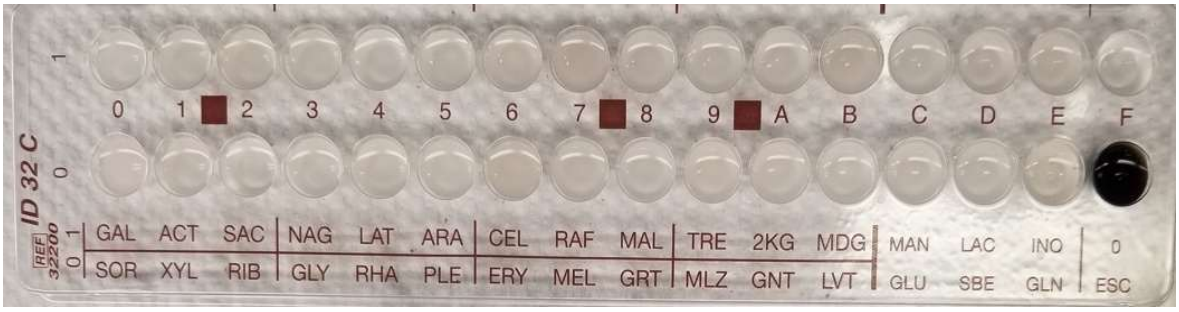
ID 32 C
REF 32200
0 1 2 3 4 5 6 7 8 9 A B C D E F
GAL ACT SAC NAG LAT ARA CEL RAF MAL TRE 2KG MDG MAN LAC INO 0
SOR XYL RIB GLY RHA PLE ERY MEL GRT MLZ GNT LVT GLU SBE GLN ESC

(o)

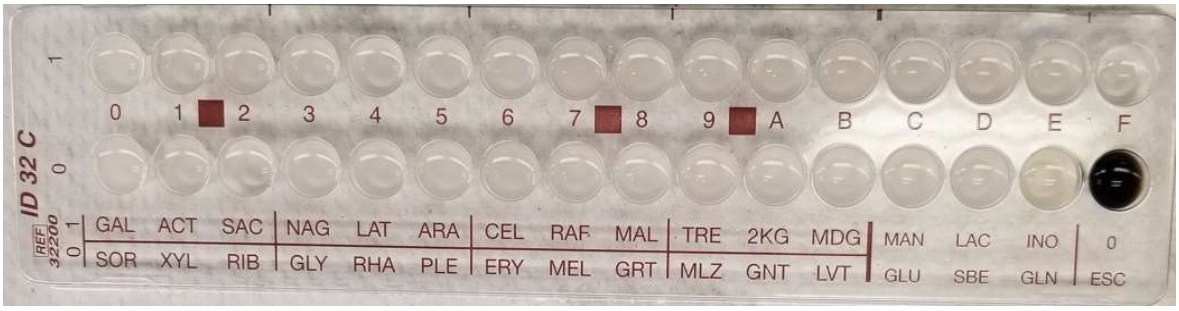
ID 32 C
REF 32200
0 1 2 3 4 5 6 7 8 9 A B C D E F
GAL ACT SAC NAG LAT ARA CEL RAF MAL TRE 2KG MDG MAN LAC INO 0
SOR XYL RIB GLY RHA PLE ERY MEL GRT MLZ GNT LVT GLU SBE GLN ESC

(p)

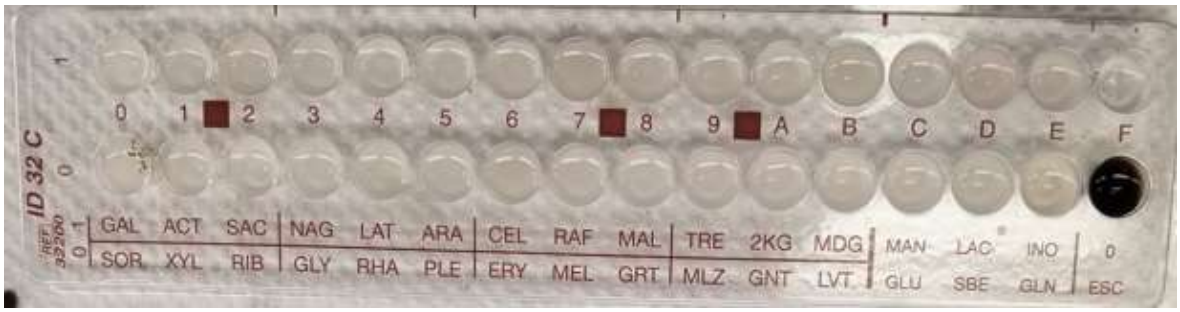

(q)

(r)

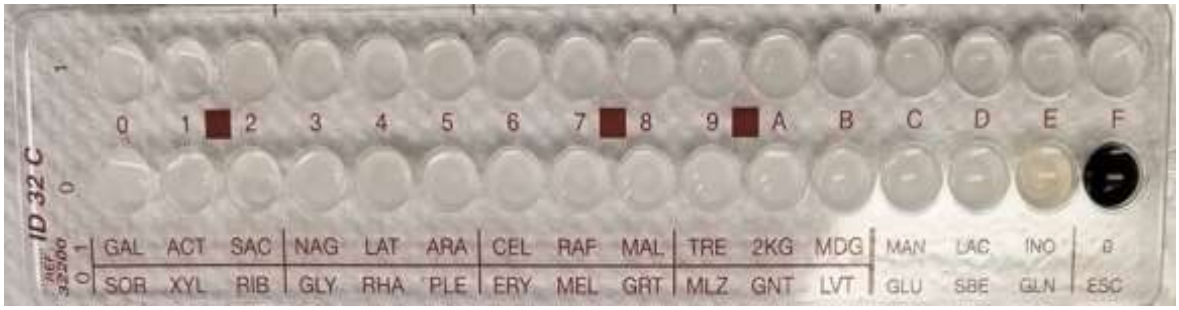

Figure S2.9: Images representing the growth of *E. dermatitidis* (a) wildtype, (b) *alb1*, (c) *alb2*, (d) *alb3,* (e) *alb4,* (f) *alb5,* (g) *alb6,* (h) *alb7,* (i) *alb8,* (j) *alb9,* (k) *alb10,* (l) *alb11,* (m) *alb12,* (n) *alb13,* (o) *alb13,* (p) *alb15,* (q) *alb16* and, (r) *alb17* on ID 32-C Strips. *Alb1, alb2 and alb3* are conditional albinos and the rest are obligate albinos. Negative control (1.F) has no substrate and positive control (0.F) includes Esculinferric citrate.

(a)

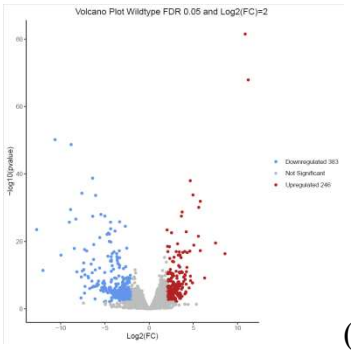

(b)

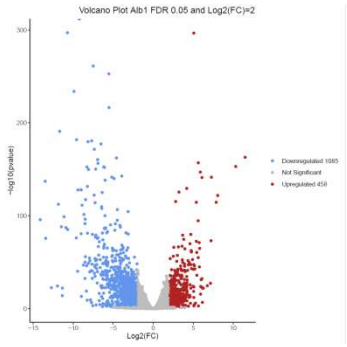

(c)

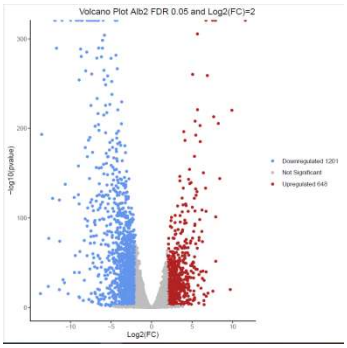

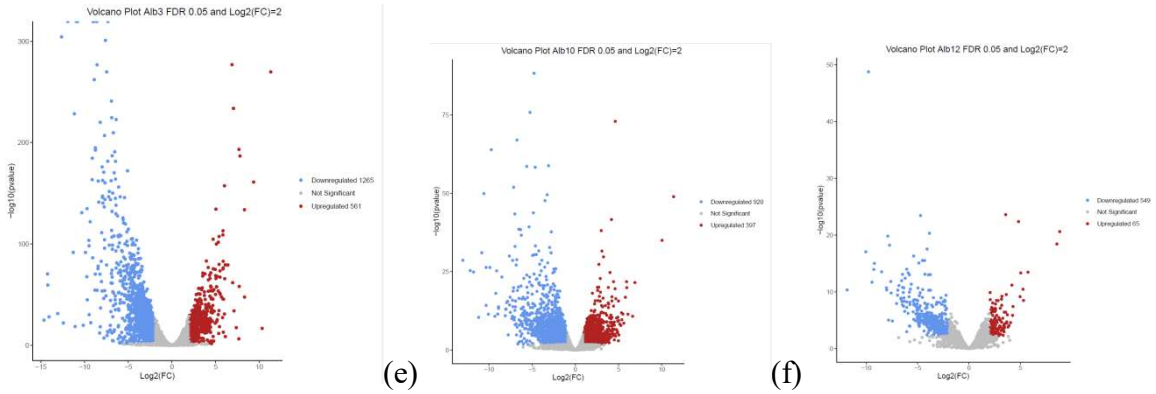

(d) (e) (f)

Figure S3.1: Volcano plots representing the number of differentially expressed upregulated (red dots) and downregulated (blue dots) genes observed on YPD vs YPG based on FDR <0.05 and Log2(FC) >2 or <-2 for (a) *E. dermatitidis* wildtype, (b) *alb1*, (c) *alb2*, (d) *alb3*, (e) *alb10*, and (f) *alb12*.

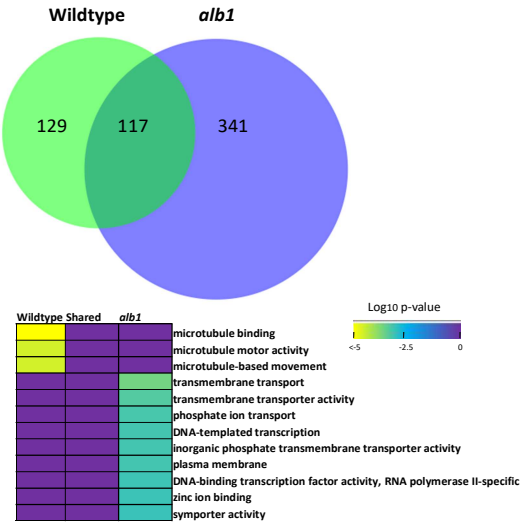

a)

b)

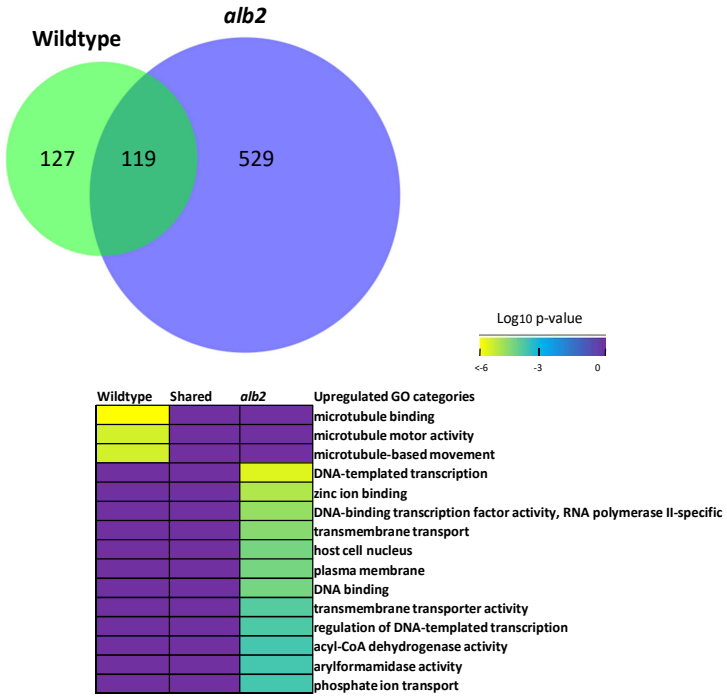
Wildtype
alb2
127
119
529
Log10 p-value
<-6
-3
0
Wildtype
Shared
alb2
Upregulated GO categories
microtubule binding
microtubule motor activity
microtubule-based movement
DNA-templated transcription
zinc ion binding
DNA-binding transcription factor activity, RNA polymerase II-specific
transmembrane transport
host cell nucleus
plasma membrane
DNA binding
transmembrane transporter activity
regulation of DNA-templated transcription
acyl-CoA dehydrogenase activity
arylformamidase activity
phosphate ion transport

c)


Wildtype
alb3
133
113
447
Log10 p-value
<-5.5
-3.5
0
Wildtype
Shared
alb3
Upregulated GO terms
microtubule binding
microtubule motor activity
microtubule-based movement
transmembrane transport
DNA-templated transcription
zinc ion binding
plasma membrane
membrane
transmembrane transporter activity
acyl-CoA dehydrogenase activity
arylformamidase activity
oxidoreductase activity
FAD binding

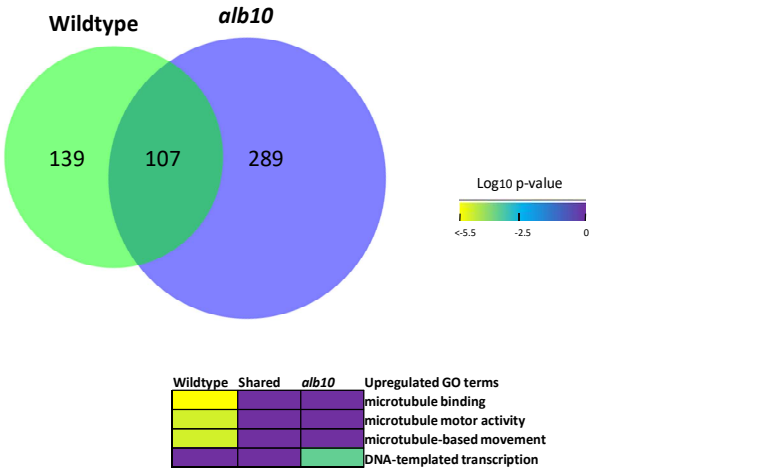
Wildtype
alb10
139
107
289
Log10 p-value
<-5.5
-2.5
0
Wildtype
Shared
alb10
Upregulated GO terms
microtubule binding
microtubule motor activity
microtubule-based movement
DNA-templated transcription

d)

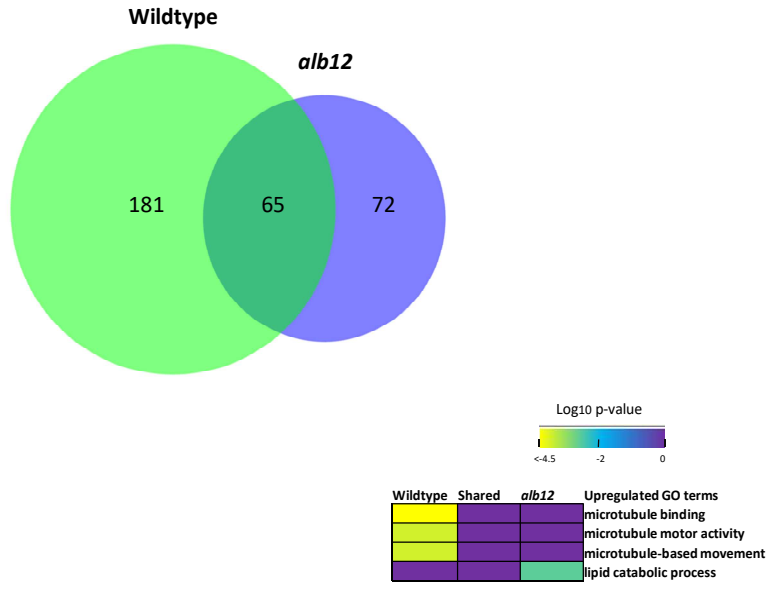
Wildtype
alb12
181
65
72
Log10 p-value
<-4.5
-2
0
Wildtype
Shared
alb12
Upregulated GO terms
microtubule binding
microtubule motor activity
microtubule-based movement
lipid catabolic process

e)

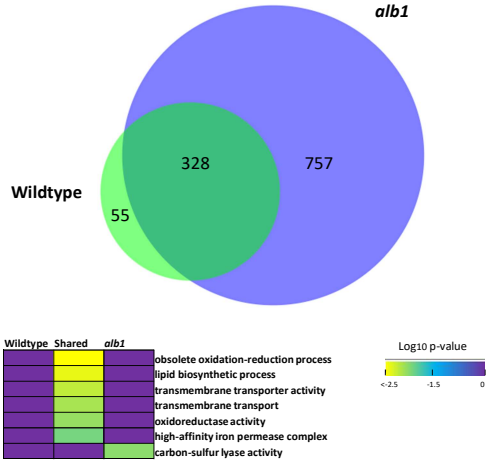
alb1
328
757
Wildtype
55
Wildtype Shared alb1
obsolete oxidation-reduction process
lipid biosynthetic process
transmembrane transporter activity
transmembrane transport
oxidoreductase activity
high-affinity iron permease complex
carbon-sulfur lyase activity
Log10 p-value
<-2.5
-1.5
0

f)

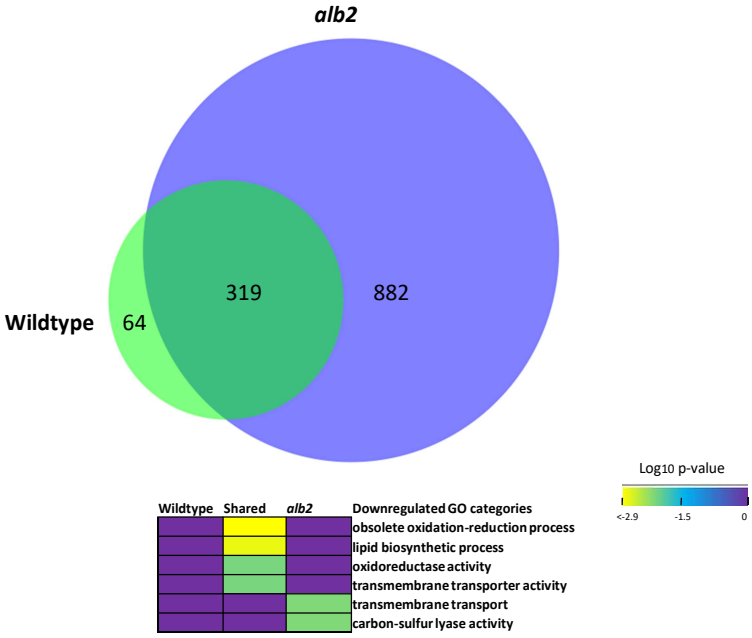
alb2
319
882
Wildtype
64
Log10 p-value
<-2.9
-1.5
0
Wildtype Shared alb2
Downregulated GO categories
obsolete oxidation-reduction process
lipid biosynthetic process
oxidoreductase activity
transmembrane transporter activity
transmembrane transport
carbon-sulfur lyase activity

g)

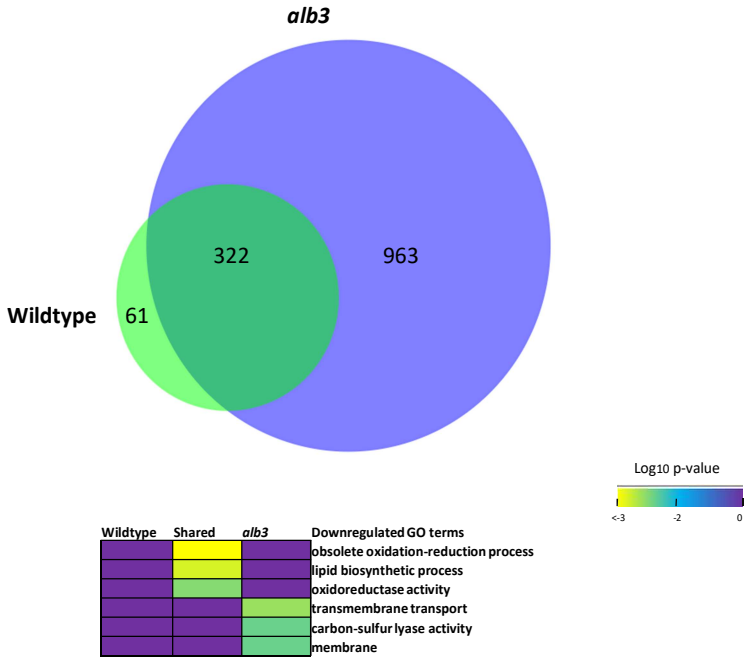
alb3
322
963
Wildtype
61
Log10 p-value
<-3
-2
0
Wildtype
Shared
alb3
Downregulated GO terms
obsolete oxidation-reduction process
lipid biosynthetic process
oxidoreductase activity
transmembrane transport
carbon-sulfur lyase activity
membrane

h)

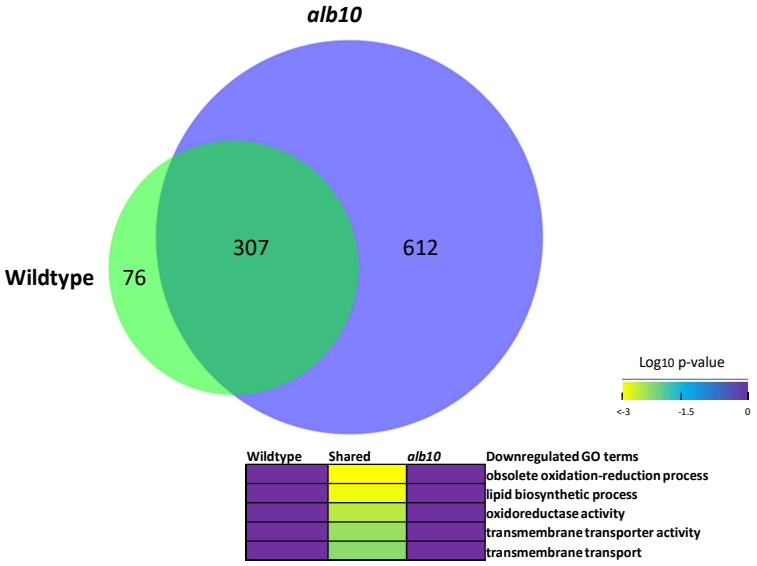
alb10
307
612
Wildtype
76
Log10 p-value
<-3
-1.5
0
Wildtype
Shared
alb10
Downregulated GO terms
obsolete oxidation-reduction process
lipid biosynthetic process
oxidoreductase activity
transmembrane transporter activity
transmembrane transport

i)

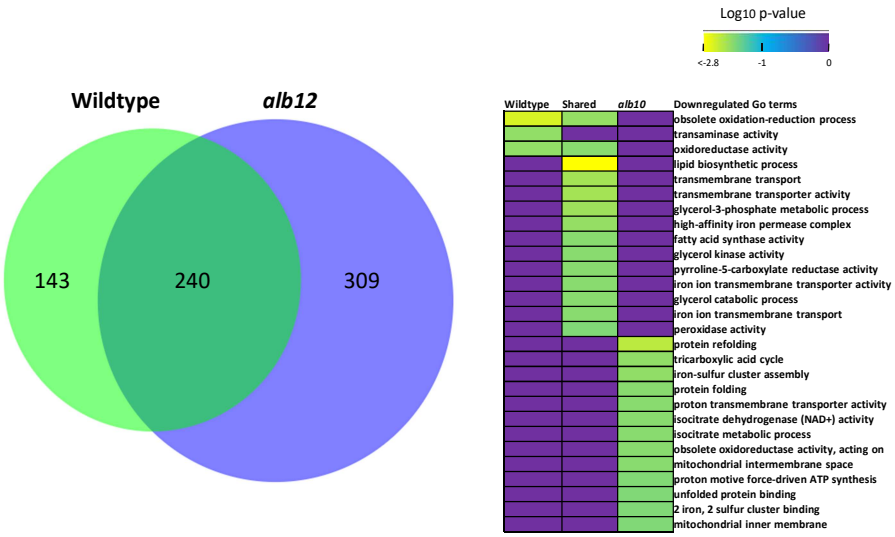

j)

Figure S3.2: Venn diagram demonstrating the overlap in differentially expressed upregulated or downregulated genes in *E. dermatitidis* wildtype (WT) and albino mutant datasets. DEGs identified using DESeq2 with a significance cutoff of $p < 0.05$ and $\log_2$ FC > 2 or < -2 (a) WT and *alb1* upregulated, (b) WT and *alb2* upregulated, (c) WT and *alb3* upregulated, (d) WT and *alb10* upregulated, (e) WT and *alb12* upregulated, (f) WT and *alb1* downregulated, (g) WT and *alb2* downregulated, (h) WT and *alb3* downregulated, (i) WT and *alb10* downregulated, (j) WT and *alb12* downregulated. Terms presented for each section include Gene Ontology- terms that are considered significantly enriched at FDR < 0.05, from FungiFun 3.0. Yellow colour = more statistically enriched, purple colour= less statistically enriched.

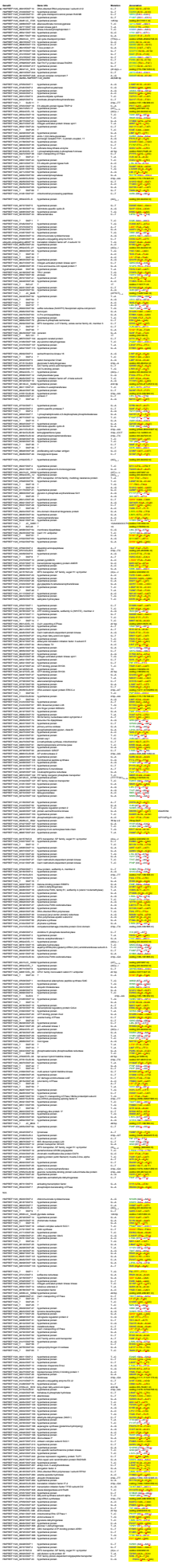

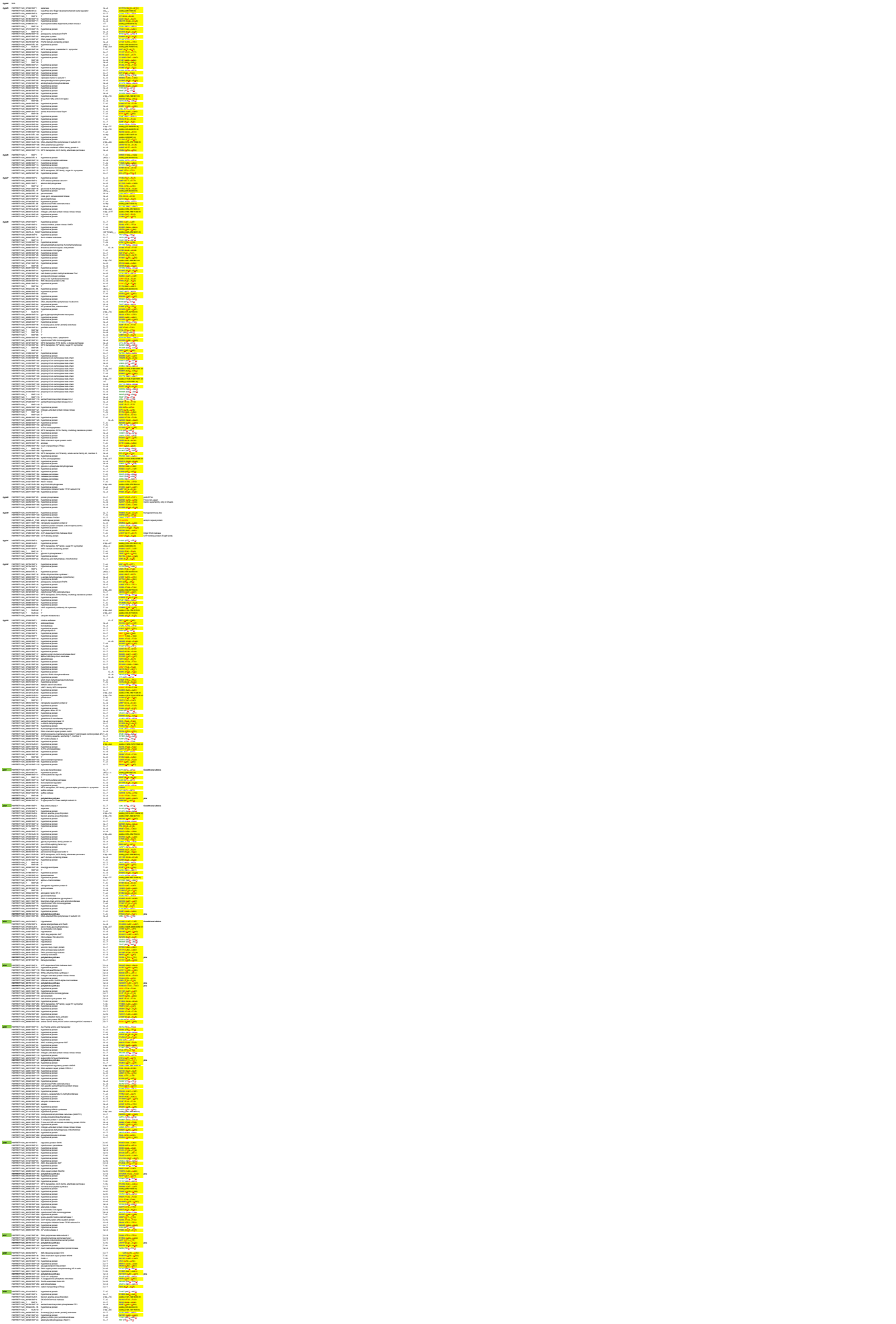

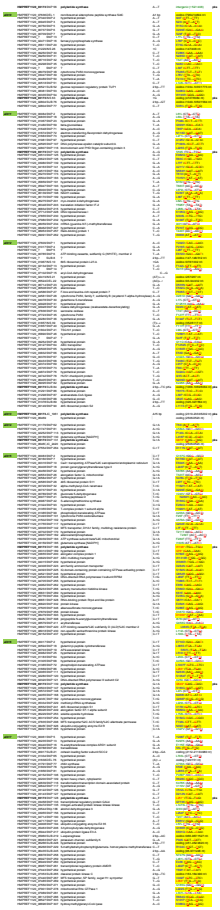

Gene	Gene Inforamtion																			
HMPREF1120_07340	hypothetical protein	Strains	hyp33	alb10															
		Annotation	L181F (CTC→TTC)	I90F (ATT→TTT)															
		Mutation	C→T	A→T															
HMPREF1120_00729	alpha-methylacyl-CoA racemase	Strains	hyp33	alb15															
		Annotation	N183D (AAT→GAT)	Y162H (TAT→CAT)															
		Mutation	C→T	T->C															
HMPREF1120_07925	hypothetical protein	Strains	hyp33	hyp21															
		Annotation	G41D (GGT→GAT)	E20K (GAA→AAA)															
		Mutation	C→T	C→T															
HMPREF1120_06975	hypothetical protein	Strains	hyp33	hyp28															
		Annotation	K468N (AAA→AAT)	G192S (GGT→AGT)															
		Mutation	A→T	G→A															
HMPREF1120_04285	hypothetical protein	Strains	hyp33	hyp22															
		Annotation	S322L (TCG→TTG)	A472V (GCT→GTT															
		Mutation	G→A	C→T															
HMPREF1120_00406	DNA mismatch repair protein msh3	Strains	hyp33	hyp28															
		Annotation	F679L (TTC→CTC)	T25R (ACA→AGA)															
		Mutation	A→G	G→C															
HMPREF1120_08863	AP endonuclease 2	Strains	hyp33	hyp10	alb6														
		Annotation	Y29Y (TAC→TAT)	coding (895-896/1350 nt)	P360L (CCT→CTT)														
		Mutation	G→A	2 bp→AA	G->A														
HMPREF1120_04739	X-Pro aminopeptidase	Strains	hyp33	hyp28															
		Annotation	L237S (TTG→TCG)	coding (3163-3164/3786 nt)															
		Mutation	A→G	2 bp→CT															
HMPREF1120_05524	hypothetical protein	Strains	hyp32	hyp28	alb17	hyp26	alb12	hyp25	hyp20	hyp16	hyp15	hyp14	hyp8	hyp5	hyp4	hyp2	hyp1	alb9	
		Annotation	coding (93-94/432 nt)	coding (93-94/432 nt)	coding (9	coding (9	coding (9	coding (9	coding (9	coding (9	coding (9	coding (9	coding (9	coding (9	coding (9	coding (9	coding (9	coding (93-94/432 nt)	
		Mutation	$(AC)_{8\rightarrow7}$	$(AC)_{8\rightarrow7}$	$(AC)_{8\rightarrow7}$	$(AC)_{8\rightarrow7}$	$(AC)_{8\rightarrow7}$	$(AC)_{8\rightarrow7}$	$(AC)_{8\rightarrow7}$	$(AC)_{8\rightarrow7}$	$(AC)_{8\rightarrow7}$	$(AC)_{8\rightarrow7}$	$(AC)_{8\rightarrow7}$	$(AC)_{8\rightarrow7}$	$(AC)_{8\rightarrow7}$	$(AC)_{8\rightarrow7}$	$(AC)_{8\rightarrow7}$	$(AC)_{8\rightarrow7}$	
HMPREF1120_07052	ataxia telangiectasia and Rad3	Strains	alb3	hyp22															
		Annotation	N1483D (AAT→GAT)	H1107R (CAT→CGT)															
		Mutation	A→G	T→C															
HMPREF1120_03173	**polyketide synthase**	Strains	alb3	alb2	alb1	alb12	alb10	alb9	alb13	alb14	alb6	alb4	alb7	alb15	alb16	alb8	alb5	alb11	alb17
		Annotation	F439L (TTC→CTC)	F764S (TTT→TCT)	N578H (A	coding (1	coding (4	intergenic	coding (2	Q978* (C	W1252S (	H2065Y (	L577P (C	W198* (T	Q649* (C	H2152Y (	F429S (T	S59S (TC	L251* (TTG→TAG)
		Mutation	T→C	T→C	A→C	2 bp→TC	+G	A→T	Δ15 bp	G->A	C->G	G->A	A->G	C->T	G->A	G->A	A→G	A→G	A→T
HMPREF1120_07637	hypothetical protein	Strains	hyp28	hyp10															
		Annotation	D8N (GAT→AAT)	D188N (GAT→AAT)															
		Mutation	C→T	C→T															
HMPREF1120_06267	hypothetical protein	Strains	hyp28	hyp22															
		Annotation	Q158Q (CAG→CAA)	R117Q (CGA→CAA)															
		Mutation	C→T	G→A															
HMPREF1120_06619	urease	Strains	hyp28	alb5															
		Annotation	Y27D (TAC→GAC)	L319F (CTC→TTC)															
		Mutation	T→G	G→A															
HMPREF1120_06469	hypothetical protein	Strains	hyp28	alb13	alb14														
		Annotation	D583N (GAT→AAT)	coding (2506/2523 nt)	coding (2506/2523 nt)														
		Mutation	G→A																
HMPREF1120_02928	malate dehydrogenase (oxaloacetate-d	Strains	hyp28	alb12															
		Annotation	N192D (AAC→GAC)	D24N (GAT→AAT)															
		Mutation	A→G	G→A															
HMPREF1120_02200	dynein heavy chain, cytoplasmic	Strains	hyp28	alb17															
		Annotation	K2210K (AAG→AAA)	R628C (CGC→TGC)															
		Mutation	C→T	C→T															
HMPREF1120_01230	propionyl-CoA carboxylase beta chain	** 14 SNPS in the same Strains.	hyp28																
HMPREF1120_03076	X-Pro aminopeptidase	Strains	hyp28	hyp4															
		Annotation	Y112H (TAT→CAT)	E766K (GAA→AAA)															
		Mutation	T→C	G→A															
HMPREF1120_07859	Ca2+-transporting ATPase	Strains	hyp4	hyp28	hyp1														
		Annotation	L67* (TTA→TGA)	Q60* (CAA→TAA)	P777S (CCG→TCG)														
		Mutation	G→A	G→A	C→T														
HMPREF1120_05292	MFS transporter, LAT3 family, solute ca	Strains	hyp28	hyp4															
		Annotation	S7L (TCA→TTA)	G70S (GGT→AGT)															
		Mutation	G→A	C→T															
HMPREF1120_04099	peroxiredoxin	Strains	hyp27	alb4															
		Annotation	I160I (ATC→ATT)	G42R (GGG→AGG)															
		Mutation	C→T	G->A															
HMPREF1120_07390	separase	Strains	alb2	hyp25															
		Annotation	D14D (GAC→GAT)	A1772V (GCC→GTC)															
		Mutation	G→A	G→A															
HMPREF1120_03423	fanconi anemia group M protein	Strains	alb2	alb9															
		Annotation	coding (391-392/447 nt)	coding (147-148/3432 nt)															
		Mutation	2 bp→TC	2 bp→TC															
HMPREF1120_00737	hypothetical protein	Strains	alb2	hyp23	hyp10	hyp3	alb10	alb15											
		Annotation	D299E (GAC→GAA)	D299E (GAC→GAA)	D299E (	D299E (	D299E (	D299E (GAC→GAA)											
		Mutation	C->A	C->A	C->A	C->A	C->A	C->A											
HMPREF1120_07029	glycosyl hydrolase, family protein 31	Strains	alb2	hyp30															
		Annotation	L458L (CTG→TTG)	N578K (AAT→AAA)															
		Mutation	G→A	T→A															
HMPREF1120_01788	hypothetical protein	Strains	alb2	hyp1															
		Annotation	E322G (GAG→GGG)	G193R (GGC→CGC)															
		Mutation	A→G	G→C															
HMPREF1120_01202	hypothetical protein	Strains	alb2	hyp13															
		Annotation	coding (966-967/1038 nt)	L160L (TTG→CTG)															
		Mutation	2 bp→TT	A→G															
HMPREF1120_04342	retrograde regulation protein 2	Strains	alb2	hyp11															
		Annotation	N41D (AAT→GAT)	S439S (TCA→TCG)															
		Mutation	A→G	T→C															
HMPREF1120_03001	DNA-directed RNA polymerase III subu	Strains	alb2	hyp25															
		Annotation	L68L (CTG→TTG)	coding (372-373/1599 nt)															
		Mutation	G→A	2 bp→AA															
HMPREF1120_02419	hypothetical protein	Strains	alb1	alb12	hyp15	hyp8	hyp6	hyp1	alb5										
		Annotation	coding (267/267 nt)	coding (267/267 nt)	coding (2	coding (2	coding (2	coding (2	F14L (TTT→TTG)										
		Mutation	$(AT)_{14\rightarrow15}$	$(AT)_{14\rightarrow15}$	$(AT)_{14\rightarrow16}$	$(AT)_{14\rightarrow16}$	2 bp→AA	$(AT)_{14\rightarrow15}$	A→C										
HMPREF1120_00785	ATP-binding cassette, subfamily G (WH	Strains	alb12	hyp10															
		Annotation	E672D (GAA→GAT)	I503I (ATT→ATC)															
		Mutation	T→A	A→G															
HMPREF1120_04586	F-box and leucine-rich repeat protein 7	Strains	alb12	hyp4															
		Annotation	P605S (CCT→TCT)	S147S (TCG→TCA)															
		Mutation	C→T	G→A															
HMPREF1120_02280	hypothetical protein	Strains	alb12	alb16															
		Annotation	S144F (TCT→TTT)	S1054F (TCT→TTT)															
		Mutation	G→A	C->T															
HMPREF1120_09254	hypothetical protein	Strains	alb12	hyp25															
		Annotation	Q11Q (CAG→CAA)	coding (128-129/201 nt)															
		Mutation	G→A	2 bp→TC															
HMPREF1120_06609	hypothetical protein	Strains	hyp25	hyp4															
		Annotation	Y117F (TAT→TTT)	Y3D (TAC→GAC)															
		Mutation	A→T	T→G															
HMPREF1120_03608	hypothetical protein	Strains	hyp25	hyp22															
		Annotation	A385T (GCC→ACC)	I172I (ATT→ATA)															
		Mutation	G→A	T→A															
HMPREF1120_04157	MFS transporter, SP family, sugar:H+ s	Strains	hyp23	hyp17	hyp12	hyp9													
		Annotation	coding (240/462 nt)	coding (240/462 nt)	coding (2	coding (240/462 nt)													
		Mutation	$(A)_{36\rightarrow37}$	$(A)_{36\rightarrow37}$	$(A)_{36\rightarrow37}$	$(A)_{36\rightarrow37}$													
HMPREF1120_05200	chloromuconate cycloisomerase	Strains	hyp20	hyp4															
		Annotation	N102N (AAT→AAC)	A657A (GCT→GCC)															
		Mutation	A→G	A→G															
HMPREF1120_05728	hypothetical protein	Strains	hyp20	hyp5															
		Annotation	H74Y (CAT→TAT)	Y113H (TAC→CAC)															
		Mutation	G→A	A→G															
HMPREF1120_04237	cohesin complex subunit SCC1	Strains	hyp20	hyp22															
		Annotation	P594P (CCT→CCC)	P336S (CCC→TCC)															
		Mutation	T→C	C→T															
HMPREF1120_01791	chitin synthase	Strains	hyp20	alb17															
		Annotation	W499* (TGG→TGA)	A703A (GCT→GCA)															
		Mutation	C→T	T→A															
HMPREF1120_08138	hypothetical protein	Strains	hyp20	hyp5															
		Annotation	L564F (CTC→TTC)	coding (4703-4714/5310 nt)															
		Mutation	G→A	Δ12 bp															
HMPREF1120_00298	hypothetical protein	Strains	hyp20	alb10															
		Annotation	V112V (GTT→GTA)	N48D (AAC→GAC)															
		Mutation	T→A	T→C															
HMPREF1120_08462	hypothetical protein	Strains	hyp20	alb11	hyp22														
		Annotation	P210T (CCG→ACG)	P210T (CCG→ACG)	P210T (CCG→ACG)														
		Mutation	C→A	C→A	C→A														
HMPREF1120_07636	nonribosomal siderophore peptide synth	Strains	hyp16	alb10															
		Annotation	I4662I (ATA→ATC)	coding (7964/14604 nt)															
		Mutation	T→G	Δ1 bp															
HMPREF1120_06770	hypothetical protein	Strains	hyp15	hyp30															
		Annotation	Q379Q (CAG→CAA)	G1471V (GGG→GTG)															
		Mutation	C→T	G→T															
HMPREF1120_01493	cytochrome P450 oxidoreductase	Strains	hyp14	alb15															
		Annotation	coding (186-187/855 nt)	F25F (TTC→TTT)															
		Mutation	2 bp→GA	G->A															
HMPREF1120_01304	phytoene synthase	Strains	hyp13	alb6															
		Annotation	L183L (CTC→CTT)	M123I (ATG→ATC)															
		Mutation	G→A	G->C															
HMPREF1120_06473	mitogen-activated protein kinase spm1	Strains	hyp10	hyp4	hyp1														
		Annotation	N312H (AAT→CAT)	Q26Q (CAG→CAA)	I285F (ATC→TTC)														
		Mutation	T→G	C→T	T→A														
HMPREF1120_07823	hypothetical protein	Strains	hyp10	hyp9															
		Annotation	N863Y (AAC→TAC)	R325W (CGG→TGG)															
		Mutation	T→A	G→A															
HMPREF1120_04809	nonribosomal peptide synthase	Strains	hyp10	alb6															
		Annotation	F11L (TTC→TTG)	D998N (GAT→AAT)															
		Mutation	C→G	C->T															
HMPREF1120_04368	hypothetical protein	Strains	hyp10	hyp1															
		Annotation	V130V (GTA→GTG)	coding (172-173/243 nt)															
		Mutation	A→G	2 bp→AA															
HMPREF1120_06773	hypothetical protein	Strains	hyp9	hyp6															
		Annotation	F46L (TTT→TTG)	F184F (TTT→TTC)															
		Mutation	A→C	T→C															
HMPREF1120_01179	hypothetical protein	Strains	hyp8	alb14															
		Annotation	A269P (GCC→CCC)	T53I (ACT→ATT)															
		Mutation	G→C	G->A															
HMPREF1120_01522	hypothetical protein	Strains	hyp8	hyp7															
		Annotation	Q159* (CAG→TAG)	coding (93-94/432 nt)															
		Mutation	A→G	$(AC)_{8\rightarrow7}$															
HMPREF1120_04169	G2/mitotic-specific cyclin-B	Strains	hyp6	hyp3															
		Annotation	E63E (GAG→GAA)	S41P (TCA→CCA)															
		Mutation	G→A	A→G															
HMPREF1120_01067	hypothetical protein	Strains	hyp4	alb11															
		Annotation	V88V (GTA→GTC)	P348L (CCT→CTT)															
		Mutation	T→G	G→A															
HMPREF1120_02538	mitogen-activated protein kinase kinase	Strains	hyp21	alb4															
		Annotation	S115P (TCT→CCT)	A572G (GCC→GGC)															
		Mutation	T→C	G->C															
HMPREF1120_04580	hypothetical protein	Strains	hyp21	hyp26															
		Annotation	coding (206-208/261 nt)	*134E (TAA→GAA)															
		Mutation	Δ3 bp	T→G															
HMPREF1120_09152	hypothetical protein	Strains	hyp21	alb15															
		Annotation	R19K (AGA→AAA)	L190L (CTA→TTA)															
		Mutation	C→T	C->T															
HMPREF1120_01747	hypothetical protein	Strains	alb14	alb6															
		Annotation	A584A (GCT→GCC)	A584A (GCT→GCC)															
		Mutation	A->G	A->G															
HMPREF1120_07614	hypothetical protein	Strains	alb4	hyp22															
		Annotation	S535L (TCG→TTG)	T3T (ACC→ACT)															
		Mutation	C->T	C→T															
HMPREF1120_01385	phospholipid-translocating ATPase	Strains	alb15	alb16															
		Annotation	A203A (GCC→GCT)	L1007F (CTC→TTC)															
		Mutation	C->T	C->T															
HMPREF1120_03159	glutamate synthase [NADPH]	Strains	alb14	alb15															
		Annotation	L416P (CTC→CCC)	I1605I (ATT→ATC)															
		Mutation	A->G	A->G															
HMPREF1120_05776	hypothetical protein	Strains	hyp27	alb15															
		Annotation	coding (350-351/528 nt)	E235G (GAA→GGA)															
		Mutation	2 bp→GA	A->G															
HMPREF1120_06229	soluble epoxide hydrolase	Strains	alb16	hyp22															
		Annotation	L158L (CTA→CTC)	Y169D (TAT→GAT)															
		Mutation	T->G	A→C															
HMPREF1120_09091	hypothetical protein	Strains	alb16	alb11															
		Annotation	V327V (GTC→GTA)	I368M (ATT→ATG)															
		Mutation	C->A	T→G															
HMPREF1120_02264	hypothetical protein	Strains	alb5	hyp22															
		Annotation	P152P (CCT→CCC)	I49V (ATT→GTT)															
		Mutation	A→G	T→C															
HMPREF1120_00084	hypothetical protein	Strains	alb11	hyp22															
		Annotation	L61L (CTA→CTT)	P412S (CCA→TCA)															
		Mutation	A→T	C→T															
HMPREF1120_06348	translation initiation factor IF-2	Strains	alb11	hyp22															
		Annotation	Y595Y (TAC→TAT)	coding (1064-1065/3169 nt)															
		Mutation	G→A	2 bp→GA															
HMPREF1120_07901	mitochondrial Rho GTPase 1	Strains	hyp22	alb17															
		Annotation	P517P (CCA→CCG)	L222S (TTG→TCG)															
		Mutation	T→C	A→G															
HMPREF1120_02447	ABC drug exporter AtrF	Strains	alb12	alb3															
		Annotation	F1263L (TTC→TTA)	N1401H (AAT→CAT)															
		Mutation	C->A	A→C															

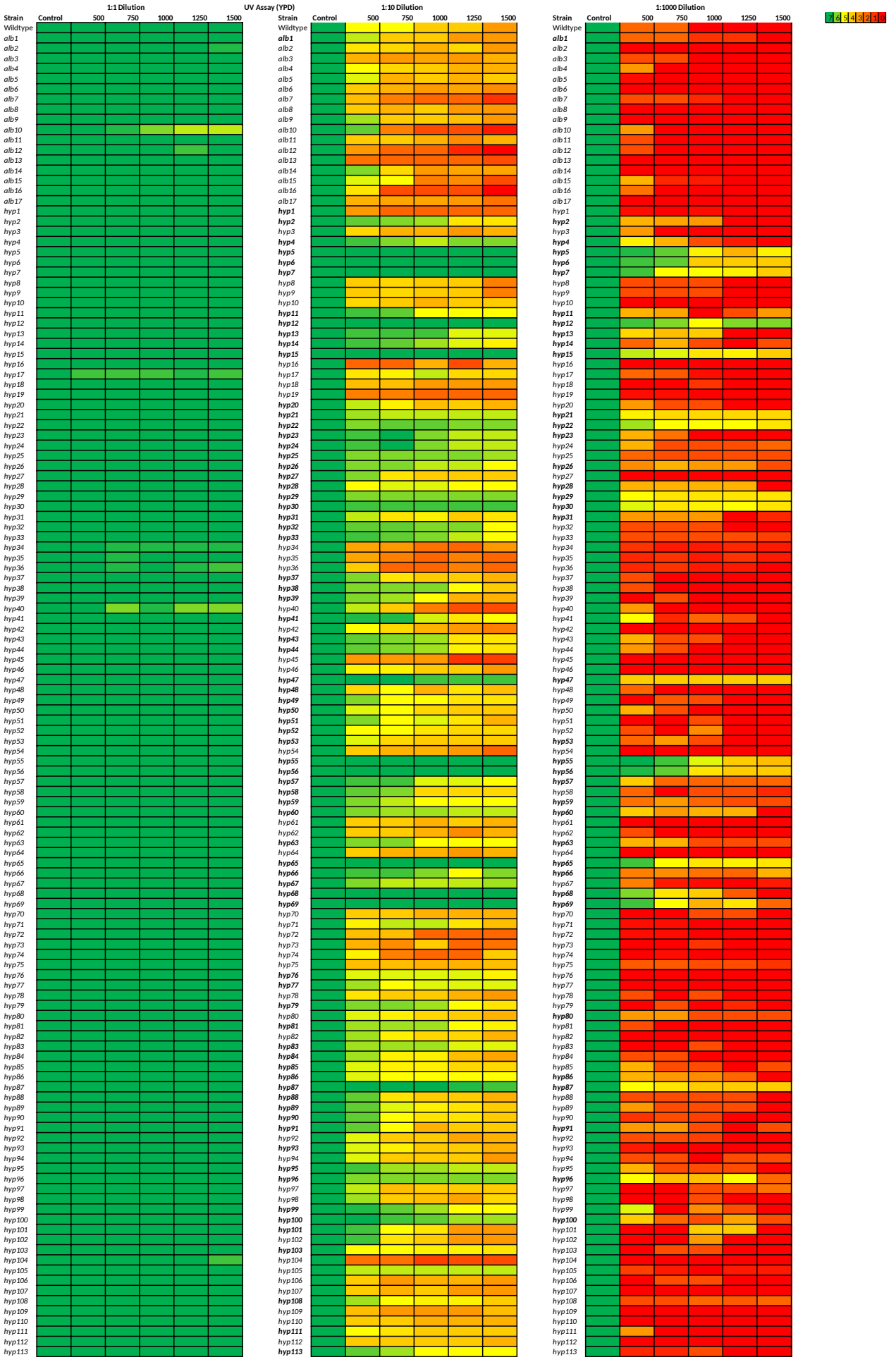
UV Assay (YPD)
1:1 Dilution
1:10 Dilution
1:1000 Dilution
Strain
Control
500
750
1000
1250
1500
7 6 5 4 3 2 1 0

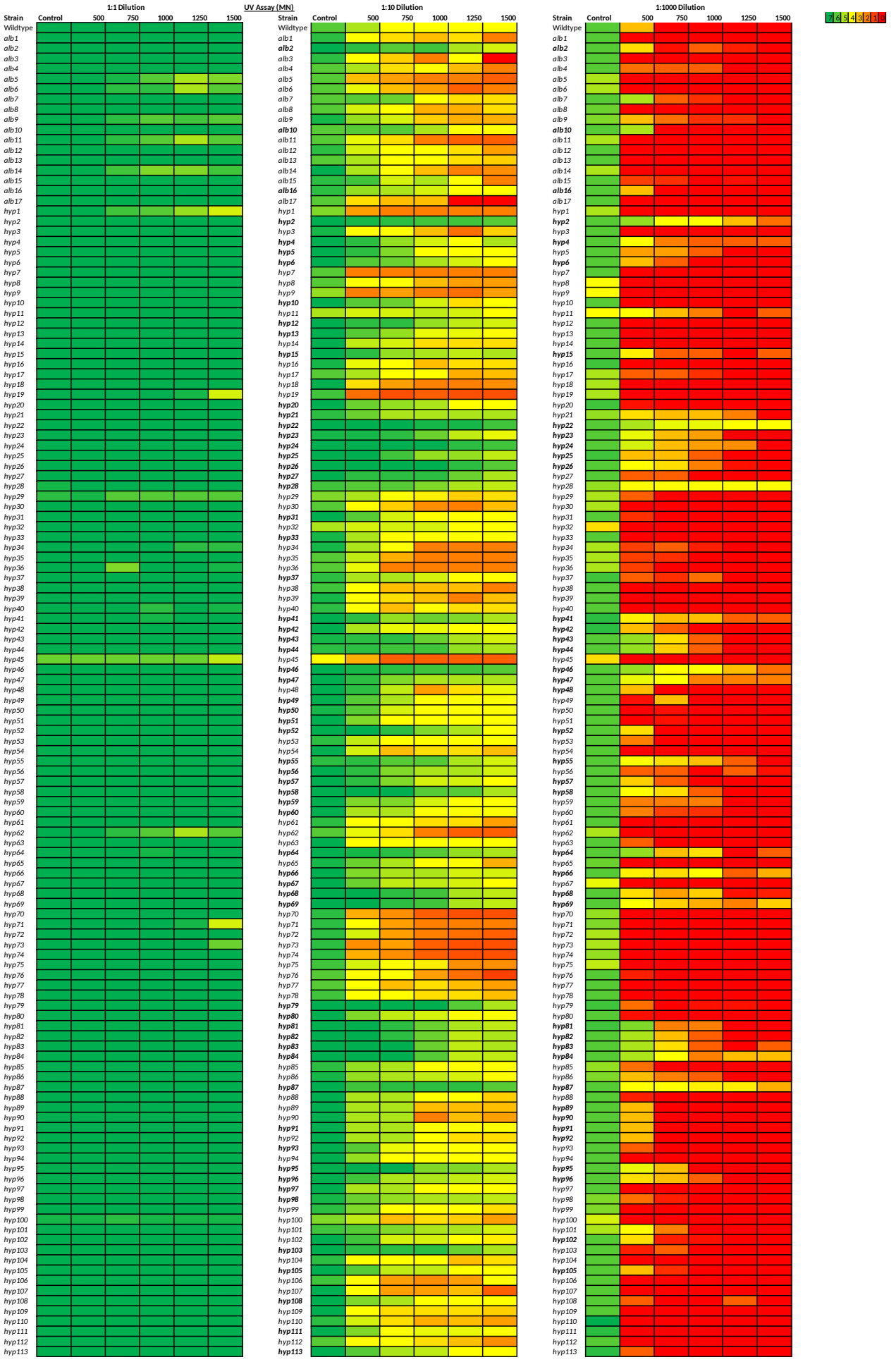
UV Assay (MN)
1:1 Dilution
1:10 Dilution
1:1000 Dilution
Strain
Control
500
750
1000
1250
1500
7 6 5 4 3 2 1 0
Wildtype
alb1
alb2
alb3
alb4
alb5
alb6
alb7
alb8
alb9
alb10
alb11
alb12
alb13
alb14
alb15
alb16
alb17
hyp1
hyp2
hyp3
hyp4
hyp5
hyp6
hyp7
hyp8
hyp9
hyp10
hyp11
hyp12
hyp13
hyp14
hyp15
hyp16
hyp17
hyp18
hyp19
hyp20
hyp21
hyp22
hyp23
hyp24
hyp25
hyp26
hyp27
hyp28
hyp29
hyp30
hyp31
hyp32
hyp33
hyp34
hyp35
hyp36
hyp37
hyp38
hyp39
hyp40
hyp41
hyp42
hyp43
hyp44
hyp45
hyp46
hyp47
hyp48
hyp49
hyp50
hyp51
hyp52
hyp53
hyp54
hyp55
hyp56
hyp57
hyp58
hyp59
hyp60
hyp61
hyp62
hyp63
hyp64
hyp65
hyp66
hyp67
hyp68
hyp69
hyp70
hyp71
hyp72
hyp73
hyp74
hyp75
hyp76
hyp77
hyp78
hyp79
hyp80
hyp81
hyp82
hyp83
hyp84
hyp85
hyp86
hyp87
hyp88
hyp89
hyp90
hyp91
hyp92
hyp93
hyp94
hyp95
hyp96
hyp97
hyp98
hyp99
hyp100
hyp101
hyp102
hyp103
hyp104
hyp105
hyp106
hyp107
hyp108
hyp109
hyp110
hyp111
hyp112
hyp113

Temp Assay	10°C				28°C			
Strain	1:1	1:10	1:100	1:1000	1:1	1:10	1:100	1:1000
Wildtype								
alb1								
alb2								
alb3								
alb4								
alb5								
alb6								
alb7								
alb8								
alb9								
alb10								
alb11								
alb12								
alb13								
alb14								
alb15								
alb16								
alb17								
hyp1								
hyp2								
hyp3								
hyp4								
hyp5								
hyp6								
hyp7								
hyp8								
hyp9								
hyp10								
hyp11								
hyp12								
hyp13								
hyp14								
hyp15								
hyp16								
hyp17								
hyp18								
hyp19								
hyp20								
hyp21								
hyp22								
hyp23								
hyp24								
hyp25								
hyp26								
hyp27								
hyp28								
hyp29								
hyp30								
hyp31								
hyp32								
hyp33								
hyp34								
hyp35								
hyp36								
hyp37								
hyp38								
hyp39								
hyp40								
hyp41								
hyp42								
hyp43								
hyp44								
hyp45								
hyp46								
hyp47								
hyp48								
hyp49								
hyp50								
hyp51								
hyp52								
hyp53								
hyp54								
hyp55								
hyp56								
hyp57								
hyp58								
hyp59								
hyp60								
hyp61								
hyp62								
hyp63								
hyp64								
hyp65								
hyp66								
hyp67								
hyp68								
hyp69								
hyp70								
hyp71								
hyp72								
hyp73								
hyp74								
hyp75								
hyp76								
hyp77								
hyp78								
hyp79								
hyp80								
hyp81								
hyp82								
hyp83								
hyp84								
hyp85								
hyp86								
hyp87								
hyp88								
hyp89								
hyp90								
hyp91								
hyp92								
hyp93								
hyp94								
hyp95								
hyp96								
hyp97								
hyp98								
hyp99								
hyp100								
hyp101								
hyp102								
hyp103								
hyp104								
hyp105								
hyp106								
hyp107								
hyp108								
hyp109								
hyp110								
hyp111								
hyp112								
hyp113								

7 6 5 4 3 2 1 0

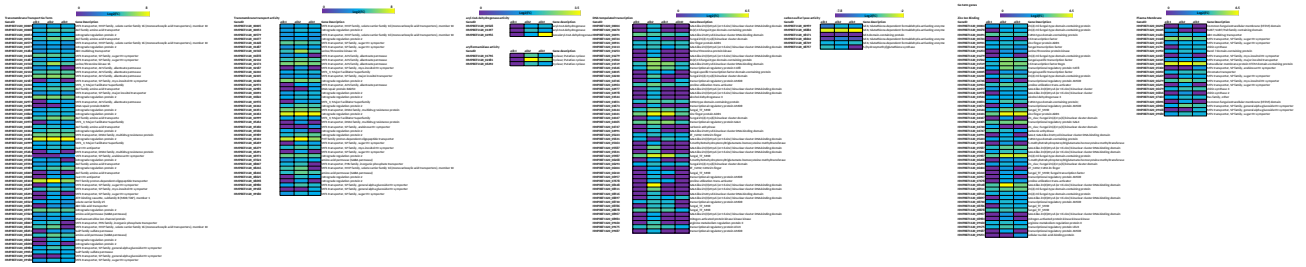

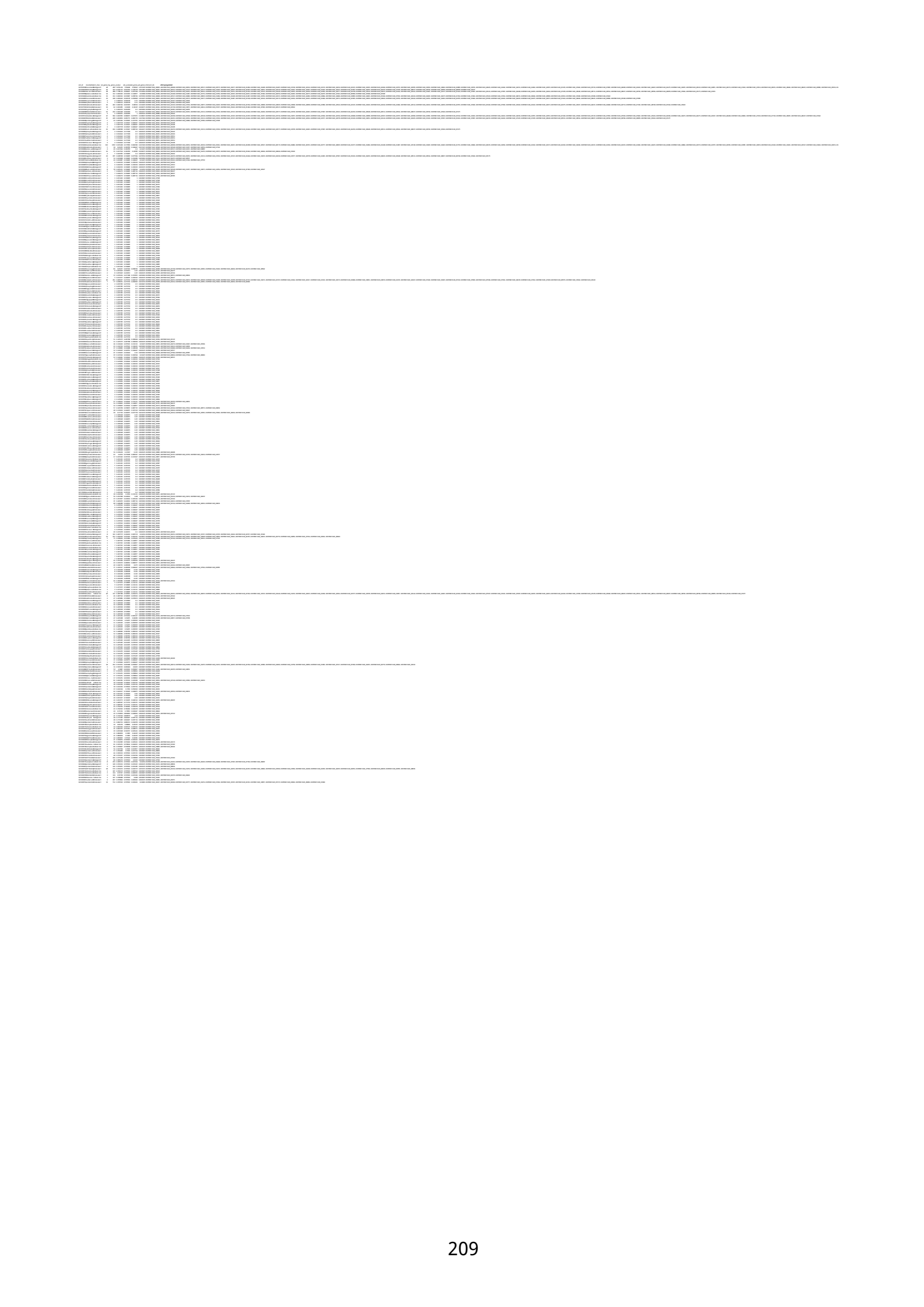

ont_id	description	ont_class	sel_genes	bg_genes	pvalue	adj_pvalue	sel_genes_intersect_ids	**alb12 upregulated**
GO:0016049	lipid catabi	Biological P	3	17	0.000335	0.019762	0.176471	0.069767 HMPREF1120_03245, HMPREF1120_03538, HMPREF1120_06140
GO:0006629	lipid metaB	Biological P	3	47	0.006716	0.08166	0.06383	0.069767 HMPREF1120_03245, HMPREF1120_03538, HMPREF1120_06140
GO:0004349	glucosamin	Molecular f	1	1	0.008304	0.08166	1	0.023256 HMPREF1120_09080
GO:0006049	-acetylgluc	Biological P	1	1	0.008304	0.08166	1	0.023256 HMPREF1120_09080
GO:0019408	dolichol bis	Biological P	1	1	0.008304	0.08166	1	0.023256 HMPREF1120_07618
GO:1904462	dehydrodec	Cellular Co	1	1	0.008304	0.08166	1	0.023256 HMPREF1120_07618
GO:0003963	methylated	Molecular f	1	2	0.016541	0.108438	0.5	0.023256 HMPREF1120_01764
GO:0004348	phosphogh	Molecular f	1	2	0.016541	0.108438	0.5	0.023256 HMPREF1120_08325
GO:0003630	racemase /	Molecular f	1	2	0.016541	0.108438	0.5	0.023256 HMPREF1120_02303
GO:0003689	DNA clamp	Molecular f	1	3	0.024712	0.132544	0.333333	0.023256 HMPREF1120_01583
GO:0005692	DNA replic	Cellular Co	1	3	0.024712	0.132544	0.333333	0.023256 HMPREF1120_01583
GO:0016789	hydrolase -	Molecular f	5	212	0.029904	0.133908	0.023585	0.116279 HMPREF1120_03245, HMPREF1120_03538, HMPREF1120_06140, HMPREF1120_07216, HMPREF1120_09167
GO:0004656	L-serine bi	Biological P	1	4	0.032815	0.133908	0.25	0.023256 HMPREF1120_08325
GO:0051216	biosynthesis	Molecular f	2	35	0.033722	0.133908	0.057143	0.046512 HMPREF1120_03468, HMPREF1120_05469
GO:0006281	DNA repair	Biological P	3	89	0.036996	0.133908	0.033708	0.069767 HMPREF1120_00792, HMPREF1120_01583, HMPREF1120_01764
GO:0006757	cellular ar	Biological P	1	5	0.040853	0.133908	0.2	0.023256 HMPREF1120_01656
GO:0008199	ferric iron b	Molecular f	1	5	0.040853	0.133908	0.2	0.023256 HMPREF1120_01656
GO:0046857	phosphatid	Biological P	1	5	0.040853	0.133908	0.2	0.023256 HMPREF1120_05001
GO:0004152	carboxyspe	Molecular f	1	6	0.048826	0.151618	0.166667	0.023256 HMPREF1120_00135
GO:0006260	DNA replic	Biological P	2	45	0.053272	0.157151	0.044444	0.046512 HMPREF1120_00792, HMPREF1120_01583
GO:0008152	metabolic p	Biological P	1	8	0.064578	0.165657	0.125	0.023256 HMPREF1120_09189
GO:0008132	O-methylth	Molecular f	1	8	0.064578	0.165657	0.125	0.023256 HMPREF1120_05344
GO:0016705	oxidoreduta	Molecular f	1	8	0.064578	0.165657	0.125	0.023256 HMPREF1120_01656
GO:0016740	transferase	Molecular f	1	9	0.072358	0.170765	0.111111	0.023256 HMPREF1120_07618
GO:0016787	hydrolase -	Molecular f	1	9	0.072358	0.170765	0.111111	0.023256 HMPREF1120_09189
GO:0032259	methylatio	Biological P	2	68	0.108915	0.247153	0.029412	0.046512 HMPREF1120_01764, HMPREF1120_05344
GO:0006310	DNA recom	Biological P	1	16	0.125077	0.273316	0.0625	0.023256 HMPREF1120_00792
GO:0051536	iron, 2 sul	Molecular f	1	17	0.132365	0.278912	0.058824	0.023256 HMPREF1120_02746
GO:0016530	protein dis	Biological P	1	18	0.139594	0.284001	0.055556	0.023256 HMPREF1120_02698
GO:0016887	hydrolase -	Molecular f	1	19	0.146764	0.288636	0.052632	0.023256 HMPREF1120_07216
GO:0006810	nitrogen ci	Biological P	1	22	0.167926	0.3196	0.045455	0.023256 HMPREF1120_02303
GO:0006464	protein gly	Biological P	1	23	0.174865	0.322407	0.043478	0.023256 HMPREF1120_07618
GO:0005576	extracellul	Cellular Co	1	24	0.181748	0.324943	0.041667	0.023256 HMPREF1120_05230
GO:0004386	helicase ac	Molecular f	1	25	0.188574	0.327232	0.04	0.023256 HMPREF1120_00651
GO:0016614	oxidoreduta	Molecular f	1	27	0.202061	0.340618	0.037037	0.023256 HMPREF1120_08325
GO:0005783	endoplasm	Cellular Co	1	32	0.234828	0.384857	0.03125	0.023256 HMPREF1120_07618
GO:0008676	-acetyltran	Molecular f	1	35	0.253853	0.404793	0.028571	0.023256 HMPREF1120_04922
GO:0016021	membrane	Cellular Co	4	314	0.262764	0.407975	0.012739	0.093023 HMPREF1120_03245, HMPREF1120_03538, HMPREF1120_06140, HMPREF1120_09168
GO:0051287	NAD bindi	Molecular f	1	40	0.28454	0.430458	0.025	0.023256 HMPREF1120_08325
GO:0022857	transmem	Molecular f	4	348	0.327373	0.482876	0.011494	0.093023 HMPREF1120_03965, HMPREF1120_04573, HMPREF1120_08216, HMPREF1120_09168
GO:0055114	oxidoreduta	Biological P	6	584	0.356525	0.513048	0.010274	0.139535 HMPREF1120_01656, HMPREF1120_02766, HMPREF1120_03571, HMPREF1120_04343, HMPREF1120_05469, HMPREF1120_08325
GO:0016021	membrane	Cellular Co	16	1769	0.396369	0.556804	0.009045	0.372093 HMPREF1120_01770, HMPREF1120_01785, HMPREF1120_02708, HMPREF1120_03156, HMPREF1120_03246, HMPREF1120_03580, HMPREF1120_03965, HMPREF1120_04480, HMPREF1120_04573, HMPREF1120_05001, HMPREF1120_07618, HMPREF1120_08216, HMPREF1120_09137, HMPREF1120_09147, HMPREF1120_09168, HMPREF1120_09258
GO:0016491	oxidoreduta	Molecular f	4	403	0.433691	0.595064	0.009926	0.093023 HMPREF1120_02766, HMPREF1120_03571, HMPREF1120_04343, HMPREF1120_05469
GO:0005506	iron ion bin	Molecular f	1	90	0.53096	0.711968	0.011111	0.023256 HMPREF1120_01656
GO:0055085	transmem	Biological P	4	489	0.58978	0.771268	0.00818	0.093023 HMPREF1120_03965, HMPREF1120_04573, HMPREF1120_08216, HMPREF1120_09168
GO:0005886	plasma me	Cellular Co	1	112	0.610999	0.783672	0.008929	0.023256 HMPREF1120_09168
GO:0005975	carbohydr	Biological P	1	122	0.642811	0.806933	0.008197	0.023256 HMPREF1120_09080
GO:0003677	DNA bindi	Molecular f	3	428	0.702568	0.861574	0.007009	0.069767 HMPREF1120_00792, HMPREF1120_01583, HMPREF1120_02746
GO:0006351	DNA-templ	Biological P	1	169	0.761353	0.916731	0.005917	0.023256 HMPREF1120_02746
GO:0046872	metal ion b	Molecular f	2	354	0.803544	0.927084	0.00565	0.046512 HMPREF1120_00135, HMPREF1120_02766
GO:0003676	nucleic acid	Molecular f	1	207	0.828232	0.927084	0.004831	0.023256 HMPREF1120_00651
GO:0000960	DNA-bindi	Molecular f	1	210	0.832652	0.927084	0.004762	0.023256 HMPREF1120_02746
GO:0008270	zinc ion bir	Molecular f	2	388	0.843823	0.927084	0.005155	0.046512 HMPREF1120_02746, HMPREF1120_03571
GO:0055085	protein bin	Molecular f	3	554	0.854016	0.927084	0.005415	0.069767 HMPREF1120_02698, HMPREF1120_08475, HMPREF1120_08769
GO:0042026	host cell nu	Cellular Co	1	234	0.864231	0.927084	0.004274	0.023256 HMPREF1120_02746
GO:0003824	catalytic ac	Molecular f	2	451	0.899635	0.947829	0.004435	0.046512 HMPREF1120_01656, HMPREF1120_01764
GO:0065007	regulation	Biological P	1	295	0.920575	0.952875	0.00339	0.023256 HMPREF1120_02746
GO:0005634	nucleus	Cellular Co	3	737	0.955907	0.958669	0.004071	0.069767 HMPREF1120_00792, HMPREF1120_01583, HMPREF1120_02746
GO:0005524	ATP bindin	Molecular f	2	570	0.958669	0.958669	0.003509	0.046512 HMPREF1120_00651, HMPREF1120_01583